Antibacterial activities of *Propionibacterium acnes* bacteriophages against a diverse collection of *P. acnes* clinical isolates: Prospects for novel alternative therapies for acne vulgaris

by

Jenna Graham

A thesis submitted in partial fulfillment
of the requirements for the degree of
Master of Science (MSc) in Biology

The Faculty of Graduate Studies
Laurentian University
Sudbury, Ontario, Canada

© Jenna Graham, 2017

THESIS DEFENCE COMMITTEE/COMITÉ DE SOUTENANCE DE THÈSE
Laurentian Université/Université Laurentienne
Faculty of Graduate Studies/Faculté des études supérieures

Title of Thesis Titre de la thèse	Antibacterial activities of Propionibacterium acnes bacteriophages against a diverse collection of P. acnes clinical isolates: Prospects for novel alternative therapies for acne vulgaris
Name of Candidate Nom du candidat	Graham, Jenna
Degree Diplôme	Master of Science
Department/Program Département/Programme	Biology
Date of Defence Date de la soutenance	August 22, 2017

APPROVED/APPROUVÉ

Thesis Examiners/Examinateurs de thèse:

Dr. Reza Nokbeh
(Co-Supervisor/Co-directeur de thèse)

Dr. Mazen Saleh
(Co-Supervisor/Co-directeur de thèse)

Dr. Céline Larivière
(Committee member/Membre du comité)

Dr. Wolfgang Köster
(External Examiner/Examinateur externe)

Approved for the Faculty of Graduate Studies
Approuvé pour la Faculté des études supérieures
Dr. David Lesbarrères
Monsieur David Lesbarrères
Dean, Faculty of Graduate Studies
Doyen, Faculté des études supérieures

ACCESSIBILITY CLAUSE AND PERMISSION TO USE

I, **Jenna Graham**, hereby grant to Laurentian University and/or its agents the non-exclusive license to archive and make accessible my thesis, dissertation, or project report in whole or in part in all forms of media, now or for the duration of my copyright ownership. I retain all other ownership rights to the copyright of the thesis, dissertation or project report. I also reserve the right to use in future works (such as articles or books) all or part of this thesis, dissertation, or project report. I further agree that permission for copying of this thesis in any manner, in whole or in part, for scholarly purposes may be granted by the professor or professors who supervised my thesis work or, in their absence, by the Head of the Department in which my thesis work was done. It is understood that any copying or publication or use of this thesis or parts thereof for financial gain shall not be allowed without my written permission. It is also understood that this copy is being made available in this form by the authority of the copyright owner solely for the purpose of private study and research and may not be copied or reproduced except as permitted by the copyright laws without written authority from the copyright owner.

Abstract

A total of 136 chronically infected Canadian acne patients from Ottawa-Gatineau and Northeastern Ontario regions accounting for 75% of subjects (12-50 years old, with 90th percentile at the age of 30) who had suffered acne vulgaris (with various acne related scarring) for a median duration of 4 years, were sources for isolation of *Propionibacterium acnes*, the etiologic agent for acne vulgaris. Eighty-four percent of patients were subjected to various treatment regimens with topical and systemic agents including in combination with 1-3 different types of antibiotics (mean duration of 7 months). A diverse collection of 224 clinical *P. acnes* isolates from Canadian and Swedish subjects were characterized for their sensitivities to infection by a Canadian collection of 67 diverse phages belonging to siphoviridae; and multiple minimal cocktails consisting of 2-3 phages were formulated to be effective on global *P. acnes* isolates. *Propionibacterium acnes* isolates were characterized by multiplex PCR to belong to phylotypes IA, IB and II, which also showed resistance against commonly used antibiotics for treating acne vulgaris (overall resistance rate of 9.5%), were sensitive to phages regardless of their type and antibiotic resistance patterns, providing ground for phages as novel alternative therapeutics for future *in vivo* trials. The phage collection was diverse by virtue of their *BamHI* restriction patterns and full genome sequences and harboured a major tail protein (MTP) that appeared to be important in contributing to their host ranges. Three dimensional structural modeling of the N-domain of *P. acnes* MTPs implicated previously unreported involvement of the α1-β4 loop (C5 loop) within N-domain amino acid sequence in contributing to the expanded host range of a mutant phage to infect a naturally phage resistant *P. acnes* clinical isolate. Given the potential of phages for rapid mutational diversification surpassing that of their bacterial hosts and the fact that phages are generally regarded as safe (GRAS), rapid and cost-effective

derivation of mutant phages with expanded host ranges provide a strong framework for improving phage cocktails for use in future personalized medicine.

Keywords

Bacteriophage, Phage, Siphoviridae, Coryneform, P. acnes, Acne vulgaris, Antibiotic resistance, Phage Therapy, phylotype, Clinical isolate, Genome, Multiplex PCR, Host-range, 3D modeling, Major Tail protein, Receptor.

Acknowledgments

I would like to express my gratitude to my supervisor, Dr. Reza Nokhbeh, for his mentorship and guidance throughout my studies. I am indebted to him for the countless hours he has spent reviewing this thesis and for the time he has worked closely with me throughout this project. His vast knowledge and expertise has been integral to the success of this project, and his continued support allowed me to investigate and address additional questions as they arose, challenging me to grow and adapt throughout its duration. The endless stories and life lessons he has shared have never been unappreciated, and the motivation which drives his research has been a source of inspiration for me throughout my studies.

My warmest thanks also goes to members of my thesis committee, Dr. Céline Larivière and Dr. Mazen Saleh. I am grateful to them for reviewing this thesis quickly, and for providing support, guidance, valuable suggestions and constructive criticism. I would like to acknowledge Dr. Gustavo Ybazeta for sharing his expertise on several occasions and to him and Nya Fraleigh for their contributions to the genomics work. I am grateful to Dr. Mery Martínez for her guidance and encouragement.

Obtaining a collection of clinical isolates was an integral component of this thesis hence I express my appreciation for our dermatologist collaborators, Dr. Sharyn Laughlin and Dr. Lyne Giroux, who so kindly agreed to collect patient samples for this project. I also would like to extend thanks to Kathryn Bernard and Dr. Anna Holmberg for contributing isolates from their collections.

To my lab and office mates- my time in Sudbury would not have been the same without you. I would especially like to thank Cassandra, Nya, Twinkle, Megan and Seb for their friendship, support and advice. Without these amazing people, I would have been lost.

Finally, I extend my deepest gratitude to my family and to my partner Kyle. I am extremely lucky that they have stuck by my side through thick and thin. This thesis would not have been possible without their endless love, extraordinary support and incredible patience.

Table of Contents

List of Tables

List of Figures

List of Abbreviations

(O)	Oral
(T)	Topical
1 KbP	1 Kb Plus (DNA Ladder)
AA	Antiandrogen
AB	Antibiotic
AD	Deep tissue isolates from Sweden
AS	Skin surface isolates from Sweden
ATCC	American Type Culture Collection
AZ	Azithromycin
BBA	Brucella laked sheep blood agar supplemented with hemin and vitamin K1
BHI	Brain-heart infusion (nutrient medium)
BioNJ	Bio neighbourjoining
Blastp	Standard protein BLAST
bp	Base pair
BPO	benzoyl peroxide
BSA	Bovine serum albumin
CADM	Congruence Among Distance Matrices
CAMP	Christie, Atkins, Munch-Peterson
CB	Columbia (nutrient medium)
CC	Closed comedone
CFU	Colony forming units
CLB	Cell lysis buffer
CLSI	Clinical and Laboratory Standards Institute
CM	Clindamycin
COC	Combined oral contraceptive
CSLU	Department of Clinical Sciences of Lund University (Lund, Sweden)
Cys/Pus	Cystic/pustular (lesion)
DC	Doxycycline
ddH_2O	Double-distilled water
DNA	Deoxyribonucleic acid
dNTPs	Deoxyribonucleotide triphosphates
DPC	Daptomycin
dsDNA	Double-stranded DNA
EM	Erythromycin
erm(X)	Erythromycin ribosome methylase resistance gene
EtBr	Ethidium bromide
Etest	Epsilometer test
EUCAST	European Committee on Antimicrobial Susceptibility Testing
FDA	American Food and Drug Administration
gDNA	Genomic DNA
gehA	Glycerol-ester hydrolase A gene
gp	Gene product
GRAS	Generally recognized as safe

GRHA	Gonadotropin-releasing hormone agonist
GUI	Graphical user interface
H_0	Null hypothesis
H_1	Alternate hypothesis
HR	High Range (DNA Ladder)
HS	High sensitivity
HβD2	Human β-defensin 2
IL-12	Interleukin-12
IL-1α	Interleukin-1α
IL-1β	Interleukin-1β
IL-8	Interleukin-8
Ion PGM	Ion Torrent Personal Genome Machine
kbp	Kilobase pair
LDG	Low-dose glucocorticoid
LE	Levofloxacin
LZ	Linezolid
MALDI-TOF	Matrix-assisted laser desorption/ionization time of flight
MC	Minocycline
MH	Mueller-Hinton (nutrient medium)
MIC	Minimal inhibitory concentration
MOI	Multiplicity of infection
MSA	Multiple sequence alignment
MTP	Major tail protein
NCBI	National Center for Biotechnology Information
NEB	New England Biolabs
NML	National Microbiology Laboratory (Winnipeg, Canada)
OC	Open comedone
OC	Oral contraceptive
OD	Samples of lesion exudate, Ottawa
ORF	Open reading frame
OS	Skin surface samples, Ottawa
p	Probability value
PABA	Para-aminobenzoic acid
PAMPs	Pathogen-associated molecular patterns
PCI	Phenol, chloroform and isoamyl alcohol
PCR	Polymerase chain reaction
p-distance	Proportion of variable sites between two sequences
PDT	Photodynamic therapy
PEG	Polyethylene glycol
PFU	Plaque forming unit
PGL	Benzylpenicillin
QC	Quality control
rDNA	DNA locus used for transcription of ribosomal RNA
recA	recombinase A gene
RI	Rifampicin
RNA	Ribonucleic acid

rrn	Genomic locus for rRNA operon
rRNA	Ribosomal RNA
r_s	Spearman's correlation coefficient
RT	Room temperature
RTD	Retinoid, topical and/or oral
SAPHO	Synovitis, acne, pustulosis, hyperostosis, osteitis
SD	Samples of lesion exudate, Sudbury
SE	Standard error
SPAUD	Scientific Panel of Antibiotic Usage in Dermatology
SPL	Spironolactone
SS	Skin surface samples, Sudbury
TAE	Tris-acetate-ethylenediaminetetraacetic acid
Taq Pol	Taq DNA polymerase
TC	Tetracycline
TEM	Transmission electron microscopy
TLRs	Toll-like receptors
TM	Trimethoprim
TNFα	Tumor necrosis factor alpha
tRNA	Transfer RNA
TS	Trimethoprim/sulfamethoxazole
TXL	Ceftriaxone
VA	Vancomycin
W	Kendall's coefficient of concordance

List of Appendices

1 Introduction

1.1 Propionibacterium acnes

1.1.1 General Microbiology

Propionibacterium acnes is a non-motile, asporogenous, Gram-positive, aerotolerant anaerobe. Described as a pleomorphic rod (Patrick & McDowell, 2012), its morphology is dependent on strain, age and culturing conditions; all of which seemingly confer variable colony morphology on agar media (Marples & McGinley, 1974). Anaerobic cultures typically exhibit coryneform morphology, representative of its earlier taxonomic nomenclature as "*Corynebacterium parvum*" (Cummins & Johnson, 1974) and "*Corynebacterium acnes*" (Bergey *et al.*, 1923). Cells range from 0.2 to 1.5µm wide by 1 to 5µm in length, however, isolates of phylotype III group exhibit filamentous morphology and have been observed to grow up to 21.8µm in length (McDowell *et al.*, 2008). On the surface of agar media, colonies may appear raised, convex or pulvinate, and range from 1 to 4mm in diameter. As colonies become larger with age, they tend to transition from pale to deep shades of yellow, beige or pink. Appearance of the colonies is dependent on the type of media.

Culturing in complex media is a necessity for this chemoorganotrophic microorganism, and renders it fastidious; its nutritional requirements may only be met by media rich in organic compounds such as sugars and polyhydroxy alcohols. Propionic acid production via fermentation of organic substrates, coupled with its aversion to aerobic conditions, was the basis by which Douglas and Gunter (Douglas & Gunter, 1946) argued to amend its original genus designation from "*Corynebacterium*" to "*Propionibacterium*".

A prominent member of the healthy human skin microbiome (Funke *et al.*, 1997; Grice & Segre, 2011), *P. acnes* thrives near-exclusively in the anoxic environment of the pilosebaceous unit, located just under the surface of the skin (Barnard *et al.*, 2016a; Bek-Thomsen *et al.*, 2008; Grice & Segre, 2011; Leeming *et al.*, 1984). The pilosebaceous unit provides a unique niche for *P. acnes*, where competition is scarce and nutrient resources are abundant.

Colonization of this lipophilic commensal tends to be concentrated over areas of the head and trunk that are rich in sebaceous glands (Roth & James, 1988). Cell-to-cell adherence is promoted by metabolizing components of the sebum secreted by the glands, such as triacylglycerols (Gribbon *et al.*, 1993; Marples *et al.*, 1971). Liberation of free fatty acids combined with the secretion of acidic metabolic products—acetic and propionic acid—imposes a decrease in the pH level of the stratum corneum, enhancing its suitability for occupation by normal flora and preventing pathogen colonization (Elias, 2007; Korting *et al.*, 1990; Ushijima *et al.*, 1984). A dominant and often exclusive occupant of the pilosebaceous unit, *P. acnes* is believed to aid in the protection against colonization of other pathogenic microbes (Bek-Thomsen *et al.*, 2008; Gallo & Nakatsuji, 2011; Shu *et al.*, 2013).

Despite its presence as a predominant skin commensal, *P. acnes* is also known to colonize other areas of the body including the gastrointestinal tract and the genitourinary tract (Delgado *et al.*, 2011, 2013; McDowell & Patrick, 2011; Montalban Arques *et al.*, 2016; Yang *et al.*, 2013). The events that lead to colonization of *P. acnes* play a major

role in its ability to illicit robust immune responses. The substantial implications of colonization in relation to pathogenicity are discussed.

1.1.2 Isolation and characterization

Recovery of *P. acnes* from patient specimens is largely dependent on the length of incubation time and atmospheric composition. Length of incubation time to recover isolates depends on the species, size and age of the inoculum. *P. acnes* isolates are typically recovered after one to fourteen days of incubation (Funke *et al.*, 1997). Isolation and cultivation require anaerobic to microaerophilic environments, however, anaerobic conditions seem to be especially favourable for the purpose of primary isolation (Funke *et al.*, 1997). Published reports of *P. acnes* isolation, from a variety of infection sources, are rapidly accumulating as a result of extending incubation periods, optimizing specimen processing (i.e. sonicating to disrupt biofilm) and culture conditions (Abdulmassih *et al.*, 2016; Bayston *et al.*, 2007; Bossard *et al.*, 2016; Butler-Wu *et al.*, 2011; Frangiamore *et al.*, 2015; Kvich *et al.*, 2016; Schäfer *et al.*, 2008).

Complex, non-selective media is employed for primary isolation and enrichment of *P. acnes* as no selective medium capable of exclusive isolation of the microbe is readily available. *P. acnes* is the primary microbial etiologic agent of acne vulgaris, however it is not the only agent involved in this polymicrobial condition (Brook, 1991; Leeming *et al.*, 1984; Marples & McGinley, 1974). There have also been reports of polymicrobial, deep-seated infections involving *P. acnes* (Bémer *et al.*, 2016). Therefore, multistep approaches beginning with culturing techniques, followed by visual inspection, biochemical testing and molecular methods to screen for and characterize clinical isolates

are employed as a reliable methodology for preparing pure clinical cultures of *P. acnes* (Bémer *et al.*, 2016; Cazanave *et al.*, 2013; Shah *et al.*, 2015).

Phylogenetic analysis of clinical *P. acnes* isolates has revealed significant associations between phylotype, virulence factors and pathologies such as acne vulgaris and deep tissue infections, among others (Barnard *et al.*, 2016b; Davidsson *et al.*, 2016; Johnson *et al.*, 2016; Kwon & Suh, 2016; Lomholt *et al.*, 2017; Lomholt & Kilian, 2010; McDowell *et al.*, 2012; Paugam *et al.*, 2017; Petersen *et al.*, 2017; Yu *et al.*, 2016). Development of methods for phylogenetic characterization of *P. acnes* isolates has revealed three main phylogenetic lineages—type I, II and III—encompassing various clades, clusters and strain types. Sequence analysis of housekeeping gene *recA*, putative hemolysin gene *tly* and CAMP factor genes led to the designation of the three major lineages and two major clades within the type I lineage—IA and IB (McDowell *et al.*, 2005, 2008; Valanne *et al.*, 2005). More recently, multilocus sequence typing (MLST) schemes have been used to further divide the lineages into clusters IA1, IA2, IB, IC, II and III (Kilian *et al.*, 2012; Lomholt & Kilian, 2010; McDowell *et al.*, 2011, 2012). Other approaches, such as ribotyping and multiplex PCR-based approaches, yield results that align with the established phylogenetic groupings and are more rapid than sequence-based techniques (Barnard *et al.*, 2015; Davidsson *et al.*, 2016; Fitz-Gibbon *et al.*, 2013; Shannon *et al.*, 2006a).

1.1.3 Clinical significance

Once acknowledged exclusively as a commensal, general perception of the relationship between *P. acnes* and its human host has evolved based on recognition of its capacity to

act as an opportunistic pathogen. Genome sequencing has exposed a plethora of encoded putative virulence factors, many of which likely contribute to its ability to damage host tissue and illicit robust inflammatory immune responses (Brüggemann *et al.*, 2004). Genome characterization combined with clinical manifestations as a result of colonization, have revealed the microbe's pathogenic potential, suggesting an alternative role for *P. acnes* as an opportunistic pathogen (Brüggemann *et al.*, 2004; Brüggemann, 2005). Accredited mainly as the primary microbial agent involved in the pathogenesis of acne vulgaris, *P. acnes* is gaining notoriety for its implication in deep-seated infections and various systemic inflammatory disorders (Perry & Lambert, 2011).

1.1.3.1 Acne vulgaris

Current consensus within the literature suggests that the pathogenesis of acne vulgaris is no longer solely dependent on abnormal desquamation and sebum overproduction (Das & Reynolds, 2014; Kircik, 2016). Acne vulgaris is a multi-factorial, complex condition of the pilosebaceous unit; perpetuated by abnormal androgen levels, sebaceous hyperplasia, microbial colonization, a cascade of inflammatory events and subsequent cornification of the follicular wall (Knutson, 1974); a process referred to as comedogenesis. The role that *P. acnes* plays in acne pathogenesis has remained elusive, however researchers continue to peel back the layers of complexity revealing evidence of the dynamic interplay between *P. acnes* and other factors (Das & Reynolds, 2014).

1.1.3.1.1 Pathogenesis

Microbial Colonization

In 1896, “acne bacilli” (*P. acnes*) were first detected in histological samples by Paul Gerson Unna while examining comedone specimens (Unna, 1896). Since then, colonization and hyperproliferation of *P. acnes* within the pilosebaceous unit has been identified as an essential process in acne pathogenesis. Follicular colonization is thought to be promoted by changes in the pilosebaceous environment resulting from excess sebum production; enhancing its capacity to foster *P. acnes* colonization. Increased nutrient availability (McGinley *et al.*, 1980), abnormal sebum composition (Gribbon *et al.*, 1993; Saint-Leger *et al.*, 1986a, b), and the formation of a follicular plug (Burkhart & Burkhart, 2007; Jeremy *et al.*, 2003; Knutson, 1974), create an ideal niche for *P. acnes* proliferation.

The sebaceous gland, a component of the pilosebaceous unit, secretes sebum; a fluid protective barrier that is critical to the overall health of the skin and hair (De Luca & Valacchi, 2010). Androgen hormones directly influence sebum production by acting as agonists of sebocyte proliferation. An increase in androgen levels; typically occurring during adolescence and an indicator of puberty onset, activate hyperplasia of the sebaceous glands. Sebaceous glands function via holocrine secretory mechanisms, therefore, sebocyte hyperproliferation upregulates sebum secretion; inciting alterations in sebum composition (Strauss *et al.*, 1962; Thiboutot, 2004). Changing sebum composition is implicated in comedogenesis and facilitates *P. acnes* colonization. Linoleic acid behaves as a barrier against microbial colonization (Elias *et al.*, 1980). As sebum is

overproduced, linoleic acid concentration declines, resulting in failure to prevent migration of *P. acnes* into the follicular space. Similarly, decreased concentration of antioxidants result in elevated sebum levels of oxidized squalene and other lipid peroxidases, which reduce oxygen tension within the follicle thereby enhancing its suitability for colonization of anaerobic inhabitants (Saint-Leger *et al.*, 1986a, b). Following colonization, lipase produced by *P. acnes* hydrolyzes sebum triglycerides. Glycerol molecules liberated from this hydrolysis reactiong provide valuable nutrient resources for the *P. acnes* while free fatty acids enhance its adherence to the follicular wall, preventing its removal with sebum secretions (Gribbon *et al.*, 1993). Other factors contributing to microbial colonization involve the formation of a follicular plug, which may be indirectly modulated by altered sebum composition and biofilm formation of *P. acnes* (Burkhart & Burkhart, 2003; Coenye *et al.*, 2007; Holmberg *et al.*, 2009; Jahns *et al.*, 2012).

Microbial Immunomodulation and Virulence

Development of acne lesions involve *P. acnes* virulence factors and host inflammatory responses to follicular colonization. Degradation and rupture of the follicular wall leads to innate immune responses resulting in inflammation—a hallmark of acne lesions. The pathogenic propensity of *P. acnes* is fueled by its extensive assortment of genome-encoded virulence factors, which instigate follicular disruption and activate innate immune receptors, resulting in subsequent release of a proinflammatory cocktail of cytokines, oxidized lipids and bacteria into the surrounding dermal layers.

Host cell carbohydrate, protein and lipid components are hydrolyzed by various glycoside hydrolases, proteases and esterases expressed by *P. acnes* (Brüggemann *et al.*, 2004; Brüggemann, 2005; Holland *et al.*, 2010; Jeon *et al.*, 2017; Miskin *et al.*, 1997). Other tissue damaging virulence factors that are associated with immunostimulatory activity include porphyrins, sialidases and Christie, Atkins, Munch-Peterson (CAMP) factors (Brüggemann *et al.*, 2004; Brüggemann, 2005; Jeon *et al.*, 2017; Lang & Palmer, 2003; Lheure *et al.*, 2016; Schaller *et al.*, 2005). Porphyrins released by *P. acnes* are thought to exert cytotoxic effects on keratinocytes due to free radical generation by molecular oxygen-porphyrin interactions in environments of relatively elevated oxygen tension, ultimately leading to tissue damage (Brüggemann, 2005). A predominant porphyrin secreted by *P. acnes*—coproporphyrin III—has been shown to elicit proinflammatory IL-8 expression by keratinocytes, leading to recruitment of lymphocytes, neutrophils and macrophages (Schaller *et al.*, 2005). Similarly, the genome of *P. acnes* encodes five homologs of pore-forming toxic proteins, known as CAMP factors (Brüggemann, 2005; Lang & Palmer, 2003; Valanne *et al.*, 2005), which act on host cells in the presence of host sphingomyelinase. A study by Nakatsuji *et al.* (2011) reports degradation and invasion of keratinocytes and macrophages due to interaction between CAMP factor 2 and sphingomyelinase. Moreover, a recent study by Lheure *et al.* (2016) demonstrates upregulation of keratinocyte-secreted IL-8 by activation of TLR-2 by *P. acnes* CAMP factor 1. Another cause of host tissue degredation and inflammatory response is the action of *P. acnes* sialidases on host cells (Nakatsuji *et al.*, 2008). Genome sequencing of *P. acnes* has revealed at least two genes encoding sialidases, which function by cleaving host cell sialoglycoconjugates to obtain energy sources (Brüggemann *et al.*, 2004;

Brüggemann, 2005). Furthermore, activation of sebocytes by sialidases induce secretion of IL-8 (Nakatsuji *et al.*, 2008; Oeff *et al.*, 2006).

Immunostimulatory activities of *P. acnes* also involves activation of pattern recognition receptors, such as the Toll-like receptors (TLRs), by pathogen-associated molecular patterns (PAMPs) of *P. acnes*, to stimulate release of proinflammatory cytokines and chemokines (Su *et al.*, 2017; Takeda & Akira, 2004; Vowels *et al.*, 1995). For example, *P. acnes* activates TLR2 pathways of keratinocytes and sebocytes, causing these cells to secrete interleukin-8 (IL-8), human β-defensin 2 (HβD2), NF-κB and AP-1 (Hisaw *et al.*, 2016; Nagy *et al.*, 2005, 2006; Su *et al.*, 2017). *P. acnes*-induced secretion of IL-8 and other chemotactic factors modulate neutrophil migration to the pilosebaceous unit, while HβD2 possesses Gram-negative microbicidal activity (Kim, 2005). Neutrophils attracted to lesion sites cause the follicular epithelium to rupture, which provokes inflammation (Webster *et al.*, 1980) by monocytic secretion of cytokines and chemokines. Monocyte TLRs and nucleotide-binding oligomerization domain receptors are activated by *P. acnes* PAMPs, resulting in release of tumor necrosis factor alpha (TNFα), interleukin-12 (IL-12), interleukin-1β (IL-1β) and IL-8 (Kim *et al.*, 2002; Kistowska *et al.*, 2014; Qin *et al.*, 2014; Vowels *et al.*, 1995).

In addition to its involvement during the later stages of lesion development and persistence, *P. acnes* may be a key factor in initiating comedogenesis. A distinctive comedonal feature (Ingham *et al.*, 1992), elevated levels of interleukin-1α (IL-1α) have been attributed to *P. acnes*-activated secretion of IL-1α from human keratinocytes via the TLR-2-mediated pathway (Graham *et al.*, 2004). Selway *et al.* (2013) showed that

specific PAMPs characteristic of Gram-positive bacteria, such as peptidoglycan and lipoteichoic acid, result in TLR-2-mediated IL-1α release from human keratinocytes. Interestingly, this study reported IL-1α-like mediated hypercornification of sebaceous glands, which provides evidence supporting the possible role of *P. acnes* during comedogenesis.

1.1.3.1.2 Scarring

Affecting up to 95% of acne patients (Layton *et al.*, 1994), scarring is a common result of the inflammation associated with acne vulgaris and is influenced by the severity and duration of inflammation (Bourdes *et al.*, 2015). According to a classification scheme devised by Jacob *et al*. (2001), which is based on morphological characteristics together with associated treatment options, acne scarring is divided into the following three categories: icepick, rolling and boxcar; the latter of which may be subdivided into shallow (0.1 to 0.5 mm) or deep (≥0.5 mm) scars. Each type of scarring requires a certain level of treatment, all involving varying degrees of invasiveness and monetary cost. Scar treatment modalities requiring surgical procedures such as punch excision, punch elevation, subcision and laser skin resurfacing, offer permanent results albeit an inherent level of invasiveness compared to non-surgical procedures. Although typically yielding improvements that are temporary and/or requiring multiple treatments, non- and partially-ablative procedures are less invasive as these approaches are limited to topical therapies, subcutaneous and dermal fillers, lasers that promote collagen remodeling and microscopic dermal injury via fractional resurfacing (Alam & Dover, 2006; Fife, 2016; Jacob *et al.*, 2001). Based on various metrics, such as the Dermatology Quality of Life

Index, those suffering from atrophic scarring as a result of acne report an overall reduction with regards to quality of life (Reinholz *et al.*, 2015).

1.1.3.1.3 Social, psychological and economic impacts

Acne vulgaris affects over 85% of adolescents (Balkrishnan *et al.*, 2006a), thereby rendering it one of the most common skin disorders (Johnson & Roberts, 1978; Rea *et al.*, 1976; Wolkenstein *et al.*, 2003). The effects of acne alone cause the United States to suffer a loss of productivity to the tune of 3 billion dollars per year (Bickers *et al.*, 2006). Aside from the physical disfiguration, there is also a psychosocial aspect that accompanies the presence of acne, which has been reported to have a direct effect on work and educational performance (Gokdemir *et al.*, 2011). In an era where self-worth is often dictated by aesthetics (Gordon *et al.*, 2013), individuals stricken with visible signs of acne and/or scarring are likely to suffer psychologically and exhibit aberrant behavior because of this (Chuah & Goh, 2015).

A report published by (Ritvo *et al.*, 2011) described the tendency towards a negative perception of teens with acne by adults and teenagers. Therefore, it is not surprising that low self-esteem, depression, anxiety, bullying, and other psychosocial effects including suicidal tendencies decrease the quality of life with those suffering with acne (Krowchuk, 2000; Law *et al.*, 2010; Lee *et al.*, 2006). Some metrics have even highlighted similarities of quality of life measurements between acne and those afflicted by psoriasis and debilitating conditions such as coronary heart disease, diabetes and chronic back pain (Cresce *et al.*, 2014; Klassen *et al.*, 2000).

1.1.3.2 Other notable pathologies

Deep tissue infections caused by *P. acnes* are commonly preceded by surgical procedures in the presence, or absence, of an implanted foreign material or device (Jakab *et al.*, 1997). Post-operative infections are often characterized as chronic having a delayed-onset, typically persisting due to microbial biofilms which coat the implant surface, protecting the infectious agents, such as *P. acnes,* from immune defence and antibiotic treatment (Bayston *et al.*, 2007; Coenye *et al.*, 2007; Holmberg *et al.*, 2009; Jakab *et al.*, 1997; Trampuz *et al.*, 2003; Tunney *et al.*, 1998). Examples of devices associated with *P. acnes* infection include intraocular lenses (Gopal *et al.*, 2008), breast implants (Del Pozo *et al.*, 2009; Rieger *et al.*, 2013), neurosurgical hardware (Chu *et al.*, 2001), cardiovascular devices (Das & Reynolds, 2014; Hinestrosa *et al.*, 2007; Kanjanauthai & Kanluen, 2008; Kestler *et al.*, 2017; Silva Marques *et al.*, 2012; van Valen *et al.*, 2016) and orthopedic implants (Butler-Wu *et al.*, 2011; Drago *et al.*, 2017; Figa *et al.*, 2017; Frangiamore *et al.*, 2015; Koh *et al.*, 2016; Mook *et al.*, 2015; Phadnis *et al.*, 2016; Portillo *et al.*, 2013; Rienmüller & Borens, 2016; Tunney *et al.*, 1999; Wang *et al.*, 2013; Zhang *et al.*, 2015). Although relatively less frequent, there have been several reports of *P. acnes* deep tissue biofilm formation in the absence of implants and, in many cases, without prior surgical intervention (Berjano *et al.*, 2016; Berthelot *et al.*, 2006; Capoor *et al.*, 2017; Chu *et al.*, 2001; Coscia *et al.*, 2016; Crowhurst *et al.*, 2016; Daguzé *et al.*, 2016; Haruki *et al.*, 2017; Kowalski *et al.*, 2007; Kranick *et al.*, 2009; Lavergne *et al.*, 2017; Nisbet *et al.*, 2007).

Clinical manifestations, as a result of most deep-seated *P. acnes* infection, are devastating due to the chronic nature of infection. For instance, the economic implications of

infections resulting from joint arthroplasty are immense (Sculco, 1993). According to a study conducted by Kurtz *et al.* (2012), the projected cost of infected knee and hip revisions in the year 2020 will exceed $1.62 billion in the United States.

It is thought that *P. acnes* takes a role as an infectious agent, exercising immunomodulatory behavior, that contributes to the pathogenesis of multifactorial systemic disorders involving genetic and immunological components (Chen & Moller, 2015; Rukavina, 2015). In 1978, Homma *et al.* (1978) observed elevated levels of *P. acnes* in biopsy specimens of sarcoid positive lymph nodes compared to controls. Since then, evidence of its participation in the etiology of the condition has continued to accumulate (Eishi, 2013; Hiramatsu *et al.*, 2003; Nakamura *et al.*, 2016; Negi *et al.*, 2012; Schupp *et al.*, 2015; Werner *et al.*, 2017; Zhao *et al.*, 2017). Other complex pathologies that demonstrate evidence of association with the immunostimulatory behavior of *P. acnes* are “SAPHO” syndrome (synovitis, acne, pustulosis, hyperostosis, osteitis) (Berthelot *et al.*, 2017; Colina *et al.*, 2007; Nguyen *et al.*, 2012) and prostate cancer (Bae *et al.*, 2014; Cavarretta *et al.*, 2017; Davidsson *et al.*, 2016; Fehri *et al.*, 2011; Kakegawa *et al.*, 2017; Olender *et al.*, 2016; Sayanjali *et al.*, 2016; Severi *et al.*, 2010; Shannon *et al.*, 2006b; Shinohara *et al.*, 2013; Yow *et al.*, 2017).

1.1.4 Current therapeutic approaches (acne vulgaris)

Acne vulgaris is a dynamic condition owing its development to a variety of pathophysiological mechanisms. A wide range of treatment modalities are available and application in a combinatorial manner is encouraged to expediently address the distinct variables that contribute to the disease state. However, despite evidence of successful

clinical outcomes, there is no shortage of side effects and limitations associated with the existing treatments routinely recommended for the management of acne vulgaris.

Establishing an effective therapeutic regimen is based on clinical assessment of acne severity (Thiboutot, 2000). Assessment of the proposed therapeutic approaches is accomplished in consideration of the patient's candidacy measured against the risk of contraindication pertaining to prospective treatments. Concomitant approaches incorporate a combination of topical antimicrobial agents, topical retinoids, systemic antibiotics and systemic retinoids (Gollnick *et al.*, 2003; Leyden, 2003); utilizing exclusive, complimentary mechanisms of action. Combination therapy is indicated for all levels of acne severity and early initiation of treatment is recommended (Alexis, 2008). Expert groups, such as the Global Alliance to Improve Outcomes in Acne, have published clinically relevant information with regards to the pathophysiology of acne vulgaris and comprehensive therapeutic guidelines (Gollnick *et al.*, 2003; Thiboutot *et al.*, 2009). The treatment algorithm presented by the Global Alliance to Improve Outcomes in Acne published by the Journal of the American Academy of Dermatology, is most commonly used by clinicians (Barber, 2011); therefore, details of the treatment modalities that follow are based on the recommendations published by this group, which align with those of the Academy's most recently published care guidelines (Zaenglein *et al.*, 2016).

1.1.4.1 Topical treatments

The first line of treatment for acne vulgaris is a topical retinoid with or without an antimicrobial agent. Monotherapy employing a topical retinoid product, such as

adapalene (a third generation retinoid), tazarotene (acetylated retinoid) and tretinoin (retinoic acid), is the primary course of treatment for mild, comedonal cases of acne. Recommended therapeutic regimens for the treatment of all other types and levels of severity incorporate topical retinoids in combination with topical and/or systemic antimicrobials. Topical antimicrobials include benzoyl peroxide and antibiotics; namely clindamycin and erythromycin. Aside from asserting antimicrobial action, topical antimicrobials exhibit anti-inflammatory properties. Topical retinoids act as mild anti-inflammatory agents in addition to serving as comedolytic agents (Bikowski, 2005).

A common, undesirable side effect of topical acne treatment is skin irritation. Despite its frequent use for the treatment of acne and maintenance, issues regularly arising as a result of benzoyl peroxide application are peeling, erythema and unpleasant skin sensations such as burning and itching (Bikowski, 2005; Mills *et al.*, 1986). Women of childbearing age must be cautious as topical retinoids are contraindicated for use by pregnant women due to the risk of teratogenicity (Kaplan *et al.*, 2015; Panchaud *et al.*, 2012). Emergence of resistant microorganisms is highly possible when antibiotics are employed (Cunliffe *et al.*, 2002) and decreases with the addition of complimentary treatment modalities (Alexis, 2008; Del Rosso, 2016; Dréno *et al.*, 2016a).

1.1.4.2 Systemic treatments

Antibiotics

Despite the nature of infection, complications with regard to efficacy of therapeutics arise on the account of increasing antibiotic resistances (Oprica & Nord, 2005; Simpson, 2001) often resulting in persistent chronic infections. Lipophilic antibiotics have been employed

for treatment of acne vulgaris for roughly 60 years (Del Rosso, 2016), including tetracyclines, macrolides, clindamycin, trimethoprim/sulfamethoxazole and levofloxacin (Ochsendorf, 2006; Ross *et al.*, 2003; Strauss *et al.*, 2007; Zaenglein *et al.*, 2016). Poor clinical response to antibiotic therapies and the prolonged nature of treatment is correlated with a rise in antibiotic resistance due to selective pressure against species susceptible to antibiotics, thereby selecting for resistant strains (Del Rosso & Zeichner, 2016). The Scientific Panel of Antibiotic Usage in Dermatology (SPAUD) estimated nine million oral prescriptions are given per year to treat infectious skin disorders in the United States (1999–2003), predominately for the treatment of acne vulgaris and rosacea (Del Rosso & Kim, 2009; James Q. Del Rosso, 2006). This figure is troubling as resistant *P. acnes* strains seem to be easily acquired through previous antibiotic treatment in addition to contact with persons carrying resistant strains (Ochsendorf, 2006). A point mutation within the nucleotide region encoding 16S ribosomal RNA (rRNA) is responsible for acquired resistance to tetracyclines (Ross *et al.*, 2001). Dictated by sub-species phenotype, point mutations in the peptidyl transferase region of 23S rRNA is reported to yield varying levels of single and cross-resistance to erythromycin and clindamycin; both of which are ineffective against strains harboring erythromycin ribosome methylase resistance gene, *erm*(X), a result of transposon-mediated resistance (Ross *et al.*, 1997, 2002). The rates of resistance varies between geographical regions as treatment regimens differ, however, in general, the abovementioned mutations are widespread with few mutations remaining unelucidated and limited to specific geographical regions (Schafer *et al.*, 2013). *P. acnes* remains most sensitive to tetracyclines with higher levels of resistance against erythromycin and clindamycin

(Ochsendorf, 2006). Second generation tetracyclines, doxycycline and minocycline, are prominent treatment options with preference given to enteric-coated doxycycline to minimize the severity of adverse gastro-intestinal side effects (Kircik, 2010; Zaenglein, 2015). For instance, European surveillance studies report that Finland has the highest outpatient use of tetracycline, which correlates with the high tetracycline resistance at 11.8% (Schafer *et al.*, 2013). Macrolides are most frequently used in Italy where resistance to erythromycin (42%) and clindamycin (21%) are very high (Oprica & Nord, 2005). Recent studies from Europe, Mexico and Chile suggest resistance to trimethoprim/sulfamethoxazole is most common, with a highest reported rate of 68% (González *et al.*, 2010; Oprica *et al.*, 2004; Ross *et al.*, 2001; Schafer *et al.*, 2013).

There are a vast array of detrimental side effects reported with prolonged antibiotic administration required for the treatment of acne such as gastrointestinal complications, photosensitivity, candidiasis, dizziness and lightheadedness, among others (Garner *et al.*, 2012; Kircik, 2010; Park & Skopit, 2016; Smith & Leyden, 2005). Multiply-resistant strains are also on the rise due to combinatorial therapies of systemic antibiotics and retinoids with topical microbicides (Ross *et al.*, 2003).

Oral retinoid

Isotretinoin (Accutane), the only available orally-administered retinoid therapy, is regarded as the most effective treatment for acne vulgaris. It acts to decrease sebum levels by approximately 90%, thereby reducing *P. acnes* load and inflammation as a secondary effect (King *et al.*, 1982; Leyden *et al.*, 1986). Isotretinoin is reserved for the treatment of severe acne and/or for patients that are at risk for scarring; regardless of the

severity of their condition (Layton *et al.*, 1997). Patients experiencing psychosocial impairment as a result of their condition may also be considered for oral retinoid therapy (Kellett & Gawkrodger, 1999).

Despite its efficacy, contraindications of isotretinoin pose limitations to the range of patients eligible for treatment. Teratogenicity is the most severe and well-documented side effect of retinoid therapy (Dai *et al.*, 1992). Despite efforts to reduce the incidence of pregnancy through extensive patient counselling and contraceptives, fetal exposure to isotretinoin remains a reality due to non-compliance (Collins *et al.*, 2014; Shin *et al.*, 2011; Tan *et al.*, 2016). Most patients experience skin dryness and cheilitis. Other side effects include conjunctivitis, hair loss, arthralgia and myalgia (Brito *et al.*, 2010; Kellett & Gawkrodger, 1999). Minor infections by *Staphylococcus aureus* are a result of alterations of skin flora composition following retinoid therapy (Başak *et al.*, 2013; Williams *et al.*, 1992). Published reports regarding other adverse effects; including depression and inflammatory bowel disease, contain conflicting evidence (Zaenglein *et al.*, 2016). However, physicians are advised to remain mindful of the guidelines for evidence-based monitoring.

Hormone therapy

Hormone therapy targets androgen levels, which play a crucial role in the onset of acne vulgaris. Androgen-induced seborrheic hyperplasia can be reduced by introducing treatment with a combined oral contraceptive (COC), antiandrogen (AA), low-dose glucocorticoid (LDG) or gonadotropin-releasing hormone agonist (GRHA) (Bettoli *et al.*, 2015). Treatment modalities act via one or more of the following mechanisms: androgen

receptor blockage (COC and AA); 5-alpha-reductase inhibition (COC and AA); down-regulation of adrenal androgen production (COC, AA and LDG); reduced production of ovarian androgens (COC, AA and GRHA); decreased levels of free testosterone in blood by upregulating sex hormone binding protein production (COC and AA); and suppression of ovulation-induced androgen production (COC) (Bettoli *et al.*, 2015).

Hormone therapies are recommended as an alternative to oral isotretinoin for the treatment of acne where scarring has occurred or there is a potential for scarring. It is also indicated as an alternative approach for the treatment of moderate to severe acne. Like other treatment methods, hormonal therapy is suggested in conjunction with a topical antimicrobial or oral antibiotic and/or topical retinoid. Hormone therapy is contraindicated for pregnant females or females wishing to become pregnant and is not a viable option for acne therapy in males (Sawaya & Hordinsky, 1993). In addition to several side effects, there is a risk of major adverse events while undergoing hormone therapy that must be considered when determining the suitability of the treatment for the individual (Bettoli *et al.*, 2015; Gollnick *et al.*, 2003). Possible serious side effects of hormone therapy include thromboembolism, hepatotoxicity, cardiovascular disease, cervical and breast cancer; more common effects include breast tenderness, headache, nausea, and irregular menstrual cycle (Bettoli *et al.*, 2015; ESHRE Capri Workshop Group, 2013; Harper, 2016; Hughes & Cunliffe, 1988; Krunic *et al.*, 2008; Miquel *et al.*, 2007; Park & Skopit, 2016; Plu-Bureau *et al.*, 2013; Savidou *et al.*, 2006; Shaw, 2000; Shaw & White, 2002; Zaenglein *et al.*, 2016). Additional criteria, in relation to patient eligibility, extends the limitation of hormone therapy further; excluding patients with a history of and/or active blood clot disorders, diabetes, hypertension, cerebrovascular

disorders, cardiac disease, liver disease and breast, endometrial or liver cancer, amongst others (Barber, 2011; Bettoli *et al.*, 2015; Harper, 2016).

1.1.4.3 Alternative treatment: light therapies

Light-based therapies have been under investigation as a fairly recent alternative option for acne treatment. The safety and efficacy of such methods are not well-known as off-label use is detrimental to the initiation of clinical efficacy trials. Another impediment to supporting the validity of light therapies is that devices are not as stringently assessed in comparison to the evaluative protocols for regulatory clearance that pharmaceuticals are subject to (Thiboutot *et al.*, 2009). Light-based therapy targets *P. acnes* and/or acts to disrupt sebaceous gland function via photochemical and/or photothermal effects, respectively (Momen & Al-Niaimi, 2015). Aside from persistent relapse, side effects that may deter patients from undergoing light therapy include discomfort, erythema, edema, pustular eruption, superinfection, blistering, crusting and peeling (Babilas *et al.*, 2010; Jih *et al.*, 2006; Momen & Al-Niaimi, 2015; Nestor *et al.*, 2016; Taub, 2007; Wiegell & Wulf, 2006).

1.1.4.4 Summary

Motley & Finlay (1989) demonstrated that “willingness-to-pay” values for a cure by ≥62% patients with acne, ranged from £100–£5000 (approx. $240–$17400 current US dollars, respectively). Monthly willingness-to-pay values of acne sufferers are reported to be higher than for individuals suffering from high cholesterol, hypertension, angina, atopic eczema and psoriasis (Parks *et al.*, 2003). Therefore, it is imperative that therapeutics aimed at resolving acne be made available.

All of the abovementioned therapeutic approaches entail a certain level of patient adherence to obtain desirable results. Elevated incidence of treatment failure may be credited to a lack of patient adherence; often attributed to the daily demand of therapeutic applications, development of undesirable side effects or persistence of the condition (Lott *et al.*, 2010; de Lucas *et al.*, 2015). Conventional treatment modalities are associated with numerous contraindications, accompanied by a risk of mild to severe adverse effects, and typically yield results after a minimum of two months. In recent years, there has been an abundance of evidence promoting the importance of maintaining a healthy, human microbiome and its role in disease prevention (Muszer *et al.*, 2015). Therapy-related consequences that impact the delicately-balanced composition of commensal flora have substantial implications (Başak *et al.*, 2013).

Therapeutic objectives sought in the treatment of acne are to eliminate lesions and to prevent relapse while taking all measures to avoid scarring (Thiboutot *et al.*, 2009). Pathogenic factors must be addressed in such a way as to minimize side effects (Alexis, 2008). Current approaches in acne therapy present numerous challenges that justify the pursuit of a viable therapeutic alternative; free of adverse effects, contraindications, potential for relapse and minimal necessity for patient adherence.

1.2 Bacteriophage therapy: a viable alternative

1.2.1 Historical background

The first-ever report of bacteriophages published in a major journal was by Fredrick Twort (Twort, 1915). In this report published by *The Lancet*, Twort had not been able to describe the nature by which the unknown entity he observed killed bacterial cultures,

however, he considered the existence of an “ultramicroscopic virus” (Twort, 1915). Prior to this, similar findings had been reported by scientists in other regions (Gamaleya, 1898; Hankin, 1896). Twort’s suspicions regarding the viral nature of his unidentified substance was supported by observations presented by Felix d’Herelle during the meeting of the Academy of Sciences in 1917 (d’Herelle, 1917). D’Herelle described zones of clearance formed on bacterial lawns by bacteria-free filtrate of the stool of dysentery patients and coined the term “bacteriophage” to describe the agents of bacterial lysis (Duckworth, 1976; d’Herelle, 1917). Just a short time after, phage therapy became globally implemented for the treatment of various life-threatening illnesses such as dysentery, cholera and bubonic plague, amongst others (d’Herelle, 1926). Beginning in the early 1920’s, large-scale commercial production of phage preparations was underway in France, India, Brazil and the United States. In the late 1930’s, the American Medical Association set out to evaluate the value and safety of bacteriophage therapy. The lack of standardization of phage formulations with respect to aspects relating to safety and efficacy, coupled with a shortage of knowledge regarding the biological mechanisms of phage efficacy, raised concerns in the Western World (Summers, 2001).

Leading up to the discovery of antibiotics, bacteriophages dominated the field of infectious disease treatment, however, just fifteen years following the discovery and initial applications of phage, antibiotics emerged and rapidly became the focus of attention for antimicrobial development. Phage therapy was so widely accepted at the time that the discovery of the new non-phage antimicrobials, e.g. penicillin, was dismissed by the Chairman of the Sir William Dunn School of Pathology of Oxford University and the project had remained dormant for several years prior to its

reinstatement (Friedman & Friedland, 1998). Nonetheless, concerns associated with phage therapy, newfound availability of broad-spectrum antibiotics and the necessity for such antimicrobials during World War II, initiated a massive push towards the development of antibiotics, resulting in near-abandonment of phage research in the Western World. Phage research and application persisted in the Soviet Union and Poland by virtue of economic and political value (Kutter *et al.*, 2010). Return of phage research to Western countries is believed to have been hindered by a reluctance to share common practices with the Soviet Union (Summers, 2001).

Since the late 1930's, phage research remained overshadowed by antibiotics in Western countries, however, the emergence of antibiotic resistance prompted a revitalized interest in the field of phage therapy. Recent attention to the importance of a balanced, healthy microbiome, coupled with escalating rates of antibiotic resistance, have presented a growing global challenge in the treatment of infectious diseases. Development of novel, highly selective and easily produced antimicrobial products is crucial to initiating a paradigm shift towards adopting safer, more effective treatment strategies without the shortcomings and detrimental effects of conventional antibiotics.

1.2.2 Important considerations and current state

Bacteriophage-based antimicrobial therapeutic strategies offer a powerful alternative to conventional antibiotics. Bacteriophage preparations, often produced as "phage cocktails", are comprised of multiple types of whole phage particles formulated to increase the likelihood of overcoming any naturally-occuring or evolved resistance among bacterial targets (Doss *et al.*, 2017; Gill & Hyman, 2010). Phage products, such as

lytic enzymes, are also of interest by virtue of their relatively negligible toxicity and targeted host specificity (Trudil, 2015).

Phage life cycles vary between lytic and temperate, the former is preferred for whole phage applications as the completion of the phage life cycle results in bacterial death, whereas the latter will result in persistence of both the host cell and the phage. The general sequence of events concerning the life cycle of a lytic phage begins with its attachment to the surface of its host. Prior to attachment, the interaction at the phage-host interface is at random, therefore selective attachment only occurs when components of the phage that confer specificity (most often the tail fibers) come into contact with a matching receptor on the surface of the host bacterium. Upon attachment, the phage inserts its genetic material into the host cytoplasm, initiating a cascade of phage-modulated events. Redirection of host replicative and metabolic machinery favors exponential propagation of new phage particles, followed by subsequent lysis of the host and release of progeny phage.

By virtue of its high degree of specificity, no threat to the delicate balance of the commensal microflora is imposed by treatment with defined phage formulations. The risk of human toxicity by phage is mitigated by the absence of tropism for eukaryotes combined with lacking the capacity to execute an infectious life cycle within mammalian cells (Mount *et al.*, 2004; Parasion *et al.*, 2014). Therefore, administration of phage may be given in higher doses than chemical antibiotics. However, high doses are not necessary as phages replicate exponentially. Therefore, unlike antibiotics, which experience exponential decay in the body, a single dose administration of phage would

suffice to rapidly eliminate the pathogen target (Doss *et al.*, 2017). Moreover, resistance to phage is rare as spontaneous mutation in the phage during exponential replication confers dynamic control over any emerging resistant populations (Parasion *et al.*, 2014). Therefore, phage therapy boasts a highly specific, natural, cost-effective approach to indiscriminately eliminating both antibiotic susceptible and resistant pathogens via mechanisms that can be either strain- or species-specific (Parasion *et al.*, 2014).

In the advent of rising concerns associated with chemical applications used for biocontrol of bacteria, there is a renewed interest in bacteriophages in the West; stimulating a revitalization of phage research and the development and implementation of commercial applications within agricultural, aquaculture and industrial sectors. Commercial applications currently in use include “Listex P100” and “ListShield”, “EcoShield” and “Salmofresh” phage preparations that are used to control foodborne human pathogens, such as *Listeria monocytogenes*, *Escherchia coli* O157:H7 and pathogenic *Salmonella* serotypes, respectively (Żaczek *et al.*, 2015). To reduce loss of agriculutural crop yields, commercial preparations that target phytobacteria, such as “AgriPhage”, provide protection against bacteria that parasitize plant hosts (Żaczek *et al.*, 2015). Making it possible to apply phage to food for human consumption, these phage preparations have been designated as “GRAS” (generally recognized as safe) by the American Food and Drug Administration (FDA). Nevertheless, certain stipulations must be adhered to; those of which relate to the nature of the phage state that the phage be lytic and must not possess any toxin or antibiotic resistance genes thus ensuring that horizontal virulent or resistance gene transfer will not occur between the phage and its bacterial hosts (Gill & Hyman, 2010; Nobrega *et al.*, 2015).

Phage therapy in humans has persevered in regions of the former Soviet Union, however, its application has been limited to compassionate use provisions in Western countries (Kutter *et al.*, 2010). Previous attempts were made to initiate clinical trials with phage in the past, however, lack of funding made it difficult to do so (Kutter *et al.*, 2010). Recently, the first industry-standard clinical trials for bacteriophage therapy have begun and are currently underway in Europe and the United States (Kingwell, 2015). In Belgium, France and Switzerland, a project sponsored by the European Union called "Phagoburn" has initiated phase I/II clinical trials of two anti-infection therapies for burn victims against *Escherichia coli* and *Pseudomonas aeruginosa* (Kingwell, 2015; Pherecydes Pharma, 2016; Servick, 2016). Furthermore, an American company—"AmpliPhi Biosciences"—has recently initiated clinical trials of a phage preparation for the treatment of chronic rhinosinusitis associated with infection by *S. aureus* (AmpliPhi Biosciences, 2016; Kingwell, 2015). Other studies have evaluated the safety of various phage preparations. Reports from Switzerland and Bangladesh have demonstrated the safety of oral *E. coli* phage preparations in healthy adults (Bruttin & Brüssow, 2005) and children hospitalized with acute bacterial diarrhea (Sarker *et al.*, 2016), respectively. Another study reported the safety of phage application in patients with chronic venous leg ulcers, which targetted *E. coli*, *S. aureus* and *P. aeruginosa* (Rhoads *et al.*, 2009). Supporting both the safety and efficacy of a phage preparation for the treatment of patients suffering from *P. aeruginosa*-associated chronic otitis, a report published in the United Kingdom by Wright *et al.* (2009) describes a significant decline in bacterial load, relief of symptoms and improved clinical presentation after just a single dose of the

phage preparation. Taken together, findings from these studies and others represent a positive direction and a promising future for antibacterial phage therapy.

1.3 Phage therapy and acne vulgaris

1.3.1 Current literature

The first phage isolation against "*C. acnes*" was reported by Brzin in 1964. Subsequent reports of *P. acnes* phage isolations offered more detailed characterization in terms of host range, physical morphology, and genome sequencing (Brown *et al.*, 2016; Brown *et al.*, 2017; Farrar *et al.*, 2007; Jong *et al.*, 1975; Liu *et al.*, 2015a; Lood *et al.*, 2008; Lood & Collin, 2011; Marinelli *et al.*, 2012; Webster & Cummins, 1978; Zierdt *et al.*, 1968). In earlier reports, host ranges of phage isolates were determined and those with unique host ranges were used to serotype *P. acnes* isolates by exploiting the association between *P. acnes* serotypes and susceptibility to phage collections (Jong *et al.*, 1975; Webster & Cummins, 1978). Later, morphological characteristics of *P. acnes* phage particles were characterized using transmission electron microscopy (TEM). Electron microscopy of *P. acnes* phages reveals only siphovirus morphology, with icosahedral heads of approximately 50 nm and a flexible, non-contractile tail approximately 150 nm in length (Ackermann, 2011; Brown *et al.*, 2017; Farrar *et al.*, 2007; Lood *et al.*, 2008; Lood & Collin, 2011; Marinelli *et al.*, 2012; Webster & Cummins, 1978).

To date, seventy-three *P. acnes* phage genomes have been sequenced; none have been isolated from environmental sources (Brown *et al.*, 2016; Brown *et al.*, 2017; Farrar *et al.*, 2007; Liu *et al.*, 2015a; Lood & Collin, 2011; Marinelli *et al.*, 2012). In 2007, Farrar *et al.* reported the first-ever *P. acnes* bacteriophage DNA sequence, phage PA6, which

was isolated from the skin of a patient in the United Kingdom. Four years later, two phages were induced from Swedish *P. acnes* isolates originating from deep tissue infection (PAD20) and skin surface (PAS50) for genome sequencing by Lood and Collin (2011). Eleven phage genomes sequenced by Marinelli *et al.* (2012) consisted of nine nasal skin isolates (Los Angeles, US) and two phages from the American Type Culture Collection (ATCC) 29399B phage stock obtained 30 years prior (Philadelphia, US). Liu *et al.* (2015a) sequenced forty-eight *P. acnes* phages collected from the retroauricular creases of acne patients and healthy individuals. More recently, a report published by Brown *et al.* (2016) presents the genome sequences of ten phages obtained from human facial skin swabbing. From these reports, we have learned that *P. acnes* phages are very similar in terms of their genome structure and organization. Phage DNA sequencing revealed genome lengths ranging between 29,017 to 29,806 base pair (bp) with guanine-cytosine content (GC-content) of 53.70% to 54.73%—slightly lower than that of their *P. acnes* hosts (approximately 60%) (Brown *et al.*, 2016; Farrar *et al.*, 2007; Liu *et al.*, 2015a; Lood & Collin, 2011; Marinelli *et al.*, 2012). Having a nucleotide identity greater than 85%, minimal genetic diversity exists at the nucleotide level across genome sequences (Brown *et al.*, 2016; Liu *et al.*, 2015a; Lood & Collin, 2011; Marinelli *et al.*, 2012). The lack of diversity is striking considering the phage collections vary significantly with respect to geographic location and temporal period of which they were collected (Brüggemann & Lood, 2013).

Specific mechanisms that phages use to interact with *P. acnes* host cells during adsorption and initiation of the infective life cycle is very limited, despite the relative abundance of *P. acnes* bacteria and their phages. Approximately 50% of phage genomes

encode putative proteins homologous to those of other *P. acnes* phages (Marinelli *et al.*, 2012). The majority of remaining gene products have up to 50% amino acid identity to proteins expressed by phages of other *Actinomycetales* species; to which no functions are assigned (Lood & Collin, 2011; Marinelli *et al.*, 2012). The genome organization and predicted products are similar to many mycobacteriophages that also exhibit siphoviral morphology (Lood & Collin, 2011; Marinelli *et al.*, 2012). Further investigation based on phage DNA sequences and corresponding phage products in relation to host protein networks will help to solve the mechanisms exploited by phage during infection.

Based on published sequences, about half of the genome (approximately 15 kbp) is comprised of structural genes and genes involved in phage packaging, located within an operon on the left side of the genome (genes 1 to 19), transcribed from left to right. The majority of genetic variation is found amongst the viral DNA replication genes located on the right side of the genomes that undergo leftward transcription using the complementary strand. The far right side of the genomes harbor up to three genes, in addition to a large, variable, non-coding region of greater than 1kbp in length, possibly containing the origin of replication. Aside from within the far-right region, there is little non-coding DNA and there are no genes encoding tRNA. Additionally, a 13bp single-stranded extension on both ends of the PA6 genome (Farrar *et al.*, 2007) and PAS50/PAD20 genomes (Lood & Collin, 2011) have been reported. However, data presented by other groups suggest an 11bp extension on both ends of the phage genomes they reported (Brown *et al.*, 2016; Liu *et al.*, 2015a; Lood & Collin, 2011; Marinelli *et al.*, 2012).

Genes 1 to 19 encoding putative structural proteins are all highly conserved at the nucleotide level, with the exception of putative minor tail protein encoded by ORF19. It appears to be highly variable in the 3' region of the gene, with a corresponding variability in the C-terminal domain of the protein product, suggesting involvement in host specificity. Due to its proximity to the genes encoding tail proteins, it may encode a component of the tail structure and is predicted to play a role in attachment to *P. acnes* surface adhesins due to its homology to collagen chain precursors (Farrar *et al.*, 2007).

Another genomic region that has been suggested for its involvement with phage entry is ORF16 encoding gene product (gp) 16, a protein having a slight homology to protease enzymes known to bind nonpolar C termini (Farrar *et al.*, 2007). Data suggests gp16 may be a minor structural protein (Marinelli *et al.*, 2012) and due to its location, Farrar *et al.* (2007) suggested the possibility of its role in host entry via degradation of cell wall peptide linkages, if it is indeed a constituent of the tail fibers. Located close to the tail protein encoding region, gp17, encodes a protein with unknown function. However, its H-type lectin domain may be capable of associating with carbohydrates suggesting a role in host receptor binding (Lood & Collin, 2011). Following this first part of the genome is the lysis cassette: genes encoding the protein products required for the release of progeny viruses from the host cell; including holin and endolysin, for cell membrane rupture and peptidoglycan degradation of the cell wall (Liu *et al.*, 2015a; Lood & Collin, 2011; Marinelli *et al.*, 2012).

With the exception of *P. acnes* phylotype III, all other *P. acnes* phylotypes have been represented among those isolated from acne lesions, the majority of which are classified

as type IA (Fitz-Gibbon *et al.*, 2013). Therefore, *P. acnes* phages with a wide species-specific host range are optimal for therapeutic phage preparations. Additionally, application of phages having broad host ranges will minimize the chance of survival of less sensitive *P. acnes* isolates. Majority of *P. acnes* phages observed to date, have been reported to exhibit a broad host range at the strain-level, thereby insinuating a low frequency of resistance to phage (Jong *et al.*, 1975; Liu *et al.*, 2015a; Marinelli *et al.*, 2012; Webster & Cummins, 1978; Zierdt *et al.*, 1968). To date, sequenced genomes of bacteriophages isolated against *P. acnes* do not encode any protein products associated with a lysogenic life cycle (Marinelli *et al.*, 2012) or any genes known to confer virulence to their bacterial hosts (Brüggemann & Lood, 2013).

1.4 Scope of this study

Reports of *Propionibacterium acnes*-specific bacteriophages, to date, provide evidence of their biological properties that are desirable for therapeutic applications. We hypothesize that phages and the antibacterial products they produce, are viable therapeutic alternatives for future acne treatment. To demonstrate proof of concept, we aim to acquire and test *P. acnes*-specific phages for the purpose of formulating minimal phage cocktails that have high levels of antibacterial activity against a wide range of clinically-relevant *P. acnes* isolates.

To address our aim, the first objective of this project is to establish a collection of geographically diverse *P. acnes* clinical isolates from a variety of superficial and deep-seated specimens, and further characterize them on the basis of their genetic properties and antimicrobial susceptibilities. The second objective is to establish a library of *P.*

acnes-specific bacteriophages, characterize them for their biological activities against the collections of clinical *P. acnes* isolates to determine their host ranges. The final objective of this project is to formulate candidate phage cocktails using phages that exhibit a broad, complementary variety of host range activities and to assess the biological properties of candidate phages through genome sequencing and deduced proteomics.

2 Materials and Methods

2.1 Materials

2.1.1 Bacterial strains and clinical isolates

Standard control strains of *P. acnes*, ATCC 6919 and ATCC 29399 (Table C.1), were included in all experiments. *Propionibacterium avidum* ATCC 25577 and *Propionibacterium granulosum* ATCC 25564 were used as negative internal controls for phage host range analysis, molecular identification and phylotyping of clinical isolates. *E. coli* K-12 MG1655 and *Streptococcus pyogenes* ATCC 12204 were applied as positive and negative catalase controls, respectively. *Bacillus subtilis* ATCC 23857, *Clostridium difficile* ATCC 9689, *E. coli* K-12 MG1655, *S. aureus* ATCC 29923, *Salmonella typhimurium* TA1535 and *S. pyogenes* ATCC 12204 were used as negative external controls in phage host range analysis. Antibiotic susceptibility testing required quality control (QC) validation by evaluating minimal inhibitory concentration (MIC) values of standard QC strains, *S. aureus* ATCC 29213, *Enterococcus faecalis* ATCC 29212 and *Streptococcus pneumoniae* ATCC 49619, against published values.

Clinical *P. acnes* isolates from patients across Canada associated with various systemic or deep tissue infections were obtained from the National Microbiology Laboratory (NML) in Winnipeg (Table C.1). Forty-five *P. acnes* isolates from skin surfaces of healthy patients (AS) and deep tissue infections (AD) were received and cultured from the collection of Dr. Anna Holmberg (Department of Clinical Sciences of Lund University, Sweden) (Table C.1). Clinical samples of swabbed skin surfaces and acne

lesion extracts were obtained from 91 patients of Dr. Lyne Giroux (Sudbury Skin Clinique, Canada) and 45 patients of Dr. Sharyn Laughlin (Laserderm, Ottawa, Canada) using M40 Transystem Amies Agar Gel swabs (Copan Diagnostics, Murrieta, USA). Bacterial stocks were maintained in 10% glycerol at -80 ºC for long-term storage, and working agar plates were used for daily culturing and short-term storage at 4 ºC.

2.1.2 Culture media, supplements, antibiotics, reagents, enzymes and kits

Columbia (CB) broth and Brain-heart infusion (BHI) broth dehydrated nutrient media and agar were purchased from Quelab (Montreal, Canada). CB and BHI were used for routine culturing of bacteria and solid CB/BHI media containing 1.6% bacteriological agar were used for colony isolation and short-term maintenance of cultures. CB/BHI media containing 0.7% bacteriological agar was used as top agar in plaque assay or for experiments requiring agar overlay. Refer to Appendix A for formulations and preparations.

Antibiotic susceptibility was determined by Epsilometer test (Etest) purchased from bioMérieux (St. Laurent, Canada). The Etest panel consisted of the following antibiotics: azithromycin (AZ) AZ 256, benzylpenicillin (PGL) VB/PGL 32 (commonly referred to as Penicillin G), ceftriaxone (TXL) VB/TXL 32, clindamycin (CM) CM 256, daptomycin (DPC) DPC 256, doxycycline (DC) DC 256, erythromycin (EM) EM 256, levofloxacin (LE) LE 32, linezolid (LZ) LZ 256, minocycline (MC) MC 256, rifampicin (RI) RI 32, tetracycline (TC) TC 256, trimethoprim/sulfamethoxazole (TS) 1/19 TS 32 and vancomycin (VA) VA 256.

Brucella broth from BD Biosciences (Sparks, USA) and Mueller-Hinton (MH) broth from Oxoid (Basingstoke, UK), were used in antibiotic susceptibility testing. Nutrient media supplements required for all antimicrobial susceptibility testing included hemin (H9030) and vitamin K_1, both of which were purchased from Sigma-Aldrich (Saint Louis, USA). To evaluate susceptibility to DPC, supplementation with calcium chloride (BioShop, Burlington, Canada) was necessary. Refer to Appendix A for formulations and preparations. Hydrogen peroxide (30%) was used in catalase test, pronase (Boehringer Mannheim GmbH, Germany) and Ribonuclease (RNase) A/T1 (2 mg/mL RNase A and 5000 U/mL RNase T1) (Thermo Scientific) were used for protein digestion and RNA degradation in genomic DNA (gDNA) isolation, respectively. Polyethylene glycol (PEG) 8000 was used to precipitate and concentrate the phage particles (Bioshop Canada). A 25:24:1 (v/v) mixture of phenol, chloroform and isoamyl alcohol (PCI) was used for phage DNA extraction (Appendix B.3). Restriction enzymes *BamHI* and *HindIII* were purchased from New England Biolabs (NEB; Ipswich, USA); *Taq* DNA polymerase (*Taq* Pol) (50 U/µl), 10 mM deoxyribonucleotide triphosphates (dNTPs), polymerase chain reaction (PCR) buffer without Mg^{+2} (10X) and 50 mM $MgCl_2$ were purchased from Invitrogen (Carlsbad, USA). NEBNext Fast DNA Fragmentation & Library Preparation set for Ion Torrent (NEB), Agencourt AMPure XP Beads (Beckman Coulter Inc., Danvers, USA) and Ion Express Barcode Adaptors 17–32 Kit (Life Technologies) were used for preparations of phage DNA libraries for genome sequencing. The library quality was assessed with the Qubit 2.0 Fluorometer using the Qubit double-stranded DNA (dsDNA) High Sensitivity (HS) Assay Kit (Life Technologies). Ion 316 Chip v2 and the Ion PGM Sequencing 200 Kit v2 (Life Technologies, Carlsbad, USA) were used for

sequencing phage genomes using the Ion Torrent Personal Genome Machine (Ion PGM) platform. Agarose gels (0.7%–2%) prepared in 1X tris-acetate-ethylenediaminetetraacetic acid (TAE) running buffer, 6X DNA loading dye, GeneRuler High Range (HR) DNA Ladder (Thermo Scientific) and/or 1 Kb Plus (1 KbP) DNA Ladder (Invitrogen) were used in DNA gel electrophoresis and the gels were stained in ethidium bromide (EtBr) (0.5 μg/mL) before imaging (Appendix B.6).

2.1.3 PCR primers

P. acnes gDNA-specific oligonucleotide primers were synthesized by Sigma-Aldrich (Oakville, Canada) and used for PCR amplification for identifying and phylotyping bacterial isolates (Table 2.2.1).

2.1.4 Equipment and other tools

Nunc OmniTrays (Thermo Scientific, Rochester, USA) and sterile 96-pin, 12 mm polypropylene replicators (Scinomix, Earth City, USA) were used for phage host range analysis in high throughput infection assay.

Anaerobic incubation was carried out in the 855-AC Controlled Atmosphere Chamber (Plas Labs, Lansing, USA). Standard microaerobic incubation of bacterial cultures (85% N_2, 10% CO_2, 5% O_2) was made possible using the Invivo2 500 Hypoxia Workstation (Baker Ruskinn, Sanford, USA). Candle jars were occasionally used with atmospheric concentration of CO_2 adjusted to 5% (Oxoid, Basingstoke, UK). Bacterial morphology was assessed using the Axio Scope.A1 (Carl Zeiss Microscopy, Thornwood, USA). Bacterial cultures with volumes more than 2 ml were precipitated by centrifugation performed in the Beckman Coulter Allegra X-12 Benchtop Centrifuge fitted with the

SX4750A rotor (Palo Alto, USA). Centrifugation of liquid volumes ≤ 2 mL were performed using the Benchtop Sorvall Legend Micro 21R Centrifuge with the standard 24-Place 1.5/2.0 mL Rotor (Thermo Scientific, Germany). PEG-precipitated phage particles were centrifuged using the Avanti J-E High-Performance Centrifuge fitted with the JA-25.50 Fixed-Angle Rotor (Beckman Coulter, Palo Alto, USA). Gel visualization and digital image acquisition were carried out using FluorChem FC3 imaging system with AlphaView Software. Concentration and purity of DNA was estimated by reading the absorbance values at 260 nm and 280 nm using a NanoDrop 2000c UV-Vis spectrophotometer (Thermo Scientific, Wilmington, USA) against double-distilled water (ddH_2O) as a blank. The PTC-100 Programmable Thermal Controller (MJ Research Inc, Watertown, USA) was used to perform PCR.

2.2 Methods

2.2.1 Culture conditions and cryopreservation of standard strains and clinical isolates

All standard bacterial strains and clinical isolates were cultured at 37 °C. *Propionibacteria* and *C. difficile* were incubated anaerobically in the 855-AC Controlled Atmosphere Chamber. Culturing *S. pneumoniae* required the use of Oxoid jars with 5% CO_2 atmospheric adjustment. All other bacterial strains were grown under aerobic conditions.

Columbia broth medium was used for recovery and maintenance of all standard bacterial strains and clinical isolates, with the exception of *S. pyogenes and S. pneumonia* grown in BHI medium.

Glycerol stocks of all standard bacterial strains and clinical isolates were prepared for long-term storage at -80 °C. Colony-purified bacteria were grown in 5 mL broth media under appropriate growing conditions for 3 to 5 days. Cultures were concentrated by centrifugation at 3250 x g for 20 min using the Allegra X-12 Benchtop Centrifuge. Bacterial pellets were resuspended in 500 µL CB broth and mixed with 500 µL 20% sterile glycerolto attain a final glycerol concentration of 10%. One millilitre concentrated glycerol stock was deposited into two 2 mL cryovials and stored at -80 °C.

2.2.2 Isolation of *P. acnes* clinical isolates from Sudbury and Ottawa

A combined total of 91 (Sudbury) and 45 (Ottawa) new and long-term acne patients served as sampling sources for *P. acnes* isolation. Patients were recruited to the study by informed consent following the Canadian Research Ethics Guidelines and approved by the Research Ethics Board of Health Sciences North (Sudbury, ON). Skin surface samples, denoted by SS (Sudbury Surface) and OS (Ottawa Surface), were collected by swabbing the skin surface. Samples of lesion exudate, denoted by SD (Sudbury Deep) and OD (Ottawa Deep), were collected by sampling the material from the extracts of acne lesions following sterilization around the site of infection with 70% ethanol or isopropyl alcohol. M40 Transystem Amies Agar Gel swabs were used for sample collection and transportation to the research lab.

Samples were streaked for bacterial colony isolation onto CB agar plates and incubated at standard growing conditions for 15 days. One isolated colony of each colony morphology type was selected for further examination under oil immersion at 1000x using the Axio Scope.A1. Bacterial isolates exhibiting coryneform or pleomorphic rod morphology were

considered for further testing. Catalase testing was performed by transferring a loopful of the candidate colonies onto a microscope slide to which a drop of 30% hydrogen peroxide was added. *S. pyogenes* ATCC 12204 and *E. coli* K-12 MG1655 were used as negative and positive controls, respectively. Colonies were considered catalase positive by observation of gas production upon contact with hydrogen peroxide. All *P. acnes* candidates testing positive for catalase production and exhibiting the prescribed morphology were sub-cultured for colony purification via selection of a single colony and streaking onto CB agar plates followed by incubation under anaerobic conditions. Each isolated colony was sub-cultured a total of three times to eliminate contamination and propagate pure cultures. Following the final purification step, a single isolated colony was split and transferred to two separate tubes, both containing 5 mL CB broth and incubated under standard growing conditions. Both cultures were centrifuged using the Allegra X-12 Benchtop Centrifuge at 3250 x g for 15 min. The bacterial pellet from one tube was used to prepare long-term glycerol stock (see Section 2.2.1). The supernatant from the second tube was discarded and the bacterial pellet was washed once with 1 mL sterile ddH_2O followed by centrifugation at 17000 x g for 5 minutes at 4 °C using the Benchtop Sorvall Legend Micro 21R Centrifuge. Pellets were stored at -80 °C prior to genome isolation.

2.2.3 Genomic DNA extraction from presumptive *P. acnes* isolates

Bacterial pellets prepared in Section 2.2.2 (stored at -80 °C) were thawed and 240 μL lysis cocktail containing 208 μL cell lysis buffer (CLB) (25 mM Tris-HCl pH 8.0, 2.5 mM EDTA pH 8.0 and 1% Triton X-100), 6 μL 20 μg/μL pronase, 24 μL 10% SDS and

2 μL RNase A/T1 (2 μg/μL, 500 U/mL) were added and mixed thoroughly followed by overnight incubation at 37 ºC on a rotating mixer set to 2 rpm. Lysed cells were incubated in a water bath adjusted to 70 °C for 10 min followed by 30 min incubation at 37 °C. A volume of 120 μL 3 M potassium acetate pH 5.5 was added to each tube and mixed by inversions, followed by centrifugation in the Benchtop Sorvall Legend Micro 21R Centrifuge at 17000 x g for 15 min at 4 °C. A volume of 320 μL supernatant was carefully removed to avoid pelleted debris and 1200 μl ethanol/0.16 M sodium acetate was added to the supernatant followed by gentle mixing until the condensed chromosomal DNA was visible. Chromosomal DNA was pelleted by centrifugation using the Benchtop Sorvall Legend Micro 21R Centrifuge at 17000 x g for 15 min at 4 °C. The supernatant was discarded and the pellet was carefully washed with 600 μL 70% ethanol chilled to -20 °C. The tube was inverted onto an absorbent surface to dry for 20 min. Residual ethanol was further evaporated in a vacuum condenser chamber for 10 min. The DNA pellet was resuspended in 400 μL sterile ddH_2O followed by qualitative and quantitative analysis by Nanodrop spectrophotometry and 0.7% agarose gel electrophoresis. Extracted gDNA was loaded in 5 μL volumes with 1 μL 6 X DNA loading dye and electrophoresed using 1 X TAE buffer against gDNA of *P. acnes* ATCC 6919 (positive control) and 2.5 μL 1 KbP DNA ladder mixed with 2.5 μL HR DNA Ladder. DNA bands were stained with 0.5 μg/mL EtBr prior to visualizing and digital image acquisition using the short wave ultraviolet transilluminator function of the FluorChem FC3 imaging system with AlphaView Software. The prepared gDNA libraries were stored at -20 °C until use.

2.2.4 Molecular identification and characterization of *P. acnes* clinical isolates

Oligonucleotide primers specific to nucleotide sequences encoding *P. acnes* 16S rRNA and glycerol-ester hydrolase A (*gehA*) lipase genes (Table 2.2.1) were used to amplify fragments by PCR to confirm the identity *P. acnes* isolates. A select group of negative and positively-identified isolates were further verified and confirmed by Matrix Assisted Laser Desorption/Ionization Time-of-Flight (MALDI-TOF). Analysis by MALDI-TOF was performed at the laboratory of Dr. Tony Mazzulli, Department of Microbiology, Mount Sinai Hospital (Toronto, Canada) using the Vitek MS manufactured by bioMérieux S.A. (Marcy-l'Étoile, France). All *P. acnes* isolates were subjected to molecular phylotyping via PCR using phylotype IA, IB and II specific primers (Table 2.2.1). Procedural details of identification and typing are given in the following sections.

2.2.4.1 Molecular identification of *P. acnes* isolates: PCR amplification of *gehA* lipase gene and 16S rRNA DNA sequencesGenomic DNA of *P. acnes* ATCC 6919 and *P. acnes* ATCC 29399 served as positive controls, while gDNA from *P. granulosum* ATCC 25564 and *P. avidum* ATCC 25577 served as negative controls. PCR amplification targeting *P. acnes gehA* gene (GenBank accession no. PPA2105) encoding a triacylglycerol lipase, and highly-conserved regions within three operons of 16S ribosomal DNA (rDNA) of candidate *P. acnes* clinical isolates, were used for molecular identification of the *P. acnes* clinical isolates. PCR primers for *gehA* and 16S rDNA, originally designed by (Nakamura *et al.*, 2003), are listed in (Table 2.2.1). Primer specificity was verified by comparing nucleotide sequences to the alignment of the *gehA* gene and 16S rDNA nucleotide sequences of known *P. acnes* strains, *P. avidum, P. granulosum, P. propionicum*, and several *S. aureus* and *E. coli* strains. Exact nucleotide

Table 2.2.1: Molecular identification and phylotyping of *P. acnes* clinical isolates. Primer nucleotide targets are based on *P. acnes* reference strain KPA171202 (GenBank accession no. AE017283).

	Primer ID	Direction	Primer sequence (5'→3')	Primer modification	Nucleotide Target	Operon/type	Amplified Region (5'→3')	Fragment size (bp)	Reference
Primers for Identification	Lip1	Forward	TCACTGATGAAGATCAACGCAC	-	*gehA*	-	2279544…2279029	515	Nakamura *et al.*, 2003
	Lip2	Forward	ACTTCTCCTGCAAGGTCAAG	-			2279306…2279029	277	
	Lip rev	Reverse	TGCGAATGTCCGACGACGTCGA	5'A17C 3'			-	-	
	PAS9	Forward	CCCTGCTTTTGTGGGGTG	-	16S rDNA (3 operons)	I	606230…607175	946	
						II	1525296…1524351		
						III	1801665…1800720		
	PAS10	Forward	CGCCTGTGACGAAGCGTG	-		I	606593…607175	583	
						II	1524933…1524351		
						III	1801302…1800720		
	PAS rev	Reverse	CGACCCCAAAAGAGGCAC	5' G16C 3'		-	-	-	
Primers for phylotyping	PR213	Forward	GACGATTACTGGGGCAAGAA	-	sequence that encodes a solute-binding protein within an ABC peptide transporter operon	Type IA	1579146…1579405	584	Shannon *et al.*, 2006
	PR216	Reverse	GGGGTGAACTTGACGTTGAT	-					
	PR256	Forward	GTCATCGGCTTCTGGATCAT	-	putative Y40U fragment [1]	Type IB	948634–949358	725	
	PR257	Reverse	CCTGGTTTCCACGATGTCTT	-					
	PR257G	Reverse	CCTGGTTTCCACGATGGCTT	5' T17G 3'					
	PR245	Forward	ATAAACCCATCGGCGGCTCGAT	-	two putative RHS-family protein genes	Type IA/IB Type II	246705–250694	3990 537 [2]	
	PR247	Reverse	AGCAAGGGAGCATTCAGTGG	-					

[1] No significant nucleotide protein homology with any known sequence
[2] See Section 2.2.4.2 for explanation

matches were found exclusively in corresponding regions of the *P. acnes* genome with the exception of *P. avidum* where the lipase gene was also amplified by the *gehA* sequence-specific primers. The conditions were optimized for double primer screening of *P. acnes* candidates by multiplex PCR reactions in 96-well plates at a final volume of 50 μL per reaction. Optimization for multiplexing the PCR reactions was achieved by adjusting the ratio of primers in order to produce nearly equivalent intensities of the amplified bands. Template DNA volumes, extracted as described in Section 2.2.3, varied between 1 μL and 5 μL to adjust for approximately 0.1 μg total DNA per reaction. Each reaction contained 1X master mix comprised of the following reagents: 5 μL *Taq* Pol PCR Buffer without $MgCl_2$ (10X) and 1.5 μL 50 mM $MgCl_2$, 1 μL 10 mM dNTPs and 1 μL 5 U/μL *Taq* Pol, a volume of gDNA equivalent to 0.1 μg and adequate ddH_2O to adjust the final reaction volume to 50 μL. Multiplex PCR amplifications of *gehA* and 16S rDNA were conducted separately with the following oligonucleotide primer sets (see Table 2.2.1): 0.6 μM Lip1, 0.2 μM Lip2, 0.4 μM Lip rev primers and 0.8 μM Pas9, 0.1 μM Pas10, and 0.4 μM Pas rev primers, respectively. Reactions were performed with the PTC-100 Programmable Thermal Controller. Optimized multiplex PCR cycle conditions were as follows: an initial denaturation step of 5 min at 94 °C, 30 cycles of denaturation at 94 °C for 30 s, primer annealing at 53 °C for 30 s and primer extension at 72 °C for 60 s, respectively. The reaction cycles were followed by a final extension step for 15 min at 72 °C. Once complete, reactions were held at 4 °C.

P. acnes identity of isolates was confirmed upon detection of DNA band sizes of 278 bp and 516 bp (corresponding with *gehA*) and 583 bp and 946 bp (corresponding with 16S

rDNA operon sequence targets), as determined by 1.5% gel electrophoresis. Amplified DNA was loaded in 10 μL volumes with 2 μL 6X DNA loading dye and electrophoresed using 1X TAE buffer against positive control strain *P. acnes* ATCC 6919, negative control strains *P. avidum* ATCC 25577 and *P. granulosum* ATCC 25564, and 3 μL 1 KbP DNA ladder. Amplified DNA bands were stained and imaged as described in Section 2.2.3.

2.2.4.2 Molecular phylotyping of *P. acnes* clinical isolates

Genomic DNA was extracted (Section 2.2.3) from Swedish *P. acnes* isolates AS13 (type IB) and AD7 (type II), previously typed based on recombinase A (*recA)* gene sequences (Holmberg *et al.*, 2009). Genomes of ATTC 6919 (type IA; (McDowell *et al.*, 2005; Valanne *et al.*, 2005) and Swedish isolates were used as positive controls for molecular phylotyping of all clinical isolates. *P. granulosum* ATCC 25564 and *P. avidum* ATCC 25577 were used as negative controls. Polymerase chain reactions using unique primer sets (Table 2.2.1) developed by (Shannon *et al.*, 2006a) to target various type-specific DNA sequences, yielded amplified PCR products that were analyzed to define each isolate as type IA, IB or II.

Amplification of the phylotype-specific genomic regions were performed by PCR in 96-well PCR plates by using single-primer sets for independent PCR reactions with a final concentration of 0.4 μM individual primer per 50 μL reaction. Template DNA volumes and 1X master mix formulation and preparations were as described in Section 2.2.4.1. Reactions were performed in the PTC-100 Programmable Thermal Controller. Optimized multiplex PCR cycle conditions were 30 cycles of DNA denaturation, annealing and

extension, executed under the following conditions: 94 °C for 30 s, 50 °C for 30 s and 72 °C for 60 s, respectively. Preceded by an initial denaturation step of 5 min at 94 °C, the reaction cycles were followed by a final extension period of 15 min at 72 °C. Once complete, reactions were held at 4 °C.

The isolates were confirmed as phylotype IA, IB or II based upon detection of 584 bp, 725 bp and 537 bp bands, respectively, as determined by 1.8% agarose gel electrophoresis. Amplified DNA was loaded in 10 μL volumes with 2 μL 6X DNA loading dye and electrophoresed using 1 X TAE buffer against amplified type-specific DNA sequences of ATCC 6919 (type IA positive control), *P. acnes* AS13 (type IB positive control), or *P. acnes* AD7 (type II positive control) in addition to 3 μL 1 KbP DNA ladder. Amplified DNA bands were stained and imaged as described in Section 2.2.3.

2.2.4.3 Antibiotic susceptibility testing of *P. acnes* clinical isolates

Antibiotic susceptibility of *P. acnes* isolates was determined by Etest. Protocols for testing, as described by the Clinical and Laboratory Standards Institute (CLSI) for susceptibility testing of anaerobic bacteria and the Etest package insert, were adhered to (bioMérieux, 2012a; Clinical and Laboratory Standards Institute, 2004). Susceptibility interpretation of MIC values for all antibiotics except DC and MC was based on breakpoints established by the CLSI and the European Committee on Antimicrobial Susceptibility Testing (EUCAST) (Clinical and Laboratory Standards Institute, 2015; EUCAST, 2016). Distribution of DC and MC MIC values for the *P. acnes* isolate

population were bimodal; breakpoints were determined to be the central MIC values falling within the troughs of the bimodal distributions (Kronvall *et al.*, 2011).

All susceptibility testing, except DPC and TS, was performed on Brucella 5% laked sheep blood agar supplemented with 5 mg/L hemin and 1 mg/L vitamin K_1 (BBA) in 150 mm diameter petri dishes. Effects of para-aminobenzoic acid (PABA) antagonists on TS activity was minimized by substituting MH base medium for Brucella base medium (bioMérieux, 2010). Susceptibility to DPC was evaluated on BBA, supplemented with 0.1 g/L $CaCl_2$ to increase Ca^{2+} concentration to levels sufficient for optimal DPC performance (bioMérieux, 2012b). To maintain consistent moisture levels, all media was prepared approximately 12 hours prior to testing and the thickness of agar medium was maintained at 0.4 mm.

Cryopreserved isolates were subcultured at least twice on BBA prior to susceptibility testing. Isolated colonies from plates were cultured in Brucella broth supplemented with vitamin K_1 and hemin and incubated for approximately 24 hours under anaerobic conditions. Etest strips were equilibrated to room temperature for a minimum of 30 min prior to opening the package. Broth cultures were standardized to a 1.0 McFarland turbidity standard and, if necessary, were diluted by adding hemin and vitamin K_1-supplemeted Brucella broth medium. Sterile, flocked swabs were used to sample the standardized bacterial suspension and streak the entire surface of the agar media three times, rotating the plate 60 degrees every time, to create an even lawn of bacterial growth. Etest strips were applied to dry plates according to standard Etest package insert (bioMérieux, 2012a). Immediately after placing the strips, plates were inverted and

incubated under anaerobic conditions at 35°C for approximately 72 h. MIC values were read and adjustments were made based on standard protocol as stated in the Etest package insert reading guide and customer information sheet “CIS007” (bioMérieux, 2012a, c).

Quality control reference strains, *E. faecalis* ATCC 29212, *S. aureus* ATCC 29212 and *S. pneumoniae* ATCC 49619, were used to evaluate and monitor experimental conditions and antibiotic performance. Quality assessments, based on comparison of observed MIC values with published MIC ranges, were carried out according to Etest standard protocols (bioMérieux, 2013). Susceptibility testing of *P. acnes* ATCC 6919 was repeated regularly to ensure consistency of test conditions.

2.2.5 Isolation of *P. acnes* bacteriophages

A collection of *P. acnes*-specific phages was previously isolated by Jelena Trifkovic, a former technician of Dr. Reza Nokhbeh. In brief, sewage samples were periodically collected over a period of 12 months from Robert O. Pickard Environmental Centre in Ottawa and Gatineau Wastewater Treatment Plants. A 50 mL sample of the collected sewer was filtered through 0.22 μm sterile syringe filters to remove debris and cellular contents. Classical agar overlay method was used to isolate and purify phage plaques as follows: approximately 200–300 μL filtered sewage samples were mixed with 300 μL overnight *P. acnes* broth cultures—strains 1 to 6, ATCC 29399 and ATCC 6919—followed by incubation at room temperature (RT) for 15 min. The mixture was added to 3 to 4 mL 0.7% molten CB top agar, cooled down to approximately 50 ºC, and overlaid on CB agar (1.6%) plates. Plates were incubated under standard microaerobic atmospheric conditions. Phage plaques were removed as agar plugs and transferred into 1 mL CB

broth followed by vigorous vortexing to resuspend the phage particles. The phage suspension was filtered through sterile 0.22 μm syringe filters to remove cells and agar debris. Phage titres were determined by plating 100 μL triplicate samples from 10-fold dilution series in CB broth using agar overlay method. Following overnight incubation of plates, the resulting plaques were counted and the titre of phage stocks were calculated using the corresponding volume and dilution factors. The secondary phage stocks were prepared following isolation of a single plaque using the primary phage stocks as inoculum. Plaque purified secondary stocks were grown and titred as above and stored at 4 ºC.

Cutaneous *P. acnes* phages were isolated from the superficial swab samples of a patient in Sudbury, ON. After the sample was streaked onto CB agar for isolation of bacterial colonies (Section 2.2.2), 5 mL CB broth was inoculated using swabs and incubated at standard growing conditions overnight. Cultures were centrifuged using the Allegra X-12 Benchtop Centrifuge at 3250 x g for 15 min. The supernatant was collected and filtered through sterile 0.22 μm syringe filters to remove cells. Classical overlay method was used to isolate and purify phages, as described above.

2.2.6 Transmission electron microscopy of phages

To characterize phages based on their morphology, phage particles were visualized by transmission electron microscopy (TEM). High-titre samples (10^8–10^9 PFU/mL) for TEM were prepared using agar overlay method by plating 100 μL volumes of 10-fold dilution series (in CB) from phage stocks. Phage on plates that exhibited confluent lysis were eluted into 2 mL sterile ddH_2O deposited onto the agar surface, then incubated at room

temperature for 30 minutes. Eluate was removed from the plates, filter-sterilized and titred. Imaging services were provided by Dr. Tim Karnauchow (Children's Hospital of Eastern Ontario, Ottawa, Ontario) and the Canadian Centre for Electron Microscopy, McMaster University (Hamilton, Canada). In short, 5 µL phage suspension was deposited onto formvar-coated copper grids and allowed to dry for two minutes. The sample was washed once with 100 µL ddH_2O and blotted with filter paper to remove excess liquid. The sample was negatively stained with 1% uranyl acetate, applied for one minute prior to blotting dry. Samples were visualized at direct magnifications ranging from 50000x to 200000x and micrographs were taken with the Philips CM12 microscope, operated at 120 kV.

2.2.7 Host range analysis of *P. acnes* bacteriophages

High throughput spot infection tests were performed by mixing 1 mL overnight *P. acnes* cultures with 5.5 mL 0.7% molten CB agar overlaid on CB agar plates (1.6%) prepared in rectangular single-well, non-treated Nunc OmniTrays followed by inoculation of 1 to 2 µL filtered phage stocks using a sterile 96-pin, 12 mm Scinomix polypropylene replicator in duplicate. Prior to performing spot infections, phage stocks were titred to ensure a concentration of 10^4 to 10^5 pfu/mL; ensuring that the volume of phage suspension (1 to 2 µL) carried by individual pins would suffice to initiate infection of the target cells. Plates were incubated under standard growing conditions for 24 to 48 h. Appearance of clearance zones around the point of inoculation by pins was considered as positive endpoint for infection. The procedure was repeated to assess the susceptibility of a set of negative controls including *S. aureus* ATCC 29923, *S. typhimurium TA1535, E. coli*

MG1655, S. pyogenes ATCC 12204, *P. granulosum* ATCC 25564 and *P. avidum* ATCC 25577.

Propionibacterium acnes strain #9 was naturally resistant to the isolated phages. Evolutionary derivation approach was followed to isolate a mutant phage from an existing phage stock with a wide host range (i.e. πα6919-4 phage). A 300 µL sample of *P. acnes* #9 overnight culture in CB broth was mixed with πα6919-4 stock at a multiplicity of infection (MOI) of ~1000 followed by incubation at RT for 15 minutes. Agar plate overlay method was utilized to isolate mutant phage plaques. Clear plaques were plucked, transferred to 1 mL CB broth and vortexed. The phage suspension was filtered through 0.22 µm syringe filter and titred. The secondary stocks were prepared as indicated above.

2.2.8 Genetic characterization of bacteriophages

In order to carry out genomic analyses, i.e. restriction enzyme fragmentation profiling and genomic sequence analysis, phages were propagated in *P. acnes* strains and the resulting lysate supernatants were collected. The cleared lysate supernatants were used to recover the phage particles, which were subsequently used for extraction of gDNA. The following sections provide the details of the procedures used for phage propagation, cleared lysate preparation, gDNA extraction, restriction enzyme fragment profiling and sequencing the phage genomes.

2.2.8.1 Propagation of bacteriophages

A volume of each bacteriophage stock, giving an approximate MOI of 0.1 to 1, was mixed with 1 mL *P. acnes* overnight cultures (~10^9 CFU/mL) of strains on which the

phages were originally isolated, followed by incubation at RT for 15 minutes. This preparation is conducted with the intent of establishing an initial infected population. The infected starter cells were mixed with 24 mL of *P. acnes* cultures in exponential growth phase and 20 mL sterile CB broth. A control set was also prepared in parallel that lacked the phage in the mixture. The phage-infected and control sets were incubated under standard growing conditions for *P. acnes* until complete bacterial lysis (clearance) was observed. The infected cultures were centrifuged at 2000 x g for 30 min at 4 ºC using the Benchtop Sorvall Legend Micro 21R Centrifuge and the lysate supernatant was filtered through sterile 0.22 μm vacuum filters. The filtrates were collected and stored at 4 °C.

2.2.8.2 Precipitation of phages and extraction of genomic DNA

A total of 25 mL filtered lysate supernatants were mixed with 5 mL 30% PEG 8000/3 M NaCl in 35 mL Corex tubes and incubated at 4 °C for 8 to 12 h. Phages were precipitated by centrifugation at 14 000 x g for 30 minutes at 4 °C using the Avanti J-E High-Performance Centrifuge. The supernatant was drained completely and the phage pellet was resuspended in 1 mL 1X phage extraction buffer (100 mM sodium chloride, 100 mM Tris-hydrochloride pH 7.5 and 25 mM EDTA (Appendix B.4). A volume of 500 μL PCI (25:24:1, v/v) solution (Appendix B.3) was added to 500 μL phage suspension and mixed vigorously for roughly 3 min followed by centrifugation at 14000 x g for 10 min at 4 ºC using the Benchtop Sorvall Legend Micro 21R Centrifuge. The DNA-containing aqueous phase was carefully transferred to a new epitube without disturbing the proteinaceous interphase and organic lower layer. The PCI extraction procedure was repeated one more time and the DNA was precipitated from the second aqueous phase by adding 1.5 mL

ethanol/0.16 M sodium acetate and incubated at -20 °C for 8 to 12 hours. The gDNA pellet was obtained by centrifugation at 14000 x g for 15 min at 4 °C and the supernatant was poured off. The DNA pellet was washed with 400 µL 70% ethanol (chilled to -20 °C) and the residual ethanol was evaporated in a vacuum evaporator for10 minutes. The dried gDNA pellet was resuspended in 50 µL sterile ddH_2O followed by qualitative and quantitative analysis by spectrophotometry and 0.7% agarose gel electrophoresis. Two microliters of the phage gDNA preparation was mixed with 4 µL 1X DNA loading dye and electrophoresed as indicated in Section 2.2.3 against isolated gDNA of bacteriophage πα33 (positive control).

2.2.8.3 BamHI restriction digestion of phage genomic DNA

Phage gDNA concentrations and the purity of preparations were estimated by the NanoDrop spectrophotometer. Digestion of the phage gDNA was carried in a 1.5 mL sterile eppendorf tube, at a total reaction volume of 50 uL. A volume of phage DNA equivalent to 2 µg was used, to which 5 µL bovine serum albumin (BSA) (1 mg/mL) and 5 µL 10X NEBuffer 3 were added, followed by volume adjustment with sterile ddH_2O, for a total of 49 µL. The reaction was started by adding 1 µL BamHI (20 U/µL), giving a final reaction volume of 50 µL, followed by mixing and incubation at 37 °C for 1 h. After incubation, the tubes were immediately placed on ice and BamHI restriction banding patterns were assessed via DNA gel electrophoresis using 0.7% agarose gel as described in Section 2.2.3. Wells were loaded with 10 µL digested phage DNA mixed with 2 µL 6X DNA loading dye then run against πα33 BamHI digested genome (positive control) and 2.5 µL 1 KbP DNA ladder combined with 2.5 µL HR DNA Ladder. BamHI digested

DNA bands were stained and imaged as described in Section 2.2.3. Banding patterns of the digested phage DNA were inspected and visually clustered.

2.2.8.4 Phage genome sequencing and analysis

Genomic libraries were prepared by Jenna Graham and Nya Fraleigh. Genome sequencing, assisted by Nya Fraleigh, and sequence assembly/annotation were done by Dr. Gustavo Ybazeta as follows.

2.2.8.4.1 Preparation of phage genomic libraries

Phage genome libraries were constructed using the NEBNext Fast DNA Fragmentation & Library Prep Set for Ion Torrent. To prepare the libraries, the concentration of each purified phage DNA sample was measured using the Qubit accompanied by the HS dsDNA for Qubit kit. Double-stranded DNA reagent was diluted into dsDNA HR buffer at a ratio of 1:200. DNA standards of 0 ng and 10 ng were prepared for the Qubit read and were made using 190 µL diluted dsDNA reagent combined separately with the 10 µL standard. One microliter DNA sample was mixed with 199 µL dilute dsDNA reagent and analyzed. The amount of DNA used for library preparation was 100 ng at a maximum volume of 15.5 µL per DNA sample. Fragmentation and end repair of DNA was conducted as indicated in the NEBNext Fast DNA Fragmentation and Library Prep protocol for approximate target fragment size of 200 to 300 bp.

The standard protocol for the preparation of adapter ligated DNA was modified to accommodate for the use of Ion Torrent barcode adaptors 17–32 kit. Added to the fragmented phage DNA samples was 9 µL sterile ddH_2O, 4 µL 10X T4 DNA Ligase Buffer (NEB), 1 µL P1 DNA Library Adaptors and 1 µL Barcode Adaptors (Life

Technologies), 1 µL *Bst* 2.0 Warm Start DNA Polymerase (NEB) and 4 µL T4 DNA Ligase (NEB). The tube content was mixed well and incubated in the Eppendorf Mastercycler Pro thermal cycler for 15 min at 25 °C, 5 min at 65 °C then reduced to a resting temperature of 4 °C. Stop Buffer (10X; NEB) was added at a volume of 5 µL and mixed well followed by the addition of 55 µL 0.1X TE buffer (NEB). Approximately 200 to 300 bp fragments were selected for via AMPure XP Bead-based dual bead size selection as recommended in the manufacturer's standard protocol.

PCR amplification and cleanup of adaptor ligated DNA was performed according to the standard protocol using 40 µL adaptor ligated DNA, 4 µL NEBNext DNA Library Primers for Ion Torrent (NEB), 6 µL sterile ddH_2O and 50 µL NEBNext High-Fidelity 2X PCR Master Mix (NEB). PCR cycling conditions were as described by the NEB protocol for 8 cycles. Genomic library quality was assessed using the Qubit with 5 µL genomic library sample mixed with 195 µL dilute dsDNA reagent as described above against 0 ng and 10 ng standards.

2.2.8.4.2 Sequencing, assembly and annotation

Genomes of *P. acnes* bacteriophages were sequenced using the Ion PGM System (Ion PGM Sequencer and PGM Torrent Server). Once fragment libraries were prepared, template preparation was performed using the Ion OneTouch 2 system and the Ion PGM OT2 Template 200 Kit. Sequencing was performed with the Ion PGM Sequencing 200 Kit v2 with the Ion 316 Chip Kit v2, with variable numbers of genome samples per chip. Raw data processing and analysis was conducted with the Torrent Suite Software.

Genome assembly was accomplished with the program MIRA version 4.0.2 (Chevreux *et al.*, 1999), using the reference *Propionibacterium acnes* phage PA6 –GenBank entry NC_009541.1 (Farrar *et al.*, 2007). Draft genomes were visually inspected for sequence artifacts using gap5 v1.2.14-r (Bonfield & Whitwham, 2010). Genome sequence format changes and visualization were done with Artemis v 16.0.0.1 - Standard (Rutherford *et al.*, 2000). The graphical user interface (GUI) Mauve (Darling *et al.*, 2004) and progressive Mauve (Darling *et al.*, 2010) were used for multi-genome alignment among the draft genomes for comparative genome analysis.

Genome annotation was performed using the Prokka pipeline v 1.11 set for bacterial genomes (Seemann, 2014). This pipeline was run with the dependencies for searches against DNA and protein databases using BLAST 2.2. 29 + (Camacho *et al.*, 2009), to conduct similarity searches for protein-coding predictions, using protein family profiles Prodigal v2.6 (Hyatt *et al.*, 2010) and HMMER v3.1 (Finn *et al.*, 2011). Bioperl was used to transform file formats for input and output (Stajich *et al.*, 2002). Downloaded from GeneBank (Nov-10-2015), a *P. acnes* phage sequence database was created to assist Prokka annotation (Table E.1). A Multiple genomic loci comparison graph was composed using GUI Easyfig v2.2.2 (Sullivan *et al.*, 2011).

2.2.8.4.3 Major tail proteins: phylogenetic analysis, homology and structure prediction

The Bio neighbour joining (BioNJ) algorithm (Gascuel, 1997) was used in Seaview to construct a phylogenetic tree based on sequences of the major tail proteins (MTPs) among the *P. acnes* phages sequenced in this study. Alignment maps of MTP sequences

were produced by Jalview v. 2.10.1 (Waterhouse *et al.*, 2009) and DNAMAN v. 9 (Lynnon Biosoft, n.d.).

To identify homologous protein sequences, sequence similarity searches were conducted using standard protein BLAST (blastp) from the National Center for Biotechnology Information (NCBI) (Altschul *et al.*, 1990) within non-redundant protein sequence database. To search for structural homologs of MTP sequences within the protein data bank (PDB), the MPI Bioinformatics Toolkit integrative platform was used (Alva *et al.*, 2016). Structural protein homology searches were conducted with HHPred (Söding *et al.*, 2005) using multiple sequence alignment (MSA) generation method HHblits (Remmert *et al.*, 2011). To further validate the structural alignment results produced by the MPI Bioinformatics Toolkit, the MTP sequences were uploaded to LOMETS (Local Meta-Threading-Server), a meta-server that runs several protein homology detection programs for the prediction of protein structure (Wu & Zhang, 2007). LOMETS conducts secondary structure prediction and threading using multiple programs and algorithms (FFAS-3D, HHsearch, MUSTER, pGenTHREADER, PPAS, PRC, PROSPECT2, SP3, and SPARKS-X). The multiple sequence alignment results with predicted secondary structures for each protein were returned, accompanied by the most probable matches among those within the PDB database. The MSA output was used by the server to model three-dimensional protein structures using MODELLER (Webb & Sali, 2016). The final PDB formatted files from LOMETS were visualized using PyMOL v.1.8 (Schrödinger, LLC, n.d.) to produce images of the predicted three-dimesional protein structures.

2.2.9 Statistical analyses

2.2.9.1 Categorical data

Statistical analysis of categorical data was performed using the GraphPad QuickCalcs Web site: http://www.graphpad.com/quickcalcs/contingency1/ (accessed March 2016), to construct two-way contingency tables and determine statistical significance through generation of p-values using Fisher exact test.

2.2.9.2 Concordance of *P. acnes* identification methods

Unweighted Cohen's kappa statistics (Cohen, 1960) was determined to assess the level of agreement between two different methods used to identify *P. acnes* isolates.

The kappa coefficient was generated at 95% confidence level with GraphPad QuickCalcs software (Web site: http://www.graphpad.com/quickcalcs/kappa1), using the probabilities of observed (P_o) and expected random (P_e) agreements in detecting the true positive and negative results (Cohen, 1960).

Validity of the multiplex PCR identification method with respect to MALDI-TOF reference method was determined and the corresponding sensitivity (proportion of true positives), specificity (proportion of true negatives) and positive and negative predictive values were calculated using GraphPad InStat Software (GraphPad InStat version 3.10, 32 bit for Windows, GraphPad Software, San Diego California USA, www.graphpad.com).

2.2.9.3 Concordance testing of *P. acnes* phage host range and major tail protein sequence diversity

Responsible for host cell receptor recognition and binding, bacteriophage tail structures are determinants of host specificity (Fokine & Rossmann, 2014; Sassi *et al.*, 2013). The

Congruence Among Distance Matrices (CADM) test was applied to examine the level of concordance between the distance matrices of phage activity spectra and phage tail-associated protein sequences equivalent to *P. acnes* phage PA6 gp11, gp14, gp15, gp16 and gp17, using gp1 (small terminase subunit) as a positive control for the null hypothesis (H_0) characterized by discordance among distance matrices (Campbell *et al.*, 2011; Legendre & Lapointe, 2004). The detailed process of CADM test and the statistical analysis is explained below.

2.2.9.3.1 Distance matrices

Multiplatform GUI 'SeaView' v.4.6.1 (Gouy *et al.*, 2010), was used to write host range binary strings and aligned protein sequences (twelve sequenced phage genomes) in PHYLIP file format to use in R v.3.3.2 software environment for statistical computing and graphics (R Core Team, 2016). First, host range profiles of all sequenced phages were converted to binary strings and written to FASTA format; binary code was denoted by successful lysis "1" and absence of lysis by "0". SeaView was used to convert FASTA files to PHYLIP format. Individual protein sequences of interest were written to FASTA format, and aligned using SeaView—Clustal Omega (Sievers *et al.*, 2011) and MUSCLE (Edgar, 2004)—and exported to PHYLIP format.

Within the R software environment, package SeqinR v.3.3-3 (Charif & Lobry, 2007) was used to read host range binary strings from PHYLIP files using function `read.alignment` and create a full character matrix based on the binary strings using function `as.matrix`. With function `dist.gene` and argument `method = percentage`, package APE v.4.0 (Paradis *et al.*, 2004) was used to calculate the

proportion of sites that were different between two sequences (p-distances) based on pairwise combinations of binary sequences representing host ranges for each of sequenced phages; using the p-distances calculated, a full distance matrix was written with function `as.matrix` for use in congruency analysis (Section 2.2.9.3.2). Similarly, package phangorn v.2.1.1 (Schliep, 2011) was used to read protein sequence alignments from PHYLIP files using function `read.phyDat` with argument `type = AA`. Protein sequences were then written as objects of class `phyDat` with function `as.phyDat`. For each pairwise combination of sequenced phages, computation of uncorrected p-distances was achieved with the `dist.hamming` function excluding pairwise sites having missing or ambiguous states. These calculations were based on the protein sequences written as objects of class `phyDat` in conjunction with arguments `ratio = TRUE` and `exclude = pairwise`. Distance matrices were written using function `as.matrix` for use in congruency analysis based on protein sequences (Section 2.2.9.3.2).

2.2.9.3.2 Congruence Among Distance Matrices (CADM)

Global congruence and Mantel tests were performed using the APE package in R by pairwise CADM tests of distance matrices derived from the phage host range dataset and tail-associated protein sequence datasets (Section 2.2.9.3.1). Prior to congruence analysis, distance matrices were bound using function `rbind`. For each set of variables tested, function `CADM.global` was used to generate an overall concordance statistic (Kendall's coefficient of concordance, W) and a test statistic (Friedman's X^2_{ref}), which was used for permutation test to determine the one-tailed probability (P-value) of the data falling under the H_0 (Legendre & Lapointe, 2004). Mantel tests were performed using Spearman's

correlation coefficient, r_s, as generated by function `CADM.post` with argument `mantel=TRUE`, producing one-tailed *P*-values based on ranking of permuted distance matrices (Legendre & Lapointe, 2004).

The global concordance statistic, Kendall's *W* (Kendall & Smith, 1939), indicated the level of discordance among distance matrices and ranged between 0 (incongruent) and 1 (completely congruent). To test the significance of *W*, Friedman's X^2 (Friedman, 1937) test statistic (X^2_{ref}) was calculated using *W* and then analyzed against a distribution of permuted X^2 values (X^2*) falling under H_0 (complete incongruence). Distributions of X^2* statistics were generated by the global CADM test through 9999 random permutations across the distance matrices in question (Campbell *et al.*, 2011; Legendre & Lapointe, 2004). Based on a level of significance α=0.05, a X^2_{ref} statistic greater than or equal to 95% of X^2* values under H_0 returned a one-tailed probability $P \leq 0.05$, resulting in rejection of H_0 and acceptance of the alternate hypothesis, H_1, which represents congruence among distance matrices (Campbell *et al.*, 2011; Legendre & Lapointe, 2004). Therefore, when $P \leq 0.05$, the variables under test—datasets corresponding to phage host range and a tail-associated protein sequence—were considered congruent at a level inferred by Kendall's *W*.

Mantel tests were performed to compliment the global test statistics associated with congruent matrices (H_1) only (Campbell *et al.*, 2011; Legendre & Lapointe, 2004). Similar in process to the global CADM test, the probability of incongruent matrices (H_0) was determined by calculating Spearman's correlation coefficient (r_s) and testing it against a distribution of the statistic (r_s*) under permutation to obtain a one-tailed *P*-value (Legendre & Lapointe, 2004).

3 Results

3.1 Participating patients from Sudbury and Ottawa

Samples were collected from the skin surface and exudate of acne lesions from 45 patients in Ottawa and 91 patients in Sudbury. The overall highest prevalence of acne was observed in participants aged 17 years (11.8%). Those aged between 12 and 21 years accounted for 71.3% of the overall patient population, while 20.6% were between the ages of 22 and 31. The remaining 8.1% of patients fell within the age range of 32–50 years (Figure 3.1). Although the overall number of female participants of both patient populations was slightly higher than that of male participants (54.4%), the difference was not significant ($p=0.544$). The proportion of male subjects aged between 12 to 18 (59.4%) is higher than female subjects ($p=0.001$), whereas there are a higher proportion of female subjects (68.7%) over the age of 18 than there are males ($p=0.001$). Based on 47 patient records, the mean duration of acne was 4.9 years, with a median of 4 years. Thirty-eight patients (81%) reported having acne for up to eight years, and the remaining patients were suffering from acne for 8–17 years (Figure 3.2).

The most commonly affected areas of body were the face, back and chest; with the highest incidence of 42.5% affecting face/back/chest simultaneously, followed by face only (31.3%) and face/back simultaneously (17.5%). Sixty-eight patient records indicate that 73.5% of patients had only one lesion type; predominantly closed comedones. Other patients exhibited a combination of lesion types as listed in Table 3.1. Overall, the majority of lesion types exhibited by patients were closed comedones (57.4%). Incidence

of cystic and/or pustule lesions was 45.6% and open comedones was 8.8%. Based on 65 patient reports, 63.1% of patients had scarring due to acne lesions (Table 3.1).

The majority of patients were treated with a combination of antibiotics, retinoids and benzoyl peroxide; less frequent treatment combinations are listed in Table 3.1. Out of 114 patient treatment records, 99 patients (86.8%) underwent treatment with topical and/or oral retinoid(s) and 80 patients (70.2%) with topical and/or oral antibiotics. Treatment with benzoyl peroxide was also reported for 80 patients, and 2 patients (1.7%) underwent photodynamic therapy (Table 3.1). Out of 100 female patient treatment records, oral contraceptives and spironolactone (antiandrogen), were used by 19 (19%) and 6 (6%) patients, respectively. Patients treated with antibiotics were exposed to a maximum of 3 different types of antibiotic (Figure 3.3). Use of specific antibiotics are detailed in Table 3.2. Having a 7-month mean treatment duration, the most frequently used topical antibiotic was clidamycin (CM) (58.8% of patients using antibiotics). The most commonly used oral antibiotic was minocycline (MC) (28.8%), followed by doxycycline (DC) (23.8%). Mean duration of treatment with oral MC was 6.2 months and DC for 7.5 months.

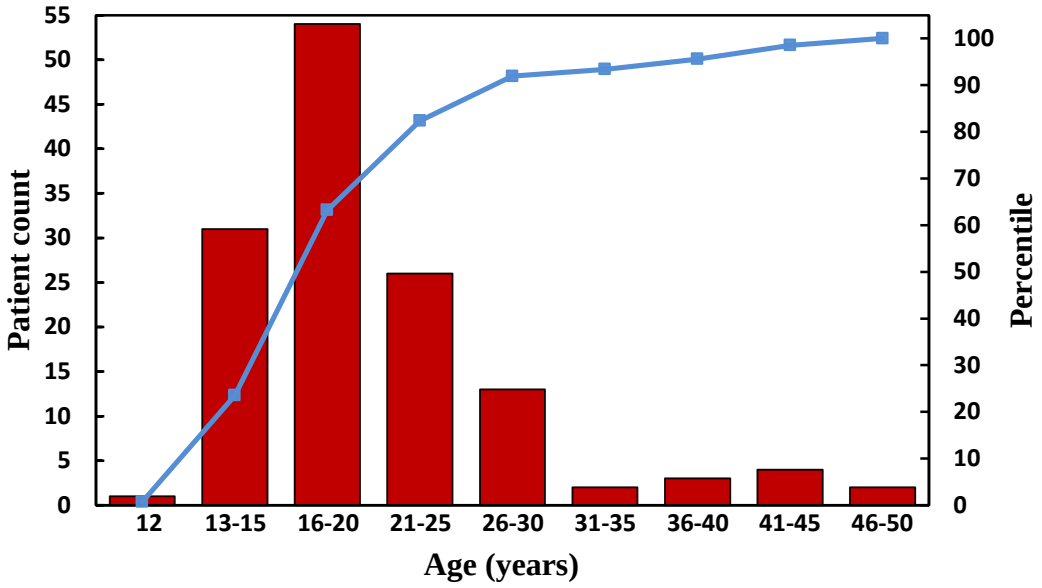

Figure 3.1: Age distribution of Ottawa and Sudbury patient populations

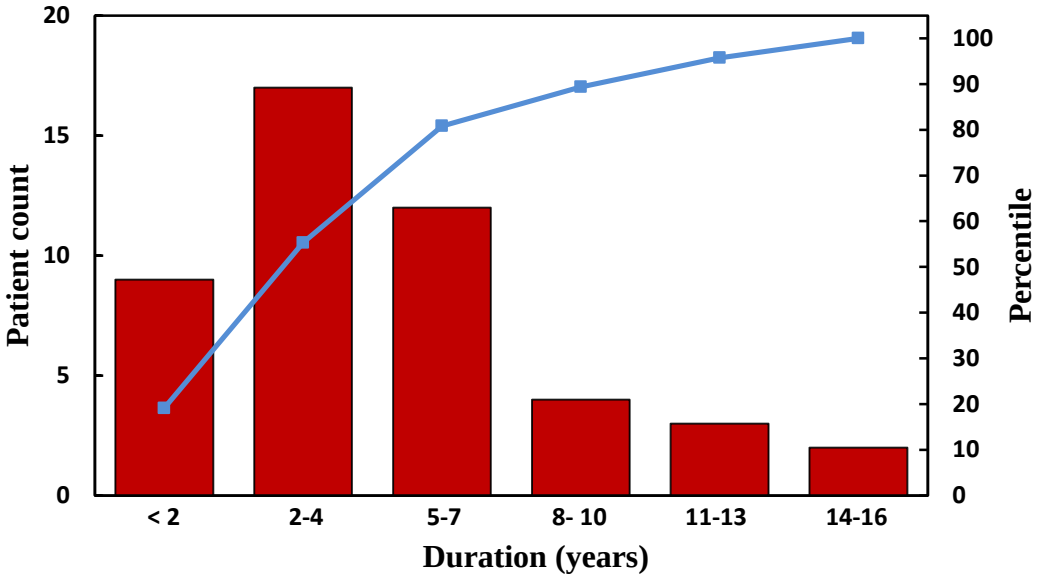

Figure 3.2: Duration of acne persistence among acne patients.

Table 3.1: Clinical presentation and treatment of acne vulgaris.

Lesion Site		Type of Lesion[1]		Treatment[2]	
Total number of records	80	Total number of records	68	Total number of records	136
Face, back and chest	34	CC only	29	RTD(s) + AB(s) + BPO	36
Face	25	Cys/Pus only	18	RTD(s)+ AB(s)	15
Face and back	14	CC + Cys/Pus	10	RTD(s)+BPO	14
Face and groin	2	OC only	3	RTD(s) only	13
Back	2	OC + Cys/Pus	3	RTD(s) + AB(s) + BPO + OC	12
Chest	1			AB(s) + BPO	8
Groin	1			AB(s) only	2
Face and chest	1	Scarring (65 records)	41	RTD(s) + BPO + OC	2
				AB(s) + BPO + OC	2
				RTD(s) + AB(s) + BPO + SPL	2
				SPL only	1
				RTD(s) + AB(s) + BPO + OC + SPL	1
				OC + SPL	1
				RTD(s) + AB(s) + SPL	1
				RTD(s) + OC	1
				BPO only	1
				PDT + RTD(s) + BPO	1
				PDT + RTD(s) + BPO + AB(s)	1

[1]OC, open comedone(s); CC, closed comedone(s); Cys/Pus, cystic/pustular lesion(s)

[2]AB, antibiotic (topical and/or oral); BPO, benzoyl peroxide; OC, oral contraceptive; PDT, photodynamic therapy; RTD, retinoid (topical and/or oral); SPL, spironolactone

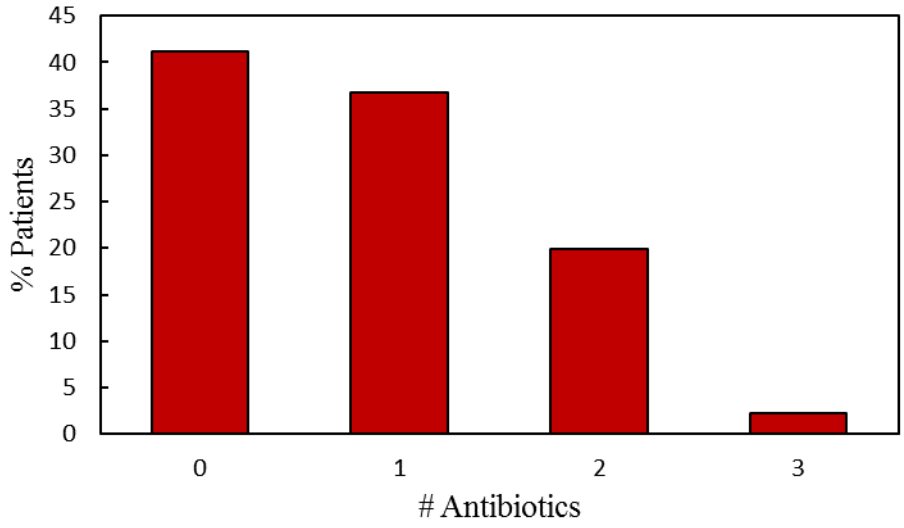

Figure 3.3: Frequency of antibiotic use among Ottawa and Sudbury patient populations.

Table 3.2: Antibiotic use among Sudbury and Ottawa patient populations (n=80 antibiotic-treated patients).

Topical		Topical & Oral		Oral	
CM	21	CM(T)/DC(O)	10	MC	15
DPS	3	CM(T)/MC(O)	6	DC	5
EM	1	CM(T)/TC(O)	2	EM	3
CM/EM	3	CM(T)/EM(O)	2	MC/TC	2
		CM(T)/EM(T)/TC(O)	1	TC	1
		CM(T)/DPS(T)/DC(O)	1	TM	1
		CM(T)/DC(O)/TC(O)	1	DC/EM	1
		DPS(T)/DC(O)	1		

(T), topical; (O), oral; CM, clindamycin; DC, doxycycline; DPS, dapsone; EM, erythromycin; MC, minocycline; TC, tetracycline; TM, trimethoprim

3.2 *P. acnes* isolate collections

A total of 222 clinical *P. acnes* isolates from various geographical regions and two ATCC strains were included in this study. Forty-five *P. acnes* isolates from Sweden were used in this study; this included 17 isolates from the foreheads of non-acne patients, and 28 isolates recovered from the tissue surrounding various types of deep-seated infections (Holmberg *et al.*, 2009). Eleven *P. acnes* isolates, recovered from systemic infection sources, superficial and deep-seated infections across Canada, were also incorporated into this study. See Table C.1 for isolate-specific details.

P. acnes isolates from Ottawa and Sudbury comprise the majority of the overall collections. Out of 91 patients from Sudbury, only the isolates derived from the first 76 sets of samples (SS1/SD1 to SS76/SD76) were characterized, which resulted in 110 confirmed *P. acnes* isolates from Sudbury. Similarly, out of 45 patients from Ottawa, only the isolates derived from the first 40 sets of samples (OS1/OD1 to OS40/OD40) were characterized, yielding 56 confirmed *P. acnes* isolates from Ottawa. See Table 3.3 for details pertaining to all *P. acnes* isolate collections.

Table 3.3: *Propionibacterium acnes* clinical isolate collections from a variety of sources and geographical regions

Geographical Origin	Patients	Sample Origin	Isolates	Total[1]	Collection Period	Source	Reference
Various locations, Canada	11	Superficial infection	2	11	2001-2007[6]	NML[2]	-
		Deep tissue infection	3				
		Systemic	6				
Sweden	45	Skin surface, non-lesional (AS)	28	45	2005-2007[6]	CSLU[3]	Holmberg *et al.*, 2009
		Deep tissue infection (AD)	17				
Sudbury	74	Lesion surface (SS)	45	110	2013 - 2014	Sudbury Skin Clinique[4]	This study
		Lesion exudate (SD)	65				
Ottawa	40	Lesion surface (OS)	19	56	2013 - 2014	Laserderm[5]	This study
		Lesion exudate (OD)	37				

[1]NML and CSLU isolates were recovered from different patients. Single and multiple isolates were recovered from Sudbury and Ottawa patients.
[2]NML, National Microbiology Laboratory (Winnipeg, Canada), courtesy of Ms. Kathryn Bernard
[3]CSLU, Department of Clinical Sciences of Lund University (Lund, Sweden), courtesy of Dr. Anna Holmberg
[4]Courtesy of Dr. Lyne Giroux
[5]Courtesy of Dr. Sharyn Laughlin
[6]approximate

3.2.1 Isolate screening

P. acnes isolates from Ottawa and Sudbury were acquired from 76 and 40 patients, respectively. Patient sampling was performed by swabbing, separately, the skin surface and exudate of acne lesions. Samples were cultured as described in Section 2.2.2 and 186 isolates were presumptively identified as *P. acnes* based on their coryneform morphology and positive catalase activity (Section 2.2.2); representative images of isolated colonies and microscopic morphology are given in Figure 3.4 and Figure 3.5.

As described in Section 2.2.4.1, identities of presumptive clinical isolates were confirmed by molecular characterization, accomplished by PCR, using *P. acnes*-specific primer sets. In order to efficiently screen the large number of presumptive isolates, the PCR-based method designed by (Nakamura *et al.*, 2003) for *P. acnes* identification was adapted for double-primer screening via multiplex PCR. Two genetic targets were used to differentiate *P. acnes* isolates from other species with a high level of accuracy—*gehA* and 16S rDNA. Primers “Lip1”, “Lip2” and “Lip rev” are complementary to sequences encoding GehA (Figure 3.6), a lipase gene specific to *P. acnes* and closely-related *Propionibacteria*. Incorporation of primers that are complementary to *gehA* gene allows for identification of both *P. acnes* and *P. avidum* as the primer set is also capable of amplifying the lipase gene of *P. avidum*, but not *P. granulosum* (Nakamura *et al.*, 2003). Primers “Pas9”, “Pas10” and “Pas rev” are complementary to sequences of the three 16S rRNA operons (*rrn* operons) of *P. acnes* only (Figure 3.6). Primer sets were comprised of three primers- two forward primers (one external and one internal) and one reverse primer (Table 2.2.1). Using internal primers for PCR improves the specificity of this

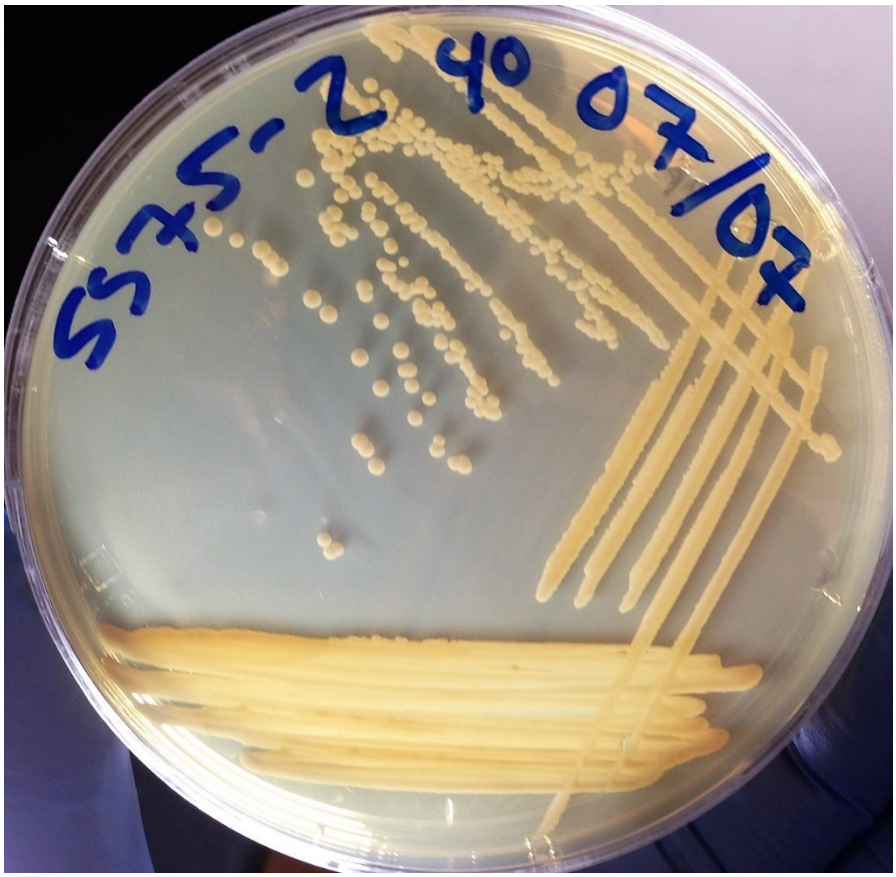

Figure 3.4: Sample plate showing colonies of *P. acnes* isolate "SS75-2", recovered from a sample taken of a lesion surface from a patient in Sudbury.

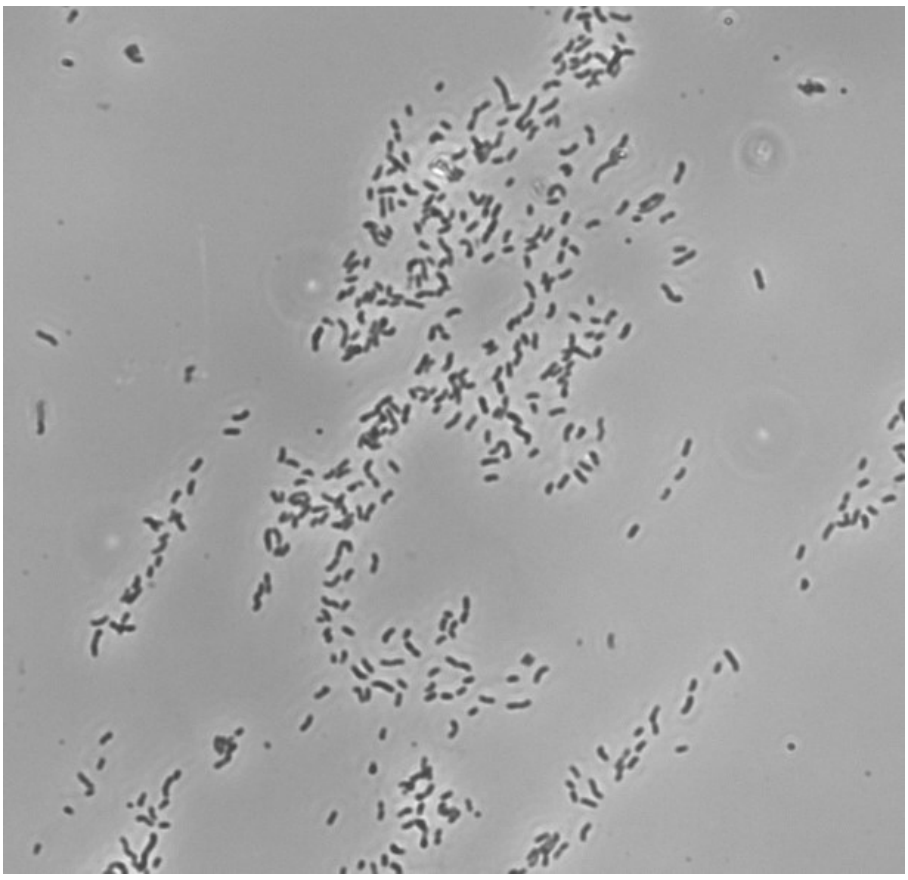

Figure 3.5: Image taken of *P. acnes* isolate "SS75-2", recovered from a sample taken of a lesion surface from a patient in Sudbury. Coryneform morphology confirmed by visual inspection at 400X magnification.

(i) Primer nucleotide targets for amplification of *gehA* lipase gene and the expected amplicon sizes (bp).

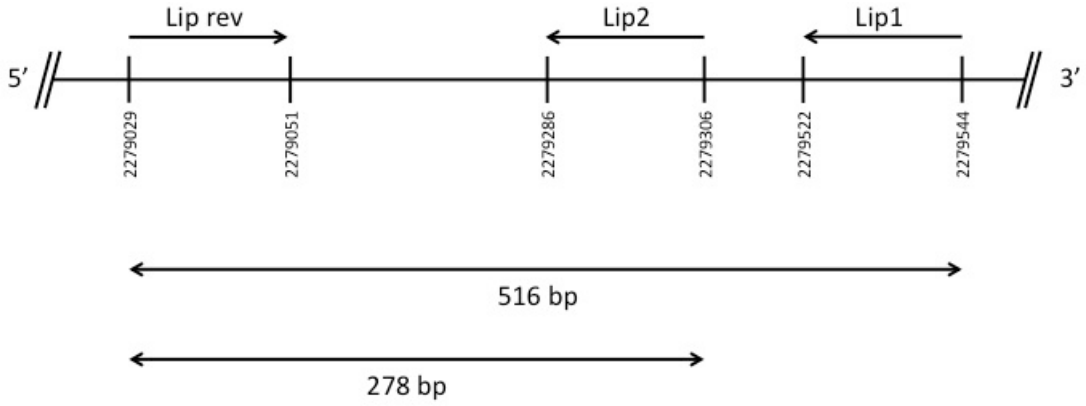

(ii) Primer genome targets for amplification of 16S rRNA gene and the expected amplicon sizes (bp).

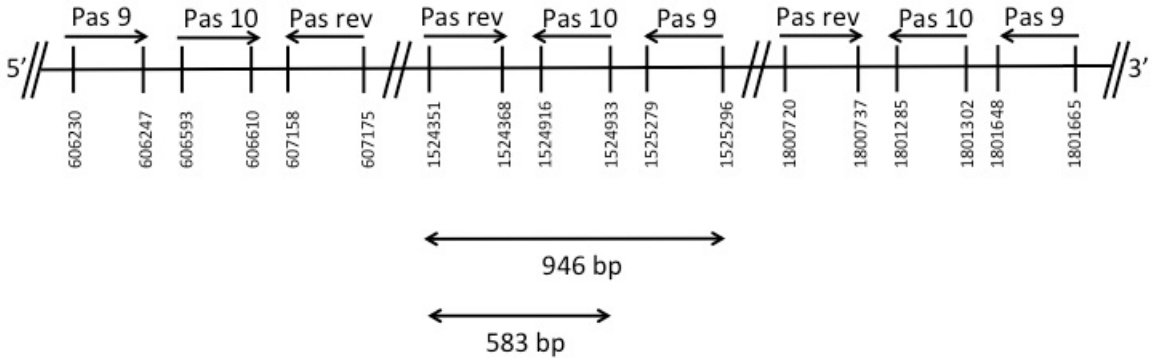

Figure 3.6: Primer targets for PCR-based identification of *P. acnes* clinical isolates. Alignments are based on reference strain *P. acnes* KPA171202 (NCBI Reference Sequence NC_006085.1).

screening method; it is unlikely that any nonspecific products will contain sequences complementary to the external and internal primers. Moreover, the longer amplicon produced by the external primers will serve as the template for internal primers, contributing to the diagnostic value of the amplified bands.

Shown in Figure 3.7, multiplex PCR was optimized using ATCC 6919 DNA as a template for all reactions with variable ratios of forward primers for each primer set—Lip1:Lip2 and Pas9:Pas10. The volume of the external forward primers (Lip1 and Pas9) ranged from 1–4 µL and volumes of the corresponding internal forward primers (Lip2 and Pas10) and reverse primers (Lip rev and Pas rev) remained constant at 1 µL and 2 µL, respectively. For positive controls, single-primer PCR was performed using all forward primers in separate reactions at a ratio of 1:1 for forward primer:reverse primer.

To determine the optimal ratio of forward primers for use in a single multiplex PCR reaction, products giving clear bands of equal intensity were considered ideal. Bands produced by the *gehA*-associated primer set were as expected, exhibiting amplicon lengths of 516 bp and 278 bp (Figure 3.6), with equal intensities achieved using 3:1 and 4:1 ratios of Lip1:Lip2 (Figure 3.7a). As shown in Figure 3.7b, the lengths of the double primer products of reactions using the *rrn* operon-specific primer set were 946 bp and 583 bp, as expected (Figure 3.6). Although no bands of equal intensity were present for any of the primer ratios, 4:1 ratio of Pas9:Pas10 produced clear bands for both internal and external primers. Positive control and single-primer reactions gave clear bands and all products were as expected. The optimal forward primers ratios were determined to be 4:1 for Pas9:Pas10 and 3:1 for Lip1:Lip2.

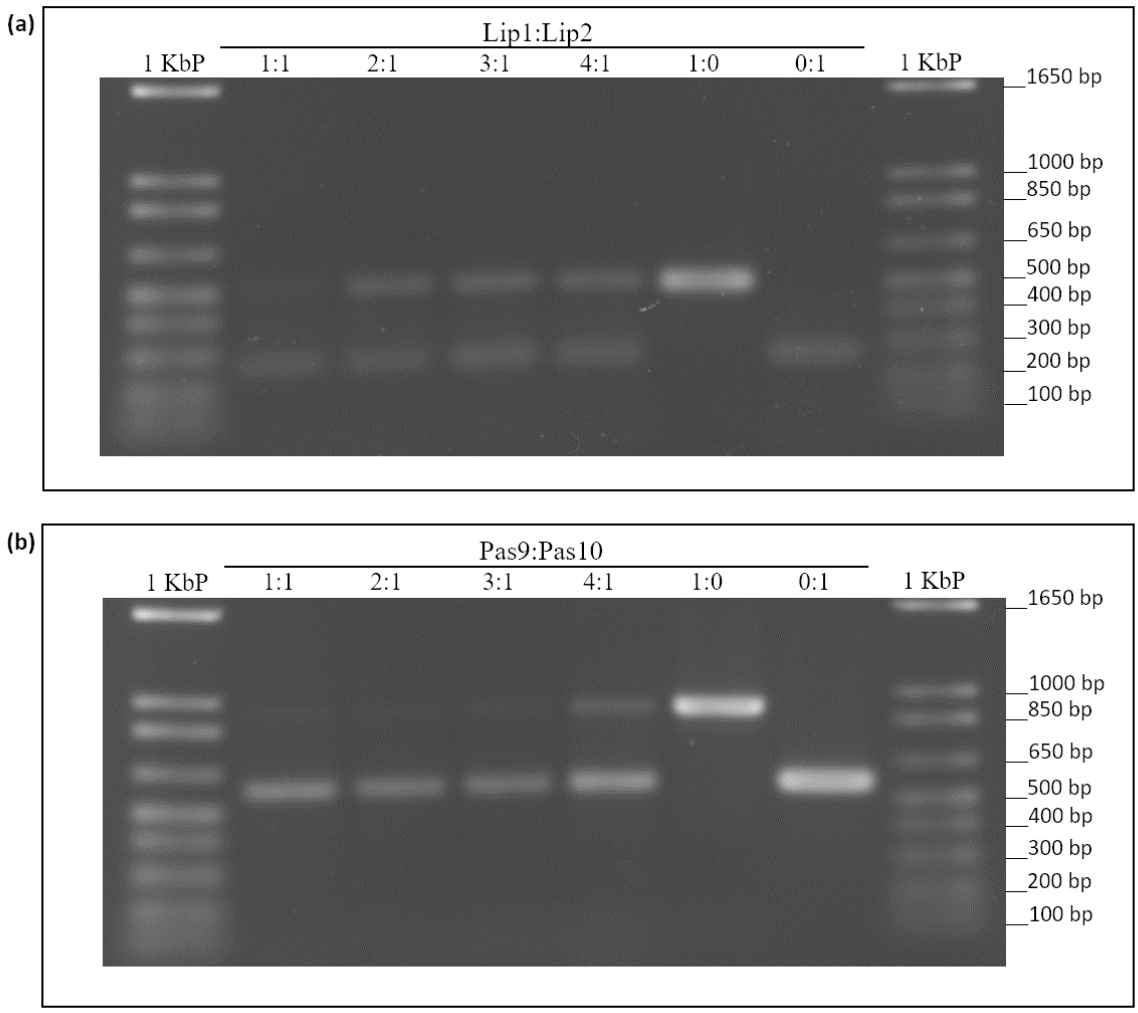

Figure 3.7: Agarose gels showing double primer optimization for multiplex PCR amplification of (a) *gehA* and (b) 16S rDNA, using ATCC 6919 genome template. Primer ratios (in µL) are indicated above each lane. Reverse primer volumes were consistent across all reactions (2 µL) with the exception of single primer reactions (1 µL). 1 KbP, 1 Kb Plus DNA ladder. See Section 2.2.4.1 for PCR and gel electrophoresis conditions.

All clinical isolates were screened under the optimized multiplex PCR conditions. As described above, clinical isolates were confirmed to be *P. acnes* based on the presence of amplified PCR products of *gehA* and *rrn* operon sequence targets depicted in Figure 3.6. *P. acnes* ATCC 6919 was used as the positive control, *P. granulosum* ATCC 25564 as the negative control for both primer sets, and *P. avidum* ATCC 25577 as the negative control for primers targeting *rrn* operon sequences only. Isolate screening returned 166 PCR-verified *P. acnes* isolates; 110 confirmed *P. acnes* isolates from the Sudbury patient population and fifty-six from Ottawa. As expected, *P. avidum* ATCC 25577 tested positive for the presence of the *gehA* gene only; 16 out of 20 *P. acnes*-negative isolates demonstrated banding patterns consistent with *P. avidum* (see example Figure 3.8).

The validity of screening of clinical isolates by multiplex PCR with reference to MALDI-TOF analysis of a sample population of 72 isolates was determined by generating kappa statistics. See Figure 3.9 for a sample of MALDI-TOF output spectra, representative of *P. acnes* ATCC 6919 and *P. avidum* ATCC 25577. As indicated in Table 3.4, results of both methods were in an excellent agreement at 95% confidence level with a kappa value of 0.824 (standard error =0.0760). Furthermore, calculated high sensitivity, specificity, PPV and NPV values (Table 3.4) supported the suitability of multiplex PCR as a rapid and relatively inexpensive method of choice for identifying the correct *P. acnes* isolates.

Further evaluation of the identity of the isolates was confirmed by their susceptibilities to infection by *P. acnes* aspecific phages. All PCR-confirmed *P. acnes* isolates were sensitive to *P. acnes* bacteriophages and were successfully genotyped (further discussion

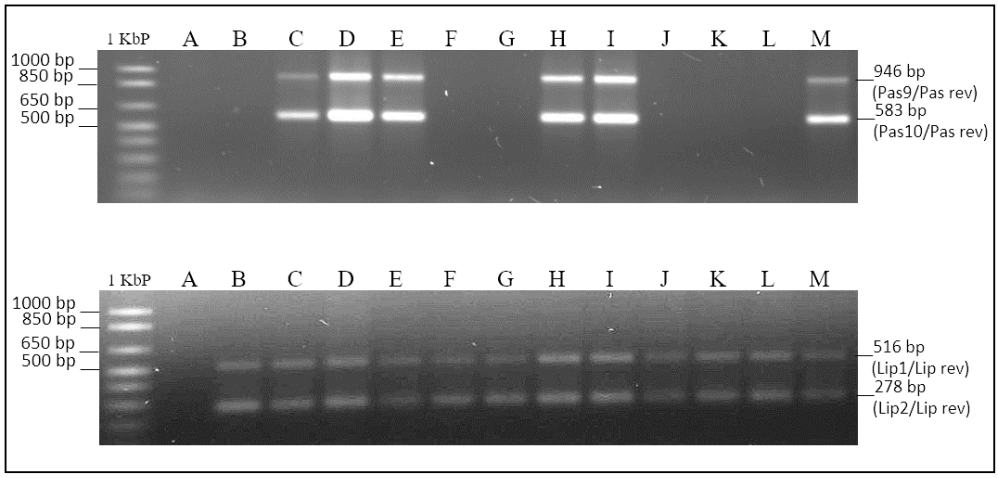

Figure 3.8: Agarose gels showing multiplex PCR screening of presumptive *P. acnes* clinical isolates. 1 KbP, 1 Kb Plus DNA ladder; A, *P. granulosum* ATCC 25564; B, *P. avidum* ATCC 25577; C, *P.acnes* ATCC 6919; D, SD26-3; E, SS27-1; F, SS27-2; G, SS27-3; H, SD27-1; I, SD27-2; J, SD27-4; K, SS29-2; L, SD29-2; M, SS30-1. See Section 2.2.4.1 for PCR and gel electrophoresis conditions.

(i)

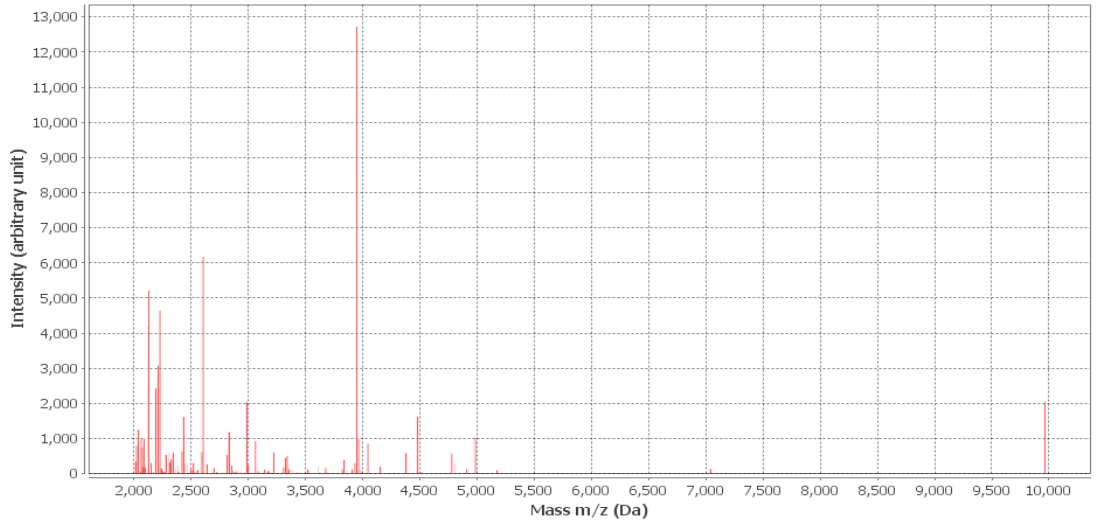

(ii)

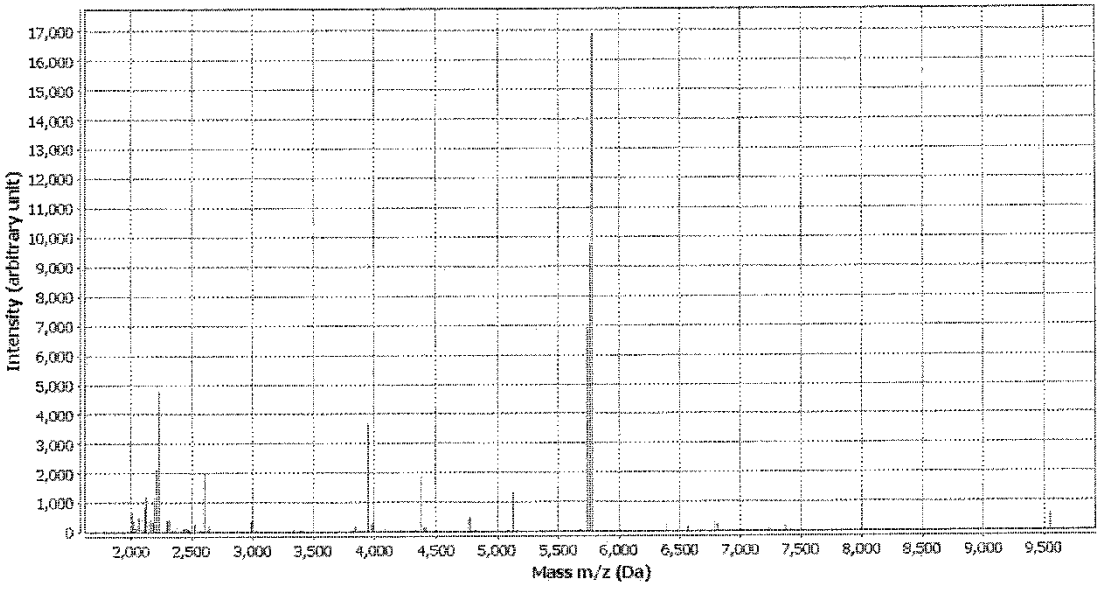

Figure 3.9: Examples of MALDI-TOF results. (i) *P. acnes* ATCC 6919 (positive control), and (ii) *P. avidum* ATCC 25577 (negative control). Note the differences in overall m/z peaks patterns between positive and negative controls and the presence of a distinctive signal at ~4000 m/z in *P. acnes* ATCC 6919.

Table 3.4: Validation of Multiplex PCR results with reference to MALDI-TOF results for identification of *P. acnes* isolates.

		MALDI-TOF		
		+	-	Total
Multiplex PCR	+	50	2	52
	-	3	17	20
	Total	53	19	72
Statistical Analysis Output				
	Sensitivity			0.9615
	Specificity			0.8500
	Positive predictive value			0.9434
	Negative predictive value			0.8947
	Kappa value			0.8240
	SE of Kappa			0.0760

of typing results to follow). Conversely, non-*P. acnes* isolates were neither typable nor sensitive to *P. acnes* bacteriophages.

3.2.1 Classification

P. acnes isolates from Sweden have been typed, previously, by *recA* sequence analysis (Table C.1) (Holmberg *et al.*, 2009). Typing of Canadian isolates was carried out using the PCR-based approach for molecular phylotyping of *P. acnes* isolates, as described in Section 2.2.4.2. Type-specific primers amplified regions of the genome that correspond to sequences known to be exclusive to each type (Table 2.2.1).

The primer set PR213/PR216 targets a sequence within an ABC-type peptide uptake operon of an 8.7 kb region specific only to type IA isolates (GenBank accession no. DQ208967). Type IB isolates were identified based on amplification with primer sets PR256/PR257 and PR256/PR257(G) wherein a nucleotide substitution, T→G at position 17, was introduced within the reverse primer sequence based on analysis of alignment with known *P. acnes* sequences. These primer sets amplify the nucleotide sequence encoding a putative Y40U fragment, which is divergent from type IA and not present or varies considerably in type II. Primer set PR245/PR247 amplifies a region within gDNA coding for two rearrangement hotspot (RHS) family proteins, which function to promote genetic diversity by genomic rearrangement (Jackson *et al.*, 2009; Tomida *et al.*, 2013). Type II isolates were distinguishable from IA and IB isolates due to an approximate 3450 base pair deletion within this region (Shannon *et al.*, 2006a). Types were distinguished by detection of PCR products with lengths of 584 bp (type IA), 725 bp (type IB) and 537 bp (type II) (Figure 3.10; Figure 3.11).

(i) Primer genome targets for amplification of phylotype IA specific amplicon and the expected amplified fragment size (bp)

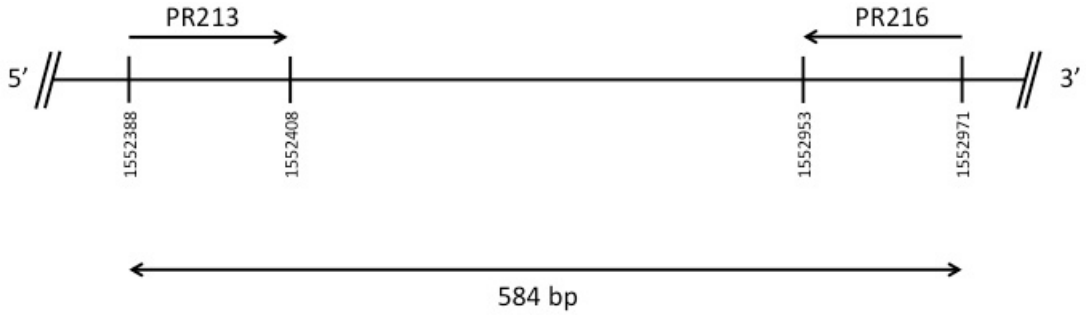

(ii) Primer genome targets for amplification of phylotype IB specific amplicon and the expected amplified fragment size (bp)

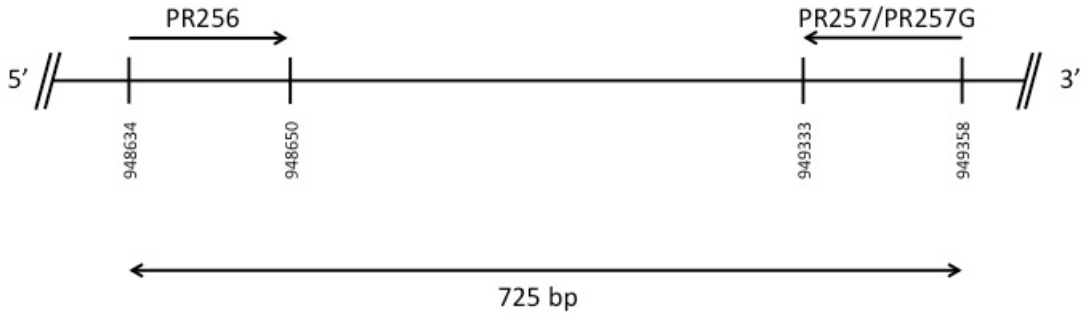

(iii) Primer genome targets for amplification of phylotype II specific amplicon and the expected amplified fragment size (bp)

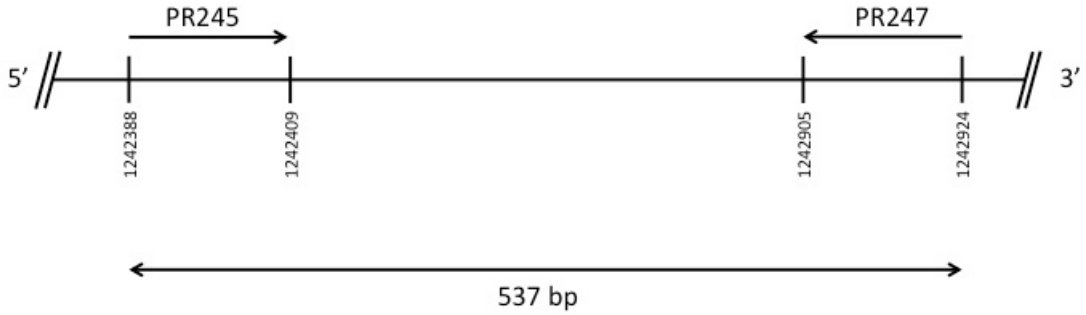

Figure 3.10: Primer targets for PCR-based phylotyping of *P. acnes* clinical isolates. Alignments are based on the following reference strains: (i) *P. acnes*33 (type IA; GenBank accession no. CP003195); (ii) *P. acnes* KPA171202 (type IB); (iii) *P. acnes* ATCC 11828 (type II; GenBank accession no. CP003084).

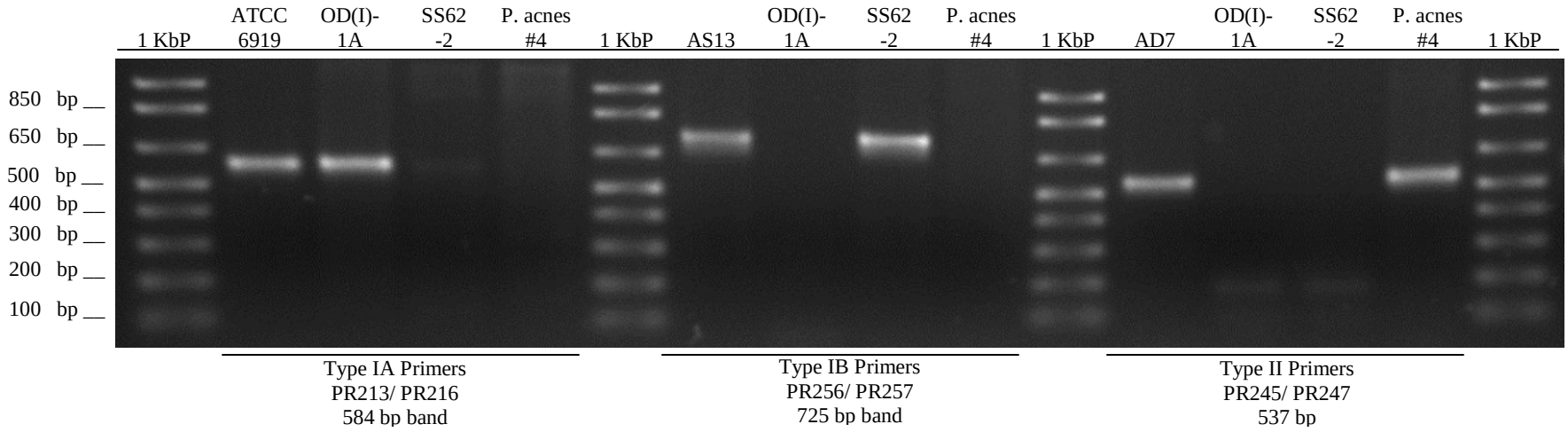

Figure 3.11: Agarose gel showing PCR phylotype screen of *P. acnes* clinical isolates. 1 KbP, 1 Kb Plus DNA ladder. *P. acnes* Type IA positive control: ATCC 6919; *P. acnes* Type IB positive control: AS13; *P. acnes* Type II positive control: AD7. See Section 2.2.4.1 for PCR and gel electrophoresis conditions.

Table 3.5: Distribution of *P. acnes* isolate phylotypes across a variety of sources and geographical origins.

Collection	Isolates	Sample Origin	Isolates	Type IA	Type IB	Type II
NML	11	Superficial infection	2	0	1	1
		Deep tissue infection	3	2	0	1
		Systemic	6	3	2	1
Sweden	45	Skin surface, non-lesional (AS)	28	14	8	6
		Deep tissue infection (AD)	17	9	3	5
Sudbury	110	Skin surface (SS)	45	37	7	1
		Lesion exudate (SD)	65	55	7	3
Ottawa	56	Skin surface (OS)	19	17	0	2
		Lesion exudate (OD)	37	34	1	2

The distribution of *P. acnes* phylotypes is given in Table 3.5. With an overall representation of 77.03%, the greatest proportion of isolates from each group was type IA. Type IB isolates represented 13.06% of the combined collections, followed by 9.91% type II isolates. *P. acnes* type IA isolates comprised 51.11% of the Swedish collection, followed by equal proportions of type IB and type II isolates (both 24.44%). Similarly, 45.45% of NML *P. acnes* isolates were type IA, followed by equal proportions of type IB and type II isolates (both 27.27%). Type IA isolates represented 83.64% and 91.07% of the Sudbury and Ottawa collections, respectively. From Sudbury, type IB isolates (12.73%) represented a larger proportion of the collection than type II isolates (3.64%). Conversely, type II isolates (7.14%) of the Ottawa collection represented a larger proportion of the collection compared to type IB isolates (1.74%). Unequal distribution of *P. acnes* phylotypes across both Sudbury and Ottawa populations was determined to be significant by chi-square analysis ($p<0.001$ for both).

Contigency tables were used to assess the independence of *P. acnes* phylotype from sampling source (lesion surface versus lesion exudate) for Sudbury and Ottawa collections. Results indicate that isolate phylotypes from both Sudbury and Ottawa collections were independent of the sampling source ($p=0.633$ and $p=0.612$, respectively). Therefore, there was no bias for phylotype distribution among samples from either the lesion surfaces or exudates.

Antibiotic susceptibility of *P. acnes* isolates are given in the following section 3.2.2. Contingency tables were used to assess the independence of *P. acnes* antibiotic resistance to one or more antibiotics from phylotype. Results indicate that *P. acnes* resistance to one

or more antibiotics is independent of phylotype for both Sudbury (p=0.316) and Ottawa (p=0.836).

3.2.2 Antibiotic susceptibility of clinical *P. acnes* isolates

Susceptibility of Sudbury, Ottawa and Lund *P. acnes* isolate collections (211 total *P. acnes* isolates), to a panel of clinically-relevant antibiotics was determined. Fourteen antibiotics, commonly indicated for treatment of superficial, deep tissue and systemic *P. acnes* infections, were selected for testing. Choice of antibiotics for treatment of acne included AZ, CM, DC, EM, MC, TC and TS (Tan & Tan, 2005). Preferred antibiotics for treatment of deep tissue infection are PGL, TXL or combination therapy using VA and RI (Brook, 2002; Levi *et al.*, 1997; Osmon *et al.*, 2013; Schreffler *et al.*, 2002; Viraraghavan *et al.*, 2004). Alternatives include CM, DPC, DC, EM, LE, LZ, MC, TC or VA (Brook, 2002; Olsson *et al.*, 2012; Osmon *et al.*, 2013; Portillo *et al.*, 2013).

P. acnes isolates susceptibility to the abovementioned antibiotics was assessed by first determining the MIC values by Etest, then by evaluating the MIC values against the clinical breakpoints listed in Table D.1. As described in Section 2.2.4.3, Etest strips impregnated with a concentration gradient of antibiotic, were laid over *P. acnes*-swab spread on agar medium. Antibiotic activity against *P. acnes* was visualized by the appearance of an ellipse-shaped zone of inhibition, a result of antibiotic diffusion from Etest strips through agar medium (Figure 3.12).

Endpoint MIC values were read according to Etest guidelines (bioMérieux, 2012a). Shown in Figure 3.12, the values printed on the front of the strips, indicated the antibiotic MIC at standard-two fold dilutions, as well as midpoint values. MIC values were read at

the point of intersection between the strip and the zone of inhibition (ellipse). MIC values of antibiotics having a bactericidal mode of action were read at the point of complete inhibition. Endpoints of antibiotics having a bacteriostatic mode of action were read at 80% inhibition, except linezolid which was read at 90% inhibition (bioMérieux, 2012a).

In accordance with Etest protocol, quality control measures were implemented. Strip performance was confirmed by achievement of acceptable MIC values for the standard strains *E. faecalis* ATCC 29212, *S. aureus* ATCC 29213 and *S. pneumoniae* ATCC 49619 (bioMérieux, 2013). *Propionibacterium acnes* strain ATCC 6919 was used routinely as an internal quality control.

Erythromycin and azithromycin

Overall, the highest frequencies of resistance observed were to antibiotics of the macrolide class. Of the whole isolate population, 19.9% were resistant to EM; closely followed by AZ with an overall frequency of 18.6%. The proportion of EM-resistant isolates from Sudbury was 2.3-fold and 4.3-fold greater than that of the Ottawa and Lund collections, respectively (p=0.002). A similar pattern was observed for resistance against AZ, with Sudbury having a frequency of resistance 2.5-fold and 4.1-fold greater when compared to Ottawa and Lund, respectively (p=0.003).

Clindamycin

Subsequent to macrolide resistance, 11.7% of isolates demonstrated resistance to CM, an antibiotic of the lincosamide class. Sudbury isolates have over two-fold higher frequency of CM resistance (16%) in comparison to those from Ottawa (7.3%) and from Lund (6.7%) (p=0.129) (Table 3.6).

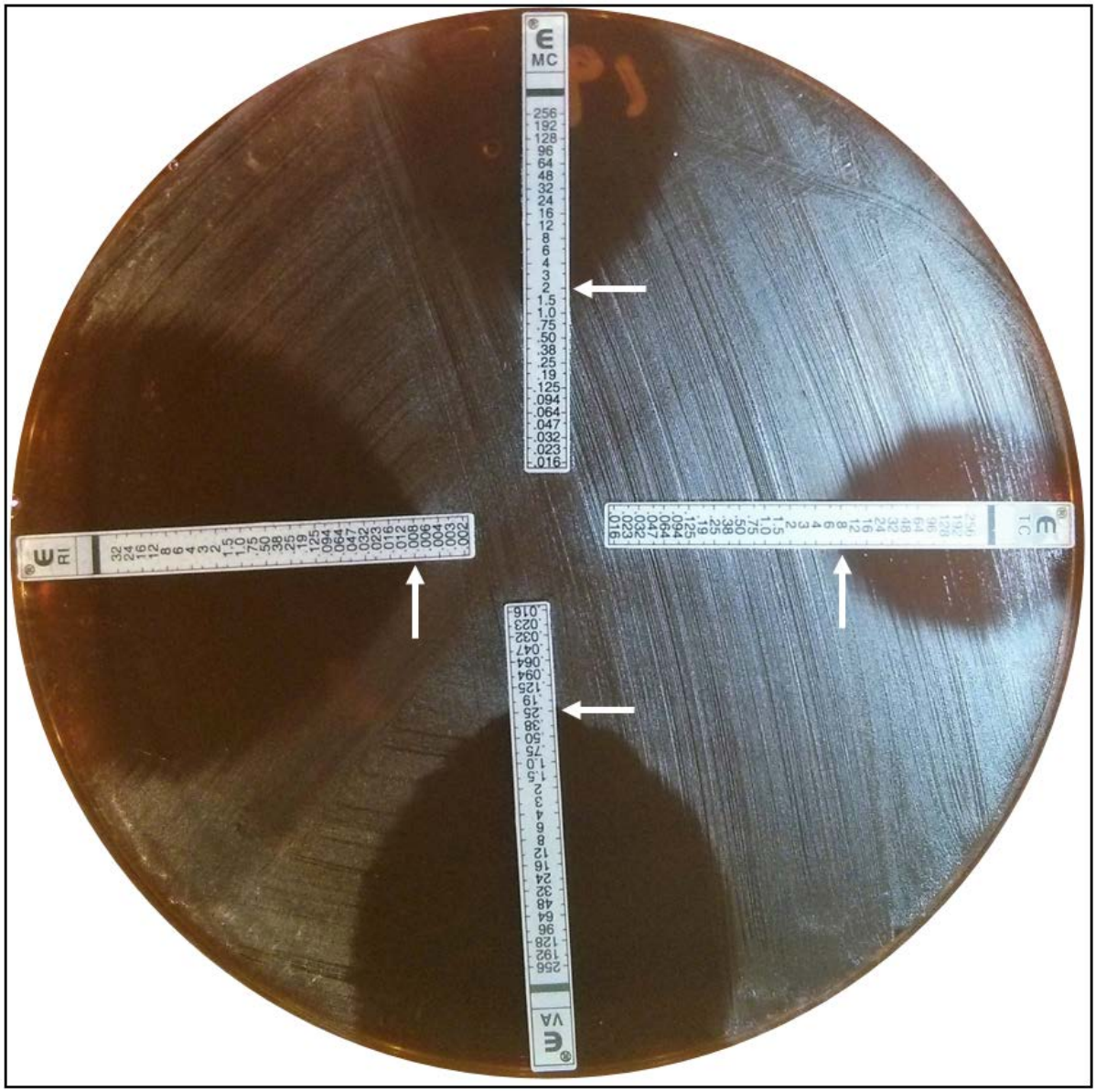

Figure 3.12: Sample photograph of antibiotic susceptibility test results for *P. acnes* clinical isolate SS18-2, from Sudbury. Etests were performed as described in Section 2.2.4.3; shown here are MC, TC, VA and RI. MIC values taken for susceptibility interpretation are shown in µg/mL.

Tetracycline, doxycycline and minocycline

P. acnes isolates, having TC MIC values extending beyond the clinical breakpoint value, were classified as “intermediate” or “resistant” (Table D.1). None of the Lund isolates were TC-resistant, however isolates from Ottawa (8.9%) and Sudbury (5.5%) did exhibit TC-resistance with a 1.6-fold difference in frequency with no significant difference (p=0.132). The proportion of “intermediate” isolates from Lund (4.4%) closely resembled those from Sudbury (4.5%) and Ottawa (5.4%) (p=0.968).

Similar patterns of resistance against MC and DC was observed across all three *P. acnes* isolate collections (Table 3.6). The proportion of MC-resistant Ottawa isolates (14.3%) was at least 2-fold greater than those from Sudbury (7.3%) and Sweden (p=0.026). The frequency of Ottawa isolates that exhibited DC resistance (14.3%) was at least 2.2-fold larger compared with those from Sudbury (6.4%) and Lund (p=0.019).

Rifampicin and Trimethoprim/sulfamethoxazole

The lowest frequencies of antibiotic resistance were observed for RI and TS, each accounting for 0.5% of the total isolate population. Resistance to RI was observed for one *P. acnes* isolate of the Lund collection (2.2%); and resistance to TS was observed for one isolate from the Ottawa collection (1.8%).

Overall resistance among three collections

Overall, 21.3% of *P. acnes* isolates from Sudbury, Ottawa and Lund combined were resistant to a minimum of one antibiotic from the panel. The overall frequencies of resistance, including isolates with intermediate MIC values, are listed in the final column of Table 3.6. The overall frequency is based on the total number of Etests performed on

isolates across each collection and includes only tests with antibiotics indicated in the table. The frequency of Sudbury *P. acnes* resistant isolates was 12%, which was 1.3-fold larger than 9.4% of Ottawa isolates and 3.6-fold larger than Lund isolates with the lowest frequency of resistant isolates at 3.3% ($p=0.0005$).

Multiplicity of resistance

Overall frequencies of singly- and multiply-resistant isolates are shown in Figure 3.13a and are further stratified on the basis of geographical origins in Figure 3.13b. Overall, only 2.2% of the antibiotic resistant *P. acnes* isolate population were resistant to one antibiotic (Ottawa collection); and 97.8% were clustered into categories of resistance to multiple antibiotics with the majority of isolates resistant to 2 or 3 antibiotic types (64.4%) (Figure 3.13a). The highest proportion of multiply-resistant *P. acnes* isolates is from Sudbury (71.1%), followed by Ottawa (22.2%) and Lund (6.7%) (Figure 3.13b). Isolate collections from Sudbury, Ottawa and Lund demonstrated patterns of multiple resistances that are significantly different from one another ($p<0.001$). Out of the overall proportion of isolates that were resistant to 2 or 3 antibiotics 82.8% were from Sudbury, accounting for over half of all resistant Sudbury isolates, followed by 10.3% and 6.9% from Ottawa and Lund, respectively (Figure 3.13b). With a frequency of 9%, isolates with resistance to 5 antibiotics are exclusively from Sudbury. Out of the overall proportion of isolates that were resistant to 4 or 6 antibiotics 54.5% were from Ottawa, followed by 36.4% and 9.1% from Sudbury and Lund, respectively (Figure 3.13b).

Table 3.6: Incidence of antibiotic resistance across *P. acnes* isolates from Sudbury, Ottawa and Lund. Observed resistance was limited to the antibiotics listed in this table; *P. acnes* isolates were susceptible to all other antibiotics tested.

	Type of Antibiotic Resistance									
P. acnes collection	EM	AZ	CM	TC	TC (I)[1]	MC	DC	RI	TS	Overall[2]
Sudbury	29.1	27.3	16.0	5.5	4.5	7.3	6.4	0.0	0.0	12.0 (876)
Ottawa	12.5	10.9	7.3	8.9	5.4	14.3	14.3	0.0	1.8	9.4 (446)
Lund	6.7	6.7	6.7	0.0	4.4	0.0	0.0	2.2	0.0	3.3 (360)
Overall	19.9	18.6	11.7	5.2	4.7	7.6	7.1	0.5	0.5	9.5 (1682)

EM, erythromycin; AZ, azithromycin; CM, clindamycin; TC, tetracycline; MC, minocycline; DC, doxycycline; RI, rifampicin; TS, trimethoprim/sulfamethoxazole.

[1] Value represents proportion of total isolates that expressed intermediate, "I", MIC values.

[2] Bracketed value represents the total number of individual antibiotic/isolate tests performed with the antibiotics given in the table.

Antibiotic exposure

Frequencies of acne-related antibiotic exposure corresponding to *P. acnes* isolates from Sudbury and Ottawa are represented in Figure 3.14. The proportion of antibiotic resistant isolates from Sudbury patients treated with one or more antibiotics (96.8%) was 2.3-fold greater than Ottawa (40%) ($p<0.001$).

Based exclusively on acne-related antibiotic exposure data, outcome of resistance among *P. acnes* isolates from Sudbury and Ottawa was associated with overall antibiotic exposure ($p<0.001$). Single or combined exposure to antibiotics interfering with the 23S rRNA—EM and/or CM—was associated with *P. acnes* isolate resistance to CM ($p=0.0280$), AZ ($p=0.0052$) and EM ($p=0.0019$). A positive correlation was also identified between the overall frequency of isolate resistance and exposure to antibiotics that interfere with the 16S rRNA—TC, MC and/or DC ($p=0.0233$).

3.3 *Propionibacterium acnes* bacteriophage library

3.3.1 Phage isolation

Seventy of the *P. acnes* phages in this study were from a collection that was isolated previously by Jelena Trifkovic, from sewage sources in Ottawa and Gatineau via agar overlay method (Section 2.2.5) using bait strains ATCC 6919, ATCC 29399 and NML *P. acnes* strains #1 through strain #6 (Table C.1). Five cutaneous phages were isolated from one patient in Sudbury, ON (Section 2.2.5) and evolutionary derivation approach was used to isolate a single phage variant with extended host range (Section 2.2.7). To isolate lytic phages, attention was paid to select phages producing clear plaques, as shown in Figure 3.15.

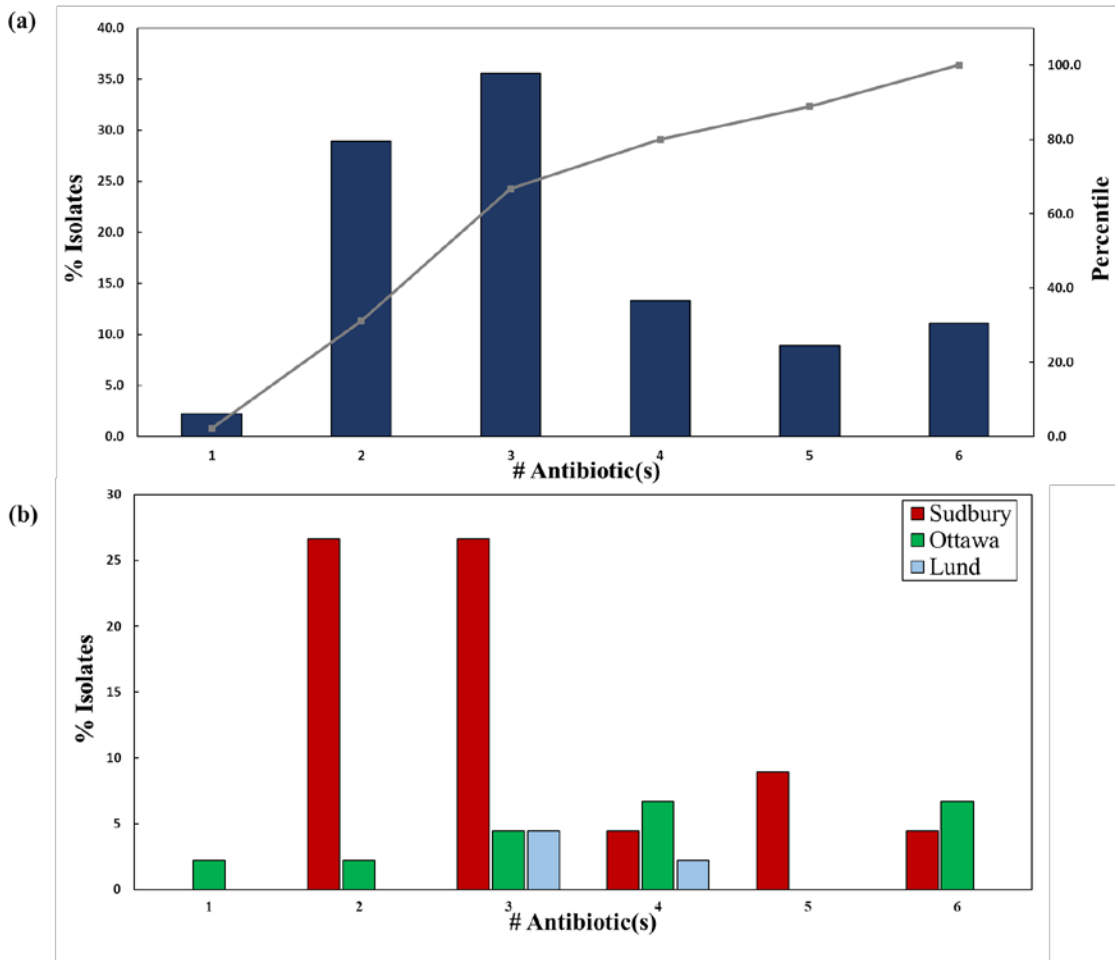

Figure 3.13: Multiplicity of antibiotic resistance among resistant *P. acnes* clinical isolates from Sudbury, Ottawa and Lund. Overall frequency of multiply-resistant isolates (a); stratified by geographical origin (b). Columns represent the frequency of isolates that have antibiotic MIC values above clinical breakpoint(s) and/or have intermediate MIC values (only tetracycline).

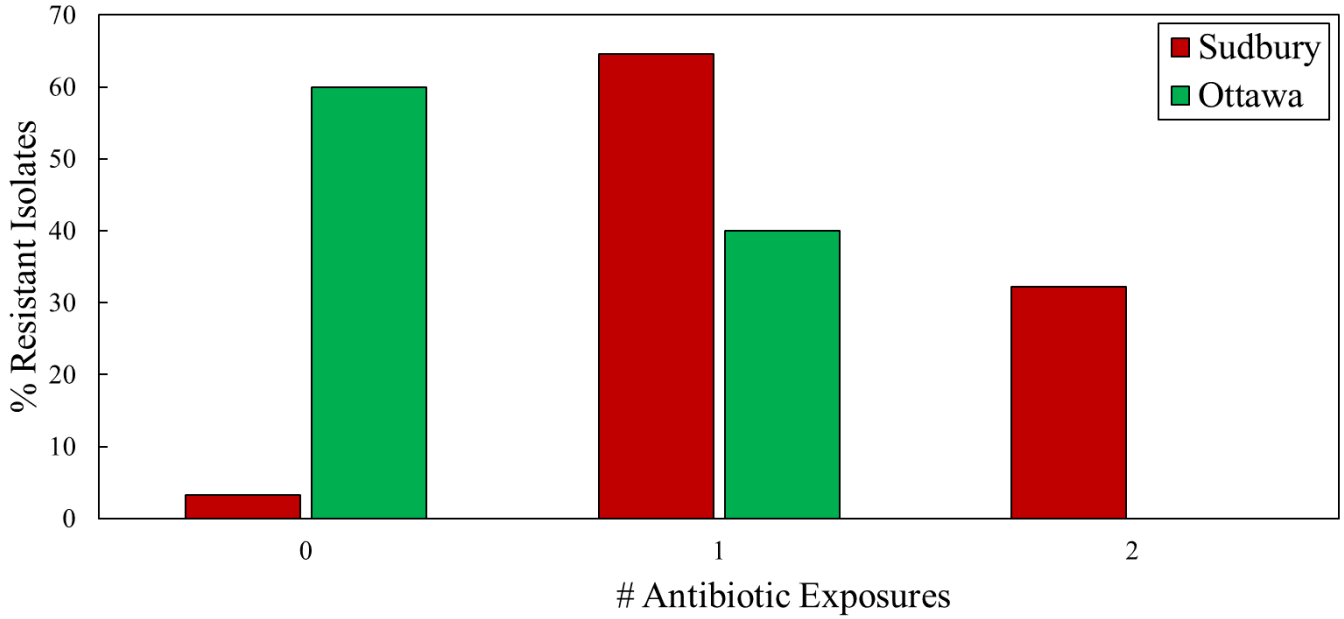

Figure 3.14: Frequency of Sudbury and Ottawa *P. acnes* isolates from patients treated with 0, 1 or 2 antibiotics.

Figure 3.15: Photograph of clear plaques formed by *P. acnes* #3 infection with πα33 via agar overlay method.

3.3.2 Morphological characterization of phage virions

To determine bacteriophage morphology, transmission electron micrographs were acquired as described in Section 2.2.6. On the basis of previous reports of *P. acnes* phage morphology (Farrar *et al.*, 2007; Lood *et al.*, 2008; Marinelli *et al.*, 2012; Webster & Cummins, 1978), all phages visualized were classified as members of the siphoviridae family of phages (Ackermann & Eisenstark, 1974). TEM imaging showed that they have non-enveloped icosahedral heads and long non-contractile tails with tail fibers extending from the tails (Figure 3.16). Dimensions of phages imaged in this study were comparable to those reported by others and similar to one another, having a mean (n=7) head diameter of 54.6±7.2 nm and mean tail length and diameter of 133.1±10.2 nm and 11.2±3.2 nm, respectively (Figure 3.16).

3.3.1 Biological activity of the bacteriophage library against *P. acnes* isolates

As described in Section 2.2.7, *in vitro* biological activity of the phage library was assessed by evaluating phage host range through high throughput spot infection tests against each *P. acnes* isolate. Phage stocks were titred prior to infection to ensure sufficient PFU/mL for infection by pin drop. *P. acnes* ATCC 6919 exhibited 100% sensitivity to all phage isolates and was employed as a positive control to monitor test conditions. The example of a spot infection test shown in Figure 3.17a demonstrates the appearance of clearance zones surrounding inoculation spots on agar plates, which were taken as a positive result, indicating successful infection of the bacterial isolate by the phage in question.

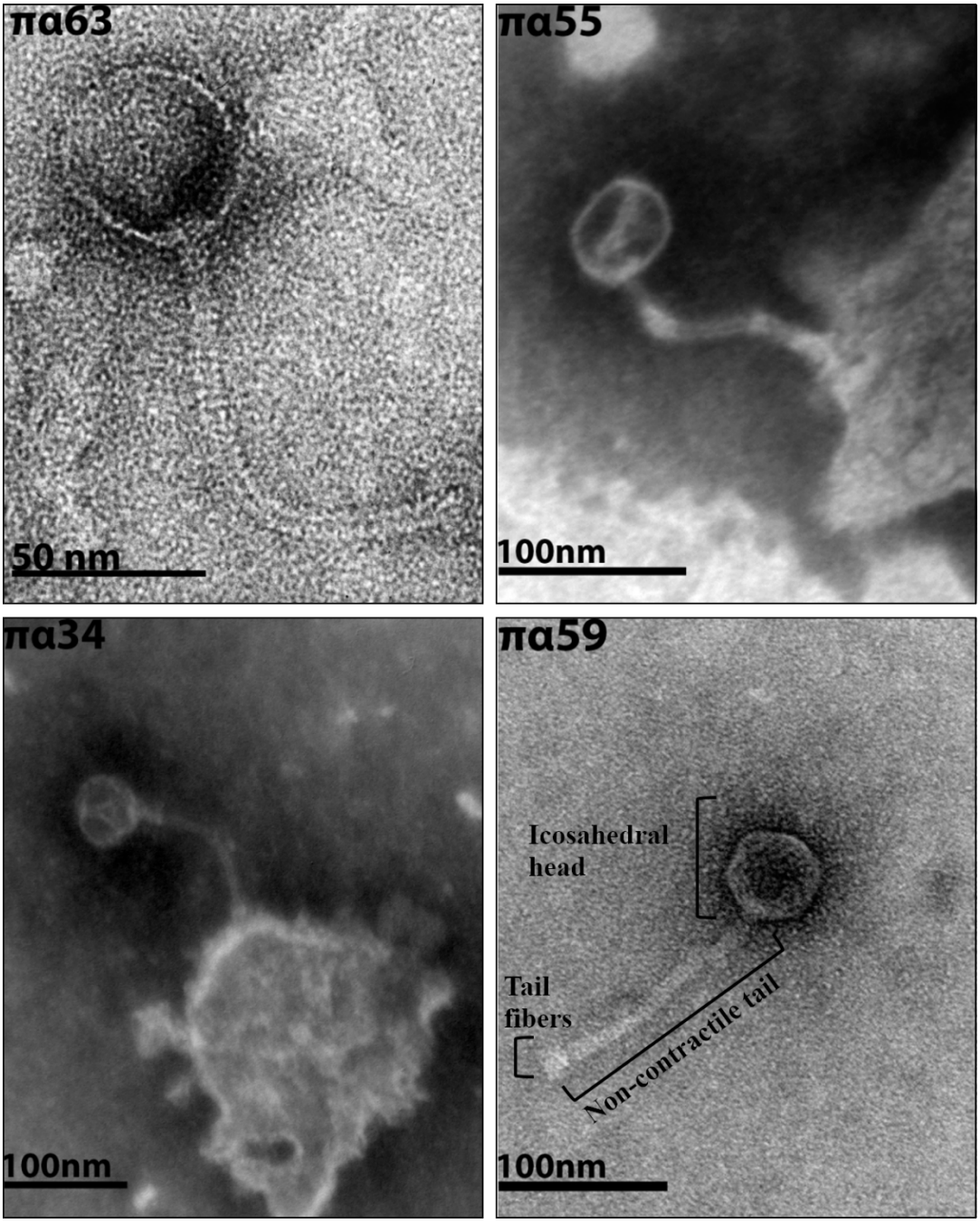

Figure 3.16: Transmission electron micrographs of negatively stained *P. acnes* phages πα34, πα55, πα63 and πα59. All phages belong to siphoviridae.

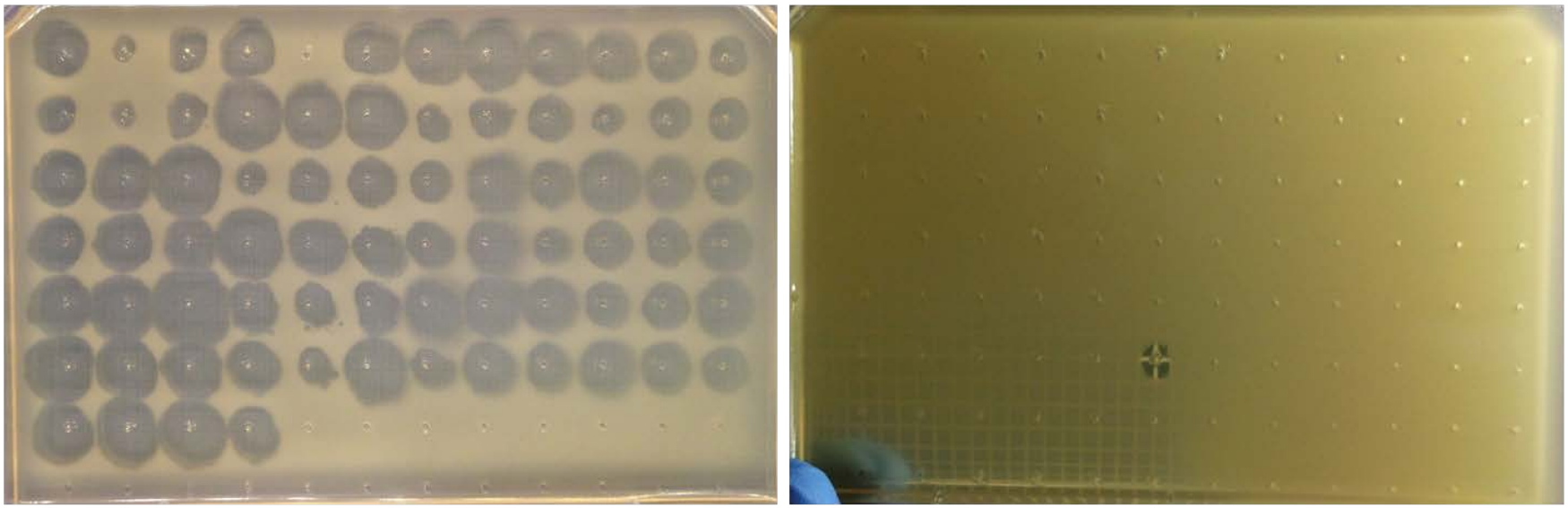

Figure 3.17: High throughput bacteriophage spot infection tests of (a) *P. acnes* ATCC6919 (100% phage sensitivity) and (b) P. acnes #9 (sensitivity to mutant phage *πα*9-6919-4). Spot infection tests were used to determine biological activity of phage collection against *P. acnes* clinical isolate population.

Infection test results were tabulated for each *P. acnes* isolate /phage combination; successful infections were denoted by "+" and unsuccessful infections by "-" (Figure 3.18). Phage host range was characterized by the number of *P. acnes* isolates that were susceptible to infection by a particular phage. Phages with identical host ranges were clustered into host range groups (HRGs) consisted of 9 (HRG1), 8 (HRG2), 4 (HRG3) and 2 (HRG4) phage isolates, possibly representing multiple isolates of similar phages. The rest of the phages showed unique host range profiles that were different from the phages grouped by host range. Rows in the phage-host interaction matrix (Figure 3.18) represent phage host range across the entire *P. acnes* population; host ranges were diverse across the various HRGs and other unique phage isolates. The overall maximum phage host range was 99.6% and the minimum was 78.1% with a median of 97.5%. Frequency analysis of phage host ranges (Figure 3.19a) was skewed to the left and revealed that 86.8% of phages could infect greater than 90% of the *P. acnes* isolate population. Therefore, a large proportion of phages were capable of infecting a large proportion of the *P. acnes* isolate population (Figure 3.19a). Despite diversity across the phage host range profiles (Figure 3.18), the phage collection exhibited a propensity for infection of a wide range of *P. acnes* isolates.

Each column of Figure 3.18 represents *P. acnes* isolates sensitivity to the phage collection. *P. acnes* isolates with identical sensitivities were stratified into one of the nine phagovar groups (PVGs), while those with unique sensitivity profiles are shown separately. Belonging to PVG1, 67.9% of *P. acnes* isolates demonstrated maximum sensitivity to 100% of phages and isolates of PVG2-PVG9 showed sensitivity to phages

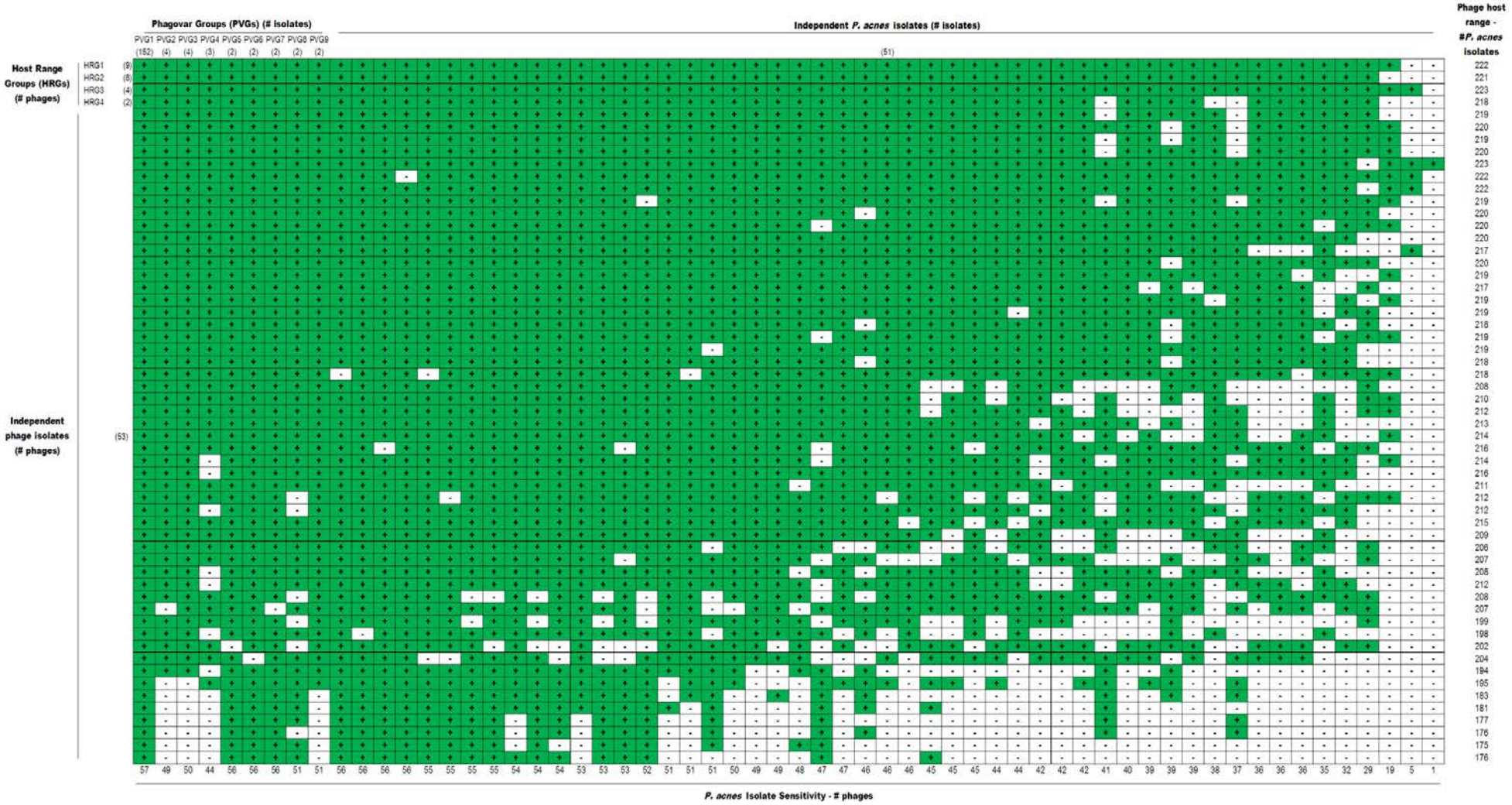

Figure 3.18: Matrix representation of phage-host interactions. Columns correspond to *P. acnes* hosts and include isolates belonging to phagovar groups (PVGs) 1 to 9 and those not belonging to PVGs (isolates with unique phage sensitivity profiles). Rows represent bacteriophages falling into specific host range group (HRG) categories 1 to 4 and phages with unique host range profiles. Green "+" cells indicate successful infection and white "-" cells denote an absence of infection.

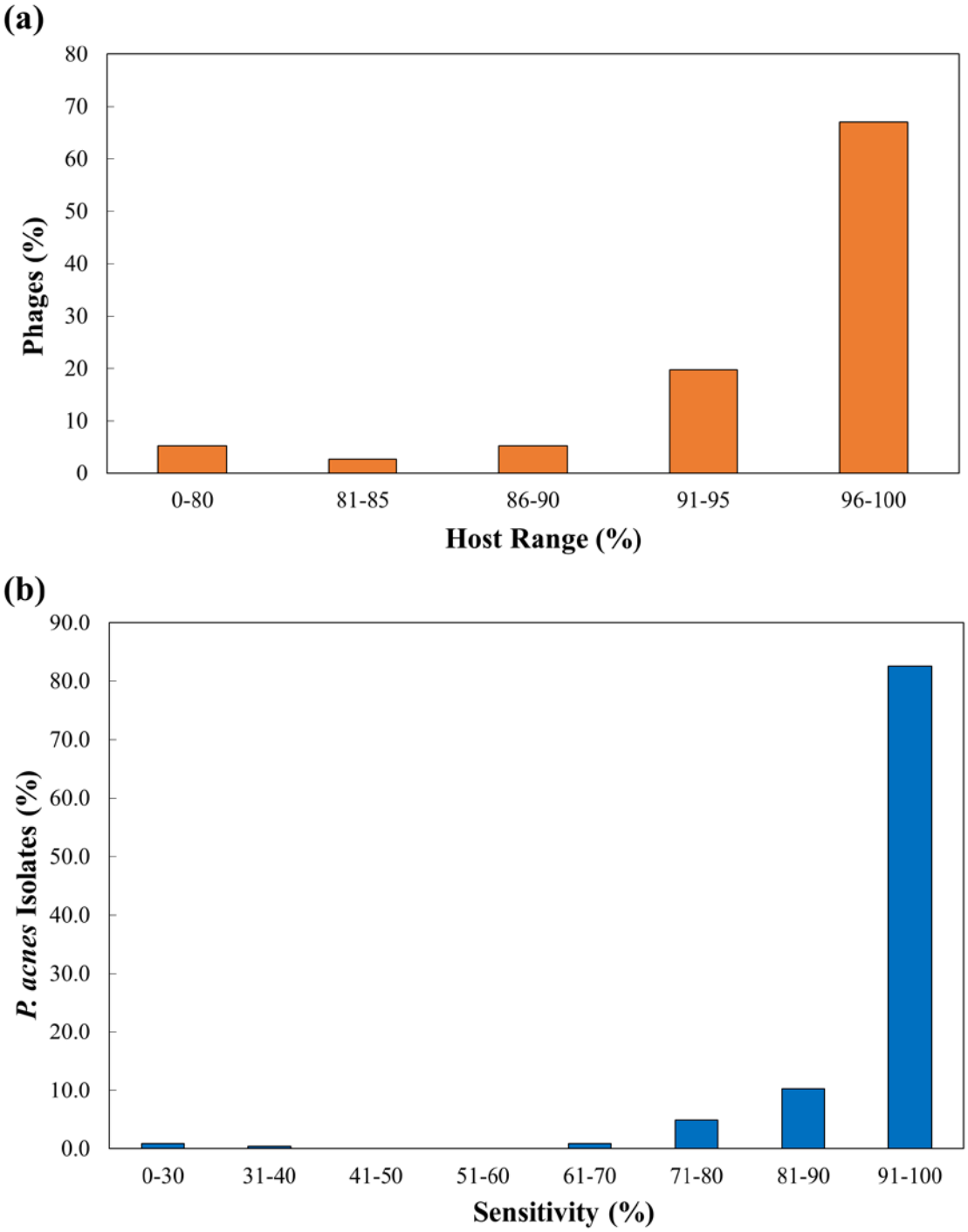

Figure 3.19: Frequency distribution of (a) phage host range (propensity of phages to infect *P. acnes* isolates) and (b) sensitivity of the *P. acnes* isolate collection (susceptibility to phage infection).

in the range of 77% to 98% (Figure 3.18). Frequency distribution of *P. acnes* isolate sensitivity to phages was skewed to the left and revealed 82.6% of *P. acnes* isolates were sensitive to greater than 90% of phages (Figure 3.19b). Although sensitivity of bacteria to a greater number of phages and broad host range of the phages are favorable for formulation of numerous phage cocktails, it does not necessarily provide an immediate solution to naturally occurring phage resistant bacteria. However, given the dynamism of phage-bacteria interplay it is possible to isolate mutant phages from the existing stocks that counter the naturally resistant bacteria. For example, initially, *P. acnes* #9 (Table C.1) exhibited natural resistance to all isolated phages. Evolutionary derivation approach was followed to isolate a mutant phage from an existing phage stock with a broad host range (i.e. πα6919-4 phage). A sample of *P. acnes* #9 overnight culture in CB broth was mixed with πα6919-4 stock at MOI of ~1000 followed by incubation at RT for 15 min. Agar plate overlay method was utilized to isolate a limited number of mutant phage plaques (total of 7 plaques). A single plaque was removed and processed as described in Section 2.2.5. High throughput spot infections were repeated in duplicate using all phage isolates (including the newly-isolated mutant phage, "πα9-6919-4") against *P. acnes* #9. As anticipated, *P. acnes* #9 was infected exclusively by the mutant phage, and the host range of the isolated phage was expanded to include strain #9 (Figure 3.17b).

In conclusion, phage libraries showed overlapping broad host ranges and the bacterial isolates were sensitive to multiple phages, which is advantageous to formulation of multiple phage cocktails.

3.4 Molecular characterization of bacteriophages

3.4.1 Restriction enzayme analysis of phage genomes

A basic evaluation of the genomic diversity across *P. acnes* phages was carried out using DNA fragment patterns produced by *Bam*HI restriction digest of phage DNA (n=64). Included were 88.7% of phages that had unique host range profiles as well as representatives from all HRGs, accounting for 77.8% of HRG1, 75% of HRG2, 100% of HRG3 and 50% of HRG4. Digestion of phage genomes revealed a diverse array of restriction fragment banding patterns. Phages were grouped into 9 clusters (Figure 3.20) based on analysis of their *Bam*HI restriction patterns (Section 2.2.8.3). Within the clusters were phages that had unique host range profiles as well as those associated with one or more HRGs; therefore, the biological activity varied between individual phages representing any single cluster. Analysis of the *Bam*HI digested genomes from phages within separate HRGs and having unique host range profiles revealed banding patterns that were diverse as well as sets of identical banding patterns. For example, although phages πα15 and πα615 have identical banding patterns, they do not share identical host range activity. However, phages πα33 and πα3-SS3-1 have both identical banding patterns and host range activity. Diversity was also observed across banding patterns produced from genomes of the phages having unique host range profiles, however, sets of identical fragment sizes were also observed. For example πα32 and πα315 exhibit different banding patterns and host range activity, while πα33 and πα314 have different banding patterns and the same host range activity. Therefore, the overall biological activity across the collection of *P. acnes* phage isolates is not represented by that of the restriction fragment banding patterns. Diversity among *Bam*HI restriction patterns is an indication of diversity across phage genomes, therefore, representatives from various clusters (Figure 3.20) were selected for genome sequencing.

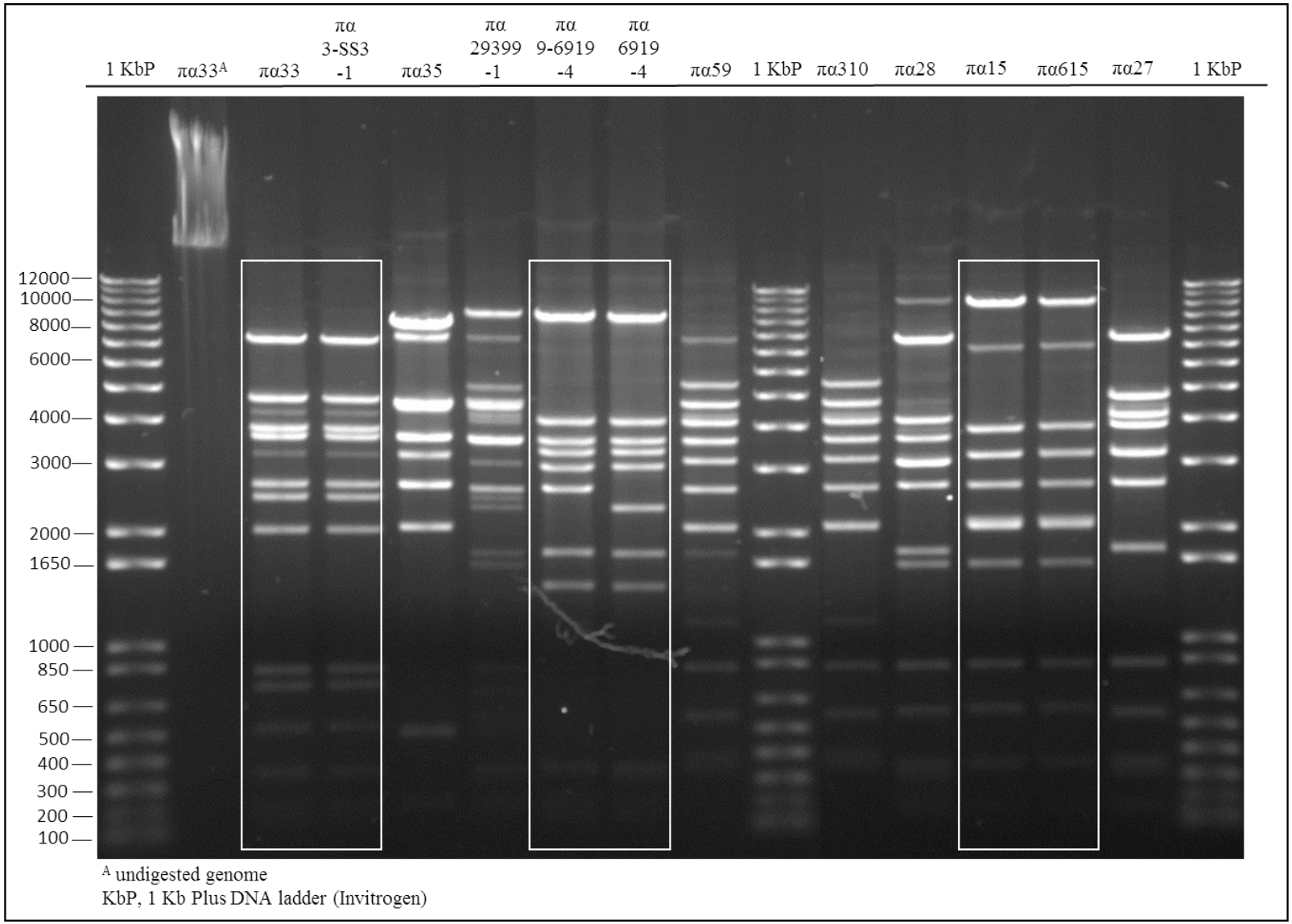

Figure 3.20: DNA gel electrophoresis of *Bam*HI digested *P. acnes* phage DNA. Representatives (n=12) from 9 *Bam*HI digested phage genome clusters are shown here (Section 3.4.1). Digested phage genome banding patterns within the white boxes appear to be identical and are grouped into a common cluster. Other unboxed DNA banding patterns belong to phage grouped into separate clusters.

3.4.2 Genome sequencing of bacteriophages

Twelve phages (Figure 3.20) were further characterized for their genomic and proteomic properties as described in Section 2.2.8.4. At the time of this report, sequence analysis was based on genomic sequence reads produced by the Ion PGM System and were restricted due to gaps and unresolved bases present in the sequence assemblies (Table 3.7). Extensive genomic analysis will be made possible by correction of inaccuracies using sequence reads recently produced by two additional platforms—MinION (Health Sciences North Research Institute) and Illumina HiSeq (McGill University and Génome Québec Innovation Centre).

A summary of sequencing and assembly results are presented in Table 3.7. Having an average coverage between 22.66 to 222.47 reads per base, each genome was assembled into one contig using MIRA v4.0.2 (Chevreux *et al.*, 1999) against reference genome of *P. acnes* phage PA6 (Farrar *et al.*, 2007). Length of the assembled genomes ranged from 29539 to 29891 base pairs, having 53.8% to 54.5% GC-content and an average of 42 open reading frames (ORFs) (Table 3.7).

3.4.2.1 Genome structure and annotation

Genome sequences provided sufficient information for functional annotation of approximately half of all gene products via Prokka pipeline v 1.11 (Seemann, 2014) using a database of 84 *P. acnes* phage reference sequences (Table E.1) according to Section 2.2.8.4.2. Sequenced phages were determined to be members of siphoviruses (TEM images) with linear dsDNA genomes based on the sequence homology searches. A summary of functional annotations for predicted gene products (gp) of sequenced phages

Table 3.7: General features and sequencing details of *P. acnes* bacteriophage genomes.

Phage ID	Genome Length (bp)	GC-Content (%)	Coding DNA (%)	Genes	Average Coverage	Unresolved Bases	Assembly Gaps
πα15	29539	54.24	87.17	46	88.44	0	1
πα27	29740	53.85	86.76	43	222.47	109	4
πα28	29762	54.18	83.85	41	65.12	119	3
πα33	29712	54.06	82.2	42	33.21	0	1
πα35	29825	54.34	73.54	38	72.53	1221	24
πα310	29724	53.95	83.85	40	36.14	56	1
πα59	29732	54.17	84.59	41	71.46	253	6
πα615	29736	54.41	87.99	47	75.56	472	8
πα6919-4	29728	54.01	84.63	44	22.66	0	2
πα9-6919-4	29891	54.07	84.79	42	55.5	0	2
πα3-SS3-1	29705	54.53	80.14	40	99.75	933	27
πα29399-1	29689	54.38	74.28	40	71.34	636	19

is given in Table 3.8. Although the function of most proteins encoded by ORFs in the right arm remain to be determined, those assigned a putative function are involved in regulatory functions (Table 3.8). Nearly all gene products encoded by ORFs in the left arm of phage genomes have been assigned functions or have properties associated with structure and virion assembly (Table 3.8).

As shown in Figure 3.21, a multiple genomic loci comparison map of all sequenced phages and reference *P. acnes* phage PA6 (Farrar *et al.*, 2007) was created using GUI Easyfig v2.2.2 (Sullivan *et al.*, 2011) to compare and contrast gross genome features. Having an overall organization analogous to other published *P. acnes* phage genomes (Farrar *et al.*, 2007; Lood and Collin, 2011; Marinelli *et al.*, 2012; Liu *et al.*, 2015; Brown *et al.*, 2016), Figure 3.21 illustrates a division of predicted ORFs into two clusters— genes of the right arm (transcribed right to left) and genes of the left arm (transcribed left to right).

Annotated open reading frames in the right arm of *P. acnes* phage genomes encode putative gene products involved in transcription, DNA replication and regulation. Sigma factors facilitate gene transcription by guiding RNA polymerase to promoter sites. A putative protein encoded by ORF equivalent of $orf24_{PA6}$ contains a sigma domain that may coordinate the transcription of phage genes by directing *P. acnes* host RNA polymerase to promoter elements on the phage genome (Farrar *et al.*, 2007). Downstream, putative nucleases are encoded by regions corresponding to $orf27_{PA6}$ and $orf37_{PA6}$. Homologous to proteins of the calcineurin-like phosphoesterase superfamily, $gp27_{PA6}$ is suspected of having nuclease activity associated with DNA repair

Table 3.8: Putative functions of predicted *P. acnes* phage gene products. Phage PA6 gene products are given as reference.

	Putative gene products: left arm of genome (rightward transcription)												Putative gene products: right arm of genome (leftward transcription)				
Phage ID	Terminase small subunit	Terminase large subunit	Portal protein	Head scaffold protein	Major head (capsid) protein	Major tail protein	Tail assembly chaperones	Tape measure protein	Minor tail subunits	Collagen-like protein	Endolysin	Holin	Sigma factor	DNA repair nuclease	DNA primase	DNA helicase	Exonuclease
PA6[A]	gp1	gp2	gp3	gp5	gp6	gp11	gp12,13	gp14	gp15,16,17,18	gp19	gp20	gp21	gp24	gp27	gp31,32	gp34	gp37
πα15	gp1	gp2	gp3	gp5	gp6	gp11	gp12,13	gp14	gp15,16,17,18	gp19	gp20	gp21	gp24	gp27	gp31	gp34,35	gp38,39
πα27	gp1	gp2	gp3	gp5	gp6	gp11	gp12,13	gp14	gp15,16,17,18	gp19	gp20	gp21	gp23	gp26	gp30	gp32	gp35
πα28	gp2	gp2	gp3	gp5	gp6	gp11	gp12,13	gp14,15	gp16,17,18	gp19	gp20	gp21	gp22	gp26	gp30	gp32	gp35
πα33	gp1	gp2	gp3,4	gp6	gp7	gp12	gp13,14	gp15,16	gp17,18,19	gp20	gp21	gp22	gp24	gp27	gp31	gp32	gp35
πα35	gp1	gp2	gp3,4	nk	gp5	gp10	gp11	gp13	gp14,15,16	gp17	gp18	gp19	gp21	gp24	gp26	gp28	gp31
πα59	gp1	gp2	gp3	gp5	gp6	gp11	gp12,13	gp14,15	gp16,17,18,19	gp20	gp21	gp22	gp24	gp27	gp31	gp33	gp36
πα615	gp1	gp2	gp3	gp6	gp7	gp12	gp13,14	gp15,16	gp17,18,19	gp21	gp22	gp23	gp25	gp28	gp33	gp36	gp40
πα6919-4	gp1	gp2	gp3	gp5	gp6	gp11	gp12,13	gp14,15	gp16,17,18,19	gp20,21	gp22	gp23	gp25	nk	gp32	gp34	gp37
πα9-6919-4	gp1	gp2	gp3	gp5	gp6	gp11	gp12,13	gp14	gp15,16,17,18	gp19	gp20	gp21	gp23	nk	gp30	gp31	gp34
πα3-SS3-1	gp1	gp2	gp3,4	nk	gp7	gp12	gp13,14	gp15	gp16,17,18	gp19	gp20	gp21	gp23	gp26	gp29	gp30	gp33
πα310	gp1	gp2	gp3	gp5	gp6	gp11	gp12,13	gp14	gp15,16,17	gp18	gp19	gp20	gp22	gp25	gp29	gp31	gp34
πα29399-1	gp1	nk	gp3	gp5	gp6	gp11	gp12,13	gp14	gp15,16,17	nk	gp18	gp19	gp21	nk	nk	nk	gp32

[A]Farrar *et al*., 2007

"gp", gene product; "nk", not known

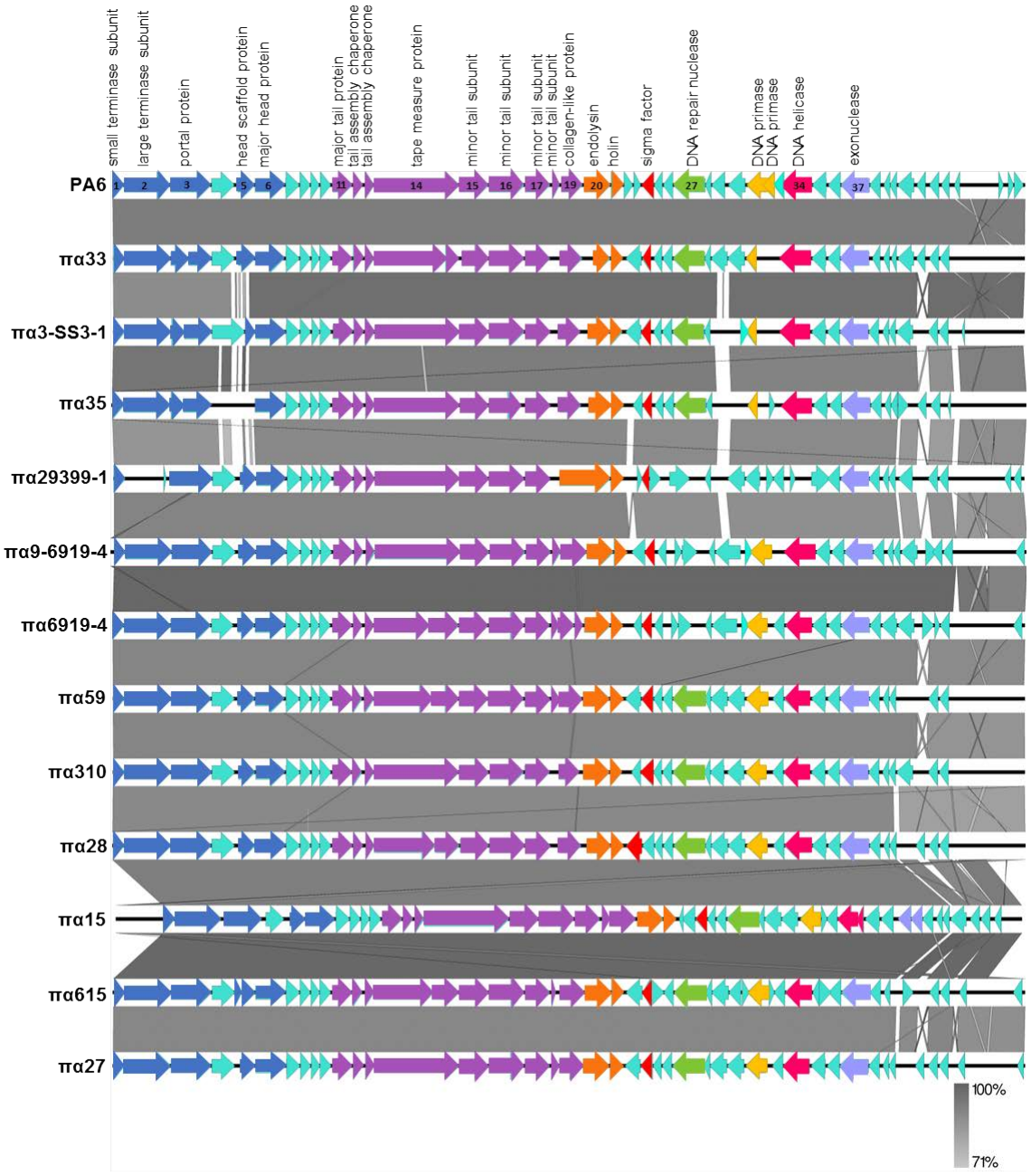

Figure 3.21: Schematic representation of *P. acnes* phage genome assemblies with annotated open reading frames. Dark blue arrows in the left arm of genomes correspond to ORFs encoding putative proteins involved in DNA packaging, and structure and assembly of the capsid. Dark purple arrows represent ORFs that encode products associated with phage tail structure and assembly.

(Aravind & Koonin, 1998), while gp27$_{PA6}$ shares sequence homology with a RecB family exonucleases (Farrar *et al.*, 2007). Putative DNA primase and helicase are encoded by ORFs equivalent to *orf*31-32$_{PA6}$ and *orf* 34$_{PA6}$ and are involved with phage DNA replication (Farrar *et al.*, 2007).

At the left end of all sequenced genomes, *orf*1 and *orf*2 encode putative small and large terminases, respectively. Immediately downstream of *orf*2, a putative portal protein equivalent to gp3 of PA6 (gp3$_{PA6}$) is encoded. The portal protein functions as a gatekeeper by effectively "plugging" the sole entry/exit point of the icosahedral capsid—a single, open vertex. Prior to tail attachment, the terminase proteins unite and interact with the portal protein to drive phage DNA through the portal opening for packaging into the capsid head (Farrar *et al.*, 2007; Fokine & Rossmann, 2014; Sassi *et al.*, 2013). Equivalent to gp5 $_{PA6}$ and gp6 $_{PA6}$, all sequenced phage genomes produce putative head scaffold protein and major head protein, respectively. The head scaffold protein provides a framework for assembly of the head proteins and is likely degraded once the capsid is assembled (Fokine & Rossmann, 2014).

Genes equivalent to *orf*11 $_{PA6}$ through *orf*18 $_{PA6}$, are responsible for construction of the phage tail and are involved in host cell recognition and binding. Minor tail proteins (gp15$_{PA6}$ through gp18 $_{PA6}$) assemble to form the tail tip complex onto which the tape measure protein (TMP; gp14 $_{PA6}$) attaches followed by elongation of the phage tail until the end of the TMP has been reached (Fokine & Rossmann, 2014). Tail assembly chaperones (gp12 $_{PA6}$ and gp13 $_{PA6}$) associate with the tape measure protein (TMP; gp14 $_{PA6}$) to assemble major tail proteins (MTP; gp11$_{PA6}$) around the entire length of the TMP

(Stockdale *et al.*, 2015). Putative minor tail proteins that are thought to be associated with the phage tail structure are encoded by *orf*15 $_{PA6}$ to *orf*18 $_{PA6}$ (Farrar *et al.*, 2007; Lood and Collin, 2011; Marinelli *et al.*, 2012; Liu *et al.*, 2015; Brown *et al.*, 2016). The gene located immediately downstream of the tail-associated ORFs (*orf*19 $_{PA6}$), encodes a putative collagen-like protein that may be involved in structural stabilization of the phage tail or may have a role in host cell attachment (Farrar *et al.*, 2007). Tail-associated structural proteins were independently evaluated for their involvement in host range determination (Section 3.4.2.2).

During the final stages of phage assembly, the capsid and tail structures are joined at the portal-occupied vertex of the capsid (Fokine & Rossmann, 2014). Once progeny phage particles have accumulated, holin (gp21 $_{PA6}$) and N-acetylmuramoyl-L-alanine amidase (gp20 $_{PA6}$) form pores in the host membrane and degrade the peptidoglycan wall, respectively, resulting in host lysis and release of progeny phage (Farrar *et al.*, 2007).

3.4.2.2 Congruence analysis of phage host range activity and protein sequences

The Congruence Among Distance Matrices (CADM) test was used to identify components of the phage tail that act as determinants of phage host range by comparison of distance matrices derived from datasets corresponding to independent protein sequences and host range for all sequenced phages (Section 2.2.9.3.2). Concordance among different types of variables can be identified by the CADM test because the test uses distance matrices (CADM input) derived from individual datasets to calculate concordance statistics (CADM output) (Campbell *et al.*, 2011; Legendre & Lapointe, 2004). Partial or complete congruence of datasets indicate a significant level of mutual

agreement or conformity among the variables associated with the datasets (Legendre & Lapointe, 2004). Therefore, the CADM test is an appropriate method to determine existing relationships between different types of variables, such as phage host range and protein sequences.

Seven distance matrices, comprised of pairwise *p*-distances between all *P. acnes* phages sequenced in this study, were constructed with respect to reliable, tail-associated protein sequences (equivalent to $gp11_{PA6}$, $gp14_{PA6}$, $gp15_{PA6}$, $gp16_{PA6}$, and $gp17_{PA6}$), small terminase subunit sequences ($gp1_{PA6}$) and host range (Section 2.2.9.3.1). The small terminase subunit is known not to come into contact with the host cell, therefore, it was selected as a negative control for congruency testing as it lacks involvement in the host recognition/adsorption process.

To determine the overall degree of concordance between phage host ranges and the proteins of interest, the global test of Congruence Among Distance Matrices (CADM) was performed. Complimentary Mantel tests (Campbell *et al.*, 2011; Legendre & Lapointe, 2004) were carried out to test for concordance among pairwise groups of individual distance matrices associated with host range against those associated with protein sequences. The global CADM test produced a concordance statistic—Kendall's coefficient of concordance, *W*—that estimated the level of congruence, between 0 (no congruence) and 1 (complete congruence), among distance matrices. Under H_0, the CADM test considers the concordance statistic "insignificant" and all matrices completely incongruent when $P > 0.05$ (Legendre, 2010). The alternate hypothesis, H_1, accepts the concordance statistic as "significant" and partial or complete congruence

among distance matrices when $P \leq 0.05$ (Legendre, 2010; Legendre & Lapointe, 2004). To determine the probability of discordance among matrices (H_0), Friedman's X^2 was calculated using W, then tested against a distribution of X^2* values derived from random permutations of all distance matrices of permuted values (Campbell *et al.*, 2011; Legendre & Lapointe, 2004). To support rejection of H_0, Mantel tests of distance matrices containing concordant data (H_1) generated one-tailed permutational probabilities based on the Spearman coefficient of correlation (r_s) statistic (Legendre & Lapointe, 2004).

As shown in Table 3.9a, results of the global CADM test revealed partial congruence among at least two distance matrices (W = 0.2705912; P = 0.0009). To determine which protein(s) demonstrated a probable association with host range, Mantel test results (Table 3.9b) were limited to those corresponding to pairwise combinations of distance matrices associated with host range versus individual protein sequences. Having an r_s value of 0.41520944 supported by a P-value of 0.0356, the Mantel test result represented a probable association between $gp11_{PA6}$ and host range (X^2 falling under H_1). All other Mantel tests produced p-values greater than 0.05. Therefore, out of all phage tail-associated proteins evaluated for their role in host recognition, the MTP was the only component that was shown to act as a determinant of phage host specificity.

3.4.2.3 Major tail protein: sequence diversity and role in host specificity of *P. acnes* phages

Shown in Figure 3.22b, construction of a phylogenetic tree using the BioNJ algorithm in Seaview v.4.6 (Section 2.2.8.4.2) demonstrates the evolutionary distance based on the MTP sequence diversity among all *P. acnes* phages sequenced in this study. Tree

Table 3.9: Results of (a) overall (global) CADM test and (b) complimentary Mantel tests, using distance matrices derived from the host range and protein sequence datasets. One-tailed *P*-values were calculated by permutation test (9999 permutations) of Friedman's X^2 (CADM test) or Spearman's coefficient of correlation,

(a) Overall CADM test		H_0: All distance matrices are incongruent ($P > 0.05$)					
Kendall's W:		0.270591					
Friedman's X^2:		123.119		$P = 0.0009000$		Reject H_0	
(b) One-tailed Mantel tests based upon ranks (Spearman correlation)		H_0: Complete pairwise incongruence among matrices ($P > 0.05$)					
		$gp1_{PA6}$	$gp11_{PA6}$	$gp14_{PA6}$	$gp15_{PA6}$	$gp16_{PA6}$	$gp17_{PA6}$
Host range	r_s	0.0538	0.4152	-0.2992	0.3180	-0.2144	0.2993
	P	0.3487	0.0356	0.9373	0.0518	0.8498	0.0540

P = permutational probability, r_s = Mantel statistic using ranks.

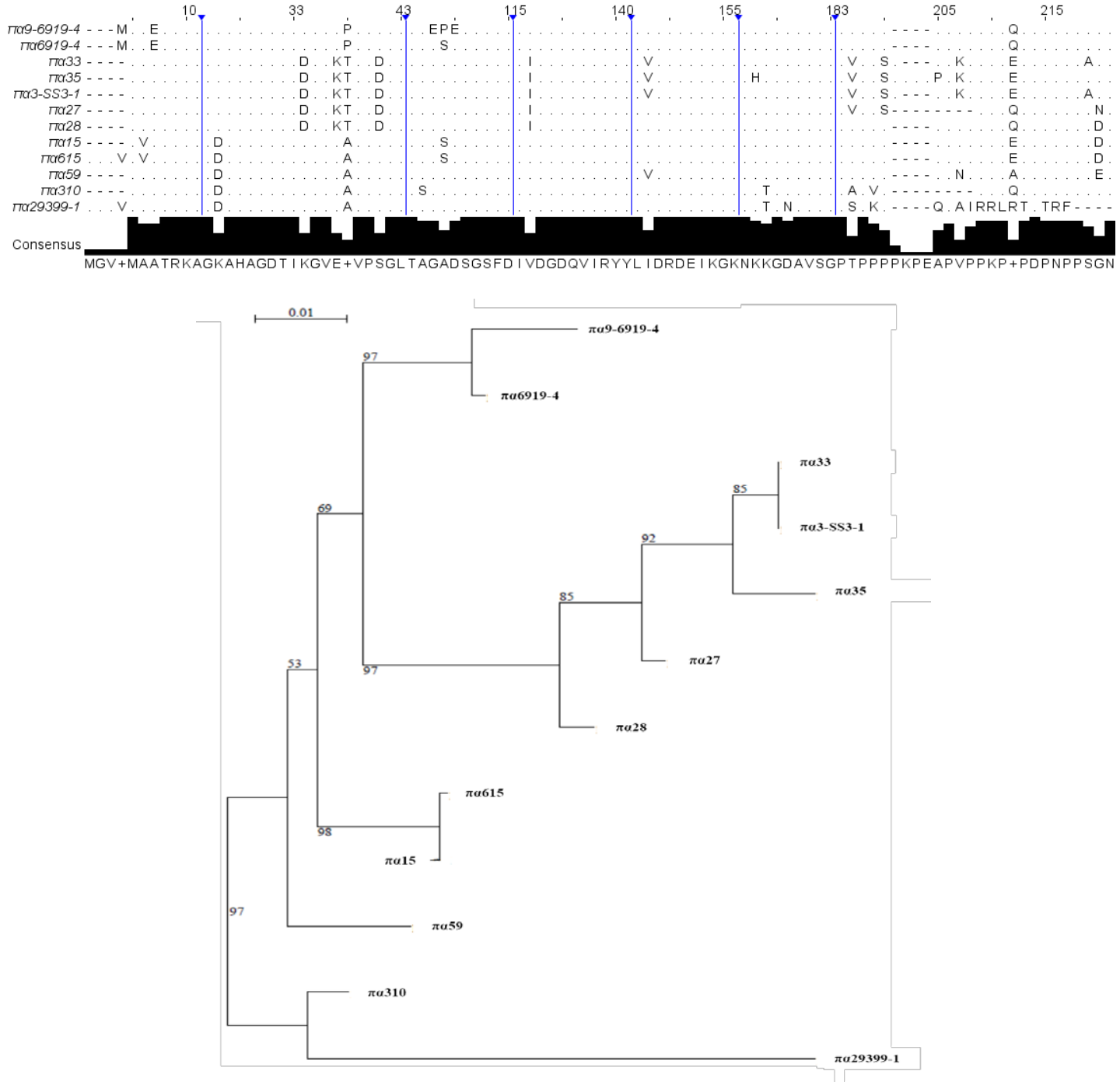

Figure 3.22. Amino acid sequence diversity of major tail proteins (MTP) associated with sequenced *P. acnes* phages. The condensed protein sequence alignment given in (a) displays non-conserved amino acids separated by breaks lines (blue) where regions of complete sequence consensus have been collapsed. The histogram under the alignment represents the consensus frequency relative to 100% (longest bars). Evolutionary distance based on the major tail protein sequences are represented by (b) a phylogenetic tree constructed using BioNJ algorithm with 1000 bootstrap replicates (bootstrap values are as indicated).

topology and differences in branch lengths is reflective of the diversity across the MTP sequences, as represented by a map of aligned non-conserved amino acids produced using Jalview v.2.10.1 (Section 2.2.8.4.2) given in Figure 3.22a. The majority of these phages exhibit differences among their MTP sequences (Figure 3.22a) that are translated into corresponding branch length differences of the phylogenetic tree (Figure 3.22b).

Based on congruence analysis results, variation across the host range profiles of all sequenced *P. acnes* phages (Figure 3.18) is reflected in the phylogenetic analysis of the MTP (Figure 3.22a). For example, two phages— πα33 and πα3-SS3-1—exhibited identical host range (Figure 3.18) and branch lengths (Figure 3.22a), based on identical MTP sequences (Figure 3.22b), as expected. Interestingly, one pair of sequenced phages— πα6919-4 and πα35—demonstrated identical host range against the collection of *P. acnes* isolates used in this study, despite variation among their MTP sequences (Figure 3.22b). It is possible that, if tested against an expanded collection of *P. acnes* isolates, they may demonstrate alternative host specificity. Despite this, the level of concordance among the MTP sequence and host range datasets was powerful enough to overcome any instance of discordant data.

Derived from *P. acnes* phage πα6919-4, mutant phage πα9-6919-4 demonstrated extended host range as it was capable of completely lysing the *P. acnes* strain #9 that was naturally resistant to the entire *P. acnes* phage collection (Section 3.3.3). Upon sequence analysis of the phage πα9-6919-4 in comparison to its parental phage πα6919-4 mutations leading to changes in one or more protein sequences implicated in phage-host interaction were detected. A condensed map of the πα6919-4 and πα9-6919-4 MTP alignment was

generated using DNAMAN v. 9 (Section 2.2.8.4.2). A relatively diverse clustered variations in MTP sequences across the sequenced phages were observed (Figure 3.22b), however, located in a fairly-conserved region of the MTP, Figure 3.23 illustrates the sequence variation between MTPs of πα6919-4 and πα9-6919-4 compared with all other known sequenced *P. acnes* phages. Figure 3.23a shows three missense mutations in the gene encoding the MTP of πα6919-4 —G_{314}→A; T_{316}→C; T_{321}→A (*gp*11 nucleotide numbering)—resulted in three tandem, non-conserved amino acid substitutions in the MTP of πα9-6919-4 (equivalent to phage PA6 bases G_{311}, G_{313} and T_{318}). Based on πα6919-4 MTP amino acid numbering, the substitutions are G_{105}→E; S_{106}→P; D_{107}→E (equivalent to phage PA6 MTP amino acids G_{105}, S_{106} and D_{107}) . Amino acid substitutions in the MTP sequence of πα9-6919-4 were unique compared to all other sequenced *P. acnes* phages to date (Figure 3.23b).

3.4.2.4 Structural modeling of the major tail protein: implications in *P. acnes* phage host range

To investigate the mechanism of tail tube-associated host specificity of *P. acnes* phages (especially for πα6919-4 and πα9-6919-4) and in order to conduct structural modeling of phage major tail proteins (MTPs), a thorough homology search within protein databases was required (Section 2.2.8.4.2). Matching entries with similar functions and with structural data (NMR or X-ray crystallography) can be used in 3D structural modeling. A blastp search using the παMTP sequences (214 amino acids) within the non-redundant protein sequence database identified a few proteins with related functions that demonstrated relatively moderate homology with major tail proteins of various

(a)

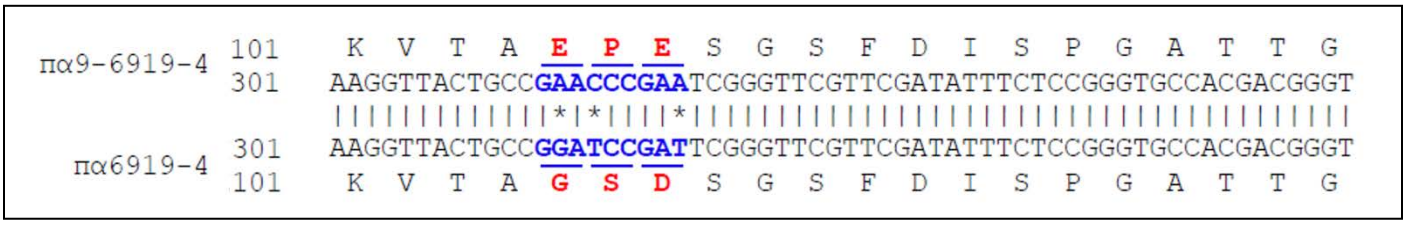

(b)

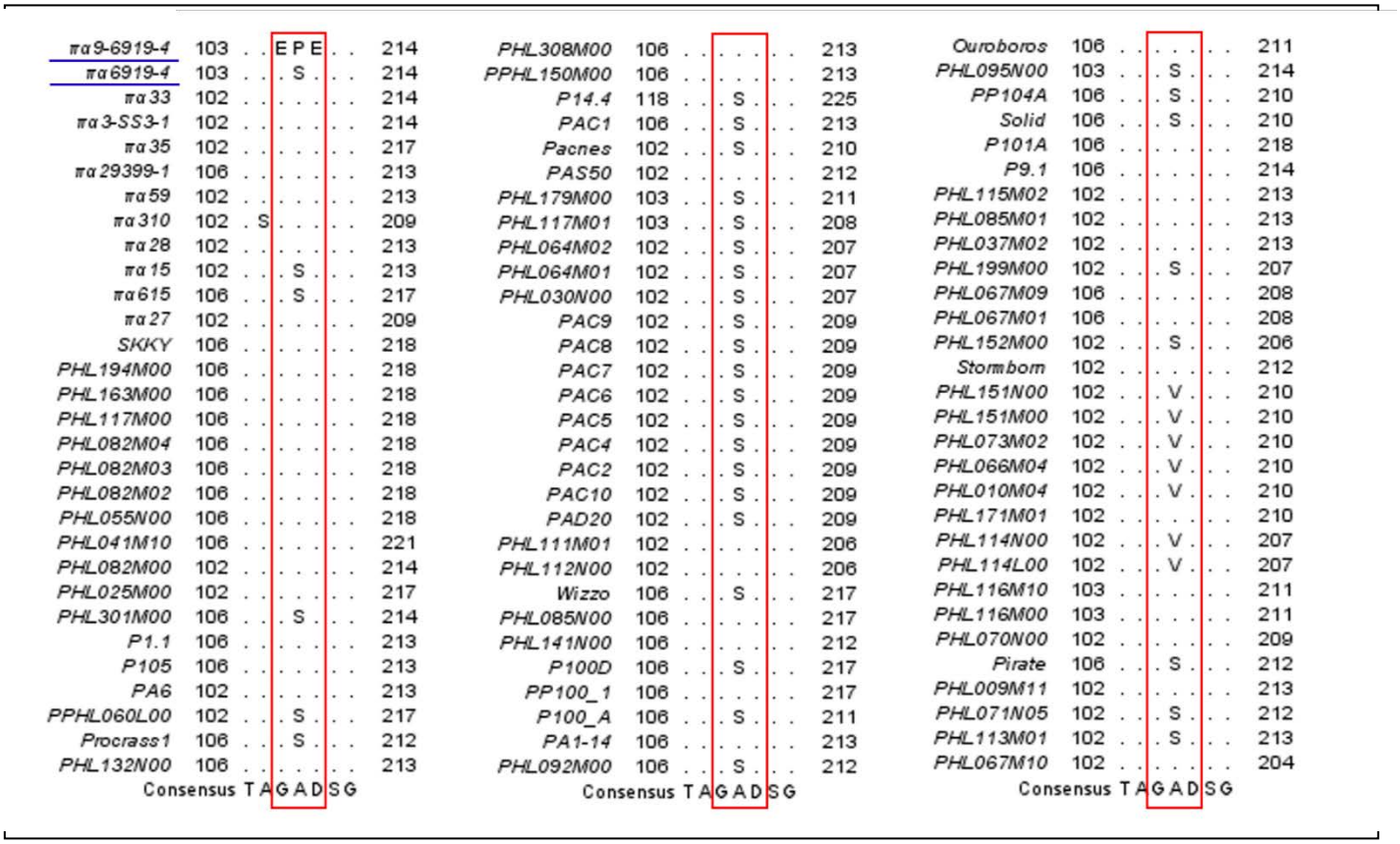

Figure 3.23. Sequence variation in a conserved region of *P. acnes* phage major tail proteins. (a) Three missense mutations present in *orf*11 of *πα*9-6919-4 resulted in substitution of three amino acids in gp11 (major tail protein). (b) Map displaying the region where sequence variation occurred in the major tail proteins of parental *P. acnes* phage *πα*6919-4, and its mutant progeny *πα*9-6919-4 (underlined blue), aligned with eighty-eight *P. acnes* MTP sequences.

Lactococcus lactis p335-group phages (p335MTPs), including ΦTIFN7 (Erkus *et al.*, 2013), r1t (van Sinderen *et al.*, 1996) and ΦLC3 (Blatny *et al.*, 2004), having the highest mean sequence identity with ΦTIFN7 (30.3% ± 0.3, e = $2.13x10^{-4} \pm 6.78x10^{-5}$). An example alignment of πα6919-4 MTP with ΦTIFN7 MTP is shown in Figure 3.24 . Sequence alignments of p335 MTPs started either at the first or forty-third παMTP N-domain residues, covering roughly 60% or 80% of the παMTPs, respectively. Homology was expected in the N-terminal region of the MTPs because N-terminal domains of siphovirus MTPs are conserved as they are the primary constituents of the homohexameric rings comprising the phage tail tube structures and are likely to share a common ancestor together with bacterial type VI secretory system (Leiman *et al.*, 2009; Pell *et al.*, 2009). Tail decorating C-terminal domains (C-domain) are absent in p335-group phages as the host adsorption strategy employed by phages of the p335 group does not involve the tail tube structure (Bebeacua *et al.*, 2013a). Therefore, aligned regions of homology between p335 MTPs and παMTPs excluded the far C-domain residues of the παMTPs, which accounted for approximately 20% of the entire παMTP length.

Having only partial alignment with low homology and, more importantly, a lack of structural data, could not support use of these proteins for structural modeling. Therefore, we sought structural alignment of παMTP sequences with those of known structure from within the PDB database. Powerful algorithms are used to generate alignments using the query protein sequence (target) and those within the PDB database (templates), ranking target-template alignments by best fit, to identify evolutionarily distant proteins that share a common ancestor and are likely have similar function, in order to produce a model of the target. Using HHPred of the MPI Bioinformatics Toolkit integrative platform, a

```
RID: EN6TDYK6013 (Expires on 04-11 04:35 am)
Query ID: lcl|Query MTP_6919_4
Molecule type: amino acid
Query Length: 214

tail protein [Lactococcus lactis subsp. cremoris TIFN7]
Sequence ID: EQC84235.1
Length: 185
Range 1: 42 to 172
Score: 50.1 bits (118)
Query Cover: 60%
Expectation value: 3x10-04
Method: Compositional matrix adjust.
Identities: 40/132 (30%)
Positives: 66/132 (50%)
Gaps: 4/132 (3%)

        MTP_6919_4  43    LGYLSDDGFKIKPERKTDDLKAWQNADVVRTVATESSIEISFQLIESKK-EVI-ELFWQS  100
                            LGY+S+DG K K   K+D +KAW   D V TV TE     S+ LIE+   EV+ E++
tail protein_TIFN7  42    LGYISEDGLKNKNSPKSDSIKAW-GGDTVATVQTEKEDTFSYTLIEALNVEVLKEVYGAG  100

        MTP_6919_4  101   KVTAGSDSGSFDISPGATTGVHALLMDIVDGDQVI-RYYFPEVELIDRDEIKGKNGEVYG  159
                            VT    +G    +       H +++D+   D V  R   P+ ++ +  +I   + +  G
tail protein_TIFN7  101   NVTGTLKTGITVKANSKELIEHPVVIDMTVRDGVFKRIVIPQGKVSEIGDISYNDSDAVG  160

        MTP_6919_4  160   YGVTLKAYPAQI  171
                            + +TL   P ++
tail protein_TIFN7  161   FEITLTGLPDKV  172
```

Figure 3.24: Protein sequence homology search result using blastp for *πα*6919-4 MTP.

structural homology search for πα6919-4 MTP was conducted (Section 2.2.8.4.2). This search was based on an initial phase of secondary structure prediction (SSPred) for segments of the primary sequence followed by aligment to proteins within PDB database with consideration of both primary sequence and secondary structure data. The παMTP returned a match with the N-domain of *E. coli* λ phage major tail tube protein (λ gpV_N) that only covered the first 156 amino acids of the πα6919-4 MTP, corresponding to its N-domain. No further match extending to its C-domain was available thus restricting our analysis to include only the N-domains of the παMTPs, which we considered useful for our analysis directed to πα6919-4 and its mutant derivative, πα9-6919-4, with extended host range. An example of the structural alignment report from the HHPred server is shown in Figure 3.25. A glance through the predicted secondary structures (ss_pred) and the known secondary structure (SS) data (ss_dssp) for λ gpV_N provides confidence for the SS predictions of the παMTP given in the MSA output. Sequence alignment showed 6% primary sequence identity with a relatively high probability of 67% and matching confidence score of 24.11 suggestive of significant structural and functional relatedness between λ gpV_N and πα MTPs. The πα6919-4 MTP included insertion of a stretch of 18 amino acids at the D104 position corresponding to the λ gpV_N sequence. This inserted stretch of amino acids was shared and highly conserved among all of our sequenced phages. It was also noted that the non-conservative tandem triple mutations in the πα9-6919-4 MTP as compared to the MTP of its parental phage πα6919-4 (G_{105}→E; S_{106}→P; D_{107}→E) was mapped to this additional 18 amino acid region.

Conducting similar searches with παMTPs using the HHSearch2 threading program via the LOMETS server predicted secondary structures and generated target-template

Figure 3.25: Structural alignment of πα6919-4 MTP and λ gpV$_N$ (2K4Q). Secondary structures were predicted by HHPred search using Bioinformatic Toolkit and aligned to λ gpV$_N$. ss_pred: predicted secondary structure; ss deep: secondary structure based on NMR atomic coordination data.

alignments with protein structures from the PDB database, generating παMTP-λ gpV_N MSA output comparable to that of HHPred. We additionally used the primary sequence of λ gpV_N, derived directly from its PDB file (2K4Q), as an internal control to validate the accuracy of the prediction and modeling by LOMETS. The MSA output from LOMETS was used to produce a PDB output file using onsite MODELLER program. The predicted 3D model for λ gpV_N produced high confidence score (C-score) for the accuracy of model and Z-score of 86.693 (cutoff threshold of 0.0339-0.0733) verifying statistical significance of the modeling process (Wu & Zhang, 2007). The predicted models for N-domains of πα6919-4 and πα9-6919-4 MTPs also had high C-scores and significant Z-scores of 11.964 and 12.991, respectively, indicating the reliability of the predicted models (Figure 3.27). Shown in Figure 3.26, we further tested the accuracy of the models by functional alignment of the amino acid sequences of our παMTAs to λ gpV_N sequence to identify the highly conserved hydrophobic residues that constitute the protein's hydrophobic core essential for its assembly and function (Pell *et al.*, 2009).

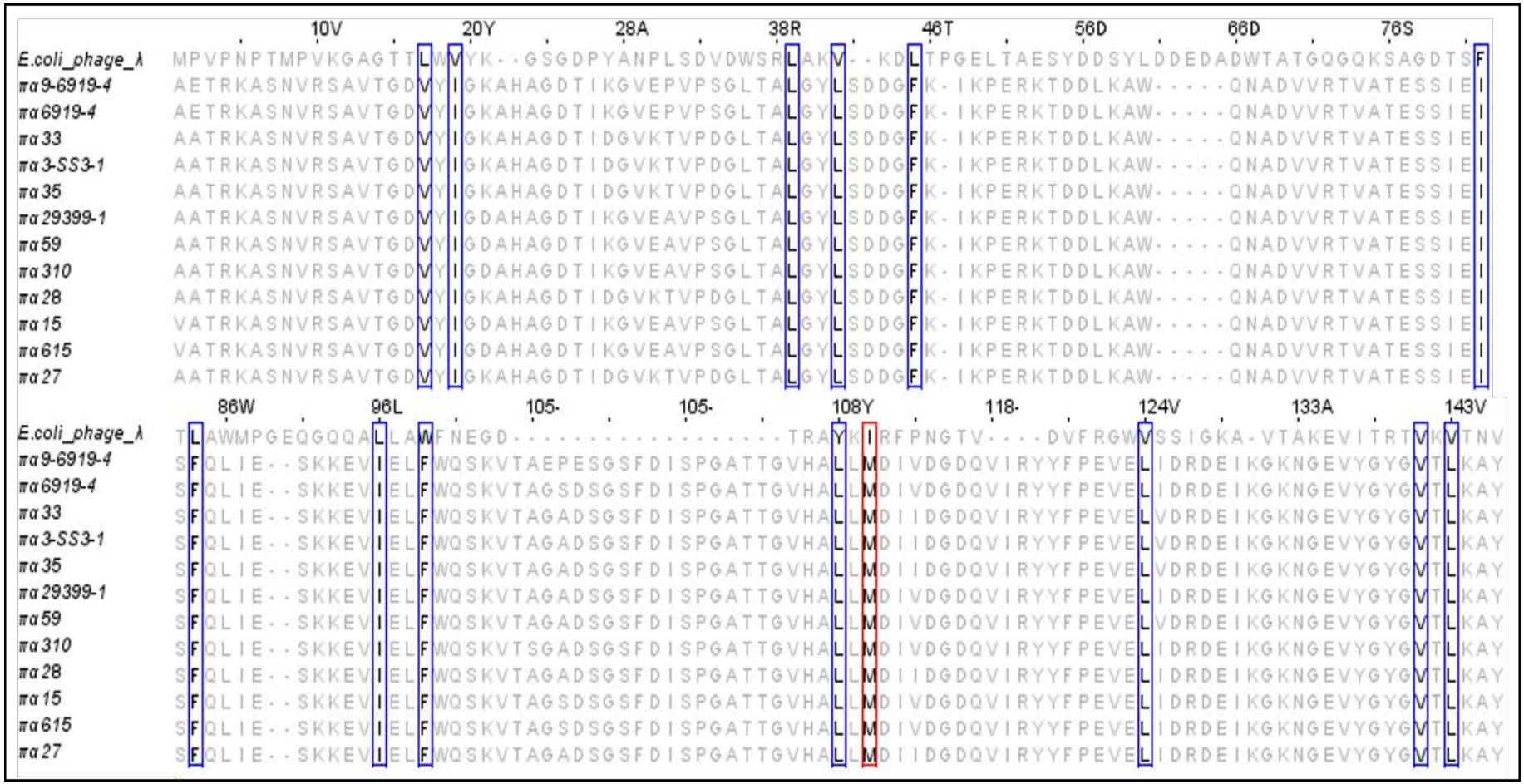

Figure 3.26: Mapping of N-domain hydrophobic core residues of παMTPs with reference to λ gpV_N sequence. Thirteen out of fourteen conserved hydrophobic residues of λ gpV_N that take part in protein's hydrophobic core are conserved in παMTPs (blue boxes). Stretch of 18 amino acids among that are present in παMTPs is shown as a gap in λ gpV_N sequence.

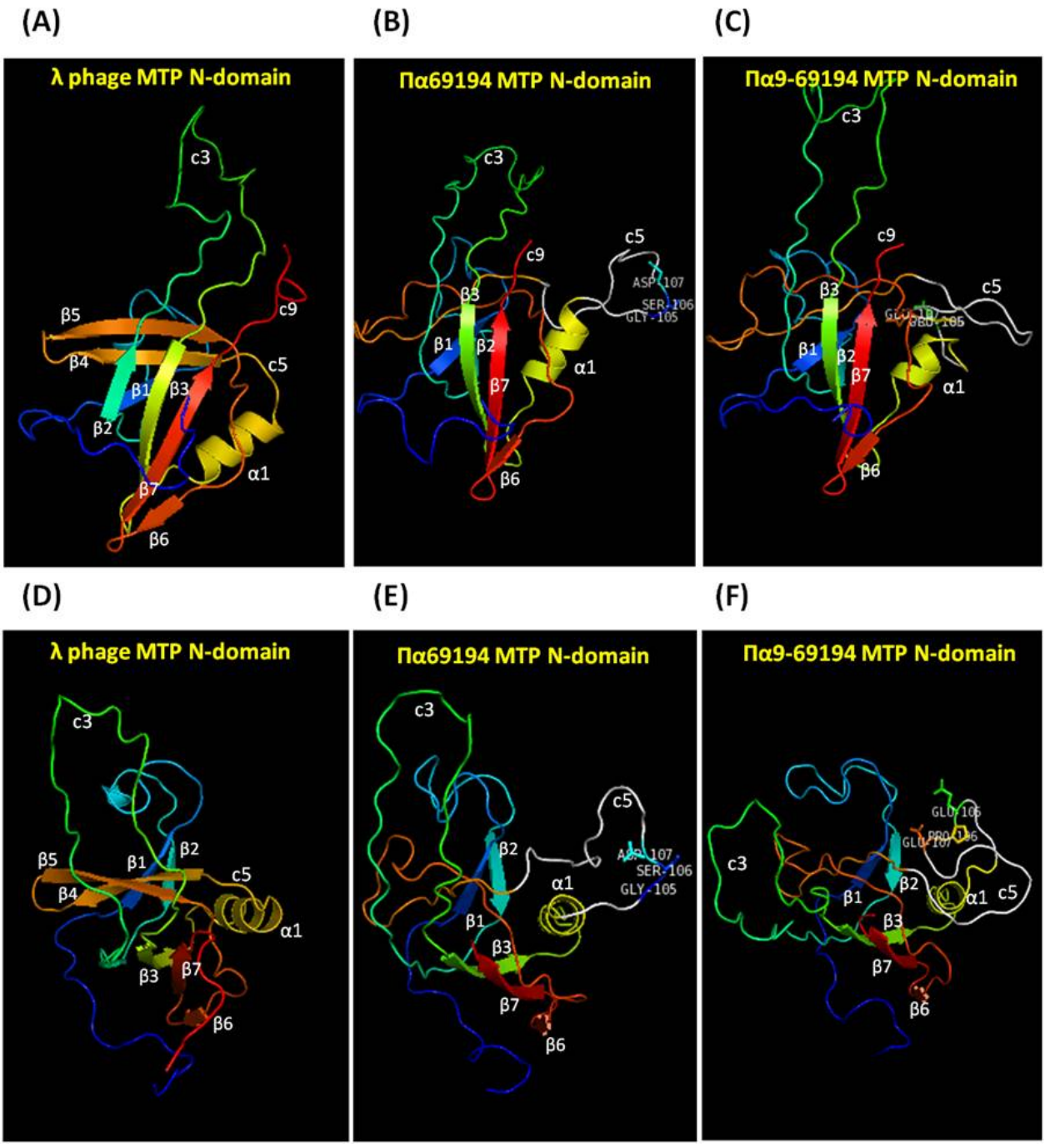

Figure 3.27: Three dimensional models of λ gpV$_N$, πα6919-4 and πα9-6919-4 MTP N-domains modelled by LOMETS. Models were built using the λ gpV$_N$ NMR data; A-C: sideview and D-F: top to bottom view.

4 Discussion

Propionibacterium acnes is a resident microflora of the human skin (Funke *et al.*, 1997; Grice & Segre, 2011). Pilosebaceous units of the head and trunk provide a habitable environment that is well-suited for this lipophilic, facultative microaerophilic anaerobe (Bek-Thomsen *et al.*, 2008; Grice & Segre, 2011; Leeming *et al.*, 1984; Roth & James, 1988). *P. acnes* has gained notoriety as an opportunistic pathogen (Brüggemann *et al.*, 2004; Brüggemann, 2005) and is mainly recognized as the primary etiologic agent associated with acne vulgaris (Das & Reynolds, 2014). Acne affects over eighty percent of individuals at least once in their lifetime and is generally considered to be a chronic condition that manifests during adolescence and early adulthood (Balkrishnan *et al.*, 2006b). Disadvantages of existing acne treatments include a wide range of adverse side effects, development of bacterial antibiotic resistance, limitations imposed by contraindications, and treatment costs, amongst others. To overcome the drawbacks associated with existing treatments, novel therapeutic modalities need to be sought. Phage therapy offers a targeted, fast-acting, cost-effective alternative to conventional antimicrobials. As a proof of concept study, the *in vitro* potential of bacteriophages as an alternative to antimicrobials and a potential future therapy for treatment of acne vulgaris is discussed.

Study participants and treatment history

Patients seeking dermatological consultation for acne in Sudbury and Ottawa (Canada), served as the largest sources of *P. acnes* isolates used in this study. The *P. acnes* collection was diversified further by the addition of donated isolates recovered from either deep tissue infections or from forehead sampling of healthy individuals from

Sweden (Table 4.1, Appendix C). The participant populations of Sudbury and Ottawa were comparable to those of other epidemiological acne studies (Aksu *et al.*, 2012; Augustin *et al.*, 2011; Bissek *et al.*, 2012; Dréno *et al.*, 2016b; Goulden *et al.*, 1997, 1999; Han *et al.*, 2016; Henderson, 1996; Kilkenny *et al.*, 1998; Layton *et al.*, 1994; Perera *et al.*, 2000; Shahzad *et al.*, 2011; Shaw & White, 2001; Shen *et al.*, 2012; Tan, 2004; Tan & Bhate, 2015; Tanghetti *et al.*, 2014; Thiboutot *et al.*, 2009; Yentzer *et al.*, 2010; Zouboulis, 2014), suggesting that the recovered *P. acnes* isolates used in this study comprise a representative collection of clinically-relevant, acne-associated phage target hosts. Consistent with reports concerning the average age of acne onset, persistence (Augustin *et al.*, 2011; Bissek *et al.*, 2012; Henderson, 1996; Perera *et al.*, 2000; Shen *et al.*, 2012; Tan, 2004; Tan & Bhate, 2015), anatomical distribution of lesions (Dréno *et al.*, 2016b; Tan, 2004) and chronic duration (Dréno *et al.*, 2016b; Tan, 2004; Thiboutot *et al.*, 2009; Zouboulis, 2014), the majority of study participants were adolescents and young adults (12-50 years old, with 90th percentile at 30 years of age). Patients in their mid-teens to early-twenties were mostly male compared to the female patient population, which exhibited a broader age distribution. The higher prevalence of adult acne among women compared to men has also been noted by several other research groups (Aksu *et al.*, 2012; Goulden *et al.*, 1999; Han *et al.*, 2016; Kaur *et al.*, 2016; Kilkenny *et al.*, 1998; Shahzad *et al.*, 2011; Shaw & White, 2001; Shen *et al.*, 2012; Tanghetti *et al.*, 2014; Yentzer *et al.*, 2010). Patients presented with lesions located on their faces in combination with the chest and/or back, whom have been afflicted with the condition for at least two years. Sixty-five participants (47.8%) reported presence of scarring; of these, the majority (63.1%) did indicate that they had developed scars as a result of acne (Table

3.1), which was expected as scarring is common among acne sufferers (Dréno *et al.*, 2016b; Goulden *et al.*, 1997; Layton *et al.*, 1994; Tanghetti *et al.*, 2014).

Used by 86.6% of treated patients, retinoids (oral and/or topical) were the most common treatment modality followed equally by both benzoyl peroxide and topical and/or oral antibiotics, both used by 70.2% of treated patients (Table 3.1). These treatments were expected to be used most often among study participants as they are indicated for all levels of acne severity (Zaenglein *et al.*, 2016), with retinoids being the first line of defense for all types of acne (Thiboutot *et al.*, 2009). Oral contraceptives and spironolactone are only indicated for the female population as an alternative treatment for moderate to severe acne (Thiboutot *et al.*, 2009; Zaenglein *et al.*, 2016), thus they have a relatively lower usage frequency of 19% and 6% of the treated female population, respectively (Table 3.1). Employed by only 1.75% of treated patients, photodynamic therapy has been recognized and evaluated as a supplementary alternative acne treatment, however, its off-label use for acne has proven successful (Haedersdal *et al.*, 2008; Thiboutot *et al.*, 2009; Zaenglein *et al.*, 2016). Similar to other studies (Tan, 2004; Yentzer *et al.*, 2010), the largest group of patients receiving treatment (31.6%) were using a combination of retinoids, benozyl peroxide and antibiotics (Table 3.1). Physicians regularly adopt combinatorial therapeutic approaches for resolving acne to address a variety of factors contributing to acne pathogenesis and attempt to reduce development of antibiotic resistance (Thiboutot *et al.*, 2009).

As shown in Table 3.2, topical clindamycin was the most frequently-used antibiotic among study participants (58.8%), followed by oral minocycline (28.8%) then oral

doxycycline (23.8%). This was as expected as these antibiotics are most commonly-employed, with topical clindamycin being indicated for all levels of acne severity and oral tetracyclines being indicated for moderate to severe acne (Del Rosso *et al.*, 2016; Zaenglein *et al.*, 2016). Regardless of whether antibiotics are used in conjunction with other treatment modalities, evidence does suggest that exposure to antibiotics can cause damage to the natural microbiome and impose selective pressure on *P. acnes* (Grech, 2014) and other bacteria in the microflora (Başak *et al.*, 2013; Lesens *et al.*, 2007; Levy *et al.*, 2003; Margolis *et al.*, 2005, 2012; Mills *et al.*, 2002; Ozuguz *et al.*, 2014; Raum *et al.*, 2008), resulting in negative treatment outcomes (Del Rosso *et al.*, 2016; Leyden, 2012; Simonart & Dramaix, 2005; Thiboutot *et al.*, 2009). With this in mind, it is worrisome that over half of the study participants underwent acne therapy with one or more antibiotics (Figure 3.3) for an approximate mean duration of seven months (Section 3.1).

Demonstrating wide representation in terms of antibiotic exposure, use of other treatment modalities, age, sex, duration of acne and primary location of lesions (sampling), Sudbury and Ottawa patient populations together with isolates from Sweden served as diverse sources of clinically-relevant *P. acnes* hosts for *in vitro* evaluation of the candidate phage collection.

Propionibacterium acnes clinical isolates

Indiscriminate lytic capacity of the phage cocktail candidates was determined by evaluating their propensity to infect and kill a diverse pool of two hundred twenty-four *P. acnes* isolates (Table 3.3). The collection of *P. acnes* isolates represent a variety of

populations contrasted by geographical origin, anatomical source of isolation, antibiotic susceptibility patterns and genetic properties. Comprising nearly seventy-five percent of the total *P. acnes* isolate pool, the largest source of clinical isolates used in this study were derived from acne patients in Sudbury and Ottawa (Table 3.3). The pool was expanded to include *P. acnes* isolates from a range of clinical sources, originating from Sweden and across Canada (Table C.1). To the best of our knowledge, this is one of the largest, most diverse pool of clinically-relevant *P. acnes* isolates assessed in terms of sensitivity to a phage collection, to date.

Genetic diversity among P. acnes isolates

Rapid, PCR-based phylotyping of both Sudbury and Ottawa clinical isolate collections revealed representation of *P. acnes* isolates belonging to major phylogenetic clades IA, IB, and II (Section 3.2.1). All PCR-confirmed *P. acnes* isolates were successfully grouped into clade IA, IB or II;like other reports, there was no evidence of type III *P. acnes* isolate recovery from acne lesions (Lomholt & Kilian, 2010; McDowell *et al.*, 2008, 2011, 2012, 2013). Corroborated by findings from several other studies that employed alternate typing schemes (Fitz-Gibbon *et al.*, 2013; Lomholt & Kilian, 2010; McDowell *et al.*, 2011, 2012, 2013), type IA isolates were frequently isolated from acne and comprised 86.14% of Sudbury and Ottawa combined *P. acnes* collections. Types IB and II isolates had lower rates of recovery from acne lesions (Table 3.5), comprising 9.04% and 4.82% of Sudbury and Ottawa combined *P. acnes* collections. Type IA *P. acnes* isolates are associated with acne, while type IB and type II isolates are associated more frequently with healthy skin and deep tissue infection (McDowell & Nagy, 2015).

Therefore, characterized by an elevated proportion of type IA isolates and lower frequencies of types IB and II isolates ($p<0.001$, Section 3.2.1), the pool of *P. acnes* isolates used in this study represents the phylogenetic composition expected from a clinically-relevant *P. acnes* population, thus this collection is a suitable target for testing the efficacy of phages as the potential antibacterials.

Statistical analysis of the frequency of *P. acnes* phylotypes recovered from lesion surfaces versus exudates revealed no bias of phylotype distribution among samples from either of these sampling sites from patients in Sudbury ($p=0.633$) and Ottawa ($p=0.612$) (Section 3.2.1). These findings suggests that *P. acnes* phylotype composition on the skin of acne patients does not vary between the surface and the interior of the acne lesion. Therefore, it is reasonable to suggest that the same *P. acnes* strains within the lesion are also on the skin surface. Phages applied to the skin surface will replicate exponentially upon application thus increasing the likelihood of treatment success by increasing the number of progeny phage particles that are capable of infecting strains on both the surface and within the lesion.

Statistical analysis of the *P. acnes* phylotypes revealed no bias relating to the presence or absence of antibiotic resistance among isolates from Sudbury ($p=0.316$) and Ottawa ($p=0.836$) (Section 3.2.1). This was expected, as phylogenetic associations between specific strain types and resistance phenotypes (Lomholt *et al.*, 2017; McDowell *et al.*, 2012) require the use of a typing methodology with a higher resolution, which could identify phylotype subgroups, clonal complexes and strain types.

Antibiotic susceptibility of P. acnes isolates

Antibiotic therapy was used by over half of the combined population of Sudbury and Ottawa patients; resistance among *P. acnes* isolates from these patients was determined to be linked to antibiotic exposure ($p<0.001$; Section 3.2.3). Other studies have documented geographical correlations with the magnitude of antibiotic exposure and corresponding resistance rates of *P. acnes* and other bacteria (Del Rosso, 2016). For instance, use of antibiotics with similar mechanisms of action, such as EM (macrolide) and CM (lincosamide), are associated with *in vivo* recovery of EM ($p=0.0019$), AZ ($p=0.0052$) and/or CM ($p=0.0280$) cross-resistant *P. acnes* in this study (Section 3.2.3), and in others (Borglund *et al.*, 1984; Grech, 2014; Oprica *et al.*, 2004; Ross *et al.*, 2003; Schafer *et al.*, 2013). Similar to other reports (Borglund *et al.*, 1984; Oprica *et al.*, 2004; Ross *et al.*, 2003), the present study revealed an association between patient exposure to one or more tetracycline-class antibiotics and recovery of *P. acnes* isolates demonstrating resistance to tetracycline, doxycycline and/or minocycline ($p=0.0233$; Section 3.2.3).

Out of two hundred eleven *P. acnes* isolates evaluated for antibiotic susceptibility, forty-five were resistant to at least one antibiotic (Section 3.2.3). Frequencies of clindamycin and erythromycin use, combined, represent the largest proportion of antibiotics used that share similar mechanisms of bacterial inhibition (Table 3.2). Therefore, given that the chronic aspect of acne and the necessity for long-term and frequent usage of antibiotics such as clindamycin and macrolides (erythromycin and azithromycin) resistance might have been descended clonally in the population, it was not surprising that the highest frequencies of resistance were to erythromycin and azithromycin, followed by

clindamycin (Table 3.6)—a trend that is corroborated by similar studies (Crane *et al.*, 2013; Fan *et al.*, 2016; Giannopoulos *et al.*, 2015; Grech, 2014; Moon *et al.*, 2012; Nakase *et al.*, 2012; Oprica & Nord, 2005; Ross *et al.*, 2003; Schafer *et al.*, 2013; Walsh *et al.*, 2016).

Macrolide and lincosamide antibiotics disrupt peptide synthesis by causing dissociation of peptidyl-tRNA from the 23S rRNA by either partial masking of the substrate-binding region of the peptidyl transferase (CM) or by blocking the ribosomal P-site used as an exit path for newly-synthesized peptide chains through induction of conformational change by binding of a region nearby the peptidyl-tRNA binding site (EM and AZ) (Dinos *et al.*, 2001; Mao & Robishaw, 1972; Tenson *et al.*, 2003). Having similar mechanisms of action, cross-resistance to macrolides (EM and AZ), lincosamides (CM) and streptogramin B antibiotics is common (Coates & Vyakrnam, 2002; Gübelin *et al.*, 2006; Ishida *et al.*, 2008; Ross *et al.*, 2003; Schafer *et al.*, 2013). In this study, over half of macrolide-resistant *P. acnes* isolates were cross-resistant to clindamycin, whereas all clindamycin-resistant isolates were cross-resistant to a macrolide (EM and/or AZ).

Resistance to macrolides, streptogramin B and/or lincosamides are often the result of a target modification by methylation or target alteration by mutation in the peptidyl transferase located within domain V of the 23S rRNA in the 50S large subunit of bacterial ribosomes (Sigmund *et al.*, 1984; Sigmund & Morgan, 1982; Weisblum, 1995). Having a variety of resistance mechanisms, such as conformational changes of the 23S rRNA secondary structure and introduction of ribosomal methyl-transferase targets (Leclercq, 2002; Vannuffel *et al.*, 1992; Weisblum, 1995), majority of *P. acnes* macrolide

and lincosamide resistance phenotypes are associated with distinct 23S rRNA mutations at *E. coli* bases 2058 (resistance group I), 2057 (group III), 2059 (group IV), or 2611, or by acquisition of the Tn5432 transposon (group II), which carries the *erm(X)* resistance gene that encodes 23S dimethylase (Nakase *et al.*, 2016; Ross *et al.*, 1997, 2001, 2002, 2003; Weisblum, 1995). Having cross-resistance to erythromycin, azithromycin and clindamycin, twenty-two *P. acnes* isolates may belong to resistance groups I (*E. coli* A2058G), II (*erm(X)* resistance gene) or IV (*E. coli* A2059G)—all of which are characterized by a high-level of macrolide resistance and moderate (group IV) to high (groups I and II) levels of clindamycin resistance (Ross *et al.*, 1997, 2002). Due to the maximum concentration of antibiotic on the Etest strips, MIC readings above 256 ug/ml could not be resolved, therefore, categorization into specific resistance groups remains uncertain. Despite this, it is clear that the isolates used in this study demonstrate a diverse range of susceptibility phenotypes to macrolides and clindamycin.

As seen in other reports, *P. acnes* rates of resistance to tetracycline-class of antibiotics in this study was lower than to macrolides and clindamycin (González *et al.*, 2010; Gübelin *et al.*, 2006; Kurokawa *et al.*, 1999; Moon *et al.*, 2012; Oprica *et al.*, 2004; Ross *et al.*, 2001, 2003; Sardana *et al.*, 2016; Walsh *et al.*, 2016) and the combined usage frequency of tetracycline-class antibiotics was linked to recovery of resistant *P. acnes* (Nakase *et al.*, 2014; Oprica *et al.*, 2005; Oprica & Nord, 2005; Ross *et al.*, 2003). Tetracyclines inhibit protein synthesis by interfering with aminoacyl-tRNA binding to the A site of 16S rRNA, of the 30S ribosomal subunit, by disruption of its tertiary structure (Chopra *et al.*, 1992; Schnappinger & Hillen, 1996). Sharing the same mechanism of action, the majority of tetracycline-resistant isolates were cross-resistant to doxycycline and/or minocycline.

Cross-resistance between tetracyclines has been documented by other studies (González *et al.*, 2010; Gübelin *et al.*, 2006; Kurokawa *et al.*, 1999; Sardana *et al.*, 2016). Common mechanisms of tetracycline resistance include efflux pumps that function to decrease the concentration of tetracycline inside the cell, ribosomal protection proteins that interfere with the tetracycline's capacity to inhibit aminoacyl tRNA binding, chemical modification of the tetracycline molecules and base mutations in the 16S rRNA (Chukwudi, 2016; Salyers *et al.*, 1990). Not all mechanisms of tetracycline resistance in *P. acnes* have been documented, however, there is evidence that a single base mutation in the 16S rRNA at *E. coli* equivalent position G1058C has been shown to confer resistance to tetracyclines in *P. acnes* (Giannopoulos *et al.*, 2015; Nakase *et al.*, 2014; Oprica *et al.*, 2005; Ross *et al.*, 1998, 2001), as well as an amino acid substitution in ribosomal protein S10 encoded by the *rpsJ* gene, which reduces susceptibility to tetracyclines prior to development of complete resistance as conferred by the G1036C mutation in 16S rRNA (Nakase *et al.*, 2017). Most studies that have attempted to elucidate the mechanism of *P. acnes* resistance to tetracycline class antibiotics have targeted the 16S rRNA of resistant *P. acnes* isolates (Giannopoulos *et al.*, 2015; Nakase *et al.*, 2014; Oprica *et al.*, 2005; Ross *et al.*, 1998, 2001). Recent studies have shown that tetracyclines are capable of binding to random, double-stranded RNA sequences, which would explain the inhibitory action of tetracyclines against non-bacterial targets (Chukwudi, 2016; Chukwudi & Good, 2016) and variation with regards to the patterns of tetracycline class antibiotic cross-resistance.

Rifampicin resistance was unexpected as the only report of *in vivo* resistance comes from a study involving a pool of 684 *P. acnes* strains isolated from a variety of specimen types

sampled from hospital patients—five of which were rifampicin-resistant (Aubin *et al.*, 2014). Rifampicin interferes with transcription via interaction with the β-subunit of RNA polymerase (Campbell *et al.*, 2001). Point mutations in the gene that encodes the β-subunit—*rpoB*— have been shown to confer *in vitro* resistance to *P. acnes* (Furustrand Tafin *et al.*, 2013). Resistance to rifampicin was demonstrated by only a single *P. acnes* isolate, derived from an infection involving a hip prosthesis originating from Lund (Table C.1; (Holmberg *et al.*, 2009)). Rifampicin is capable of penetrating *S. aureus* and *P. acnes* biofilms, which are involved in implant-associated infections, thus it is used in combination with other antibiotics to treat infections of this nature (Achermann *et al.*, 2014; Furustrand Tafin *et al.*, 2012; Zimmerli, 2014). Therefore, it is possible that the rifampicin-resistant *P. acnes* isolate originated from a patient treated with this antibiotic.

Contrary to two reports of high rates of resistance to trimethoprim/sulfamethoxazole (TS)—68% (González *et al.*, 2010) and 26.3% (Schafer *et al.*, 2013)—only one TS-resistant *P. acnes* isolate was recovered in this study (Table 3.6), similar to other reports (Cunliffe *et al.*, 1999; Moon *et al.*, 2012; Ross *et al.*, 2001). The mechanism of *P. acnes* resistance remains unknown. In this study, TS susceptibility testing was performed using MH media with low thymidine concentration to ensure that thymidine from an exogenous source was not available for conversion to thymine by *P. acnes* that may result in evasion of the inhibitory effects of TS on folate synthesis. In other studies, thymidine content of the media used for TS susceptibility testing was not indicated, therefore it is possible that the TS-resistant *P. acnes* isolates may have been less susceptible to inhibition by TS if exogenous sources of thymidine were available.

With the exception of TS, the resistance frequencies determined in this study follow Global antibiotic resistance trends as summarized in a comprehensive review by (Sardana *et al.*, 2015), which suggests that the general prevalence of *P. acnes* resistance to macrolides, TS and CM is greater than rates of resistance to tetracyclines. As reported by many other studies (Crane *et al.*, 2013; Goldstein *et al.*, 2003, 2004; Olsson *et al.*, 2012; Oprica & Nord, 2005; Ross *et al.*, 2001; Shames *et al.*, 2006), all isolates were susceptible to benzylpenicillin (penicillin G), ceftriaxone, levofloxacin, linezolid, vancomycin and daptomycin.

Twenty of the forty-five antibiotic resistant *P. acnes* isolates were multiply-resistant to combinations of macrolides and tetracyclines—all of which lacked susceptibility to both erythromycin and a tetracycline-class antibiotic (Figure 3.13). Other studies have documented multiply-resistant *P. acnes* isolates (Giannopoulos *et al.*, 2015), however, none as many as reported by the present study. This is troubling as therapeutic failure of various antibiotics, such as erythromycin (Eady *et al.*, 1989) and tetracycline (Ozolins *et al.*, 2004), has been associated with recovery of antibiotic resistant *P. acnes*. Having a subpopulation of antibiotic resistant clinically-relevant *P. acnes* isolates was relevant to this study as it provides a justification for evaluating the efficacy of the phage cocktail candidates against a group of isolates that may otherwise be associated with treatment failure in a clinical setting.

Given the antibiotic resistance properties and the phylogenetic diversities found among our *P. acnes* clinical isolates it appeared as a plausible question to address whether there exists a pattern for phage susceptibility among these clinical isolates. In the following

sections we discuss the biological properties of the phage isolates followed by their functional properties as potential antibacterials.

Phage isolates

To this end, seventy-six *P. acnes* bacteriophages were isolated and evaluated for their lytic properties against two hundred twenty-four *Propionibacterium acnes* clinical isolates that were recovered from clinical samples collected from sources across Canada and Sweden (Table 4.1, Appendix C). A large collection of highly diverse *P. acnes* phages were isolated using agar overlay method (Figure 3.15). Seventy phages from sewage samples of urban wastewater treatment plants (Ottawa, ON and Gatineau, QC) comprised the majority of our phage collection, five phage isolates were obtained from patient samples, and one isolate via evolutionary derivation approach (Section 3.3.1 and Section 3.3.3). Imaging by TEM revealed typical siphovirus morphology for all imaged phages (Figure 3.16). Intact virion structures were characterized by the presence of a non-enveloped icosahedral head that spanned a diameter of approximately 55 nm, which was attached to a non-contractile tail that was roughly 133 nm long, 11 nm in diameter and possessed short tail fibers (Figure 3.16). To date, all reports of *P. acnes* phage structures that have been resolved by TEM have described phages belonging to siphoviridea with comparable dimensions (Ackermann & Eisenstark, 1974; Farrar *et al.*, 2007; Lood *et al.*, 2008; Marinelli *et al.*, 2012; Webster & Cummins, 1978). Predicted structural protein homology between the *P. acnes* phages in this study and well-characterized proteins belonging to other siphoviruses will be discussed.

Having an overall median host range of 97.5% (Section 3.3.3), high throughput phage spot infections (Figure 3.17) revealed that the phages in our collection have an overall propensity for lytic activity against the diverse population of clinical *P. acnes* isolates (Figure 3.19a), with no preference for a specific *P. acnes* phylotype or antibiotic susceptibility properties. Similar to other studies (Pulverer *et al.*, 1973; Jong *et al.*, 1975; G F Webster and Cummins, 1978; Lood *et al.*, 2008; Marinelli *et al.*, 2012; Liu *et al.*, 2015), all phages demonstrated broad host ranges (maximum and minimum host ranges of 99.6% and 78.1%, respectively) and were unable to infect a variety of common Gram-positive and Gram negative commensals and pathogens—*P. granulosum* ATCC 25564, *P. avidum* ATCC 25577, *E. coli MG1655*, *S. aureus* ATCC 29923, *S. typhimurium TA1535* and *S. pyogenes* ATCC 12204 (Section 2.2.7) (Bek-Thomsen *et al.*, 2008; Fitz-Gibbon *et al.*, 2013; Grice & Segre, 2011; Leeming *et al.*, 1984; Puhvel *et al.*, 1975; Roth & James, 1988). Accounting for only 30.2% of phages, four host range groups (HRGs) were established (HRG1,11.8%; HRG2, 10.5%; HRG3, 5.3%; and HRG4, 2.6%), each containing phages with identical activity spectra against the population of *P. acnes* used in this study. The rest of the phages (69.8%) that comprosed the majority of phages exhibited entirely unique activity spectra. Contrary to previous studies which described *P. acnes* phages as highly similar (Pulverer *et al.*, 1973; Jong *et al.*, 1975; Webster and Cummins, 1978; Lood *et al.*, 2008; Marinelli *et al.*, 2012), our phage collection demonstrated a high degree of variation in their activity spectra (host ranges) (Figure 3.18), which reflects the relatively high level of biological diversity among phages in this collection. The limited genomic and biological diversity among other phage collections is in part due to the limitation in the sampling strategies that other groups established to

isolate their phages. For example, most reports describe isolation of *P. acnes* phages from samples taken from a limited number of human subjects (Brown *et al.*, 2016; Farrar *et al.*, 2007; Marinelli *et al.*, 2012).

Overall, *P. acnes* isolates were sensitive to infection by the majority of the members of our phage collection (Figure 3.19b). Sensitive to the entire phage collection, *P. acnes* isolates of PVG1 (phagovar group 1) comprise the majority of the *P. acnes* population (67.9%). Other PVGs vary in terms of their level of susceptibilities, however, all were susceptible to at least 77% of the phage collection (Figure 3.18). Only three isolates were sensitive to under 50% of the phage collection (Figure 3.18); of these, a single isolate—*P. acnes* #9—was naturally-resistant to all phages prior to evolutionary derivation of a phage with extended host range that was able to infect #9 (Section 3.3.3).

Compared to other studies, the proportion of *P. acnes* isolates that were sensitive to less than 50% (below median) of the phages in this study (1.3%) was over three times less than that of *P. acnes* isolates described by other reports (10.3%, Jong *et al.*, 1975; 12.1%, Lood and Collin, 2011; 7.4%, Marinelli *et al.*, 2012; 4.5%, Liu *et al.*, 2015). These groups of insensitive *P. acnes* isolates (Pulverer *et al.*, 1973; Jong *et al.*, 1975; Webster and Cummins, 1978; Lood *et al.*, 2008; Marinelli *et al.*, 2012) have challenged the prospect of developing phage-based cocktail formulations for acne treatment. The relative proportion of *P. acnes* phages in all except one (Marinelli *et al.*, 2012) of these studies is larger than the relative proportion of phages in this study (Jong *et al.*, 1975; Liu *et al.*, 2015b; Lood & Collin, 2011); therefore, simply increasing the proportion of *P. acnes* phages relative to the number of hosts will not reduce the small groups of highly-insensitive isolates. Thus, the variation between the level of sensitivity observed for *P.*

acnes in this study compared to others is by virtue of composition (diversity), not size, of the phage collection. Previous studies have cited direct cutaneous sampling of a limited number of human subjects, spontaneous lysis or induction of pseudolysogens from *P.* acnes using mitomycin C, as sources for isolation of *P. acnes* phages, which have been characterized by limited variation in terms of host activity spectra and genome sequence (Pulverer *et al.*, 1973; Jong *et al.*, 1975; Webster and Cummins, 1978; Farrar *et al.*, 2007; Lood *et al.*, 2008; Lood and Collin, 2011; Marinelli *et al.*, 2012; Liu *et al.*, 2015; Brown *et al.*, 2016). The bacterial composition of the pilosebaceous units are regularly limited to, or overwhelmingly dominated, by *P. acnes* (Puhvel *et al.*, 1975; Leeming *et al.*, 1984; Roth and James, 1988; Bek-Thomsen *et al.*, 2008; Grice and Segre, 2011; Marinelli *et al.*, 2012; Fitz-Gibbon *et al.*, 2013). The pilosebaceous unit provides a unique, protected niche where *P. acnes* (and their phages) can survive and proliferate with minimal challenge by selective pressures that may otherwise function to diversify the species and its phage populations. Therefore, based on previous studies, *P. acnes* phages derived from sources of limited microbial diversity will not challenge naturally-resistant *P. acnes* isolates.

Frequency of *P. acnes* isolates with phage insensitivity is reduced by increasing the genetic diversity across phages. Based on this assumption, increasing the level of diversity across the phage collection further skews the frequency distribution of *P. acnes* sensitivity presented in Figure 3.19b leftward, resulting in an overall higher level of sensitivity among *P. acnes* isolates. Thus, overcoming acquired or natural resistance of *P. acnes* strains to bacteriophage infection requires access to a diverse range of *P. acnes* phages and is necessary for development of a phage-based cocktails for application in

future acne treatment. Obtaining *P. acnes* phages from sewage was the underlying reason for the diversity among our phage collection. The raw sewage is a dense milieu of richly diverse microbial populations (Sulakvelidze & Barrow, 2004). The larger and multi-ethnically diverse the human communities become as in metropolitan cities, the more globally diverse microbial communities will be represented in the raw sewer. . Therefore, choosing the raw sewer of a large multi-ethnically populated urban area of over one million inhabitants such as Ottawa-Gatineau resulted in a diverse collection of phages with a broader activity spectra against *P. acnes* isolates, which would otherwise be more insensitive to less diverse phage collections.

Phage diversity can also be increased through evolutionary derivation of mutant phages. Defined as the number of mutations per base pair per replication, the rate by which phage mutants are generated is roughly two orders of magnitude above that of their bacterial hosts (Drake, 1991; Drake *et al.*, 1998). Therefore, in an actively replicating population of phages, production of mutant phage progeny can serve to infect emergent and/or naturally-resistant bacterial hosts that may have otherwise evaded phage infection (Kysela & Turner, 2007). Demonstrating the ease by which resistance can be counteracted absolute insensitivity of *P. acnes* strain #9 to all phages was overcome by exploiting the dynamism of the phage-host interaction using a phage that had the broadest *P. acnes* host range—πα6919-4; and a high-titre phage stock. High titre phage inoculum was generated via infection of *P. acnes* ATCC6919 by phage πα6919-4 giving rise to a sub-population of mutant phage derivatives. Inoculation of resistant cells with a high titre dose of πα6919-4 made it possible to select for and isolate a few plaques of variant phage with extended host range that had the capacity to successfully lyse naturally-resistant *P.*

acnes #9 (Figure 3.17). The *in vitro* evolutionary selection of variant phage πα9-6919-4 in this study proved the value of application of a high-density phage inoculums to directly select for a limited number of mutant phages that were capable of infecting the initial population of resistant *P. acnes* #9, while minimizing the likelihood of emergence of further naturally-resistant *P. acnes* populations. Kysela and Turner showed that peak population sizes of initial and emergent bacterial populations can be controlled by the titre of the initial phage inoculum administered (Kysela & Turner, 2007). This principle has a great applied value in practicing phagetherapy. Administration of a highly-dense initial dose of phage decreases peak populations of both the initial and emergent bacterial populations, whereas administration of a low titre phage inoculum increases the exponential replication of phage *in situ* and decreases the peak population of emergent bacteria (Kysela & Turner, 2007). Therefore, to eliminate both initial and emergent *P. acnes* populations, the ideal phage cocktail preparation would be a dense inoculum of phages that, when combined, demonstrate complete, overlapping host range coverage of all *P. acnes* isolates used in this study. The importance of evolutionary derivation of mutant phages with modified properties can be understood further if one assumes that it is almost analogous to a derivation of modified antibiotics from a pool of parental formulations with highly valuable advantages as; i) the derivation process is extremely cost effective (a few plates and high-titre phage stock), while the derivation of antibiotics with modified chemistry requires at the least about half a billion to one billion dollars in investment, ii) the duration of time needed for phage derivation is less than 48 hours, while for antibiotics it takes an average of about 5 years of continuous work, iii) phages are considered GRAS and therefore, regulatory hurdles to drive them to application is

highly simplified and mitigated, and iv) modern medicine is trending towards application of personalized treatments, which is in excellent alignment with application of personalized phage cocktails.

Overall, the phages assessed in this study demonstrated broad (Figure 3.19a) and diverse activity spectra against clinical *P. acnes* isolates (Figure 3.18), which were highly variable in terms of their antibiotic susceptibility profiles (Table 3.6), geographical origin, anatomical site of isolation and phylotype (Table 3.5).Thus, majority of phages in this collection are ideal candidates for minimal cocktail formulations due to their highly-targeted inter-species specificity combined with indiscriminate intra-species lytic activities. To be evaluated in future *in vivo* studies, the following demonstrate broad, overlapping lytic activities against the *P. acnes* isolates used in this study, making them ideal candidates for minimal phage cocktail formulations for acne treatment: the formulation will include phages of any member of "HRG1" (πα32; πα33; πα314; πα54; πα6919-3; πα6919-8; πα29399-3; πα3-SS3-1; πα3-SS3-2), a member from phages of group "HRG3" (πα35; πα313; πα6919-4; πα29399-4), πα315, πα43 and πα9-6919-4 (Figure 3.18).

Molecular characterization of phages

According to previous studies, sequence diversity among the *P. acnes* phage genomes is relatively low, especially in comparison to the level of diversity demonstrated within *Mycobacterium*, *Staphylococcus* and *Pseudomonas* phage groups (Marinelli *et al.*, 2012). However, based on the diverse range of activity spectra (host range) demonstrated by phages in this study, diversity at the genomic level was expected. Digestion of sixty-four *P. acnes* phage genomes with *BamHI* produced an array of restriction fragment banding

patterns (Figure 3.20); phages were visually grouped into nine clusters based on their banding patterns. Such a diverse restriction banding patterns coincides with differences in the number and positions of *BamHI* restriction recognition sites, thereby it can be an indication of sequence diversity among the *P. acnes* phage genomes in our collection. To further examine the level of diversity at the genomic level and to gain insight into the genetic determinants of functional activity, phage isolates with a variety of host ranges were selected from each *BamHI* clusters for genome sequencing.

Sequencing of twelve *P. acnes* phage genomes revealed a high degree of structural (Table 3.7) and organizational (Figure 3.21) similarities, but vast diversities at nucleotide and amino acid levels among those sequenced in this study and compared with other available sequences. Shown in Table 3.7, average genome length (29732 bp), G-C content (54.52%) and number of open reading frames (42) were within the ranges of those previously reported (Farrar *et al.*, 2007; Lood and Collin, 2011; Marinelli *et al.*, 2012; Liu *et al.*, 2015; Brown *et al.*, 2016). Described in detail in Section 3.4.2.1, gross arrangement and annotation of ORFs corresponding to phage genomes sequenced in this study were similar to those of other *P. acnes* phage genomes, with *orf*1_{PA6} to *orf*21_{PA6} in the left arm transcribed rightward and encoding gene products involved in assembly and host lysis, while *orf*22_{PA6} to *orf*48_{PA6} in the right arm were transcribed leftward and encoded gene products having regulatory functions (Figure 3.21; Table 3.8). Due to gaps and unresolved bases present in the sequenced genomes, overall sequence identity among the sequenced phage genomes cannot be determined at the time of this writing, however, it was possible to analyze reliably complete individual gene sequences.

Although the prevalence of phage-resistant *P. acnes* is relatively rare, naturally-resistant

strains commonly demonstrate widespread insensitivity to infection by phages that have been reported by other studies (Figure 3.19b; Marinelli *et al.*, 2012). Broad susceptibility patterns of *P. acnes* isolates to phages is in part due to the diversity of *P. acnes* phages. Therefore, resistance can be overcome by diversifying the phage components involved in host specificity. Phage receptor mutations commonly result inimpairment of phage adsorption to host leading to resistance to phage (Labrie *et al.*, 2010). Resistance may be evaded by counter-mutations leading to conformational alteration of phage tail structures involved in receptor recognition and binding. Previous studies have speculated on the roles of various *P. acnes* phage tail components in host cell adsorption (Farrar *et al.*, 2007; Lood *et al.*, 2008; Marinelli *et al.*, 2012; Brüggemann and Lood, 2013; Liu *et al.*, 2015; Brown *et al.*, 2016), this study sought to reveal evidence of functional associations between tail components and host range of *P. acnes* phages.

Molecular basis of phage host range diversity

Several of the structural genes in the left arm of the genome (*orf*1_{PA6}-*orf*22_{PA6}) were fully sequenced without error (Figure 3.21). Tail-associated proteins equivalent to gp11_{PA6}, gp14_{PA6}, gp15_{PA6}, gp16_{PA6}, gp17_{PA6}, gp18_{PA6} and gp19_{PA6}, are functional at the phage-host interface during infection (Table 3.8). Reliable sequences were available for all except for two proteins encoded by *orf*18_{PA6} and *orf*19_{PA6}. To gain insight into the structural determinant(s) of *P. acnes* phage host range, the level of congruence between known amino acid sequences of tail-associated components—gp11_{PA6}, gp14_{PA6}, gp15_{PA6}, gp16_{PA6}, and gp17_{PA6}—were assessed against phage host range data using global CADM analysis and complimentary Mantel tests, with gp1_{PA6} as a negative control. As shown in Table 3.9, results of the global CADM test (W = 0.2705912; P = 0.0009) followed by

Mantel test, revealed concordance among the datasets corresponding to phage host range and gp11 (r_s=0.4152, P=0.0356). Spanning genome bases 7172 to 7813 (*P. acnes* phage PA6 numbering), *orf*11_{PA6} encodes gp11—the major tail protein (MTP). As the primary structural component of the siphovirus tail, MTPs assemble into homohexameric rings that stack on top of one another to form the hollow tail tube assembled around and in contact with the tape measure protein extended from the base of the icosahedral head to the lower tail components (Fokine & Rossmann, 2014; Pell *et al.*, 2009). The role of the phage tail tube in host range determination has not been a focus of *P. acnes* phage studies. However, previous studies have speculated on the involvement of the tail tube with host adsorption based on the presence of protrusions that decorate the outer surface of the tail tubes of some siphoviruses, namely *B. subtilis* phage SPP1 (Auzat *et al.*, 2008), *E.coli* phage λ (Pell *et al.*, 2010), *Lactococcus lactis* phage p2 (Bebeacua *et al.*, 2013b), and *Mycobacterium abscessus* subsp. *bolletii* phage Araucaria (Sassi *et al.*, 2013). Comprised of MTP C-terminal domain residues (C-domain), the protrusions on the external surfaces of the hexameric rings are presumed to mediate phage adsorption onto e.g. the sugar moieties on the cell walls of Gram-positive hosts (Auzat *et al.*, 2008; Bebeacua *et al.*, 2013b; Pell *et al.*, 2010; Sassi *et al.*, 2013). This initial adsorption, which lands the phage horizontally on the cell surface, is mediated by the MTP C-domain and positions the phage in the vicinity of the receptor involved in inititation of infection that is mediated by the tail fibers providing strong interaction and binding to the receptor. There is no report that N-terminal domain of MTP plays a role in this process.

To gain insight into involvement of MTP in host specificity and host range of phages, especially the πα9-6919-4 that had extended host range, we sought to identify some of the

MTP homologs that preferably would have reported structural data. As shown in results Section 3.4.2.4, there was only a handful of proteins identified by BlastP search, neither of them had a PDB file to provide structural information. Moreover, homology alignments were restricted to only the N-domain of the MTPs and no matches were found to C-domain. Having no significant homology with proteins of other phage groups that use the C-domain for cell adsorption, the C-domain residues of the παMTPs may confer specificity to the *P. acnes* phages together with tail fibers through interaction with the surface receptor on *P. acnes* hosts.

Since blastP homology search failed to identify significant alignments to other phage MTPs that use the C-domain protrusions for host cell adsorption, we reasoned that a search additionally based on domain secondary structure prediction may identify distant proteins with related functions, which can also be used for structural modeling. Structural similarity search of πα6919-4 MTP with HHPred (according to Section 2.2.8.4.3) using the entire παMTP amino acid sequence was conducted to identify MTP homologues of phages. Full-length παMTP exhibited low sequence homology (i.e. 6% identity) with the $gpV_{N,}$ of phage λ, which encodes the N-domain of phage λ MTP, but not the C-domain consisted of 48 amino acid residues (Figure 3.25). Lack of alignment of MTP C-domain is considered as the specificity of this domain for *P. acnes* confirming the blastP results. Regardless of the role that C-domain might play in host recognition and possibly the intraphage differences with regard to their host ranges, the lack of structural information hindered us from further analysis. However, involvement of N-domain in host recognition has not been reported for any of known phages. Therefore, it appeared that we could only investigate the differences between πα6919-4 and πα9-6919-4 MTPs.

Hydrophobic side chains of fourteen highly-conserved residues of λ gpV_N are essential components of the hydrophobic gpV_N core (Pell *et al.*, 2009). HHPred search based structural alignment map identified hydrophobic residues in πα6919-4 MTP and πα9-6919-4 MTP corresponding to those in phage λ gpV_N. Across all παMTP sequences, hydrophobicity is conserved for thirteen παMTP residues aligned to core hydrophobic gpV_N residues (Figure 3.26). Moreover, structural alignment consistently identified insertion of an 18 consecutive amino acids within N-domains of παMTPs at D104 corresponding to gpV_N numbering (Figure 3.25). Given the probability of structural homology between the παMTPs and gpV_N combined with conservation of hydrophobic side chains of παMTPs residues corresponding to the gpV_N core residues, gpV_N of *E. coli* phage λ can potentially serve as a model to predict the 3D structure of the παMTP and might offer an explanation for the activity of the mutant πα9-6919-4 phage.

Structural modeling of MTP

Three-dimensional structures of N-domains of πα6919-4 MTP and πα9-6919-4 MTP were modeled upon phage λ gpV_N NMR data using LOMETS (See section 2.2.8.4.3) (Wu & Zhang, 2007) . The λ gpV_N amino acid sequence derived from its PDB (2K4Q) file was used as an internal control to validate prediction accuracy of LOMETS. High score hits for λ gpV_N PDB data, as well as for 3D models of παMTP, were suggested on the basis of λ gpV_N structural data (Figure 3.27). The overall structure of gpV_N is conserved in πα6919-4 and πα9-6919-4 models except for the β4 and β5 strands that appeared to be disordered in both πα MTPs (Figure 3.27a-c). The hydrophobic core consisted of β1-β7 and C3 loop (between β2-β3) are known for contributing to the formation of hydrophobic interfaces through which the MTP monomers assemble into

hexameric ring state. These interfaces facilitate the assembly of tail tube by providing protein-protein interactions between lateral interfaces of monomers and on the surfaces at the top and bottom of the hexameric rings. The relatively extended C3 loop is preserved in the παMTP models and most likely facilitates the interaction between stacking hexameric rings at top-bottom interfaces (Pell *et al.*, 2009). The β7 strand and amino acids past this region gradually become disordered. It is suggested that these disordered string of residues function as a transitional linker to connect the N-domain to the C-domain. The C-domain is believed to face the external surface of the tail tube where in some phages it takes part in recognition and transient binding of phage to its cell surface receptors (Bebeacua *et al.*, 2013b; Pell *et al.*, 2009). The β4 strand is immediately preceeded by a disordered loop (C5) past a single α-helix. The intervening α1-β4 loop showed a drastic difference between three models in terms of their length and amino acid compositions. Interestingly, this region contains the three sole sites of sequence variation between MTPs of πα69194 and πα9-69194, characterized by three adjacent amino acid substitutions (GSD → EPE) (Figure 3.23), indicating a functional role for this loop in extending the host range of the mutant phage πα9-6919-4. The C5 loop between α1 helix and β4 strand of lambda phage MTP gpV_N domain is short and includes only 3 amino acids (G106 -T108). Insertion of a stretch of an additional 18 amino acids into the C5 loop of πα6919-4 and πα9-6919-4 MTPs has progressively resulted in unwinding of α1 helix increasing the C5 loop length to 21 and 24 amino acids, respectively (Figure 4.1 and Figure 3.27d-f; Figure 4.1). By the most conservative measures if one considers this as the minimal length added to C5 loop and together with their amino acid compositions, it has elevated the negatively charged electrostatic state of the protein in this region

contributing to its tendency to scape hydrophobic interactions and most probably to face the external solvent environment. It is noteworthy that the amino acid changes in πα9-6919-4 from GSD to EPE is not only a contributing factor to the overall change in electrostatic state of πα9-6919-4 C5-loop, also by non-conservaive Ser→Pro mutation an additional proline residue is added to the existing proline at position 115. This is important given the dynamic structural interconversions that proline resides cause especially in a relatively disordered stretches of amino acids in coils and loops providing fuctional properties to these structures. In the absence of empirically determined structural data for παMTP we speculate that in order for these drastic mutations together with C5 loop play a role in contributing to the extended host range of the phage πα9-69194, the C5 loop must be positioned on the outer surface of the hexameric rings on the phage tail tube to be accessible to cell surface receptors. A similar loop to C5 in gpV_N and an α1 helix-like structures have been identified in Hcp1 protein of SS6 protein secretory system in *P. aeruginosa* (Figure 4.1a) (Leiman *et al.*, 2009; Mougous *et al.*, 2006; Pell *et al.*, 2009). Mougous *et al.* (2006) showed stacked hexameric structures composed of Hcp1 protein that form a tube with an internal diameter of 40 angstroms that function as type VI bacterial protein secretory apparatus (Figure 4.1b). Hcp1 in monomeric and hexameric states resemble the gpV_N. Most often present in hexameric from in solution, the single α1 helix and the proceeding disordered loop assemble in a hexagonal symmetry with α1 helix and the loop facing outward when viewed from the top of the hexameric assemblies (Figure 4.2b) (Mougous *et al.*, 2006). Interestingly, despite the fact that the C5 loop is located between four of the fourteen conserved hydrophobic residues in gpV_N (Figure 3.26), its structural alignment with Hcp1 was

significant and provided support to our hypothesis of a role, previously not described, for the C5 loop in host recognition in addition to C-domain (Figure 4.3). Both gpV_N and the predicted πα6919-4/96919-4 MTP structures given in Figure 3.27 show residues at the C-terminal end of the πα6919-4 MTP/gpV_N alignment that are located at the external surface of the hexameric rings, and thus may serve as an anchoring point for a tail tube decorating C-domain of gpV_N (Pell *et al.*, 2009) and πα6919-4/9-6919-4 MTPs. If the πα6919-4 MTP does indeed contain a C-terminus tail decorating domain, it must have been comprised of approximately forty-eight residues that do not exhibit any significant structural homology with gpV_C . The process of mutational bypassing the highly-resistant *P. acnes* strain #9 that affected the C5 loop can only be explained if a role for the N-domain be considered in host recognition reasonably leading to active infection. Based on this study and supporting observations by others, it is reasonable to propose a hypothetical binding/infection model that the residues located in the C5 loop region are involved in host specificity by acting as an auxiliary receptor recognition structures in cooperation with C-domain and tail fibers. They might achieve this either by assuming a properly folded stable structures or might be induced to assume a conformational change in the hexameric ring structure in such a way as to make adsorption to the host receptor possible. Overall, this observation provides further evidence in support of the significance of the MTP in determining host specificity of *P. acnes* phages while demonstrating the relative ease by which phages may adapt to compensate for resistance in nature by virtue of the dynamic phage-host relationship, unlike the static mechanism of action by conventional antibiotics.

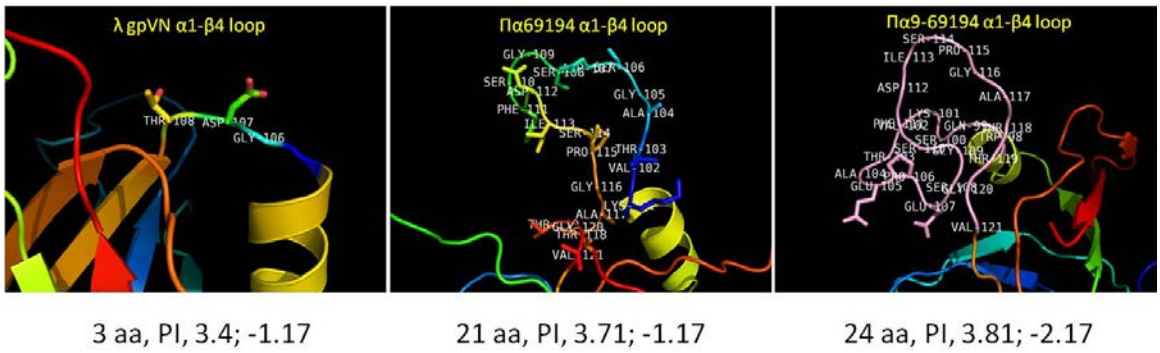

Figure 4.1: A close up view to the α1-β4 loop (C5 loop) in λgpV$_N$, πα6919-4 and πα9-6919-4 MTP models.

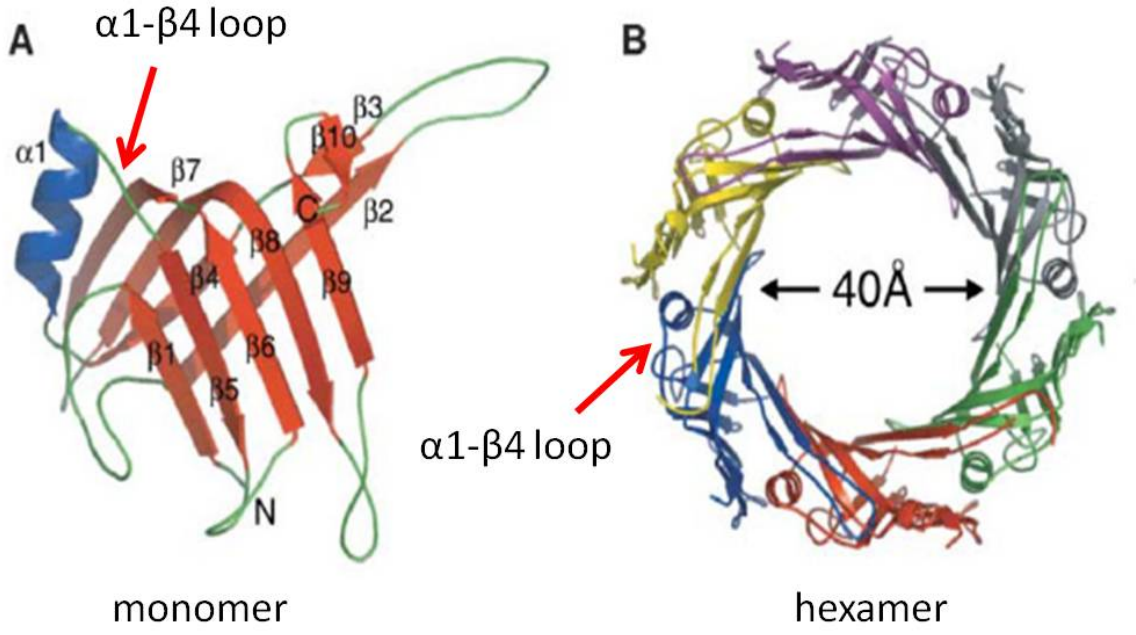

Figure 4.2: Prosed models for three dimensional structures of Hcp1 protein in A) monomeric state and B) top-bottom view of hexameric Hcp1. Red arrows point to the position of a a helix-loop structure in Hcp1 equivalent to λ gpV_N α1 helix and α1-β4 loop. Note the position of helix-loop structures at the outer surface of hexamric ring and their exposure to solvent (Mougous *et al.*, 2006).

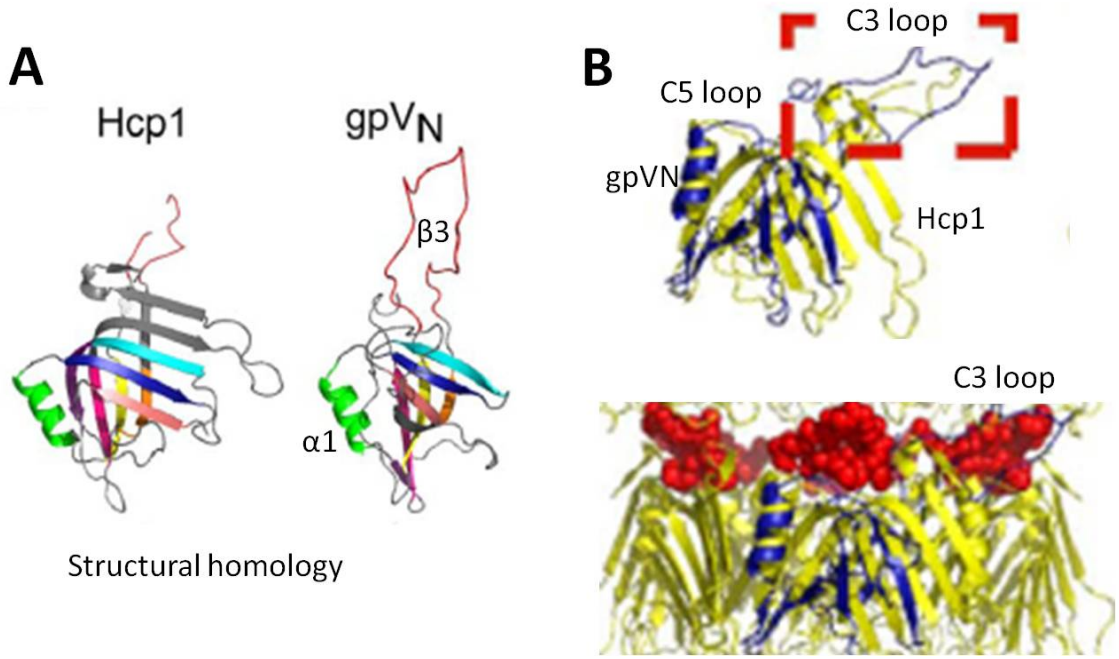

Figure 4.3: Structural homology of gpV$_N$ and Hcp1 proteins. A) conservation of α1 helix and C3 and C5 loops are shown. B) Superimposition of a single monomer of gpV$_N$ on Hcp1 in monomeric state (upper panel) and Hcp1 in hexameric state (Pell *et al.*, 2009).

As previously discussed, acne vulgaris is the most common skin condition worldwide, thus this study aimed to evaluate the therapeutic potential of a phage collection for a broad population of acne sufferers. The *P. acnes* collections in this study do not represent a global population of clinically relevant isolates, therefore this is a limitation of this study. Although the isolate collections used in this study originated from Lund and various locations within Canada, it would be reasonable to assess the biological activity of our phage collection against isolates acquired from other regions of the world in support of the therapeutic potential of our phage collection.

Another limitation of this study is the lack of complete genome sequence information for all phages in our collection. Acquiring this information would provide the opportunity to assess the congruency between all phage proteins and host range and would allow us to further strengthen our statistical analysis of the association between phage MTP and host range. There are also limitations involved with structural prediction of phage MTP that extend beyond the inherent computational limitations that may only be resolved by experimental data. The MTP structure was predicted based on a template, therefore any unaligned regions between the template (gpV_N) and target (MTP) sequences remain unresolved in the predicted protein target structure. Furthermore, identification of templates that share a high level of homology with MTP sequences would increase the accuracy of the secondary and tertiary structure.

5 Conclusion

As discussed, acne vulgaris is the most prevalent skin condition among adolescents and young adults globally (Johnson & Roberts, 1978; Rea *et al.*, 1976; Wolkenstein *et al.*, 2003). The role of *P. acnes* in the development and persistence of acne has been established (Das & Reynolds, 2014). Treatment is indicated for all levels of severity and is often accompanied by a wide range of adverse side effects (Zaenglein *et al.*, 2016). Antibiotics are commonly-used for treatment of moderate to severe acne, resulting in the rise of widespread, global resistance among *P. acnes* and other bacteria (Del Rosso & Zeichner, 2016). Phage therapy may offer a promising alternative to conventional acne treatments.

In this study, a diverse collection of 224 clinically-relevant *P. acnes* isolates was established from patient samples of healthy and infected superficial and deep tissue sites from patients in Canada and Lund, Sweden. All *P. acnes* phylotype groups were represented within the collection, with the largest number of isolates of type IA. The frequency of antibiotic resistance among *P. acnes* isolates was highest for macrolides, followed by clindamycin and tetracyclines; as anticipated, a history of antibiotic treatment was associated with antibiotic resistant *P. acnes* phenotypes.

Seventy *P. acnes* phages were isolated from raw sewage and six from human subjects, then tested against our diverse collection of *P. acnes* isolates. Just three *P. acnes* isolates in our entire collection were sensitive to less than 50% of our phages thus demonstrating the high level of diversity among phages isolated from raw sewage. Unlike the static nature of antibiotics, the phage-host relationship is dynamic and can be exploited to

overcome any naturally-occuring or evolved resistance, even among multi-drug resistant bacteria. Rapid *in vitro* derivation of a mutant phage that has lytic activity against a previously uninfectable *P. acnes* isolate demonstrates the ease by which *P. acnes* resistance may be overcome. Overall, our phages demonstrated broad host ranges; their individual host ranges were highly variable and could be combined to produce a variety of minimal phage cocktails having overlapping host ranges to achieve 100% *in vitro* efficacy against all *P. acnes* isolates in our collection.

Although we were unable to obtain complete genome sequences for the twelve sequenced phages, the information available at the time of this study revealed congruency between *P. acnes* phage MTP sequences and corresponding host ranges. Structural homology searches suggest that παMTP N-domain may share a common evolutionary ancestor with *E. coli* λ phage gpV_N, while no distant homologs were identified for παMTP N-domain, suggesting this domain may be involved in host recognition. Furthermore, modelling of the παMTP N-domain revealed a stretch of 18 amino acids which may also be involved in host recognition. Relative to the resources required to identify, develop and test traditional synthetic antibiotics, the isolation, characterization and assessment of therapeutic phage candidates is significantly less expensive and highly accessible in nature. In the advent of an increased interest and reliance on personalized medicine, phage-based therapeutics offer highly targeted antibacterial alternatives to conventional antibiotics, which are widely accessible in nature and easily isolated.

Future studies

Future studies are needed to demonstrate the therapeutic potential of the phage cocktail proposed in this study. Efficacy testing of the phage cocktail formulations in animal models can support subsequent preclinical trials. To increase the range of phage-based acne treatment options, known antibacterial phage products, such as endolysins, may be expressed as chimeric proteins to modulate antibacterial specificity. To gain a better understanding of the biology of the phages within our collection, orfs of unknown function can be functionally characterized, thus revealing new phage products that may be considered as candidates for therapeutic applications.

To further investigate the role of P. acnes phage MTPs in host specificity, structural studies of MTPs may be conducted through X-ray crystallography or NMR in conjunction with mutagenesis studies. Additionally, host specificity conferred by MTP or other tail fibres may be exploited as drug carriers for targetted drug delivery to reduce toxicity and dosage, or to delivery higher dosages for short treatment durations.

References

Abdulmassih, R., Makadia, J., Como, J., Paulson, M., Min, Z. & Bhanot, N. (2016). Propionibacterium acnes: Time-to-Positivity in Standard Bacterial Culture From Different Anatomical Sites. *J Clin Med Res* **8**, 916–918.

Achermann, Y., Goldstein, E. J. C., Coenye, T. & Shirtliffa, M. E. (2014). Propionibacterium acnes: From Commensal to opportunistic biofilm-associated implant pathogen. *Clin Microbiol Rev* **27**, 419–440.

Ackermann, H. W. & Eisenstark, A. (1974). The present state of phage taxonomy. *Intervirology* **3**, 201–219.

Ackermann, H.-W. (2011). Bacteriophage Taxonomy. *Microbiol Aust* **32**, 90–94.

Aksu, A. E. K., Metintas, S., Saracoglu, Z. N., Gurel, G., Sabuncu, I., Arikan, I. & Kalyoncu, C. (2012). Acne: prevalence and relationship with dietary habits in Eskisehir, Turkey. *J Eur Acad Dermatol Venereol JEADV* **26**, 1503–1509.

Alam, M. & Dover, J. S. (2006). Treatment of acne scarring. *Skin Ther Lett* **11**, 7–9.

Alexis, A. F. (2008). Clinical considerations on the use of concomitant therapy in the treatment of acne. *J Dermatol Treat* **19**, 199–209.

Altschul, S. F., Gish, W., Miller, W., Myers, E. W. & Lipman, D. J. (1990). Basic local alignment search tool. *J Mol Biol* **215**, 403–410.

Alva, V., Nam, S.-Z., Söding, J. & Lupas, A. N. (2016). The MPI bioinformatics Toolkit as an integrative platform for advanced protein sequence and structure analysis. *Nucleic Acids Res* **44**, W410-415.

AmpliPhi Biosciences. **(2016, March 7).** AmpliPhi Signs Clinical Trial Agreement with University of Adelaide to Conduct a Phase I Trial of Bacteriophage Therapy for Treating Staphylococcus aureus Infections. *AmpliPhi Biosci*.

Aravind, L. & Koonin, E. V. (1998). Phosphoesterase domains associated with DNA polymerases of diverse origins. *Nucleic Acids Res* **26**, 3746–3752.

Aubin, G. G., Portillo, M. E., Trampuz, A. & Corvec, S. (2014). Propionibacterium acnes, an emerging pathogen: from acne to implant-infections, from phylotype to resistance. *Médecine Mal Infect* **44**, 241–250.

Augustin, M., Herberger, K., Hintzen, S., Heigel, H., Franzke, N. & Schäfer, I. (2011). Prevalence of skin lesions and need for treatment in a cohort of 90 880 workers. *Br J Dermatol* **165**, 865–873.

Auzat, I., Dröge, A., Weise, F., Lurz, R. & Tavares, P. (2008). Origin and function of the two major tail proteins of bacteriophage SPP1. *Mol Microbiol* **70**, 557–569.

Babilas, P., Schreml, S., Szeimies, R.-M. & Landthaler, M. (2010). Intense pulsed light (IPL): a review. *Lasers Surg Med* **42**, 93–104.

Bae, Y., Ito, T., Iida, T., Uchida, K., Sekine, M., Nakajima, Y., Kumagai, J., Yokoyama, T., Kawachi, H. & other authors. **(2014).** Intracellular Propionibacterium acnes infection in glandular epithelium and stromal macrophages of the prostate with or without cancer. *PloS One* **9**, e90324.

Balkrishnan, R., Kulkarni, A. S., Cayce, K. & Feldman, S. R. (2006a). Predictors of Healthcare Outcomes and Costs Related to Medication Use in Patients With Acne in the United States. *Cutis* **77**, 251–255.

Balkrishnan, R., Kulkarni, A. S., Cayce, K. & Feldman, S. R. (2006b). Predictors of healthcare outcomes and costs related to medication use in patients with acne in the United States. *Cutis* **77**, 251–255.

Barber, K. (2011). Acne Management for Canadian Primary Care. Elsevier Canada.

Barnard, E., Nagy, I., Hunyadkürti, J., Patrick, S. & McDowell, A. (2015). Multiplex Touchdown PCR for Rapid Typing of the Opportunistic Pathogen Propionibacterium acnes. *J Clin Microbiol* **53**, 1149–1155.

Barnard, E., Shi, B., Kang, D., Craft, N. & Li, H. (2016a). The balance of metagenomic elements shapes the skin microbiome in acne and health. *Sci Rep* **6**.

Barnard, E., Liu, J., Yankova, E., Cavalcanti, S. M., Magalhães, M., Li, H., Patrick, S. & McDowell, A. (2016b). Strains of the Propionibacterium acnes type III lineage are associated with the skin condition progressive macular hypomelanosis. *Sci Rep* **6**, 31968.

Başak, P. Y., Cetin, E. S., Gürses, I. & Ozseven, A. G. (2013). The effects of systemic isotretinoin and antibiotic therapy on the microbial floras in patients with acne vulgaris. *J Eur Acad Dermatol Venereol JEADV* **27**, 332–336.

Bayston, R., Ashraf, W., Barker-Davies, R., Tucker, E., Clement, R., Clayton, J., Freeman, B. J. C. C. & Nuradeen, B. (2007). Biofilm formation by Propionibacterium acnes on biomaterials in vitro and in vivo: impact on diagnosis and treatment. *J Biomed Mater Res A* **81**, 705–709.

Bebeacua, C., Lai, L., Vegge, C. S., Brøndsted, L., van Heel, M., Veesler, D. & Cambillau, C. (2013a). Visualizing a complete Siphoviridae member by single-particle electron microscopy: the structure of lactococcal phage TP901-1. *J Virol* **87**, 1061–1068.

Bebeacua, C., Tremblay, D., Farenc, C., Chapot-Chartier, M.-P., Sadovskaya, I., van Heel, M., Veesler, D., Moineau, S. & Cambillau, C. (2013b). Structure, Adsorption to Host, and Infection Mechanism of Virulent Lactococcal Phage p2. *J Virol* **87**, 12302–12312.

Bek-Thomsen, M., Lomholt, H. B. & Kilian, M. (2008). Acne is Not Associated with Yet-Uncultured Bacteria. *J Clin Microbiol* **46**, 3355–3360.

Bémer, P., Léger, J., Tandé, D., Plouzeau, C., Valentin, A. S., Jolivet-Gougeon, A., Lemarié, C., Kempf, M., Héry-Arnaud, G. & other authors. (2016). How Many Samples and

How Many Culture Media To Diagnose a Prosthetic Joint Infection: a Clinical and Microbiological Prospective Multicenter Study. *J Clin Microbiol* **54**, 385–391.

Bergey, D. H., Harrison, F. C., Breed, R. S., Hammer, B. W. & Huntoon, F. M. (1923). *Bergey's Manual of Determinative Bacteriology*, 1st edn. Baltimore: The Williams & Wilkins Co.

Berjano, P., Villafañe, J. H., Lo Re, D., Ismael, M., Damilano, M., Bertozzi, L., Romanò, C. L. & Drago, L. (2016). Is propionibacterium acnes related to disc degeneration in adults? A systematic review. *J Neurosurg Sci*.

Berthelot, J.-M., Corvec, S. & Hayem, G. (2017). SAPHO, autophagy, IL-1, FoxO1, and Propionibacterium (Cutibacterium) acnes. *Jt Bone Spine Rev Rhum*.

Berthelot, P., Carricajo, a, Aubert, G., Akhavan, H., Gazielly, D., Lucht, F. F., A Carricajo, M. D., G Aubert, M. D., H Akhavan, M. D. & D Gazielly, M. D. (2006). Outbreak of postoperative shoulder arthritis due to Propionibacterium acnes infection in nondebilitated patients. *Infect Control Hosp Epidemiol Off J Soc Hosp Epidemiol Am* **27**, 987–90.

Bettoli, V., Zauli, S. & Virgili, A. (2015). Is hormonal treatment still an option in acne today? *Br J Dermatol* **172 Suppl 1**, 37–46.

Bickers, D. R., Lim, H. W., Margolis, D., Weinstock, M. A., Goodman, C., Faulkner, E., Gould, C., Gemmen, E. & Dall, T. (2006). The burden of skin diseases: 2004. A joint project of the American Academy of Dermatology Association and the Society for Investigative Dermatology. *J Am Acad Dermatol* **55**, 490–500.

Bikowski, J. B. (2005). Mechanisms of the comedolytic and anti-inflammatory properties of topical retinoids. *J Drugs Dermatol JDD* **4**, 41–47.

bioMérieux. **(2010).** Quality Control of Trimethoprim/sulfamethoxazole MIC testing with S. pneumoniae ATCC 49619. Etest Customer Information Sheet (CIS 013; 16267 A-en-2010/11). Marcy-l'Étoile, France: bioMérieux.

bioMérieux. **(2012a).** Antimicrobial Susceptibility Testing. Etest Package Insert (9302553C - en - 2012/01). Marcy-l'Étoile, France: bioMérieux.

bioMérieux. **(2012b).** Etest Daptomycin (DPC)- technical variable that may cause discrepencies in MIC results. Etest Customer Information Sheet (CIS 014; 14268-en-2012/12). Marcy-l'Étoile, France: bioMérieux.

bioMérieux. **(2012c).** Reading sharp and hazy endpoints. Etest Customer Information Sheet (CIS 007; 16264 B-en-2012/07). Marcy-l'Étoile, France: bioMérieux.

bioMérieux. **(2013).** Table 1. Summary of Etest Performance, Interpretive Criteria and Quality Control Ranges (15211G - 2013/12). bioMérieux SA, France.

Bissek, A.-C. Z.-K., Tabah, E. N., Kouotou, E., Sini, V., Yepnjio, F. N., Nditanchou, R., Nchufor, R. N., Defo, D., Dema, F. & other authors. **(2012).** The spectrum of skin diseases in a rural setting in Cameroon (sub-Saharan Africa). *BMC Dermatol* **12**, 7.

Blatny, J. M., Godager, L., Lunde, M. & Nes, I. F. (2004). Complete genome sequence of the Lactococcus lactis temperate phage phiLC3: comparative analysis of phiLC3 and its relatives in lactococci and streptococci. *Virology* **318**, 231–244.

Bonfield, J. K. & Whitwham, A. (2010). Gap5—editing the billion fragment sequence assembly. *Bioinformatics* **26**, 1699–1703.

Borglund, E., Hägermark, O. & Nord, C. E. (1984). Impact of topical clindamycin and systemic tetracycline on the skin and colon microflora in patients with acne vulgaris. *Scand J Infect Dis Suppl* **43**, 76–81.

Bossard, D. A., Ledergerber, B., Zingg, P. O., Gerber, C., Zinkernagel, A. S., Zbinden, R. & Achermann, Y. (2016). Optimal Length of Cultivation Time for Isolation of Propionibacterium acnes in Suspected Bone and Joint Infections Is More than 7 Days. *J Clin Microbiol* **54**, 3043–3049.

Bourdes, V., Faure, C., Petit, L., Bettoli, V., Bissonnette, R., Dreno, B., Layton, A., Tan, J., Torres, V. & other authors. **(2015).** Modeling of natural history of primary acne lesions and evolution to acne scars. *J Am Acad Dermatol* **72**.

Brito, M. de F. de M., Sant'Anna, I. P., Galindo, J. C. S., Rosendo, L. H. P. de M. & Santos, J. B. dos. **(2010).** Evaluation of clinical adverse effects and laboratory alterations in patients with acne vulgaris treated with oral isotretinoin. *An Bras Dermatol* **85**, 331–337.

Brook, I. (1991). Pathogenicity of Propionibacterium acnes in mixed infections with facultative bacteria. *J Med Microbiol* **34**, 249–252.

Brook, I. (2002). Propionibacterium acnes. In *Antimicrob Ther Vaccines*, 2nd edn., pp. 533–535. Edited by V. L. Yu, G. Edwards, P. S. McKinnon, C. Peolquin & G. D. Morse. New York, USA: Apple Tree Productions, LLC.

Brown, T. L., Petrovski, S., Dyson, Z. A., Seviour, R. & Tucci, J. (2016). The Formulation of Bacteriophage in a Semi Solid Preparation for Control of Propionibacterium acnes Growth. *PloS One* **11**, e0151184.

Brown, T. L., Tucci, J., Dyson, Z. A., Lock, P., Adda, C. G. & Petrovski, S. (2017). Dynamic interactions between prophages induce lysis in Propionibacterium acnes. *Res Microbiol* **168**, 103–112.

Brüggemann, H. (2005). Insights in the Pathogenic Potential of Propionibacterium acnes From Its Complete Genome. *Semin Cutan Med Surg* **24**, 67–72.

Brüggemann, H. & Lood, R. (2013). Bacteriophages Infecting Propionibacterium acnes. *BioMed Res Int* **2013**, 1–10.

Brüggemann, H., Henne, A., Hoster, F., Liesegang, H., Wiezer, A., Strittmatter, A., Hujer, S., Dürre, P. & Gottschalk, G. (2004). The complete genome sequence of Propionibacterium acnes, a commensal of human skin. *Science* **305**, 671–673.

Bruttin, A. & Brüssow, H. (2005). Human Volunteers Receiving Escherichia coli Phage T4 Orally: a Safety Test of Phage Therapy. *Antimicrob Agents Chemother* **49**, 2874–2878.

Brzin, B. (1964). STUDIES ON THE CORYNEBACTERIUM ACNES. *Acta Pathol Microbiol Scand* **60**, 599–608.

Burkhart, C. G. & Burkhart, C. N. (2007). Expanding the microcomedone theory and acne therapeutics: Propionibacterium acnes biofilm produces biological glue that holds corneocytes together to form plug. *J Am Acad Dermatol* **57**, 722–724.

Burkhart, C. N. & Burkhart, C. G. (2003). Microbiology's principle of biofilms as a major factor in the pathogenesis of acne vulgaris. *Int J Dermatol* **42**, 925–927.

Butler-Wu, S. M., Burns, E. M., Pottinger, P. S., Magaret, A. S., Rakeman, J. L., Matsen, F. A. & Cookson, B. T. (2011). Optimization of Periprosthetic Culture for Diagnosis of Propionibacterium acnes Prosthetic Joint Infection. *J Clin Microbiol* **49**, 2490–2495.

Camacho, C., Coulouris, G., Avagyan, V., Ma, N., Papadopoulos, J., Bealer, K. & Madden, T. L. (2009). BLAST+: architecture and applications. *BMC Bioinformatics* **10**, 421.

Campbell, E. A., Korzheva, N., Mustaev, A., Murakami, K., Nair, S., Goldfarb, A. & Darst, S. A. (2001). Structural mechanism for rifampicin inhibition of bacterial rna polymerase. *Cell* **104**, 901–912.

Campbell, V., Legendre, P. & Lapointe, F.-J. (2011). The performance of the Congruence Among Distance Matrices (CADM) test in phylogenetic analysis. *BMC Evol Biol* **11**, 64.

Capoor, M. N., Ruzicka, F., Schmitz, J. E., James, G. A., Machackova, T., Jancalek, R., Smrcka, M., Lipina, R., Ahmed, F. S. & other authors. **(2017).** Propionibacterium acnes biofilm is present in intervertebral discs of patients undergoing microdiscectomy. *PloS One* **12**, e0174518.

Cavarretta, I., Ferrarese, R., Cazzaniga, W., Saita, D., Lucianò, R., Ceresola, E. R., Locatelli, I., Visconti, L., Lavorgna, G. & other authors. **(2017).** The Microbiome of the Prostate Tumor Microenvironment. *Eur Urol*.

Cazanave, C., Greenwood-Quaintance, K. E., Hanssen, A. D., Karau, M. J., Schmidt, S. M., Gomez Urena, E. O., Mandrekar, J. N., Osmon, D. R., Lough, L. E. & other authors. **(2013).** Rapid molecular microbiologic diagnosis of prosthetic joint infection. *J Clin Microbiol* **51**, 2280–2287.

Charif, D. & Lobry, J. R. (2007). SeqinR 1.0-2: A Contributed Package to the R Project for Statistical Computing Devoted to Biological Sequences Retrieval and Analysis. In *Struct Approaches Seq Evol*, Biological and Medical Physics, Biomedical Engineering, pp. 207–232. Edited by D. U. Bastolla, P. D. M. Porto, D. H. E. Roman & D. M. Vendruscolo. Springer Berlin Heidelberg.

Chen, E. S. & Moller, D. R. (2015). Etiologies of Sarcoidosis. *Clin Rev Allergy Immunol* **49**, 6–18.

Chevreux, B., Wetter, T. & Suhai, S. (1999). Genome sequence assembly using trace signals and additional sequence information. *Ger Conf Bioinforma* **99**, 45–56.

Chopra, I., Hawkey, P. M. & Hinton, M. (1992). Tetracyclines, molecular and clinical aspects. *J Antimicrob Chemother* **29**, 245–277.

Chu, R. M., Tummala, R. P. & Hall, W. A. (2001). Focal intracranial infections due to Propionibacterium acnes: report of three cases. *Neurosurgery* **49**, 717–720.

Chuah, S. Y. & Goh, C. L. (2015). The Impact of Post-Acne Scars on the Quality of Life Among Young Adults in Singapore. *J Cutan Aesthetic Surg* **8**, 153–158.

Chukwudi, C. U. (2016). rRNA Binding Sites and the Molecular Mechanism of Action of the Tetracyclines. *Antimicrob Agents Chemother* **60**, 4433–4441.

Chukwudi, C. U. & Good, L. (2016). Interaction of the tetracyclines with double-stranded RNAs of random base sequence: new perspectives on the target and mechanism of action. *J Antibiot (Tokyo)* **69**, 622–630.

Clinical and Laboratory Standards Institute. **(2004).** Methods for Antimicrobial Susceptibility Testing of Anaerobic Bacteria. Approved Standard—Sixth Edition. CLSI document M11-A6. Wayne, PA: Clinical and Laboratory Standards Institute.

Clinical and Laboratory Standards Institute. **(2015).** Performance Standards for Antimicrobial Testing; Twenty-Fifth Informational Supplement. CLSI document M100-S25 (ISBN 1-56238-989-0 [Print]; ISBN 1-56238-990-4 [Electronic]). Clinical and Laboratory Standards Institute, 950 West VAley Road, Suite 2500, Wayne, Pennsylvania 19087 USA.

Coates, P. & Vyakrnam, S. (2002). Prevalence of antibiotic-resistant propionibacteria on the skin of acne patients: 10-year surveillance data and snapshot distribution study. *Br J Dermatol* **146**, 840–848.

Coenye, T., Peeters, E. & Nelis, H. J. (2007). Biofilm formation by Propionibacterium acnes is associated with increased resistance to antimicrobial agents and increased production of putative virulence factors. *Res Microbiol* **158**, 386–392.

Cohen, J. (1960). A Coefficient of Agreement for Nominal Scales. *Educ Psychol Meas* **20**, 37–46.

Colina, M., Monaco, A. L., Khodeir, M. & Trotta, F. (2007). Propionibacterium acnes and SAPHO syndrome: a case report and literature review. *Clin Exp Rheumatol* **25**, 457–460.

Collins, M.-K., Moreau, J. F., Opel, D., Swan, J., Prevost, N., Hastings, M., Bimla Schwarz, E. & Korb Ferris, L. (2014). Compliance with pregnancy prevention measures during isotretinoin therapy. *J Am Acad Dermatol* **70**, 55–59.

Coscia, M. F., Denys, G. A. & Wack, M. F. (2016). Propionibacterium acnes, Coagulase-Negative Staphylococcus, and the “Biofilm-like” Intervertebral Disc. *Spine* **41**, 1860–1865.

Crane, J. K., Hohman, D. W., Nodzo, S. R. & Duquin, T. R. (2013). Antimicrobial susceptibility of Propionibacterium acnes isolates from shoulder surgery. *Antimicrob Agents Chemother* **57**, 3424–3426.

Cresce, N. D., Davis, S. A., Huang, W. W. & Feldman, S. R. (2014). The quality of life impact of acne and rosacea compared to other major medical conditions. *J Drugs Dermatol JDD* **13**, 692–697.

Crowhurst, T., Tieu, J., Fowler, S. & Burnet, S. (2016). De novo Propionibacterium acnes septic arthritis. *BMJ Case Rep* **2016**.

Cummins, C. S. & Johnson, J. L. (1974). Corynebacterium parvum: a synonym for Propionibacterium acnes? *J Gen Microbiol* **80**, 433–442.

Cunliffe, W. J., Aldana, O. L. & Goulden, V. (1999). Oral trimethoprim: a relatively safe and successful third-line treatment for acne vulgaris. *Br J Dermatol* **141**, 757–758.

Cunliffe, W. J., Holland, K. T., Bojar, R. & Levy, S. F. (2002). A randomized, double-blind comparison of a clindamycin phosphate/benzoyl peroxide gel formulation and a matching clindamycin gel with respect to microbiologic activity and clinical efficacy in the topical treatment of acne vulgaris. *Clin Ther* **24**, 1117–1133.

Daguzé, J., Frénard, C., Saint-Jean, M., Dumont, R., Touchais, S., Corvec, S. & Dréno, B. (2016). Two cases of non-prosthetic bone and joint infection due to Propionibacterium acnes. *J Eur Acad Dermatol Venereol JEADV* **30**, e136–e137.

Dai, W. S., LaBraico, J. M. & Stern, R. S. (1992). Epidemiology of isotretinoin exposure during pregnancy. *J Am Acad Dermatol* **26**, 599–606.

Darling, A. C. E., Mau, B., Blattner, F. R. & Perna, N. T. (2004). Mauve: multiple alignment of conserved genomic sequence with rearrangements. *Genome Res* **14**, 1394–1403.

Darling, A. E., Mau, B. & Perna, N. T. (2010). progressiveMauve: multiple genome alignment with gene gain, loss and rearrangement. *PloS One* **5**, e11147.

Das, S. & Reynolds, R. V. (2014). Recent advances in acne pathogenesis: implications for therapy. *Am J Clin Dermatol* **15**, 479–488.

Davidsson, S., Mölling, P., Rider, J. R., Unemo, M., Karlsson, M. G., Carlsson, J., Andersson, S.-O., Elgh, F., Söderquis, B. & Andrén, O. (2016). Frequency and typing of Propionibacterium acnes in prostate tissue obtained from men with and without prostate cancer. *Infect Agent Cancer* **11**.

De Luca, C. & Valacchi, G. (2010). Surface lipids as multifunctional mediators of skin responses to environmental stimuli. *Mediators Inflamm* **2010**, 321494.

Del Pozo, J. L., Tran, N. V., Petty, P. M., Johnson, C. H., Walsh, M. F., Bite, U., Clay, R. P., Mandrekar, J. N., Piper, K. E. & other authors. (2009). Pilot study of association of bacteria on breast implants with capsular contracture. *J Clin Microbiol* **47**, 1333–1337.

Del Rosso, J. Q. (2016). Topical and oral antibiotics for acne vulgaris. *Semin Cutan Med Surg* **35**, 57–61.

Del Rosso, J. Q. & Kim, G. (2009). Optimizing use of oral antibiotics in acne vulgaris. *Dermatol Clin* **27**, 33–42.

Del Rosso, J. Q. & Zeichner, J. A. (2016). The Clinical Relevance of Antibiotic Resistance: Thirteen Principles That Every Dermatologist Needs to Consider When Prescribing Antibiotic Therapy. *Dermatol Clin* **34**, 167–173.

Del Rosso, J. Q., Webster, G. F., Rosen, T., Thiboutot, D., Leyden, J. J., Gallo, R., Walker, C., Zhanel, G. & Eichenfield, L. (2016). Status Report from the Scientific Panel on Antibiotic Use in Dermatology of the American Acne and Rosacea Society: Part 1: Antibiotic Prescribing Patterns, Sources of Antibiotic Exposure, Antibiotic Consumption and Emergence of Antibiotic Resistance, Impact of Alterations in Antibiotic Prescribing, and Clinical Sequelae of Antibiotic Use. *J Clin Aesthetic Dermatol* **9**, 18–24.

Delgado, S., Suárez, A. & Mayo, B. (2011). Identification, typing and characterisation of Propionibacterium strains from healthy mucosa of the human stomach. *Int J Food Microbiol* **149**, 65–72.

Delgado, S., Cabrera-Rubio, R., Mira, A., Suárez, A. & Mayo, B. (2013). Microbiological survey of the human gastric ecosystem using culturing and pyrosequencing methods. *Microb Ecol* **65**, 763–772.

Dinos, G. P., Michelinaki, M. & Kalpaxis, D. L. (2001). Insights into the mechanism of azithromycin interaction with an Escherichia coli functional ribosomal complex. *Mol Pharmacol* **59**, 1441–1445.

Doss, J., Culbertson, K., Hahn, D., Camacho, J. & Barekzi, N. (2017). A Review of Phage Therapy against Bacterial Pathogens of Aquatic and Terrestrial Organisms. *Viruses* **9**.

Douglas, H. C. & Gunter, S. E. (1946). The taxonomic position of corynebacterium acnes. *J Bacteriol* **52**, 15–23.

Drago, L., De Vecchi, E., Bortolin, M., Zagra, L., Romanò, C. L. & Cappelletti, L. (2017). Epidemiology and Antibiotic Resistance of Late Prosthetic Knee and Hip Infections. *J Arthroplasty*.

Drake, J. W. (1991). A constant rate of spontaneous mutation in DNA-based microbes. *Proc Natl Acad Sci U S A* **88**, 7160–7164.

Drake, J. W., Charlesworth, B., Charlesworth, D. & Crow, J. F. (1998). Rates of spontaneous mutation. *Genetics* **148**, 1667–1686.

Dréno, B., Lambert, J. & Bettoli, V. (2016a). Are retinoid/antibiotic fixed-dose combination acne treatments associated with antibiotic resistance? *Eur J Dermatol EJD* **26**, 90–91.

Dréno, B., Jean-Decoster, C. & Georgescu, V. (2016b). Profile of patients with mild-to-moderate acne in Europe: a survey. *Eur J Dermatol EJD* **26**, 177–184.

Duckworth, D. H. (1976). 'Who discovered bacteriophage?'. *Bacteriol Rev* **40**, 793–802.

Eady, E. A., Cove, J. H., Holland, K. T. & Cunliffe, W. J. (1989). Erythromycin resistant propionibacteria in antibiotic treated acne patients: association with therapeutic failure. *Br J Dermatol* **121**, 51–57.

Edgar, R. C. (2004). MUSCLE: multiple sequence alignment with high accuracy and high throughput. *Nucleic Acids Res* **32**, 1792–1797.

Eishi, Y. (2013). Etiologic link between sarcoidosis and Propionibacterium acnes. *Respir Investig* **51**, 56–68.

Elias, P. M., Brown, B. E. & Ziboh, V. A. (1980). The permeability barrier in essential fatty acid deficiency: evidence for a direct role for linoleic acid in barrier function. *J Invest Dermatol* **74**, 230–233.

Elias, P. M. (2007). The skin barrier as an innate immune element. *Semin Immunopathol* **29**, 3–14.

Erkus, O., de Jager, V. C., Spus, M., van Alen-Boerrigter, I. J., van Rijswijck, I. M., Hazelwood, L., Janssen, P. W., van Hijum, S. A., Kleerebezem, M. & Smid, E. J. (2013). Multifactorial diversity sustains microbial community stability. *ISME J* **7**, 2126–2136.

ESHRE Capri Workshop Group. **(2013).** Venous thromboembolism in women: a specific reproductive health risk. *Hum Reprod Update* **19**, 471–482.

EUCAST. **(2016).** The European Committee on Antimicrobial Susceptibility Testing. Breakpoint tables for interpretation of MICs and zone diameters. Version 6.0. http://www.eucast.org.

Fan, Y., Hao, F., Wang, W., Lu, Y., He, L., Wang, G. & Chen, W. (2016). Multicenter cross-sectional observational study of antibiotic resistance and the genotypes of Propionibacterium acnes isolated from Chinese patients with acne vulgaris. *J Dermatol* **43**, 406–413.

Farrar, M. D., Howson, K. M., Bojar, R. A., West, D., Towler, J. C., Parry, J., Pelton, K. & Holland, K. T. (2007). Genome Sequence and Analysis of a Propionibacterium acnes Bacteriophage. *J Bacteriol* **189**, 4161–4167.

Fehri, L. F., Mak, T. N., Laube, B., Brinkmann, V., Ogilvie, L. A., Mollenkopf, H., Lein, M., Schmidt, T., Meyer, T. F. & Brüggemann, H. (2011). Prevalence of Propionibacterium acnes in diseased prostates and its inflammatory and transforming activity on prostate epithelial cells. *Int J Med Microbiol* **301**, 69–78.

Fife, D. (2016). Evaluation of Acne Scars: How to Assess Them and What to Tell the Patient. *Dermatol Clin* **34**, 207–213.

Figa, R., Muñetón, D., Gómez, L., Matamala, A., Lung, M., Cuchi, E. & Corona, P. S. (2017). Periprosthetic joint infection by Propionibacterium acnes: Clinical differences between monomicrobial versus polymicrobial infection. *Anaerobe* **44**, 143–149.

Finn, R. D., Clements, J. & Eddy, S. R. (2011). HMMER web server: interactive sequence similarity searching. *Nucleic Acids Res* **39**, W29-37.

Fitz-Gibbon, S., Tomida, S., Chiu, B.-H., Nguyen, L., Du, C., Liu, M., Elashoff, D., Erfe, M. C., Loncaric, A. & other authors. **(2013).** Propionibacterium acnes strain populations in the human skin microbiome associated with acne. *J Invest Dermatol* **133**, 2152–2160.

Fokine, A. & Rossmann, M. G. (2014). Molecular architecture of tailed double-stranded DNA phages. *Bacteriophage* **4**.

Frangiamore, S. J., Saleh, A., Grosso, M. J., Alolabi, B., Bauer, T. W., Iannotti, J. P. & Ricchetti, E. T. (2015). Early Versus Late Culture Growth of Propionibacterium acnes in Revision Shoulder Arthroplasty. *J Bone Joint Surg Am* **97**, 1149–1158.

Friedman, M. & Friedland, G. W. (1998). Alexander Fleming and Antibiotics. In *Med 10 Gt Discov*, pp. 168–191. New Haven & London: Yale University Press.

Friedman, M. (1937). The Use of Ranks to Avoid the Assumption of Normality Implicit in the Analysis of Variance. *J Am Stat Assoc* **32**, 675–701.

Funke, G., von Graevenitz, A., Clarridge, J. E. & Bernard, K. A. (1997). Clinical microbiology of coryneform bacteria. *Clin Microbiol Rev* **10**, 125–159.

Furustrand Tafin, U., Corvec, S., Betrisey, B., Zimmerli, W. & Trampuz, A. (2012). Role of rifampin against Propionibacterium acnes biofilm in vitro and in an experimental foreign-body infection model. *Antimicrob Agents Chemother* **56**, 1885–1891.

Furustrand Tafin, U., Trampuz, A. & Corvec, S. (2013). In vitro emergence of rifampicin resistance in Propionibacterium acnes and molecular characterization of mutations in the rpoB gene. *J Antimicrob Chemother* **68**, 523–528.

Gallo, R. L. & Nakatsuji, T. (2011). Microbial symbiosis with the innate immune defense system of the skin. *J Invest Dermatol* **131**, 1974–1980.

Gamaleya, N. F. (1898). Bacteriolysins—ferments destroying bacteria. *Russ Arch Pathol Clin Med Bacteriol* **6**, 607–613.

Garner, S. E., Eady, A., Bennett, C., Newton, J. N., Thomas, K. & Popescu, C. M. (2012). Minocycline for acne vulgaris: efficacy and safety. *Cochrane Database Syst Rev*.

Gascuel, O. (1997). BIONJ: an improved version of the NJ algorithm based on a simple model of sequence data. *Mol Biol Evol* **14**, 685–695.

Giannopoulos, L., Papaparaskevas, J., Refene, E., Daikos, G., Stavrianeas, N. & Tsakris, A. (2015). MLST typing of antimicrobial-resistant Propionibacterium acnes isolates from patients with moderate to severe acne vulgaris. *Anaerobe* **31**, 50–54.

Gill, J. J. & Hyman, P. (2010). Phage choice, isolation, and preparation for phage therapy. *Curr Pharm Biotechnol* **11**, 2–14.

Gokdemir, G., Fisek, N., Köşlü, A. & Kutlubay, Z. (2011). Beliefs, perceptions and sociological impact of patients with acne vulgaris in the Turkish population. *J Dermatol* **38**, 504–507.

Goldstein, E. J. C., Citron, D. M., Merriam, C. V., Warren, Y. a, Tyrrell, K. L., Fernandez, H. T., Goldstein, E. J. C., Citron, D. M., Merriam, C. V. & other authors. **(2003).** In Vitro Activities of Daptomycin , Linezolid , and Five Other Antimicrobials against 307 Gram-Positive Anaerobic and 31 Corynebacterium Clinical Isolates In Vitro Activities of Daptomycin , Vancomycin , Quinupristin- Dalfopristin , Linezolid , and Five O **47**, 337–341.

Goldstein, E. J. C., Citron, D. M., Merriam, C. V., Warren, Y. A., Tyrrell, K. L. & Fernandez, H. T. (2004). In Vitro Activities of the New Semisynthetic Glycopeptide Telavancin (TD-6424), Vancomycin, Daptomycin, Linezolid, and Four Comparator Agents against Anaerobic Gram-Positive Species and Corynebacterium spp. *Antimicrob Agents Chemother* **48**, 2149–2152.

Gollnick, H., Cunliffe, W., Berson, D., Dreno, B., Finlay, A., Leyden, J. J., Shalita, A. R., Thiboutot, D. & Global Alliance to Improve Outcomes in Acne. **(2003).** Management of acne: a report from a Global Alliance to Improve Outcomes in Acne. *J Am Acad Dermatol* **49**, S1-37.

González, R., Welsh, O., Ocampo, J., Hinojosa-Robles, R. M., Vera-Cabrera, L., Delaney, M. L. & Gómez, M. (2010). In vitro antimicrobial susceptibility of Propionibacterium acnes isolated from acne patients in northern Mexico. *Int J Dermatol* **49**, 1003–1007.

Gopal, L., Nagpal, A. & Verma, A. (2008). Direct aspiration of capsular bag material in a case of sequestered endophthalmitis. *Indian J Ophthalmol* **56**, 155–157.

Gordon, R. A., Crosnoe, R. & Wang, X. (2013). Physical attractiveness and the accumulation of social and human capital in adolescence and young adulthood: assets and distractions. *Monogr Soc Res Child Dev* **78**, 1–137.

Goulden, V., Clark, S. M. & Cunliffe, W. J. (1997). Post-adolescent acne: a review of clinical features. *Br J Dermatol* **136**, 66–70.

Goulden, V., Stables, G. I. & Cunliffe, W. J. (1999). Prevalence of facial acne in adults. *J Am Acad Dermatol* **41**, 577–580.

Gouy, M., Guindon, S. & Gascuel, O. (2010). SeaView version 4: A multiplatform graphical user interface for sequence alignment and phylogenetic tree building. *Mol Biol Evol* **27**, 221–224.

Graham, G. M., Farrar, M. D., Cruse-Sawyer, J. E., Holland, K. T. & Ingham, E. (2004). Proinflammatory cytokine production by human keratinocytes stimulated with Propionibacterium acnes and P. acnes GroEL. *Br J Dermatol* **150**, 421–428.

Grech, I. (2014). Susceptibility profiles of Propionibacterium acnes isolated from patients with acne vulgaris. *J Glob Antimicrob Resist* **2**, 35–38.

Gribbon, E. M., Cunliffe, W. J. & Holland, K. T. (1993). Interaction of Propionibacterium acnes with skin lipids in vitro. *J Gen Microbiol* **139**, 1745–1751.

Grice, E. A. & Segre, J. A. (2011). The skin microbiome. *Nat Rev Microbiol* **9**, 244–253.

Gübelin, W., Martínez, M. A., Molina, M. T., Zapata, S. & Valenzuela, M. E. (2006). Antimicrobial susceptibility of strains of Propionibacterium acnes isolated from inflammatory acne. *Rev Latinoam Microbiol* **48**, 14–6.

Haedersdal, M., Togsverd-Bo, K. & Wulf, H. C. (2008). Evidence-based review of lasers, light sources and photodynamic therapy in the treatment of acne vulgaris. *J Eur Acad Dermatol Venereol JEADV* **22**, 267–278.

Han, X. D., Oon, H. H. & Goh, C. L. (2016). Epidemiology of post-adolescence acne and adolescence acne in Singapore: a 10-year retrospective and comparative study. *J Eur Acad Dermatol Venereol JEADV*.

Hankin, M. E. (1896). L'action bactéricide des eaux de la Jumna et du Gange sur le vibrion du choléra. *Ann Inst Pasteur Paris* **10**, 511–523.

Harper, J. C. (2016). Use of Oral Contraceptives for Management of Acne Vulgaris: Practical Considerations in Real World Practice. *Dermatol Clin* **34**, 159–165.

Haruki, Y., Hagiya, H., Takahashi, Y., Yoshida, H., Kobayashi, K., Yukiue, T., Tsuboi, N. & Sugiyama, T. (2017). Risk factors for Propionibacterium acnes infection after neurosurgery: A case-control study. *J Infect Chemother Off J Jpn Soc Chemother* **23**, 256–258.

Henderson, C. A. (1996). Skin disease in rural Tanzania. *Int J Dermatol* **35**, 640–642.

d'Herelle, F. (1917). Sur un microbe invisible antagoniste des bacilles dysentérique. In D, pp. 373–375. Presented at the Comptes Rendus de l'Académie des Sciences, Paris.

d'Herelle, F. (1926). *The Bacteriophage and Its Behavior* (G. H. Smith, Tran.). Baltimore, MD., USA: Williams & Wilkins Company.

Hinestrosa, F., Djurkovic, S., Bourbeau, P. P. & Foltzer, M. a. (2007). Propionibacterium acnes as a cause of prosthetic valve aortic root abscess. *J Clin Microbiol* **45**, 259–261.

Hiramatsu, J., Kataoka, M., Nakata, Y., Okazaki, K., Tada, S., Tanimoto, M. & Eishi, Y. (2003). Propionibacterium acnes DNA detected in bronchoalveolar lavage cells from patients with sarcoidosis. *Sarcoidosis Vasc Diffuse Lung Dis Off J WASOG World Assoc Sarcoidosis Granulomatous Disord* **20**, 197–203.

Hisaw, L. D., Qin, M., Park, A., Agak, G. W., Pirouz, A., Phan, J., Fernandez, C., Garbán, H. J., Nelson, A. & other authors. (2016). Antimicrobial Activity of Sebocytes against

Propionibacterium acnes via Toll-Like Receptor 2 and Lysosomal Pathway. *J Invest Dermatol* **136**, 2098–2101.

Holland, C., Mak, T. N., Zimny-Arndt, U., Schmid, M., Meyer, T. F., Jungblut, P. R. & Brüggemann, H. (2010). Proteomic identification of secreted proteins of Propionibacterium acnes. *BMC Microbiol* **10**, 230.

Holmberg, A., Lood, R., Mörgelin, M., Söderquist, B., Holst, E., Collin, M., Christensson, B. & Rasmussen, M. (2009). Biofilm formation by Propionibacterium acnes is a characteristic of invasive isolates. *Clin Microbiol Infect* **15**, 787–795.

Homma, J. Y., Abe, C., Chosa, H., Ueda, K., Saegusa, J., Nakayama, M., Homma, H., Washizaki, M. & Okano, H. (1978). Bacteriological investigation on biopsy specimens from patients with sarcoidosis. *Jpn J Exp Med* **48**, 251–255.

Hughes, B. R. & Cunliffe, W. J. (1988). Tolerance of spironolactone. *Br J Dermatol* **118**, 687–691.

Hyatt, D., Chen, G.-L., Locascio, P. F., Land, M. L., Larimer, F. W. & Hauser, L. J. (2010). Prodigal: prokaryotic gene recognition and translation initiation site identification. *BMC Bioinformatics* **11**, 119.

Ingham, E., Eady, E. A., Goodwin, C. E., Cove, J. H. & Cunliffe, W. J. (1992). Pro-inflammatory levels of interleukin-1 alpha-like bioactivity are present in the majority of open comedones in acne vulgaris. *J Invest Dermatol* **98**, 895–901.

Ishida, N., Nakaminami, H., Noguchi, N., Kurokawa, I., Nishijima, S. & Sasatsu, M. (2008). Antimicrobial susceptibilities of Propionibacterium acnes isolated from patients with acne vulgaris. *Microbiol Immunol* **52**, 621–4.

Jackson, A. P., Thomas, G. H., Parkhill, J. & Thomson, N. R. (2009). Evolutionary diversification of an ancient gene family (rhs) through C-terminal displacement. *BMC Genomics* **10**, 584.

Jacob, C. I., Dover, J. S. & Kaminer, M. S. (2001). Acne scarring: a classification system and review of treatment options. *J Am Acad Dermatol* **45**, 109–117.

Jahns, A. C., Lundskog, B., Ganceviciene, R., Palmer, R. H., Golovleva, I., Zouboulis, C. C., McDowell, A., Patrick, S. & Alexeyev, O. A. (2012). An increased incidence of Propionibacterium acnes biofilms in acne vulgaris: a case-control study: Increased incidence of P. acnes biofilms in acne vulgaris. *Br J Dermatol* **167**, 50–58.

Jakab, E., Zbinden, R., Gubler, J., Ruef, C., Graevenitz, A. V. & Krause, M. (1997). Severe Infections Caused by Propionibacterium acnes: An Underestimated Pathogen in Late Postoperative Infections. *Yale J Biol Med* **69**, 477–482.

James Q. Del Rosso. **(2006).** The Scientific Panel on Antibiotic Usage in Dermatology (SPAUD). Part I: Summary Report on Usage Patterns, Management Challenges and Recommendations. *Extensions* 1–3. Malvern, PA.

Jeon, J., Mok, H. J., Choi, Y., Park, S. C., Jo, H., Her, J., Han, J.-K., Kim, Y.-K., Kim, K. P. & Ban, C. (2017). Proteomic analysis of extracellular vesicles derived from Propionibacterium acnes. *Proteomics Clin Appl* **11**.

Jeremy, A. H. T., Holland, D. B., Roberts, S. G., Thomson, K. F. & Cunliffe, W. J. (2003). Inflammatory events are involved in acne lesion initiation. *J Invest Dermatol* **121**, 20–27.

Jih, M. H., Friedman, P. M., Goldberg, L. H., Robles, M., Glaich, A. S. & Kimyai-Asadi, A. (2006). The 1450-nm diode laser for facial inflammatory acne vulgaris: dose-response and 12-month follow-up study. *J Am Acad Dermatol* **55**, 80–87.

Johnson, M.-L. T. & Roberts, J. (1978). Skin conditions and related need for medical care among persons 1-74 years. United States, 1971-1974. *Vital Health Stat* **11**, i–v, 1-72.

Johnson, T., Kang, D., Barnard, E. & Li, H. (2016). Strain-Level Differences in Porphyrin Production and Regulation in Propionibacterium acnes Elucidate Disease Associations. *mSphere* **1**.

Jong, E. C., Ko, H. L. & Pulverer, G. (1975). Studies on bacteriophages of Propionibacterium acnes. *Med Microbiol Immunol (Berl)* **161**, 263–271.

Kakegawa, T., Bae, Y., Ito, T., Uchida, K., Sekine, M., Nakajima, Y., Furukawa, A., Suzuki, Y., Kumagai, J. & other authors. **(2017).** Frequency of Propionibacterium acnes Infection in Prostate Glands with Negative Biopsy Results Is an Independent Risk Factor for Prostate Cancer in Patients with Increased Serum PSA Titers. *PLoS ONE* **12**.

Kanjanauthai, S. & Kanluen, T. (2008). Propionibacterium acnes: A rare cause of late prosthetic valve endocarditis and aortic root abscess. *Int J Cardiol* **130**, e66–e68.

Kaplan, Y. C., Ozsarfati, J., Etwel, F., Nickel, C., Nulman, I. & Koren, G. (2015). Pregnancy outcomes following first-trimester exposure to topical retinoids: a systematic review and meta-analysis. *Br J Dermatol* **173**, 1132–1141.

Kaur, S., Verma, P., Sangwan, A., Dayal, S. & Jain, V. K. (2016). Etiopathogenesis and Therapeutic Approach to Adult Onset Acne. *Indian J Dermatol* **61**, 403–407.

Kellett, S. C. & Gawkrodger, D. J. (1999). The psychological and emotional impact of acne and the effect of treatment with isotretinoin. *Br J Dermatol* **140**, 273–282.

Kendall, M. G. & Smith, B. B. (1939). The Problem of m Rankings. *Ann Math Stat* **10**, 275–287.

Kestler, M., Muñoz, P., Marín, M., Goenaga, M. A., Idígoras Viedma, P., de Alarcón, A., Lepe, J. A., Sousa Regueiro, D., Bravo-Ferrer, J. M. & other authors. **(2017).** Endocarditis caused by anaerobic bacteria. *Anaerobe* **47**, 33–38.

Kilian, M., Scholz, C. F. P. & Lomholt, H. B. (2012). Multilocus sequence typing and phylogenetic analysis of Propionibacterium acnes. *J Clin Microbiol* **50**, 1158–65.

Kilkenny, M., Merlin, K., Plunkett, A. & Marks, R. (1998). The prevalence of common skin conditions in Australian school students: 3. acne vulgaris. *Br J Dermatol* **139**, 840–845.

Kim, J. (2005). Review of the Innate Immune Response in Acne vulgaris: Activation of Toll-Like Receptor 2 in Acne Triggers Inflammatory Cytokine Responses. *Dermatology* **211**, 193–198.

Kim, J., Ochoa, M.-T., Krutzik, S. R., Takeuchi, O., Uematsu, S., Legaspi, A. J., Brightbill, H. D., Holland, D., Cunliffe, W. J. & Akira, S. (2002). Activation of toll-like receptor 2 in acne triggers inflammatory cytokine responses. *J Immunol* **169**, 1535–1541.

King, K., Jones, D. H., Daltrey, D. C. & Cunliffe, W. J. (1982). A double-blind study of the effects of 13-cis-retinoic acid on acne, sebum excretion rate and microbial population. *Br J Dermatol* **107**, 583–590.

Kingwell, K. (2015). Bacteriophage therapies re-enter clinical trials. *Nat Rev Drug Discov* **14**, 515–516.

Kircik, L. H. (2010). Doxycycline and minocycline for the management of acne: a review of efficacy and safety with emphasis on clinical implications. *J Drugs Dermatol* **9**, 1407–1411.

Kircik, L. H. (2016). Advances in the Understanding of the Pathogenesis of Inflammatory Acne. *J Drugs Dermatol JDD* **15**, s7–s10.

Kistowska, M., Gehrke, S., Jankovic, D., Kerl, K., Fettelschoss, A., Feldmeyer, L., Fenini, G., Kolios, A., Navarini, A. & other authors. **(2014).** IL-1β drives inflammatory responses to propionibacterium acnes in vitro and in vivo. *J Invest Dermatol* **134**, 677–685.

Klassen, A. F., Newton, J. N. & Mallon, E. (2000). Measuring quality of life in people referred for specialist care of acne: comparing generic and disease-specific measures. *J Am Acad Dermatol* **43**, 229–233.

Knutson, D. D. (1974). Ultrastructural observations in acne vulgaris: the normal sebaceous follicle and acne lesions. *J Invest Dermatol* **62**, 288–307.

Koh, C. K., Marsh, J. P., Drinković, D., Walker, C. G. & Poon, P. C. (2016). Propionibacterium acnes in primary shoulder arthroplasty: rates of colonization, patient risk factors, and efficacy of perioperative prophylaxis. *J Shoulder Elbow Surg* **25**, 846–852.

Korting, H. C., Hübner, K., Greiner, K., Hamm, G. & Braun-Falco, O. (1990). Differences in the skin surface pH and bacterial microflora due to the long-term application of synthetic detergent preparations of pH 5.5 and pH 7.0. Results of a crossover trial in healthy volunteers. *Acta Derm Venereol* **70**, 429–431.

Kowalski, T. J., Berbari, E. F., Huddleston, P. M., Steckelberg, J. M. & Osmon, D. R. (2007). Propionibacterium acnes Vertebral Osteomyelitis: Seek and Ye Shall Find? *Clin Orthop* **PAP**.

Kranick, S. M., Vinnard, C. & Kolson, D. L. (2009). Propionibacterium acnes brain abscess appearing 10 years after neurosurgery. *Arch Neurol* **66**, 793–795.

Kronvall, G., Giske, C. G. & Kahlmeter, G. (2011). Setting interpretive breakpoints for antimicrobial susceptibility testing using disk diffusion. *Int J Antimicrob Agents* **38**, 281–290.

Krowchuk, D. P. (2000). Managing acne in adolescents. *Pediatr Clin North Am* **47**, 841–857.

Krunic, A., Ciurea, A. & Scheman, A. (2008). Efficacy and tolerance of acne treatment using both spironolactone and a combined contraceptive containing drospirenone. *J Am Acad Dermatol* **58**, 60–62.

Kurokawa, I., Nishijima, S. & Kawabata, S. (1999). Antimicrobial susceptibility of Propionibacterium acnes isolated from acne vulgaris. *Eur J Dermatol EJD* **9**, 25–28.

Kurtz, S. M., Lau, E., Watson, H., Schmier, J. K. & Parvizi, J. (2012). Economic burden of periprosthetic joint infection in the United States. *J Arthroplasty* **27**, 61–65.e1.

Kutter, E., De Vos, D., Gvasalia, G., Alavidze, Z., Gogokhia, L., Kuhl, S. & Abedon, S. T. (2010). Phage therapy in clinical practice: treatment of human infections. *Curr Pharm Biotechnol* **11**, 69–86.

Kvich, L., Jensen, P. Ø., Justesen, U. S. & Bjarnsholt, T. (2016). Incidence of Propionibacterium acnes in initially culture-negative thioglycollate broths-a prospective cohort study at a Danish University Hospital. *Clin Microbiol Infect Off Publ Eur Soc Clin Microbiol Infect Dis* **22**, 941–945.

Kwon, H. H. & Suh, D. H. (2016). Recent progress in the research about Propionibacterium acnes strain diversity and acne: pathogen or bystander? *Int J Dermatol* **55**, 1196–1204.

Kysela, D. T. & Turner, P. E. (2007). Optimal bacteriophage mutation rates for phage therapy. *J Theor Biol* **249**, 411–421.

Labrie, S. J., Samson, J. E. & Moineau, S. (2010). Bacteriophage resistance mechanisms. *Nat Rev Microbiol* **8**, 317–27.

Lang, S. & Palmer, M. (2003). Characterization of Streptococcus agalactiae CAMP factor as a pore-forming toxin. *J Biol Chem* **278**, 38167–38173.

Lavergne, V., Malo, M., Gaudelli, C., Laprade, M., Leduc, S., Laflamme, P. & Rouleau, D. M. (2017). Clinical impact of positive Propionibacterium acnes cultures in orthopedic surgery. *Orthop Traumatol Surg Res OTSR* **103**, 307–314.

Law, M. P. M., Chuh, A. A. T., Lee, A. & Molinari, N. (2010). Acne prevalence and beyond: acne disability and its predictive factors among Chinese late adolescents in Hong Kong: Acne disability and its predictive factors among Chinese late adolescents. *Clin Exp Dermatol* **35**, 16–21.

Layton, A. M., Henderson, C. A. & Cunliffe, W. J. (1994). A clinical evaluation of acne scarring and its incidence. *Clin Exp Dermatol* **19**, 303–308.

Layton, A. M., Seukeran, D. & Cunliffe, W. J. (1997). Scarred for life? *Dermatol Basel Switz* **195 Suppl 1**, 15-21; discussion 38-40.

Leclercq, R. (2002). Mechanisms of resistance to macrolides and lincosamides: nature of the resistance elements and their clinical implications. *Clin Infect Dis Off Publ Infect Dis Soc Am* **34**, 482–492.

Lee, S. H., Cho, H. S., Seung, N. R., Jung, S. J., Kim, C. W., Jo, H. J., Kim, K. H. & Kim, K. J. (2006). Quality of life of acne patients. *Korean J Dermatol* **44**, 688–695.

Leeming, J. P., Holland, K. T. & Cunliffe, W. J. (1984). The microbial ecology of pilosebaceous units isolated from human skin. *J Gen Microbiol* **130**, 803–807.

Legendre, P. (2010). Coefficient of concordance. In *Encycl Res Des*, pp. 164–169. Edited by N. J. Salkind. Los Angeles: SAGE Publications, Inc.

Legendre, P. & Lapointe, F.-J. (2004). Assessing congruence among distance matrices: single-malt scotch whiskies revisited. *Aust N Z J Stat* **46**, 615–629.

Leiman, P. G., Basler, M., Ramagopal, U. A., Bonanno, J. B., Sauder, J. M., Pukatzki, S., Burley, S. K., Almo, S. C. & Mekalanos, J. J. (2009). Type VI secretion apparatus and phage tail-associated protein complexes share a common evolutionary origin. *Proc Natl Acad Sci U S A* **106**, 4154–4159.

Lesens, O., Haus-Cheymol, R., Dubrous, P., Verret, C., Spiegel, A., Bonnet, R., Bes, M., Laurichesse, H., Beytout, J. & other authors. **(2007).** Methicillin-susceptible, doxycycline-resistant Staphylococcus aureus, Côte d'Ivoire. *Emerg Infect Dis* **13**, 488–490.

Levi, a D., Dickman, C. a & Sonntag, V. K. (1997). Management of postoperative infections after spinal instrumentation. *J Neurosurg* **86**, 975–980.

Levy, R. M., Huang, E. Y., Roling, D., Leyden, J. J. & Margolis, D. J. (2003). Effect of antibiotics on the oropharyngeal flora in patients with acne. *Arch Dermatol* **139**, 467–471.

Leyden, J. J., McGinley, K. J. & Foglia, A. N. (1986). Qualitative and quantitative changes in cutaneous bacteria associated with systemic isotretinoin therapy for acne conglobata. *J Invest Dermatol* **86**, 390–393.

Leyden, J. J. (2003). A review of the use of combination therapies for the treatment of acne vulgaris. *J Am Acad Dermatol* **49**, S200–S210.

Leyden, J. J. (2012). In vivo antibacterial effects of tretinoin-clindamycin and clindamycin alone on Propionibacterium acnes with varying clindamycin minimum inhibitory. *J Drugs Dermatol JDD* **11**, 1434–1438.

Lheure, C., Grange, P. A., Ollagnier, G., Morand, P., Désiré, N., Sayon, S., Corvec, S., Raingeaud, J., Marcelin, A.-G. & other authors. **(2016).** TLR-2 Recognizes Propionibacterium acnes CAMP Factor 1 from Highly Inflammatory Strains. *PloS One* **11**, e0167237.

Liu, J., Yan, R., Zhong, Q., Ngo, S., Bangayan, N. J., Nguyen, L., Lui, T., Liu, M., Erfe, M. C. & other authors. **(2015a).** The diversity and host interactions of Propionibacterium acnes bacteriophages on human skin. *ISME J* **9**, 2116.

Liu, J., Yan, R., Zhong, Q., Ngo, S., Bangayan, N. J., Nguyen, L., Lui, T., Liu, M., Erfe, M. C. & other authors. **(2015b).** The diversity and host interactions of Propionibacterium acnes bacteriophages on human skin. *ISME J* 1–16.

Liu, J., Yan, R., Zhong, Q., Ngo, S., Bangayan, N. J., Nguyen, L., Lui, T., Liu, M., Erfe, M. C. & other authors. **(2015c).** The diversity and host interactions of Propionibacterium acnes bacteriophages on human skin. *ISME J* **9**, 2078–2093.

Lomholt, H. B., Scholz, C. F. P., Brüggemann, H., Tettelin, H. & Kilian, M. (2017). A comparative study of Cutibacterium (Propionibacterium) acnes clones from acne patients and healthy controls. *Anaerobe* **47**, 57–63.

Lomholt, H. B. & Kilian, M. (2010). Population genetic analysis of Propionibacterium acnes identifies a subpopulation and epidemic clones associated with acne. *PloS One* **5**, e12277.

Lood, R. & Collin, M. (2011). Characterization and genome sequencing of two Propionibacterium acnes phages displaying pseudolysogeny. *BMC Genomics* **12**, 198.

Lood, R., Mörgelin, M., Holmberg, A., Rasmussen, M. & Collin, M. (2008). Inducible Siphoviruses in superficial and deep tissue isolates of Propionibacterium acnes. *BMC Microbiol* **8**, 139.

Lott, R., Taylor, S. L., O'Neill, J. L., Krowchuk, D. P. & Feldman, S. R. (2010). Medication adherence among acne patients: a review. *J Cosmet Dermatol* **9**, 160–166.

de Lucas, R., Moreno-Arias, G., Perez-López, M., Vera-Casaño, Á., Aladren, S., Milani, M. & ACTUO Investigators study group. **(2015).** Adherence to drug treatments and adjuvant barrier repair therapies are key factors for clinical improvement in mild to moderate acne: the ACTUO observational prospective multicenter cohort trial in 643 patients. *BMC Dermatol* **15**, 17.

Lynnon Biosoft. **(n.d.).** *DNAMAN v. 9*. USA: Lynnon Biosoft.

Mao, J. C. & Robishaw, E. E. (1972). Erythromycin, a peptidyltransferase effector. *Biochemistry (Mosc)* **11**, 4864–4872.

Margolis, D. J., Bowe, W. P., Hoffstad, O. & Berlin, J. A. (2005). Antibiotic treatment of acne may be associated with upper respiratory tract infections. *Arch Dermatol* **141**, 1132–1136.

Margolis, D. J., Fanelli, M., Kupperman, E., Papadopoulos, M., Metlay, J. P., Xie, S. X., DiRienzo, J. & Edelstein, P. H. (2012). Association of pharyngitis with oral antibiotic use for the treatment of acne: a cross-sectional and prospective cohort study. *Arch Dermatol* **148**, 326–332.

Marinelli, L. J., Fitz-Gibbon, S., Hayes, C., Bowman, C., Inkeles, M., Loncaric, A., Russell, D. A., Jacobs-Sera, D., Cokus, S. & other authors. **(2012a).** Propionibacterium acnes

Bacteriophages Display Limited Genetic Diversity and Broad Killing Activity against Bacterial Skin Isolates. *mBio* **3**, e00279-12-e00279-12.

Marinelli, L. J., Fitz-Gibbon, S., Hayes, C., Bowman, C., Inkeles, M., Loncaric, A., Russell, D. A., Jacobs-Sera, D., Cokus, S. & other authors. **(2012b).** Propionibacterium acnes bacteriophages display limited genetic diversity and broad killing activity against bacterial skin isolates. *mBio* **3**.

Marinelli, L. J., Fitz-Gibbon, S., Hayes, C., Bowman, C., Inkeles, M., Loncaric, A., Russell, D. A., Jacobs-Sera, D., Cokus, S. & other authors. **(2012c).** Propionibacterium acnes bacteriophages display limited genetic diversity and broad killing activity against bacterial skin isolates. *mBio* **3**.

Marinelli, L. J., Fitz-Gibbon, S., Hayes, C., Bowman, C., Inkeles, M., Loncaric, A., Russell, D. A., Jacobs-Sera, D., Cokus, S. & other authors. **(2012d).** Propionibacterium acnes Bacteriophages Display Limited Genetic Diversity and Broad Killing Activity against Bacterial Skin Isolates. *mBio* **3**, 1–13.

Marples, R. R., Downing, D. T. & Kligman, A. M. (1971). Control of free fatty acids in human surface lipids by Corynebacterium acnes. *J Invest Dermatol* **56**, 127–131.

Marples, R. & McGinley, K. (1974). Corynebacterium acnes and other anaerobic diptheroids from human skin. *J Med Microbiol* **7**, 349–357.

Martínez, J. L., Coque, T. M. & Baquero, F. (2015). What is a resistance gene? Ranking risk in resistomes. *Nat Rev Microbiol* **13**, 116–123.

McDowell, A., Valanne, S., Ramage, G., Tunney, M. M., Glenn, J. V., McLorinan, G. C., Bhatia, A., Maisonneuve, J.-F., Lodes, M. & other authors. **(2005).** Propionibacterium acnes Types I and II Represent Phylogenetically Distinct Groups. *J Clin Microbiol* **43**, 326–334.

McDowell, A., Perry, A. L., Lambert, P. A. & Patrick, S. (2008). A new phylogenetic group of Propionibacterium acnes. *J Med Microbiol* **57**, 218–224.

McDowell, A. & Nagy, I. (2015). Chapter 46. Propionibacteria and Disease. In *Mol Med Microbiol*, 2nd edn., pp. 837–858. Elsevier.

McDowell, A. & Patrick, S. (2011). Chapter 13: Propionibacterium. In *Mol Detect Hum Bact Pathog*. Boca Raton, FL: CRC press.

McDowell, A., Gao, A., Barnard, E., Fink, C., Murray, P. I., Dowson, C. G., Nagy, I., Lambert, P. a & Patrick, S. (2011). A novel multilocus sequence typing scheme for the opportunistic pathogen Propionibacterium acnes and characterization of type I cell surface-associated antigens. *Microbiol Read Engl* **157**, 1990–2003.

McDowell, A., Barnard, E., Nagy, I., Gao, A., Tomida, S., Li, H., Eady, A., Cove, J., Nord, C. E. & Patrick, S. (2012). An Expanded Multilocus Sequence Typing Scheme for Propionibacterium acnes: Investigation of 'Pathogenic', 'Commensal' and Antibiotic Resistant Strains. *PLoS ONE* **7**, e41480 (H. Tse, Ed.).

McDowell, A., Nagy, I., Magyari, M., Barnard, E. & Patrick, S. (2013). The opportunistic pathogen Propionibacterium acnes: insights into typing, human disease, clonal diversification and CAMP factor evolution. *PloS One* **8**, e70897.

McGinley, K. J., Webster, G. F., Ruggieri, M. R. & Leyden, J. J. (1980). Regional variations in density of cutaneous propionibacteria: correlation of Propionibacterium acnes populations with sebaceous secretion. *J Clin Microbiol* **12**, 672–675.

Mills, O. H., Kligman, A. M., Pochi, P. & Comite, H. (1986). Comparing 2.5%, 5%, and 10% benzoyl peroxide on inflammatory acne vulgaris. *Int J Dermatol* **25**, 664–667.

Mills, O., Thornsberry, C., Cardin, C. W., Smiles, K. A. & Leyden, J. J. (2002). Bacterial resistance and therapeutic outcome following three months of topical acne therapy with 2% erythromycin gel versus its vehicle. *Acta Derm Venereol* **82**, 260–265.

Miquel, M., Soler, A., Vaqué, A., Ojanguren, I., Costa, J. & Planas, R. (2007). Suspected cross-hepatotoxicity of flutamide and cyproterone acetate. *Liver Int Off J Int Assoc Study Liver* **27**, 1144–1147.

Miskin, J. E., Farrell, A. M., Cunliffe, W. J. & Holland, K. T. (1997). Propionibacterium acnes, a resident of lipid-rich human skin, produces a 33 kDa extracellular lipase encoded by gehA. *Microbiology* **143**, 1745–1755.

Momen, S. & Al-Niaimi, F. (2015). Acne vulgaris and light-based therapies. *J Cosmet Laser Ther Off Publ Eur Soc Laser Dermatol* **17**, 122–128.

Montalban -Arques, A., W u B., Högenauer, C., Langner, C. & Gorkiewicz, G. (2016). Propionibacterium acnes overabundance and natural killer group 2 member D system activation in corpus□dominant lymphocytic gastritis. *J Pathol* **240**, 425–436.

Mook, W. R., Klement, M. R., Green, C. L., Hazen, K. C. & Garrigues, G. E. (2015). The Incidence of Propionibacterium acnes in Open Shoulder Surgery: A Controlled Diagnostic Study. *J Bone Joint Surg Am* **97**, 957–963.

Moon, S. H., Roh, H. S., Kim, Y. H., Kim, J. E., Ko, J. Y. & Ro, Y. S. (2012). Antibiotic resistance of microbial strains isolated from Korean acne patients. *J Dermatol* **39**, 833–837.

Motley, R. J. & Finlay, A. Y. (1989). How much disability is caused by acne? *Clin Exp Dermatol* **14**, 194–198.

Mougous, J. D., Cuff, M. E., Raunser, S., Shen, A., Zhou, M., Gifford, C. A., Goodman, A. L., Joachimiak, G., Ordoñez, C. L. & other authors. (2006). A Virulence Locus of Pseudomonas aeruginosa Encodes a Protein Secretion Apparatus. *Science* **312**, 1526–1530.

Mount, J. D., Samoylova, T. I., Morrison, N. E., Cox, N. R., Baker, H. J. & Petrenko, V. A. (2004). Cell targeted phagemid rescued by preselected landscape phage. *Gene* **341**, 59–65.

Muszer, M., Noszczyńska, M., Kasperkiewicz, K. & Skurnik, M. (2015). Human Microbiome: When a Friend Becomes an Enemy. *Arch Immunol Ther Exp (Warsz)* **63**, 287–298.

Nagy, I., Pivarcsi, A., Koreck, A., Széll, M., Urbán, E. & Kemény, L. (2005). Distinct strains of Propionibacterium acnes induce selective human β-defensin-2 and interleukin-8 expression in human keratinocytes through toll-like receptors. *J Invest Dermatol* **124**, 931–938.

Nagy, I., Pivarcsi, A., Kis, K., Koreck, A., Bodai, L., McDowell, A., Seltmann, H., Patrick, S., Zouboulis, C. C. & Kemény, L. (2006). Propionibacterium acnes and lipopolysaccharide induce the expression of antimicrobial peptides and proinflammatory cytokines/chemokines in human sebocytes. *Microbes Infect* **8**, 2195–2205.

Nakamura, M., Kametani, I., Higaki, S. & Yamagishi, T. (2003). Identification of Propionibacterium acnes by polymerase chain reaction for amplification of 16S ribosomal RNA and lipase genes. *Anaerobe* **9**, 5–10.

Nakamura, T., Furukawa, A., Uchida, K., Ogawa, T., Tamura, T., Sakonishi, D., Wada, Y., Suzuki, Y., Ishige, Y. & other authors. **(2016).** Autophagy Induced by Intracellular Infection of Propionibacterium acnes. *PloS One* **11**, e0156298.

Nakase, K., Nakaminami, H., Noguchi, N., Nishijima, S. & Sasatsu, M. (2012). First report of high levels of clindamycin-resistant Propionibacterium acnes carrying erm(X) in Japanese patients with acne vulgaris. *J Dermatol* **39**, 794–796.

Nakase, K., Nakaminami, H., Takenaka, Y., Hayashi, N., Kawashima, M. & Noguchi, N. (2014). Relationship between the severity of acne vulgaris and antimicrobial resistance of bacteria isolated from acne lesions in a hospital in Japan. *J Med Microbiol* **63**, 721–728.

Nakase, K., Nakaminami, H., Takenaka, Y., Hayashi, N., Kawashima, M. & Noguchi, N. (2016). A novel 23S rRNA mutation in Propionibacterium acnes confers resistance to 14-membered macrolides. *J Glob Antimicrob Resist* **6**, 160–161.

Nakase, K., Nakaminami, H., Takenaka, Y., Hayashi, N., Kawashima, M. & Noguchi, N. (2017). Propionibacterium acnes is developing gradual increase in resistance to oral tetracyclines. *J Med Microbiol* **66**, 8–12.

Nakatsuji, T., Liu, Y.-T., Huang, C.-P., Gallo, R. L. & Huang, C.-M. (2008). Vaccination Targeting a Surface Sialidase of P. acnes: Implication for New Treatment of Acne Vulgaris. *PLoS ONE* **3**, e1551 (H. Bruggemann, Ed.).

Nakatsuji, T., Tang, D. C., Zhang, L., Gallo, R. L. & Huang, C.-M. (2011). Propionibacterium acnes CAMP Factor and Host Acid Sphingomyelinase Contribute to Bacterial Virulence: Potential Targets for Inflammatory Acne Treatment. *PLoS ONE* **6**, e14797 (M. J. Horsburgh, Ed.).

Negi, M., Takemura, T., Guzman, J., Uchida, K., Furukawa, A., Suzuki, Y., Iida, T., Ishige, I., Minami, J. & other authors. **(2012).** Localization of Propionibacterium acnes in granulomas supports a possible etiologic link between sarcoidosis and the bacterium. *Mod Pathol* **25**, 1284–1297.

Nestor, M. S., Swenson, N. & Macri, A. (2016). Physical Modalities (Devices) in the Management of Acne. *Dermatol Clin* **34**, 215–223.

Nguyen, M. T., Borchers, A., Selmi, C., Naguwa, S. M., Cheema, G. & Gershwin, M. E. (2012). The SAPHO syndrome. *Semin Arthritis Rheum* **42**, 254–265.

Nisbet, M., Briggs, S., Ellis-Pegler, R., Thomas, M. & Holland, D. (2007). Propionibacterium acnes: an under-appreciated cause of post-neurosurgical infection. *J Antimicrob Chemother* **60**, 1097–1103.

Nobrega, F. L., Costa, A. R., Kluskens, L. D. & Azeredo, J. (2015). Revisiting phage therapy: new applications for old resources. *Trends Microbiol* **23**, 185–191.

Ochsendorf, F. (2006). Systemic antibiotic therapy of acne vulgaris. *JDDG* **4**, 828–841.

Oeff, M. K., Seltmann, H., Hiroi, N., Nastos, A., Makrantonaki, E., Bornstein, S. R. & Zouboulis, C. C. (2006). Differential regulation of Toll-like receptor and CD14 pathways by retinoids and corticosteroids in human sebocytes. *Dermatol Basel Switz* **213**, 266.

Olender, A., Radej, S., Płaza, P., Bar, K. & Maciejewski, R. (2016). Propionibacterium acnes infection associated with cancerous prostate hypertrophy. *Pol Arch Med Wewn* **126**, 697–699.

Olsson, J., Davidsson, S., Unemo, M., Mölling, P., Andersson, S.-O., Andrén, O., Söderquist, B., Sellin, M. & Elgh, F. (2012). Antibiotic susceptibility in prostate-derived Propionibacterium acnes isolates. *APMIS Acta Pathol Microbiol Immunol Scand* **120**, 778–785.

Oprica, C. & Nord, C. E. (2005). European surveillance study on the antibiotic susceptibility of Propionibacterium acnes. *Clin Microbiol Infect* **11**, 204–213.

Oprica, C., Emtestam, L., Lapins, J., Borglund, E., Nyberg, F., Stenlund, K., Lundeberg, L., Sillerström, E. & Nord, C. E. (2004). Antibiotic-resistant Propionibacterium acnes on the skin of patients with moderate to severe acne in Stockholm. *Anaerobe* **10**, 155–164.

Oprica, C., Löfmark, S., Lund, B., Edlund, C., Emtestam, L. & Nord, C. E. (2005). Genetic basis of resistance in Propionibacterium acnes strains isolated from diverse types of infection in different European countries. *Anaerobe* **11**, 137–143.

Osmon, D. R., Berbari, E. F., Berendt, A. R., Lew, D., Zimmerli, W., Steckelberg, J. M., Rao, N., Hanssen, A., Wilson, W. R. & Infectious Diseases Society of America. (2013). Diagnosis and management of prosthetic joint infection: clinical practice guidelines by the Infectious Diseases Society of America. *Clin Infect Dis Off Publ Infect Dis Soc Am* **56**, e1–e25.

Ozolins, M., Eady, E. A., Avery, A. J., Cunliffe, W. J., Po, A. L. W., O'Neill, C., Simpson, N. B., Walters, C. E., Carnegie, E. & other authors. (2004). Comparison of five

antimicrobial regimens for treatment of mild to moderate inflammatory facial acne vulgaris in the community: randomised controlled trial. *Lancet Lond Engl* **364**, 2188–2195.

Ozuguz, P., Callioglu, E. E., Tulaci, K. G., Kacar, S. D., Balta, I., Asik, G., Karatas, S. & Karaca, S. (2014). Evaluation of nasal and oropharyngeal flora in patients with acne vulgaris according to treatment options. *Int J Dermatol* **53**, 1404–1408.

Panchaud, A., Csajka, C., Merlob, P., Schaefer, C., Berlin, M., De Santis, M., Vial, T., Ieri, A., Malm, H. & other authors. **(2012).** Pregnancy outcome following exposure to topical retinoids: a multicenter prospective study. *J Clin Pharmacol* **52**, 1844–1851.

Paradis, E., Claude, J. & Strimmer, K. (2004). APE: Analyses of Phylogenetics and Evolution in R language. *Bioinforma Oxf Engl* **20**, 289–290.

Parasion, S., Kwiatek, M., Gryko, R., Mizak, L. & Malm, A. (2014). Bacteriophages as an alternative strategy for fighting biofilm development. *Pol J Microbiol* **63**, 137–145.

Park, H. & Skopit, S. (2016). Safety Considerations and Monitoring in Patients Treated with Systemic Medications for Acne. *Dermatol Clin* **34**, 185–193.

Parks, L., Balkrishnan, R., Hamel-Gariépy, L. & Feldman, S. R. (2003). The importance of skin disease as assessed by ‘willingness-to-pay’. *J Cutan Med Surg* **7**, 369–371.

Patrick, S. & McDowell, A. (2012). Propionibacterium Orla-Jensen 1909, 337AL. In *Actinobacteria Bergey’s Man Syst Bacteriol*, 2nd edn. Edited by M. Goodfellow, P. Kämpfer, H. J. Busse, M. Trujillo, K. Suzuki, W. Ludwig & W. B. Whitman. New York, NY: Springer.

Paugam, C., Corvec, S., Saint-Jean, M., Le Moigne, M., Khammari, A., Boisrobert, A., Nguyen, J. M., Gaultier, A. & Dréno, B. (2017). Propionibacterium acnes phylotypes and acne severity: an observational prospective study. *J Eur Acad Dermatol Venereol JEADV*.

Pell, L. G., Kanelis, V., Donaldson, L. W., Lynne Howell, P. & Davidson, A. R. (2009). The phage λ major tail protein structure reveals a common evolution for long-tailed phages and the type VI bacterial secretion system. *Proc Natl Acad Sci U S A* **106**, 4160–4165.

Pell, L. G., Gasmi-Seabrook, G. M. C., Morais, M., Neudecker, P., Kanelis, V., Bona, D., Donaldson, L. W., Edwards, A. M., Howell, P. L. & other authors. **(2010).** The solution structure of the C-terminal Ig-like domain of the bacteriophage λ tail tube protein. *J Mol Biol* **403**, 468–479.

Perera, A., Atukorale, D. N., Sivayogan, S., Ariyaratne, V. S. & Karunaratne, L. A. (2000). Prevalence of skin diseases in suburban Sri Lanka. *Ceylon Med J* **45**, 123–128.

Perry, A. & Lambert, P. (2011). Propionibacterium acnes: infection beyond the skin. *Expert Rev Anti Infect Ther* **9**, 1149–1156.

Petersen, R. L. W., Scholz, C. F. P., Jensen, A., Brüggemann, H. & Lomholt, H. B. (2017). Propionibacterium Acnes Phylogenetic Type III is Associated with Progressive Macular Hypomelanosis. *Eur J Microbiol Immunol* **7**, 37–45.

Phadnis, J., Gordon, D., Krishnan, J. & Bain, G. I. (2016). Frequent isolation of Propionibacterium acnes from the shoulder dermis despite skin preparation and prophylactic antibiotics. *J Shoulder Elbow Surg* **25**, 304–310.

Pherecydes Pharma. **(2016).** *Evaluation of Phage Therapy for the Treatment of Escherichia Coli and Pseudomonas Aeruginosa Wound Infections in Burned Patients*. ClinicalTrials.gov. Clinical Trial, Bethesda (MD): National Library of Medicine (US).

Plu-Bureau, G., Maitrot-Mantelet, L., Hugon-Rodin, J. & Canonico, M. (2013). Hormonal contraceptives and venous thromboembolism: an epidemiological update. *Best Pract Res Clin Endocrinol Metab* **27**, 25–34.

Portillo, M. E., Corvec, S., Borens, O. & Trampuz, A. (2013). Propionibacterium acnes: an underestimated pathogen in implant-associated infections. *BioMed Res Int* **2013**, 804391.

Puhvel, S. M., Reisner, R. M. & Amirian, D. A. (1975). Quantification of bacteria in isolated pilosebaceous follicles in normal skin. *J Invest Dermatol* **65**, 525–531.

Pulverer, G., Sorgo, W. & Ko, H. L. (1973). [Bacteriophages of Propionibacterium acnes (author's transl)]. *Zentralblatt Bakteriol Parasitenkd Infekt Hyg Erste Abt Orig Reihe Med Mikrobiol Parasitol* **225**, 353–363.

Qin, M., Pirouz, A., Kim, M.-H., Krutzik, S. R., Garbán, H. J. & Kim, J. (2014). Propionibacterium acnes Induces IL-1β secretion via the NLRP3 inflammasome in human monocytes. *J Invest Dermatol* **134**, 381–388.

R Core Team. **(2016).** *R: A Language and Environment for Statistical Computing*. Vienna, Austria: R Foundation for Statistical Computing.

Raum, E., Lietzau, S., von Baum, H., Marre, R. & Brenner, H. (2008). Changes in Escherichia coli resistance patterns during and after antibiotic therapy: a longitudinal study among outpatients in Germany. *Clin Microbiol Infect Off Publ Eur Soc Clin Microbiol Infect Dis* **14**, 41–48.

Rea, J. N., Newhouse, M. L. & Halil, T. (1976). Skin disease in Lambeth. A community study of prevalence and use of medical care. *Br J Prev Soc Med* **30**, 107–114.

Reinholz, M., Poetschke, J., Schwaiger, H., Epple, A., Ruzicka, T. & Gauglitz, G. G. (2015). The dermatology life quality index as a means to assess life quality in patients with different scar types. *J Eur Acad Dermatol Venereol JEADV* **29**, 2112–2119.

Remmert, M., Biegert, A., Hauser, A. & Söding, J. (2011). HHblits: lightning-fast iterative protein sequence searching by HMM-HMM alignment. *Nat Methods* **9**, 173–175.

Rhoads, D. D., Wolcott, R. D., Kuskowski, M. A., Wolcott, B. M., Ward, L. S. & Sulakvelidze, A. (2009). Bacteriophage therapy of venous leg ulcers in humans: results of a phase I safety trial. *J Wound Care* **18**, 237–238, 240–243.

Rieger, U. M., Mesina, J., Kalbermatten, D. F., Haug, M., Frey, H. P., Pico, R., Frei, R., Pierer, G., Lüscher, N. J. & Trampuz, A. (2013). Bacterial biofilms and capsular contracture in patients with breast implants. *Br J Surg* **100**, 768–774.

Rienmüller, A. & Borens, O. (2016). Propionibacterium prosthetic joint infection: experience from a retrospective database analysis. *Eur J Orthop Surg Traumatol* **26**, 429–434.

Ritvo, E., Del Rosso, J. Q., Stillman, M. A. & La Riche, C. (2011). Psychosocial judgements and perceptions of adolescents with acne vulgaris: A blinded, controlled comparison of adult and peer evaluations. *Biopsychosoc Med* **5**, 11.

Ross, J. I., Eady, E. A., Cove, J. H., Jones, C. E., Ratyal, A. H., Miller, Y. W., Vyakrnam, S. & Cunliffe, W. J. (1997). Clinical resistance to erythromycin and clindamycin in cutaneous propionibacteria isolated from acne patients is associated with mutations in 23S rRNA. *Antimicrob Agents Chemother* **41**, 1162–1165.

Ross, J. I., Eady, E. A., Cove, J. H. & Cunliffe, W. J. (1998). 16S rRNA mutation associated with tetracycline resistance in a gram-positive bacterium. *Antimicrob Agents Chemother* **42**, 1702–1705.

Ross, J. I., Snelling, A. M., Eady, E. A., Cove, J. H., Cunliffe, W. J., Leyden, J. J., Collignon, P., Dreno, B., Reynaud, A. & Fluhr, J. (2001). Phenotypic and genotypic characterization of antibiotic-resistant Propionibacterium acnes isolated from acne patients attending dermatology clinics in Europe, the USA, Japan and Australia. *Br J Dermatol* **144**, 339–346.

Ross, J. I., Snelling, A. M., Carnegie, E., Coates, P., Cunliffe, W. J., Bettoli, V., Tosti, G., Katsambas, A., Galvan Peréz Del Pulgar, J. I. & other authors. **(2003).** Antibiotic-resistant acne: lessons from Europe. *Br J Dermatol* **148**, 467–478.

Ross, J. I., Eady, E. A., Carnegie, E. & Cove, J. H. (2002). Detection of transposon Tn5432-mediated macrolide-lincosamide-streptogramin B (MLSB) resistance in cutaneous propionibacteria from six European cities. *J Antimicrob Chemother* **49**, 165–168.

Roth, R. R. & James, W. D. (1988). Microbial ecology of the skin. *Annu Rev Microbiol* **42**, 441–464.

Rukavina, I. (2015). SAPHO syndrome: a review. *J Child Orthop* **9**, 19–27.

Rutherford, K., Parkhill, J., Crook, J., Horsnell, T., Rice, P., Rajandream, M. A. & Barrell, B. (2000). Artemis: sequence visualization and annotation. *Bioinforma Oxf Engl* **16**, 944–945.

Saint-Leger, D., Bague, A., Cohen, E. & Chivot, M. (1986a). A possible role for squalene in the pathogenesis of acne. I. In vitro study of squalene oxidation. *Br J Dermatol* **114**, 535–542.

Saint-Leger, D., Bague, A., Lefebvre, E., Cohen, E. & Chivot, M. (1986b). A possible role for squalene in the pathogenesis of acne. II. In vivo study of squalene oxides in skin surface and intra-comedonal lipids of acne patients. *Br J Dermatol* **114**, 543–552.

Salyers, A. A., Speer, B. S. & Shoemaker, N. B. (1990). New perspectives in tetracycline resistance. *Mol Microbiol* **4**, 151–156.

Sardana, K., Gupta, T., Garg, V. K. & Ghunawat, S. (2015). Antibiotic resistance to Propionobacterium acnes: worldwide scenario, diagnosis and management. *Expert Rev Anti Infect Ther* **13**, 883–896.

Sardana, K., Gupta, T., Kumar, B., Gautam, H. K. & Garg, V. K. (2016). Cross-sectional Pilot Study of Antibiotic Resistance in Propionibacterium Acnes Strains in Indian Acne Patients Using 16S-RNA Polymerase Chain Reaction: A Comparison Among Treatment Modalities Including Antibiotics, Benzoyl Peroxide, and Isotretinoin. *Indian J Dermatol* **61**, 45–52.

Sarker, S. A., Sultana, S., Reuteler, G., Moine, D., Descombes, P., Charton, F., Bourdin, G., McCallin, S., Ngom-Bru, C. & other authors. **(2016).** Oral Phage Therapy of Acute Bacterial Diarrhea With Two Coliphage Preparations: A Randomized Trial in Children From Bangladesh. *EBioMedicine* **4**, 124–137.

Sassi, M., Bebeacua, C., Drancourt, M. & Cambillau, C. (2013). The First Structure of a Mycobacteriophage, the Mycobacterium abscessus subsp. bolletii Phage Araucaria. *J Virol* **87**, 8099–8109.

Savidou, I., Deutsch, M., Soultati, A. S., Koudouras, D., Kafiri, G. & Dourakis, S. P. (2006). Hepatotoxicity induced by cyproterone acetate: a report of three cases. *World J Gastroenterol* **12**, 7551–7555.

Sawaya, M. E. & Hordinsky, M. K. (1993). The antiandrogens. When and how they should be used. *Dermatol Clin* **11**, 65–72.

Sayanjali, B., Christensen, G. J. M., Al-Zeer, M. A., Mollenkopf, H.-J., Meyer, T. F. & Brüggemann, H. (2016). Propionibacterium acnes inhibits FOXM1 and induces cell cycle alterations in human primary prostate cells. *Int J Med Microbiol IJMM* **306**, 517–528.

Schafer, F., Fich, F., Lam, M., Gárate, C., Wozniak, A. & Garcia, P. (2013). Antimicrobial susceptibility and genetic characteristics of Propionibacterium acnes isolated from patients with acne. *Int J Dermatol* **52**, 418–425.

Schäfer, P., Fink, B., Sandow, D., Margull, A., Berger, I. & Frommelt, L. (2008). Prolonged Bacterial Culture to Identify Late Periprosthetic Joint Infection: A Promising Strategy. *Clin Infect Dis* **47**, 1403–1409.

Schaller, M., Loewenstein, M., Borelli, C., Jacob, K., Vogeser, M., Burgdorf, W. H. C. & Plewig, G. (2005). Induction of a chemoattractive proinflammatory cytokine response after stimulation of keratinocytes with Propionibacterium acnes and coproporphyrin III. *Br J Dermatol* **153**, 66–71.

Schliep, K. P. (2011). phangorn: phylogenetic analysis in R. *Bioinforma Oxf Engl* **27**, 592–593.

Schnappinger, D. & Hillen, W. (1996). Tetracyclines: antibiotic action, uptake, and resistance mechanisms. *Arch Microbiol* **165**, 359–369.

Schreffler, R. T., Schreffler, A. J. & Wittler, R. R. (2002). Treatment of cerebrospinal fluid shunt infections: a decision analysis. *Pediatr Infect Dis J* **21**, 632–636.

Schrödinger, LLC. (n.d.). *The PyMOL Molecular Graphics System, Version 1.8.*

Schupp, J. C., Tchaptchet, S., Lützen, N., Engelhard, P., Müller-Quernheim, J., Freudenberg, M. A. & Prasse, A. (2015). Immune response to Propionibacterium acnes in patients with sarcoidosis--in vivo and in vitro. *BMC Pulm Med* **15**, 75.

Sculco, T. P. (1993). The economic impact of infected total joint arthroplasty. *Instr Course Lect* **42**, 349–351.

Seemann, T. (2014). Prokka: rapid prokaryotic genome annotation. *Bioinforma Oxf Engl* **30**, 2068–2069.

Selway, J. L., Kurczab, T., Kealey, T. & Langlands, K. (2013). Toll-like receptor 2 activation and comedogenesis: implications for the pathogenesis of acne. *BMC Dermatol* **13**, 10.

Servick, K. (2016). DRUG DEVELOPMENT. Beleaguered phage therapy trial presses on. *Science* **352**, 1506.

Severi, G., Shannon, B. A., Hoang, H. N., Baglietto, L., English, D. R., Hopper, J. L., Pedersen, J., Southey, M. C., Sinclair, R. & other authors. (2010). Plasma concentration of Propionibacterium acnes antibodies and prostate cancer risk: results from an Australian population-based case-control study. *Br J Cancer* **103**, 411–415.

Shah, N. B., Tande, A. J., Patel, R. & Berbari, E. F. (2015). Anaerobic prosthetic joint infection. *Anaerobe* **36**, 1–8.

Shahzad, N., Nasir, J., Ikram, U., Asmaa-ul-Haque, null, Qadir, A. & Sohail, M. A. (2011). Frequency and psychosocial impact of acne on university and college students. *J Coll Physicians Surg--Pak JCPSP* **21**, 442–443.

Shames, R., Satti, F., Vellozzi, E. M. & Smith, M. A. (2006). Susceptibilities of Propionibacterium acnes Ophthalmic Isolates to Ertapenem, Meropenem, and Cefepime. *J Clin Microbiol* **44**, 4227–4228.

Shannon, B. A., Cohen, R. J. & Garrett, K. L. (2006a). Polymerase chain reaction-based identification of Propionibacterium acnes types isolated from the male urinary tract: evaluation of adolescents, normal adults and men with prostatic pathology. *BJU Int* **98**, 388–392.

Shannon, B. A., Garrett, K. L. & Cohen, R. J. (2006b). Links between Propionibacterium acnes and prostate cancer. *Future Oncol Lond Engl* **2**, 225–232.

Shaw, J. C. (2000). Low-dose adjunctive spironolactone in the treatment of acne in women: a retrospective analysis of 85 consecutively treated patients. *J Am Acad Dermatol* **43**, 498–502.

Shaw, J. C. & White, L. E. (2001). Persistent acne in adult women. *Arch Dermatol* **137**, 1252–1253.

Shaw, J. C. & White, L. E. (2002). Long-term safety of spironolactone in acne: results of an 8-year followup study. *J Cutan Med Surg* **6**, 541–545.

Shen, Y., Wang, T., Zhou, C., Wang, X., Ding, X., Tian, S., Liu, Y., Peng, G., Xue, S. & other authors. (2012). Prevalence of acne vulgaris in Chinese adolescents and adults: a community-based study of 17,345 subjects in six cities. *Acta Derm Venereol* **92**, 40–44.

Shin, J., Cheetham, T. C., Wong, L., Niu, F., Kass, E., Yoshinaga, M. A., Sorel, M., McCombs, J. S. & Sidney, S. (2011). The impact of the iPLEDGE program on

isotretinoin fetal exposure in an integrated health care system. *J Am Acad Dermatol* **65**, 1117–1125.

Shinohara, D. B., Vaghasia, A. M., Yu, S.-H., Mak, T. N., Brüggemann, H., Nelson, W. G., De Marzo, A. M., Yegnasubramanian, S. & Sfanos, K. S. (2013). A mouse model of chronic prostatic inflammation using a human prostate cancer-derived isolate of Propionibacterium acnes. *The Prostate* **73**, 1007–1015.

Shu, M., Wang, Y., Yu, J., Kuo, S., Coda, A., Jiang, Y., Gallo, R. L. & Huang, C.-M. (2013). Fermentation of Propionibacterium acnes, a commensal bacterium in the human skin microbiome, as skin probiotics against methicillin-resistant Staphylococcus aureus. *PloS One* **8**, e55380.

Sievers, F., Wilm, A., Dineen, D., Gibson, T. J., Karplus, K., Li, W., Lopez, R., McWilliam, H., Remmert, M. & other authors. (2011). Fast, scalable generation of high-quality protein multiple sequence alignments using Clustal Omega. *Mol Syst Biol* **7**, 539.

Sigmund, C. D. & Morgan, E. A. (1982). Erythromycin resistance due to a mutation in a ribosomal RNA operon of Escherichia coli. *Proc Natl Acad Sci U S A* **79**, 5602–5606.

Sigmund, C. D., Ettayebi, M. & Morgan, E. A. (1984). Antibiotic resistance mutations in 16S and 23S ribosomal RNA genes of Escherichia coli. *Nucleic Acids Res* **12**, 4653–4663.

Silva Marques, J., Varela, M. G., Ferreira, R., Nobre, A., Almeida, A. G. & de Sousa, J. (2012). Intracardiac sterile pacemaker lead thrombosis. *Rev Esp Cardiol Engl Ed* **65**, 193–194.

Simonart, T. & Dramaix, M. (2005). Treatment of acne with topical antibiotics: lessons from clinical studies. *Br J Dermatol* **153**, 395–403.

Simpson, N. (2001). Antibiotics in acne: time for a rethink. *Br J Dermatol* **144**, 225–227.

van Sinderen, D., Karsens, H., Kok, J., Terpstra, P., Ruiters, M. H., Venema, G. & Nauta, A. (1996). Sequence analysis and molecular characterization of the temperate lactococcal bacteriophage r1t. *Mol Microbiol* **19**, 1343–1355.

Smith, K. & Leyden, J. J. (2005). Safety of doxycycline and minocycline: a systematic review. *Clin Ther* **27**, 1329–1342.

Söding, J., Biegert, A. & Lupas, A. N. (2005). The HHpred interactive server for protein homology detection and structure prediction. *Nucleic Acids Res* **33**, W244-248.

Stajich, J. E., Block, D., Boulez, K., Brenner, S. E., Chervitz, S. A., Dagdigian, C., Fuellen, G., Gilbert, J. G. R., Korf, I. & other authors. **(2002).** The Bioperl toolkit: Perl modules for the life sciences. *Genome Res* **12**, 1611–1618.

Stockdale, S. R., Collins, B., Spinelli, S., Douillard, F. P., Mahony, J., Cambillau, C. & van Sinderen, D. (2015). Structure and Assembly of TP901-1 Virion Unveiled by Mutagenesis. *PloS One* **10**, e0131676.

Strauss, J. S., Kligman, A. M. & Pochi, P. E. (1962). The effect of androgens and estrogens on human sebaceous glands. *J Invest Dermatol* **39**, 139–155.

Strauss, J. S., Krowchuk, D. P., Leyden, J. J., Lucky, A. W., Shalita, A. R., Siegfried, E. C., Thiboutot, D. M., Van Voorhees, A. S., Beutner, K. A. & other authors. **(2007).** Guidelines of care for acne vulgaris management. *J Am Acad Dermatol* **56**, 651–663.

Su, Q., Grabowski, M. & Weindl, G. (2017). Recognition of Propionibacterium acnes by human TLR2 heterodimers. *Int J Med Microbiol IJMM* **307**, 108–112.

Sulakvelidze, A. & Barrow, P. (2004). Chapter 13: Phage Therapy in Animals and Agribusiness. In *Bacteriophages Biol Appl*. Edited by E. Kutter & A. Sulakvelidze. Boca Raton, FL: Taylor & Francis Group, LLC.

Sullivan, M. J., Petty, N. K. & Beatson, S. A. (2011). Easyfig: a genome comparison visualizer. *Bioinforma Oxf Engl* **27**, 1009–1010.

Summers, W. C. (2001). Bacteriophage therapy. *Annu Rev Microbiol* **55**, 437–451.

Takeda, K. & Akira, S. (2004). Microbial recognition by Toll-like receptors. *J Dermatol Sci* **34**, 73–82.

Tan, A. W. & Tan, H.-H. (2005). Acne vulgaris: a review of antibiotic therapy. *Expert Opin Pharmacother* **6**, 409–418.

Tan, J. K. L. & Bhate, K. (2015). A global perspective on the epidemiology of acne. *Br J Dermatol* **172 Suppl 1**, 3–12.

Tan, J., Boyal, S., Desai, K. & Knezevic, S. (2016). Oral Isotretinoin: New Developments Relevant to Clinical Practice. *Dermatol Clin* **34**, 175–184.

Tan, J. K. L. (2004). The canadian acne epidemiological survey: baseline demographics and interim analysis. *J Am Acad Dermatol* **50**, P15.

Tanghetti, E. A., Kawata, A. K., Daniels, S. R., Yeomans, K., Burk, C. T. & Callender, V. D. (2014). Understanding the burden of adult female acne. *J Clin Aesthetic Dermatol* **7**, 22–30.

Taub, A. F. (2007). A comparison of intense pulsed light, combination radiofrequency and intense pulsed light, and blue light in photodynamic therapy for acne vulgaris. *J Drugs Dermatol JDD* **6**, 1010–1016.

Tenson, T., Lovmar, M. & Ehrenberg, M. (2003). The mechanism of action of macrolides, lincosamides and streptogramin B reveals the nascent peptide exit path in the ribosome. *J Mol Biol* **330**, 1005–1014.

Thiboutot, D. (2000). New treatments and therapeutic strategies for acne. *Arch Fam Med* **9**, 179–187.

Thiboutot, D. (2004). Regulation of human sebaceous glands. *J Invest Dermatol* **123**, 1–12.

Thiboutot, D., Gollnick, H., Bettoli, V., Dréno, B., Kang, S., Leyden, J. J., Shalita, A. R., Lozada, V. T., Berson, D. & other authors. **(2009).** New insights into the management of

acne: an update from the Global Alliance to Improve Outcomes in Acne group. *J Am Acad Dermatol* **60**, S1-50.

Tomida, S., Nguyen, L., Chiu, B.-H., Liu, J., Sodergren, E., Weinstock, G. M. & Li, H. (2013). Pan-genome and comparative genome analyses of propionibacterium acnes reveal its genomic diversity in the healthy and diseased human skin microbiome. *mBio* **4**, e00003-00013.

Trampuz, A., Osmon, D. R., Hanssen, A. D., Steckelberg, J. M. & Patel, R. (2003). Molecular and antibiofilm approaches to prosthetic joint infection. *Clin Orthop* 69–88.

Trudil, D. (2015). Phage lytic enzymes: a history. *Virol Sin* **30**, 26–32.

Tunney, M. M., Patrick, S., Gorman, S. P., Nixon, J. R., Anderson, N., Davis, R. I., Hanna, D. & Ramage, G. (1998). Improved detection of infection in hip replacements. A currently underestimated problem. *J Bone Joint Surg Br* **80**, 568–572.

Tunney, M. M., Patrick, S., Curran, M. D., Ramage, G., Hanna, D., Nixon, J. R., Gorman, S. P., Davis, R. I. & Anderson, N. (1999). Detection of prosthetic hip infection at revision arthroplasty by immunofluorescence microscopy and PCR amplification of the bacterial 16S rRNA gene. *J Clin Microbiol* **37**, 3281–3290.

Twort, F. W. (1915). An investigation on the nature of ultra-microscopic viruses. *The Lancet*, Originally published as Volume 2, Issue 4814 **186**, 1241–1243.

Tyrrell, K. L., Citron, D. M., Warren, Y. A., Fernandez, H. T., Merriam, C. V. & Goldstein, E. J. C. (2006). In Vitro Activities of Daptomycin, Vancomycin, and Penicillin against Clostridium difficile, C. perfringens, Finegoldia magna, and Propionibacterium acnes. *Antimicrob Agents Chemother* **50**, 2728–2731.

Unna, P. G. (1896). The histopathology of disease of the skin, translated by N. Walker. In *Histopathol Dis Skin Transl N Walk*, pp. 352–366. New York, USA: The Macmillan Co.

Ushijima, T., Takahashi, M. & Ozaki, Y. (1984). Acetic, propionic, and oleic acid as the possible factors influencing the predominant residence of some species of Propionibacterium and coagulase-negative Staphylococcus on normal human skin. *Can J Microbiol* **30**, 647–652.

Valanne, S., McDowell, A., Ramage, G., Tunney, M. M., Einarsson, G. G., O'Hagan, S., Wisdom, G. B., Fairley, D., Bhatia, A. & other authors. **(2005).** CAMP factor homologues in Propionibacterium acnes: a new protein family differentially expressed by types I and II. *Microbiology* **151**, 1369–1379.

van Valen, R., de Lind van Wijngaarden, R. A. F., Verkaik, N. J., Mokhles, M. M. & Bogers, A. J. J. C. (2016). Prosthetic valve endocarditis due to Propionibacterium acnes. *Interact Cardiovasc Thorac Surg* **23**, 150–155.

Vannuffel, P., Di Giambattista, M., Morgan, E. A. & Cocito, C. (1992). Identification of a single base change in ribosomal RNA leading to erythromycin resistance. *J Biol Chem* **267**, 8377–8382.

Viraraghavan, R., Jantausch, B. & Campos, J. (2004). Late-onset central nervous system shunt infections with Propionibacterium acnes: diagnosis and management. *Clin Pediatr (Phila)* **43**, 393–397.

Vowels, B. R., Yang, S. & Leyden, J. J. (1995). Induction of proinflammatory cytokines by a soluble factor of Propionibacterium acnes: implications for chronic inflammatory acne. *Infect Immun* **63**, 3158–3165.

Walsh, T. R., Efthimiou, J. & Dréno, B. (2016). Systematic review of antibiotic resistance in acne: an increasing topical and oral threat. *Lancet Infect Dis* **16**, e23-33.

Wang, B., Toye, B., Desjardins, M., Lapner, P. & Lee, C. (2013). A 7-year retrospective review from 2005 to 2011 of Propionibacterium acnes shoulder infections in Ottawa, Ontario, Canada. *Diagn Microbiol Infect Dis* **75**, 195–199.

Waterhouse, A. M., Procter, J. B., Martin, D. M. ., Clamp, M. & Barton, G. J. (2009). Jalview version 2: A Multiple Sequence Alignment and Analysis Workbench. *Bioinformatics* **25**, 1189–1191.

Webb, B. & Sali, A. (2016). Comparative Protein Structure Modeling Using MODELLER. *Curr Protoc Protein Sci* **86**, 2.9.1-2.9.37.

Webster, G. F. & Cummins, C. S. (1978). Use of bacteriophage typing to distinguish Propionibacterium acne types I and II. *J Clin Microbiol* **7**, 84–90.

Webster, G. F., Leyden, J. J., Tsai, C.-C., Baehni, P. & McArthur, W. P. (1980). Polymorphonuclear leukocyte lysosomal release in response to Propionibacterium acnes in vitro and its enhancement by sera from inflammatory acne patients. *J Invest Dermatol* **74**, 398–401.

Weisblum, B. (1995). Erythromycin resistance by ribosome modification. *Antimicrob Agents Chemother* **39**, 577–585.

Werner, J. L., Escolero, S. G., Hewlett, J. T., Mak, T. N., Williams, B. P., Eishi, Y. & Núñez, G. (2017). Induction of Pulmonary Granuloma Formation by Propionibacterium acnes Is Regulated by MyD88 and Nox2. *Am J Respir Cell Mol Biol* **56**, 121–130.

Wiegell, S. R. & Wulf, H. C. (2006). Photodynamic therapy of acne vulgaris using methyl aminolaevulinate: a blinded, randomized, controlled trial. *Br J Dermatol* **154**, 969–976.

Williams, R. E., Doherty, V. R., Perkins, W., Aitchison, T. C. & Mackie, R. M. (1992). Staphylococcus aureus and intra-nasal mupirocin in patients receiving isotretinoin for acne. *Br J Dermatol* **126**, 362–366.

Wolkenstein, P., Grob, J.-J., Bastuji-Garin, S. & Ruszczynski, S. (2003). French people and skin diseases Results of a survey using a representative sample. *Arch Dermatol* **139**, 1614–1619.

Wright, A., Hawkins, C. H., Anggård, E. E. & Harper, D. R. (2009). A controlled clinical trial of a therapeutic bacteriophage preparation in chronic otitis due to antibiotic-resistant Pseudomonas aeruginosa; a preliminary report of efficacy. *Clin Otolaryngol Off J ENT-UK Off J Neth Soc Oto-Rhino-Laryngol Cervico-Facial Surg* **34**, 349–357.

Wu, S. & Zhang, Y. (2007). LOMETS: A local meta-threading-server for protein structure prediction. *Nucleic Acids Res* **35**, 3375–3382.

Yang, I., Nell, S. & Suerbaum, S. (2013). Survival in hostile territory: the microbiota of the stomach. *FEMS Microbiol Rev* **37**, 736–761.

Yentzer, B. A., Hick, J., Reese, E. L., Uhas, A., Feldman, S. R. & Balkrishnan, R. (2010). Acne vulgaris in the United States: a descriptive epidemiology. *Cutis* **86**, 94–99.

Yow, M. A., Tabrizi, S. N., Severi, G., Bolton, D. M., Pedersen, J., Giles, G. G. & Southey, M. C. (2017). Characterisation of microbial communities within aggressive prostate cancer tissues. *Infect Agent Cancer* **12**.

Yu, Y., Champer, J., Agak, G. W., Kao, S., Modlin, R. L. & Kim, J. (2016). Different Propionibacterium acnes Phylotypes Induce Distinct Immune Responses and Express Unique Surface and Secreted Proteomes. *J Invest Dermatol* **136**, 2221–2228.

Żaczek, M., Weber-Dąbrowska, B. & Górski, A. (2015). Phages in the global fruit and vegetable industry. *J Appl Microbiol* **118**, 537–556.

Zaenglein, A. L. (2015). Psychosocial Issues in Acne Management: Disease Burden, Treatment Adherence, and Patient Support. *Semin Cutan Med Surg* **34**, S92–S94.

Zaenglein, A. L., Pathy, A. L., Schlosser, B. J., Alikhan, A., Baldwin, H. E., Berson, D. S., Bowe, W. P., Graber, E. M., Harper, J. C. & other authors. **(2016).** Guidelines of care for the management of acne vulgaris. *J Am Acad Dermatol*.

Zhang, A. L., Feeley, B. T., Schwartz, B. S., Chung, T. T. & Ma, C. B. (2015). Management of deep postoperative shoulder infections: is there a role for open biopsy during staged treatment? *J Shoulder Elbow Surg* **24**, e15-20.

Zhao, M.-M., Du, S.-S., Li, Q.-H., Chen, T., Qiu, H., Wu, Q., Chen, S.-S., Zhou, Y., Zhang, Y. & other authors. **(2017).** High throughput 16SrRNA gene sequencing reveals the correlation between Propionibacterium acnes and sarcoidosis. *Respir Res* **18**.

Zierdt, C. H., Webster, C. & Rude, W. S. (1968). Study of the anaerobic corynebacteria. *Int J Syst Bacteriol* **18**, 33–47.

Zimmerli, W. (2014). Clinical presentation and treatment of orthopaedic implant-associated infection. *J Intern Med* **276**, 111–119.

Zouboulis, C. C. (2014). Acne as a chronic systemic disease. *Clin Dermatol* **32**, 389–396.

http://www.graphpad.com/quickcalcs/contingency1/ (accessed March 2016). **(n.d.).** *GraphPad Softw QuickCalcs*.

http://www.graphpad.com/quickcalcs/kappa1/ (accessed April 2016). **(n.d.).** *GraphPad Softw QuickCalcs*.

GraphPad InStat version 3.10, 32 bit for Windows, GraphPad Software, San Diego California USA, www.graphpad.com. **(n.d.).** .

Appendix A

Microbiological Techniques, Bacterial Culturing and Stock Maintenance

A.1 Reagents, supplements and additives

95 % (v/v) ethanol (EtOH) working solution:
Added 5mL ddH_2O to 95mL anhydrous EtOH, mixed well

128.4 mg/mL calcium chloride ($CaCl_2$) working solution:
Dissolved 12.84g $CaCl_2$ in 100mL ddH_2O

1 M sodium hydroxide (NaOH) working solution:
Dissolved 40g NaOH (ACS certified) in 1L ddH_2O

0.85 % (w/v) sodium chloride (NaCl) solution, sterile
Dissolved 0.85g NaCl in 100mL ddH_2O
Sterilized by autoclave, using liquid cycle at 121°C and 15 Psi for 30 minutes

5 mg/mL hemin working solution
Mixed 0.5g hemin powder (#H9039, Sigma) into 10mL of 1 M NaOH until hemin was completely dissolved
Added ddH_2O to bring the final volume to 100mL
Sterilized by autoclave, using liquid cycle at 121°C for 15 minutes
Cooled to room temperature then stored in darkness at 4°C for a maximum of 30 days

10 mg/mL vitamin K_1 stock solution
Mixed 0.2mL Vitamin K_1 (pre-sterilized) solution with 20mL 95% EtOH
Stored in darkness at 4°C

1 mg/mL vitamin K_1 working solution
Mixed 1mL Vitamin K_1 stock solution (10mg/mL) with 9mL sterile ddH_2O
Stored in darkness at 4°C for a maximum of 30 days

Laked sheep blood
Froze sterile, whole, defibrinated sheep blood at -20°C for a minimum of 8 hours
Warmed blood to 37°C in a water bath
Mixed well by inversion prior to use

20% (v/v) glycerol:
Mixed 0.1L glycerol with 0.4L ddH_2O
Sterilized by autoclave, using liquid cycle at 121°C and 15 Psi for 30 minutes.

A.2 Nutrient media

Brain-heart infusion (BHI) broth:

Approximate formula per litre:

Casein Peptone	15.0 g
Meat peptone/brain heart infusion	12.0 g
Dipotassium phosphate	2.5 g
Dextrose	2.0 g
Yeast extract	5.0 g
Sodium chloride	5.5 g

A total of 42g dehydrated B-HI broth media was dissolved in 1L ddH_2O then sterilized by autoclave, using liquid cycle at 121°C and 15 Psi for 30 minutes.

BHI agar (1.6%):

1L BHI broth
16 g bacteriological agar

Sterilized by autoclave, using liquid cycle at 121°C and 15 Psi for 30 minutes.

Brucella broth w/ hemin and vitamin K_1 :

Approximate formula per litre:

Pancreatic digest of casein	10.0 g
Peptic digest of animal tissue	10.0 g
Dextrose	1.0 g
Yeast extract	2.0 g
Sodium chloride	5.0 g
Sodium bisulfite	0.1 g
Hemin	0.005 g
Vitamin K_1	0.001 g

A total of 28g dehydrated brucella broth media was dissolved in 1L ddH_2O. One millilitre hemin working solution (5mg/mL) and 1 mL vitamin K_1 working solution (1mg/mL) were added to the brucella solution then sterilized by autoclave, using liquid cycle at 121°C and 15 Psi for 30 minutes.

Brucella agar (1.6%) w/ hemin, vitamin K_1 and 5% laked sheep blood (BBA):

1 L brucella broth w/ hemin and vitamin K_1
16 g bacteriological agar
50 mL laked sheep blood

Sterilized by autoclave, using liquid cycle at 121°C and 15 Psi for 30 minutes. Cooled medium to 50°C and added pre-warmed (37°C) laked sheep blood. Mixed media well with magnetic stir bar and dispensed 67mL media into 150mm petri dishes for an optimal nutrient agar depth of 0.4mm +/- 0.5mm.

BBA w/ 0.1284 mg/L Ca^{2+} supplement (~ 40 mg/L final [Ca^{2+}]):

1 L BBA
1 mL $CaCl_2$ working solution (128.4 mg/mL)

Prepared BBA solution without blood and added $CaCl_2$ working solution, mixed well. Sterilized media by autoclave, using liquid cycle at 121°C and 15 Psi for 30 minutes. Cooled medium to 48°C to 50°C and added pre-warmed (37°C) laked sheep blood. Mixed media well with magnetic stir bar and dispensed 42mL media into 92mm petri dishes for an optimal nutrient agar depth of 0.4mm +/- 0.5mm.

Columbia (CB) broth:

Approximate formula per litre:

Special peptone mix	23.0 g
Sodium chloride	5.0 g
L-cysteine	0.1 g
Sodium carbonate	0.6 g
Dextrose	2.5 g
Magnesium sulfate	0.1 g
Ferrous sulfate	0.02 g
Tris	0.83 g
Tris, hydrochloride	2.86 g

A total of 35g dehydrated CB broth media was dissolved in 1L deionized water (ddH_2O) then sterilized by autoclave, using liquid cycle at 121°C and 15 Psi for 30 minutes.

CB agar (1.6%):

1 L CB broth (see above)
16 g bacteriological agar

Sterilized by autoclave, using liquid cycle at 121°C for 30 minutes.

CB top agar (0.7%):

1 L CB broth (see above)
7 g bacteriological agar

Sterilized by autoclave, using liquid cycle at 121°C and 15 Psi for 30 minutes.

Mueller-Hinton (MH) broth w/ hemin and vitamin K_1:

Approximate formula per litre:

Dehydrated infusion from beef	300.0 g
Casein hydrolysate	17.5 g
Starch	1.5 g
Hemin	0.005 g
Vitamin K_1	0.001 g

A total of 21g dehydrated MH broth media was dissolved in 1L ddH_2O. One millilitre hemin working solution (5mg/mL) and 1 mL vitamin K_1 working solution (1mg/mL) were added to the media solution then sterilized by autoclave, using liquid cycle at 121°C and 15 Psi for 30 minutes.

MH agar (1.6%) w/ hemin, vitamin K_1 and 5% laked sheep blood (MHB):

1 L MH broth w/ hemin and vitamin K_1 (see above)

16 g bacteriological agar
50 mL laked sheep blood

Sterilized by autoclave, using liquid cycle at 121°C and 15 Psi for 30 minutes. Cooled medium to 48°C to 50°C and added pre-warmed (37°C) laked sheep blood. Mixed media well with magnetic stir bar and dispensed 42mL media into 92mm petri dishes for an optimal nutrient agar depth of 0.4mm +/- 0.5mm.

Appendix B

Molecular Techniques: Buffer and Reagent Preparation

B.1 Common buffers

1M Tris-HCl, pH 8.0:

Dissolved 121.1 g Tris base in 800ml ddH_2O
Added concentrated HCl until pH 8.0 was achieved
Added ddH_2O to a final volume of 1000ml, mixed well

0.5M EDTA, pH 8.0:

Mixed 186.12 g $EDTA.Na_2.2H_2O$ in 800 ml ddH_2O
While mixing vigorously, NaOH was added into the solution until pH 8.0 was achieved
Added ddH_2O to a final volume of 1000 ml, mixed well

B.2 Bacterial cell lysis

Cell lysis buffer (CLB), pH 8.0:

Added 250 ml 0.1M Tris-HCl pH 8.0 to 735 ml ddH_2O
Added 5 ml 0.5 mM EDTA pH, 8.0
Added 10 ml 100% Triton X-100
Mixed solution well

10% Sodium dodecyl sulphate (SDS):

Added 100g SDS to 800 ml ddH_2O and stirred on a magnetic stirrer until dissolved
Added ddH_2O to a final volume of 1000 ml, mixed well

6 μg/μL pronase:

Added 60 mg pronase to 10 mL ddH_2O

3 M potassium acetate (KOAc), pH 5.5:

Mixed 294.42 g KOAc into 500 mL ddH_2O and stirred on a magnetic stirrer until dissolved
Adjusted pH to 5.5 with addition of glacial acetic acid (approximately 110 mL)
Add ddH2O to a final volume of 1000 mL

B.3 Phenol-chloroform extraction

25:24:1 phenol chloroform isoamyl alcohol (PCI):

Mixed 50 ml phenol (containing 0.2% 8-hydroxyquinoline), 48 ml chloroform and 2 ml isoamyl alcohol
Added 50 ml 0.1M Tris-HCl pH 8.0, mixed vigorously to saturate with buffer

Solution settled to allow for phase separation
A fraction of the upper phase, containing 0.1 M Tris-HCl pH 8.0, was removed resulting in a thin layer of Tris-HCl to cover the PCI solution

B.4 PEG precipitation

30% PEG/3 M NaCl solution:

Dissolved 175.5g NaCl in 200 ml ddH_2O
Added 300g PEG 8000, mixed until fully dissolved
Added ddH_2O to a final volume of 1000 ml, mixed well

1X Phage extraction buffer, pH 7.5:

5.84g NaCl dissolved in 800 ml ddH_2O
Added 100 ml 1 M Tris-HCl, pH 7.5
Added 50 ml 0.5 M EDTA, pH 8.0
Added ddH_2O to a final volume of 1000 ml, mixed well

B.5 Ethanol precipitation

3M NaOAc solution:

Dissolved 246.01g anhydrous sodium acetate in 800 ml ddH_2O
Added ddH_2O to a final volume of 1000 ml, mixed well

EtOH/0.16M NaOAc solution:

Added 852 ml anhydrous ethanol (100%) to 95 ml ddH_2O
Added 53 ml 3M sodium acetate, mixed well

B.6 Agarose gel electrophoresis

50X Tris acetate (TAE), pH 8.3:

Dissolved 242g Tris base in 500 ml ddH_2O
Added 57.1 ml 1M Glacial acetic acid and 100 ml 0.5M EDTA pH, 8.0
Added ddH_2O to a final volume of 1000 ml, mixed well (no pH adjustment necessary)

1X TAE running buffer:

Diluted 80 mL 50X TAE concentrated stock solution in ddH_2O to a final volume of 4 L

0.7% (w/v) agarose gel:

Added 0.7g electrophoresis grade agarose to 100 ml 1X TAE running buffer
Mixed well while heating until solution reached boiling point

1.5% (w/v) agarose gel:

Added 1.5g electrophoresis grade agarose to 100 ml 1X TAE running buffer

Mixed well while heating until solution reached boiling point

1.8% (w/v) agarose gel:

Added 1.8g electrophoresis grade agarose to 100 ml 1X TAE running buffer
Mixed well while heating until solution reached boiling point

2.0% (w/v) agarose gel:

Added 2.0g electrophoresis grade agarose to 100 ml 1X TAE running buffer
Mixed well while heating until solution reached boiling point

6X DNA loading buffer pH 8.0:

Combined the following, mixed well:
2.0 ml ddH_2O
6.0 ml glycerol
1.0 ml 0.5M EDTA pH 8.0
1.0 ml 1% bromophenol blue in ddH_2O
Distributed 1.0 ml to 2.0 ml screw-capped tubes and stored at -20°C

0.5 µg/mL EtBr solution:

Diluted 25 µL 10 mg/mL EtBr stock solution with 500 mL ddH_2O

Appendix C

Propionibacterium acnes Collection

Table C.1: Sources of *P. acnes* isolates used in this study (Sudbury and Ottawa excluded).

Strain Identifier	Specimen	Type	Source	Reference
ATCC 6919	Facial acne (severe case)	IA	ATCC	(Zierdt *et al.*, 1968)
ATCC 29399	Forehead (healthy individual)	IA		(Marples & McGinley, 1974)
01-A-087	Blood culture	IA	NML	none
02-A-018	Pleural fluid	IB		
05-A-026	Blood culture	IB		
00-0196	Neck abscess node	II		
03-A-023	Cerebral spinal fluid	IA		
06-0893	Tissue (allograft)	IA		
01-A-009	Blood culture	II		
03-A-024	Fluid- left frontal lesion	IB		
04-A-028	Neck wound	IA		
60743	Abdominal sterile pad	II		
70241	Blood culture	IA		
AD1	Knee prosthesis	IA	CSLU	(Holmberg *et al.*, 2009)
AD2	Sternal Wire	IA		
AD3	Sternal Wire	IB		
AD6	Bone tissue, finger	IA		
AD7	Knee prosthesis	II		
AD8	Hip prosthesis	IA		
AD9	Hip prosthesis	IA		
AD10	Bone tissue, skull	II		
AD11	Hip prosthesis	IA		
AD12	Hip prosthesis	IB		
AD14	Bone tissue, femur	II		
AD15	Prosthetic device, vertebra	IA		
AD16	Bone tissue, skull	II		
AD33	Knee prosthesis	IB		
AD47	Hip prosthesis	IA		
AD48	Prosthetic device, vertebra	IA		
AD49	Bone tissue, skull	II		
AS1	Forehead	IB		
AS2	Forehead	IA		
AS3	Forehead	IB		

Strain Identifier	Specimen	Type	Source	Reference
AS4	Forehead	IA		
AS5	Forehead	IA		
AS6	Forehead	IA		
AS7	Forehead	IA		
AS9	Forehead	II		
AS10	Forehead	IA		
AS11	Forehead	IB		
AS13	Forehead	IB		
AS16	Forehead	IB		
AS18	Forehead	IB		
AS20	Forehead	II		
AS21	Forehead	II		
AS22	Forehead	II	CSLU	(Holmberg *et al.*, 2009)
AS24	Forehead	IA		
AS25	Forehead	IA		
AS27	Forehead	IA		
AS28	Forehead	II		
AS30	Forehead	IA		
AS31	Forehead	IA		
AS32	Forehead	IA		
AS33	Forehead	IA		
AS37	Forehead	IB		
AS38	Forehead	IB		
AS39	Forehead	II		
AS50	Forehead	IA		

NML, National Microbiology Laboratory (Winnipeg, Canada), courtesy of Ms. Kathryn Bernard; ATCC, American Type Culture Collection (Manassas, USA); CSLU, Department of Clinical Sciences of Lund University (Lund, Sweden), courtesy of Dr. Anna Holmberg; AD, isolated from sites of deep infection; AS, isolated from skin of healthy individuals.

Appendix D

Antibiotic Susceptibility Testing: Interpretive Criteria

Table D.2: Clinical breakpoints used as interpretive criteria for antibiotic susceptibility of *P. acnes* clinical isolates. Clinical breakpoint does not necessarily distinguish wild-type from non-wild-type organisms, however, it does distinguish treatable organisms from organisms that will likely not respond to treatment with the antibiotic in question (Martínez *et al.*, 2015).

Antibiotic	MIC (mg/L)			Reference(s)
	S	I	R	
Azithromycin [2]	≤ 2	-	> 2	(Achermann *et al.*, 2014; EUCAST, 2016; Olsson *et al.*, 2012)
Benzylpenicillin	≤ 0.25	-	> 0.5	(EUCAST, 2016)
Ceftriaxone	≤ 16	32	≥ 64	(Clinical and Laboratory Standards Institute, 2015)
Clindamycin	≤ 4	-	> 4	(EUCAST, 2016)
Doxycycline [3]	≤ 4	-	> 4	-
Erythromycin	< 0.5	-	≥ 0.5	(Oprica *et al.*, 2004; Oprica & Nord, 2005)
Levofloxacin [1]	≤ 1	-	> 2	(Achermann *et al.*, 2014; EUCAST, 2016)
Linezolid [1]	≤ 2	-	> 4	(Achermann *et al.*, 2014; EUCAST, 2016)
Minocycline [3]	≤2	-	> 2	-
Tetracycline	≤ 4	8	≥ 16	(Clinical and Laboratory Standards Institute, 2015)
Rifampicin [2]	≤ 0.5	-	> 0.5	(Achermann *et al.*, 2014; EUCAST, 2016; Olsson *et al.*, 2012)
Vancomycin	≤2	-	> 2	(EUCAST, 2016)
Daptomycin [2]	≤ 1	-	> 1	(Achermann *et al.*, 2014; Clinical and Laboratory Standards Institute, 2015; EUCAST, 2016; Olsson *et al.*, 2012; Tyrrell *et al.*, 2006)
Trimethoprim/sulfamethoxazole	< 1	-	≥ 1	(Oprica *et al.*, 2004)

[1]Values are non-species specific.
[2]Breakpoint values do not exist for anaerobes, therefore breakpoints for other Gram-positive organisms were used.
[3]Interpretive MIC values of DC and MC were set as described in Section 2.2.4.3.

Appendix E

Phage Genome Annotation: Reference Sequences

Table E.3: *P. acnes* phage sequence database for annotation with the Prokka pipeline v 1.11 (Seemann, 2014).

Propionibacterium phage: Complete Genome ID	NCBI Reference Sequence (RefSeq; Accession.Version) [A]	Genbank (Accession.Version)
ATCC29399B_C	NC_018851.1	JX262225.1
ATCC29399B_T	NC_018847.1	JX262224.1
Attacne	NC_027629.1	KR337651.1
Keiki	-	KR337649.1
Kubed	NC_027625.1	KR337645.1
Lauchelly	NC_027628.1	KR337650.1
MrAK	NC_027620.1	KR337643.1
Ouroboros	NC_027630.1	KR337654.1
P100_1	NC_018840.1	JX262222.1
P100_A	NC_018838.1	JX262221.1
P100D	NC_018852.1	JX262220.1
P101A	NC_018841.1	JX262217.1
P104A	NC_018845.1	JX262218.1
P105	NC_018849.1	JX262219.1
P11	NC_018842.1	JX262223.1
P144	NC_018839.1	JX262216.1
P91	NC_018834.1	JX262215.1
PA1-14	NC_028694.1	KT934381.1
PA6	NC_009541.1[B]	DQ431235.1
PAC1	NC_028967.1	KR902978.1
PAC10	-	KR902987.1
PAC2	-	KR902979.1
PAC3	-	KR902980.1
PAC4	-	KR902981.1
PAC5	-	KR902982.1
PAC6	-	KR902983.1
PAC7	-	KR902984.1
PAC8	-	KR902985.1
PAC9	-	KR902986.1

Propionibacterium phage: Complete Genome ID	NCBI Reference Sequence (RefSeq; Accession.Version) [A]	Genbank (Accession.Version)
Pacnes 2012-15	NC_027371.1	KJ722067.1
PAD20	NC_015454.1	FJ706171
PAS50	NC_015453.1	FJ706172
PHL009M11	NC_027336.1	KJ578758.1
PHL010M04	NC_022336.1	JX570704.1
PHL025M00	NC_027357.1	KJ578759.1
PHL030N00	NC_027373.1	KJ578760.1
PHL037M02	-	JX570706.1
PHL041M10	NC_027391.1	KJ578761.1
PHL055N00	NC_027400.1	KJ578762.1
PHL060L00	NC_022338.1	JX570705.1
PHL064M01	-	KJ578763.1
PHL064M02	-	KJ578764.1
PHL066M04	-	JX570711.1
PHL067M01	-	KJ578765.1
PHL067M09	-	KJ578766.1
PHL067M10	NC_022335.1	JX570709.1
PHL070N00	NC_027333.1	KJ578767.1
PHL071N05	NC_022337.1	JX570710.1
PHL073M02	-	JX570703.1
PHL082M00	NC_027359.1	KJ578768.1
PHL082M02	-	KJ578769.1
PHL082M03	-	KJ578770.1
PHL082M04	-	KJ578771.1
PHL085M01	-	JX570707.1
PHL085N00	NC_027361.1	KJ578772.1
PHL092M00	NC_027385.1	KJ578773.1
PHL095N00	NC_027401.1	KJ578774.1
PHL111M01	NC_022342.1	JX570702.1
PHL112N00	NC_022334.1	JX570714.1
PHL113M01	NC_022341.1	JX570713.1
PHL114L00	NC_022340.1	JX570712.1
PHL114N00	-	KJ578775.1
PHL115M02	-	JX570708.1

Propionibacterium phage: Complete Genome ID	NCBI Reference Sequence (RefSeq; Accession.Version) [A]	Genbank (Accession.Version)
PHL116M00	NC_027362.1	KJ578776.1
PHL116M10	-	KJ578777.1
PHL117M00	-	KJ578778.1
PHL117M01	-	KJ578779.1
PHL132N00	NC_027367.1	KJ578780.1
PHL141N00	NC_027389.1	KJ578781.1
PHL150M00	NC_027294.1	KJ578782.1
PHL151M00	-	KJ578783.1
PHL151N00	-	KJ578784.1
PHL152M00	NC_027386.1	KJ578785.1
PHL163M00	-	KJ578786.1
PHL171M01	NC_027346.1	KJ578787.1
PHL179M00	NC_027370.1	KJ578788.1
PHL194M00	-	KJ578789.1
PHL199M00	NC_027295.1	KJ578790.1
PHL301M00	NC_027354.1	KJ578791.1
PHL308M00	-	KJ578792.1
Pirate	NC_027623.1	KR337653.1
Procrass1	NC_027626.1	KR337644.1
SKKY	NC_027624.1	KR337648.1
Solid	NC_027627.1	KR337647.1
Stormborn	NC_027622.1	KR337652.1
Wizzo	NC_027621.1	KR337646.1

[A] Reference sequence identical to Genbank sequence except where indicated otherwise

[B] Reference sequence derived from Genbank sequence